LOAD AND DEFORMATION MEASUREMENTS OF HUMAN THIGHS AND SEAT CUSHION FOAMS

By

Akram Ali

A THESIS

Submitted to
Michigan State University
in partial fulfillment of the requirements
of the degree of

MASTER OF SCIENCE

Department of Material Science and Mechanics

1997

ABSTRACT

LOAD AND DEFORMATION MEASUREMENTS OF HUMAN THIGHS AND SEAT CUSHION FOAMS

By
Akram Ali

In recent years much attention has been paid to applying physical principles and engineering methods to the behavior of parts of the human body, considering it a structure and a machine. This study describes the measurement of loads, deformations, and contours of human thighs and seat cushion materials. Deformation of soft tissues and seat cushion foams are significant factors in determining the interface contours between the seat and the back of the thigh. The goal of this work is to represent the human interactions with seats and to provide quantitative data to develop deformable human models. This study was conducted with related work to develop finite element models of human and seat interactions.

A contour measurement system was built that uses wires through the seat cushion foam samples to transfer the surface contours to a video camera with computer interface.. The contour system was used to measure deflections of people's soft tissues with seat cushion foams of different stiffness and thickness. While raising the foam sample and contour system into the back of the thigh, measurements of force, and deformation of the foam and thigh were collected.

The force versus deflection responses of the thighs did not vary significantly with different foam stiffnesses. This work helps the automotive seat designer understand the complex problem of contact between human soft tissues and seat cushion foams.

DEDICATION

To my parents

ACKNOWLEDGMENTS

The author like to express his sincerest gratitude to following people, for their efforts, advice and encouragement:

Co-workers and friends for their help and support: Chris Gedraitis, Nate Radcliffe, Barry Frost, Bruce Liu, Tanisha Gordon, Frank Mills, Melissa Sloan, Robert Boughner, Kristy Satchell., Jamillah Gross, Jeff Basas, Damien Fron, and Theresa Atkinson.

Tammy Bush, for her friendship and time to review my work.

Clifford Beckett, for his help and idea to develop contour measurement system used in this study.

Richard Setyabudhy, for his cooperation.

The staff in MSU Anatomy Laboratory

Dr. Norman Sauer and David Barondess, for their help and advice.

Johnson Controls, Inc., for their generous funding of this project and staff in Comfort Laboratory for their help.

Dr. Ronald Averill and Dr. Roger Haut for reviewing my work and serving on my committee.

To my graduate advisor, Dr. Robert P. Hubbard, for your friendship, guidance and help me keeps focused these past two years. Working with you helped me to learn and explore biomechanics. I appreciate your help and support for everything. I am proud of this accomplishments and you made it possible for me. Thank you.

TABLE OF CONTENTS

LEST OF TABLES

LIST OF FIGURES

CHAPTER 1

BACKGROUND AND OBJECTIVES

"With the exception of astronauts traveling in space, human bodies are supported by surfaces, such as floors, chairs or beds, pressing against the skin with a total force equal to the body weight." [1]

A knowledge of the pressure distribution and the contour of the interaction surfaces are important in design of supporting devices which will be comfortable for normal people to use and avoid pressure lesions in mobilized patients. However few measurement methods of body contour and pressure distribution have been reported.

Lindan et al. [1] used a supporting surface consisting of multiple independent springs and nails to measure the contact pressure (Figure 1.1) by the principle of spring compression. He concluded that when the person was in a seated position with their back vertical, the points of greatest pressure were under the ischial tuberosities. The position of the legs and trunk were important factors in determining the pressure distribution under the buttocks of a seated subject. Figure 1.2A illustrates the degree to which the maximum pressure exerted under the ischial tuberosities in a seated subject was influenced by allowing the feet to hang unsupported. If the feet were supported by a balance pan which was positioned to bear some of the weight of the legs, there was a distinct transfer of pressure from the thighs to ischial tuberosities so that the pressure on the latter was markedly increased (Figure 1.2B).

Figure 1.1 Subject lying on "Bed of Springs and Nails"[1].

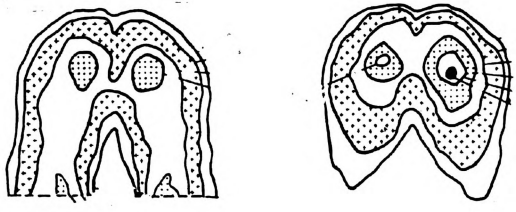

A B

Figure 1.2 Pressure Distribution under the Buttocks of Seated Subject with (A) Feet Hanging Freely, and (B) Feet Supported on a Balance Pan [1].

Mooney et al. [2] designed a special chair (Figure 1.3) to evaluate seat cushions by measuring pressure distributions. The chair, with variable back angle, variable seat angle, and variable leg angle, could be adjusted to suit the anatomy of each subject. The tests were performed with both legs weighted equally, as tested by scales under each foot. The subject was tested with his hands resting on the thighs and the thighs parallel to the floor and the seat. The pressure was measured by pneumatic cell pressure sensors developed especially for the study. This experiment confirmed that the greatest pressures were under the ischial tuberosities. Measurement of pressure under the ischial tuberosities effectively measures the seat cushion's capability to distribute these pressures. Distribution of these pressures may mean transfer of the weight to the thigh area. This would reduce the sharp pressure gradients between the ischial tuberostites and surrounding tissue. Other means of transferring pressure would be to recline or lower the knees and the legs so the weight is borne over a larger area.

The important contribution of design of seat cushions is to equalize and minimize pressure. Pressure can be measured and can be subjectively related to comfort for the healthy subject [2]. Several other specifications for seat design also are important, such as heat and moisture exchange, material stability, cushion weight, and cost. There are two characteristics of seats for seat cushion stiffness, soft and firm. In a soft seat, the cushion deforms to a level where pressure distribution is spread over a larger area of the body. In a firm seat little deformation occurs, therefore the human body can be said to be more correctly sitting on the seat [3]. In the latter case, efforts to achieve proper pressure distributions on the body are incorporated into the contour of the seat cushion. Custom

contours (Figure 1.4) that fit people in wheel chair are used to equalize the pressure distribution on their body [4].

The above studies show that the thigh is important in pressure distributions between seat cushions and people in seated postures. For this study of measurement of human thigh and seat cushion interactions in seated postures, thigh anatomy and engineering literature were reviewed.

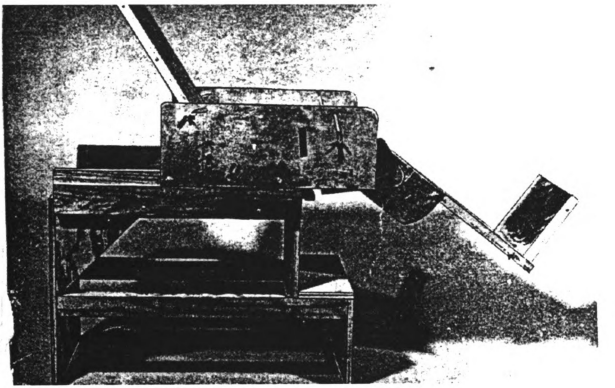

Figure 1.3 Experimental Chair Used to Evaluate The Pressure Distribution in Seat Cushions [2].

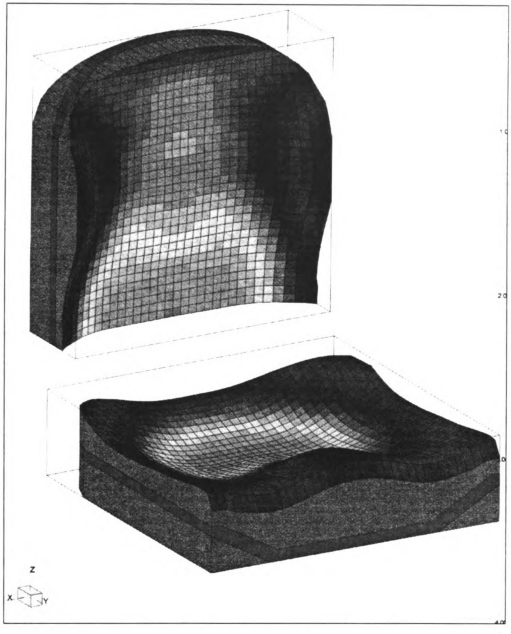

Figure 1.4. Custom Seat Contour [4].

1.1 THIGH ANATOMY

The thigh tissues consist of the following major anatomical components: bone, muscle, subcutaneous fat, and skin. The largest component of the tissues in thigh is the muscles [5]. The muscles of the adult thigh are divided into anterior, medial, and posterior compartments by intermuscular septa. The thigh posterior compartment interacts with seat cushion when people sit in chairs. The muscles of the posterior compartment of the thigh are biceps femurs, semitendinosus, and semimembranosus, and they all arise from the ischial tuberosity. The three muscles of posterior compartment are collectively known as the hamstrings, "ham" referring to the fleshy part of the thigh and "strings" referring to the long tendons of these muscles (Figure 1.5). The distal tendon of the biceps femoris, the lateral hamstring, inserts on the lateral side of the tibia, while the tendons of semitendinosus and semimembranosus, the medial hamstrings, insert on the medial side of the tibia. The three hamstrings assist the posterior hip muscles in extending the thigh and are the chief hip flexors of the leg [6].

The muscles provide strength and protection to the skeleton by distributing load, absorbing shock, and enabling the bones to move at the joints. Such movement usually represents the action of muscle groups rather than of individual muscles. The muscles perform both dynamic and static work. Dynamic work permits locomotion and the positioning of the body segments in space. Static work maintains body posture.

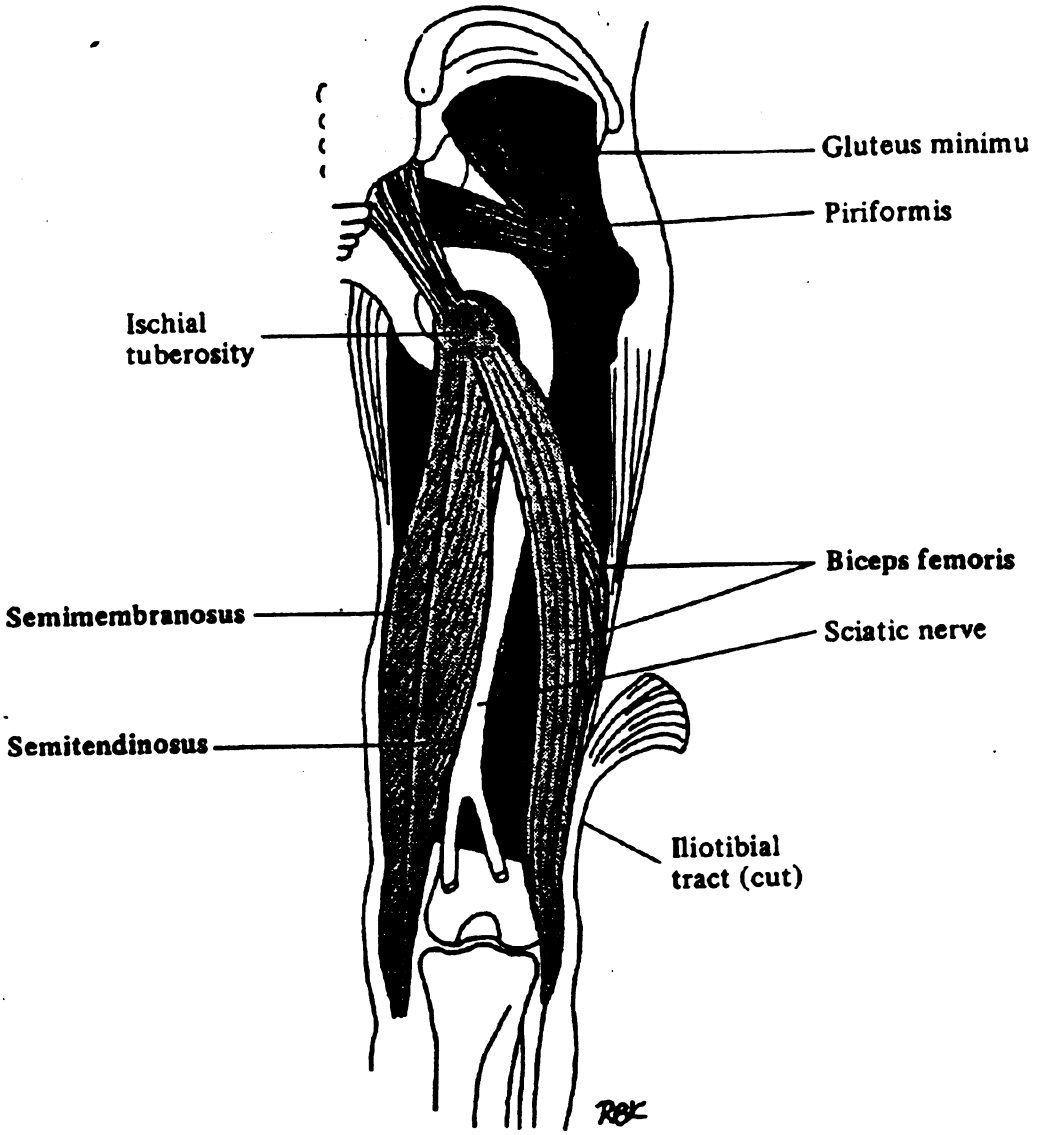

Figure 1.5 Thigh Posterior Muscles Compartment [6].

1.2 BIOMECHANICS OF SOFT TISSUE

Data describing the behavior of the bulk muscular tissue under contact loads are necessary in mechanical analyses of thigh-seat cushion interaction. Mechanical properties of biological tissues were described as being nonlinear, anisotropic and viscoelastic [7]. Viscoelasticity is associated with hysteresis, relaxation, and creep responses [7]. When a body is suddenly strained and then the strain is maintained constant afterward, the corresponding stresses induced in the body decrease with time. This phenomenon is called stress relaxation, or relaxation. If the body is suddenly stressed and then the stress is maintained constant afterward, the body continues to deform, and the phenomenon is called creep. Figure 1.6 shows the creep and relaxation functions. If the body is subjected to a cyclic loading, the stress-strain relationship in the loading process is usually different from that in the unloading process, and the phenomenon is called hysteresis.

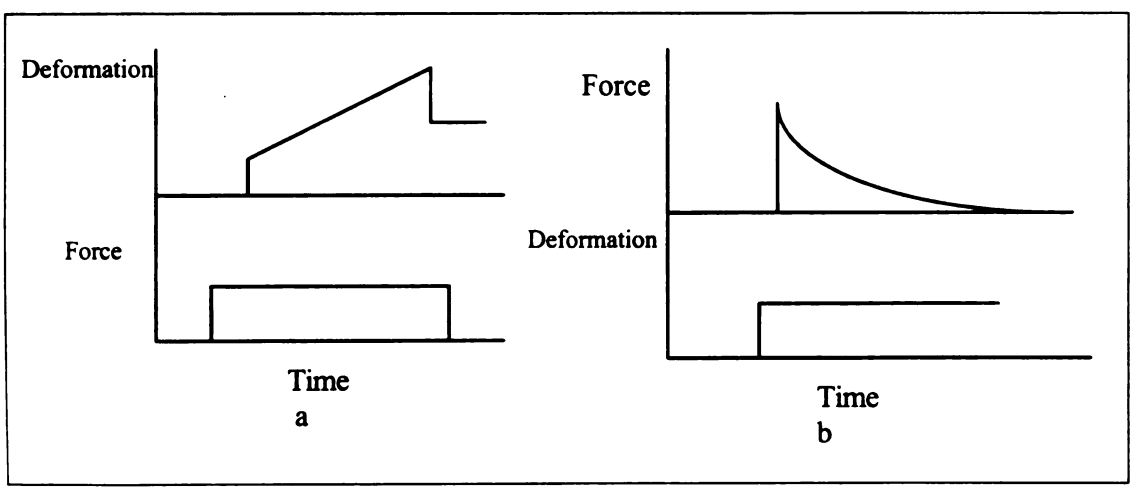

Figure 1.6 (a) Creep Function and (b) Relaxation Function (Maxwell Model) [7].

Some literature related to mechanical properties of bulk muscular have been considered as references for this thesis.

In Vannah and Childress [8], they used a quasi-static test of bulk muscle tissue to measure the load-deformation responses of the posterior muscle belly of the lower legs of living human subjects. A high distortion indentation test was chosen to deform the tissue in order to estimate the composite stiffness of the tissue. The stiffness of the calf was measured using the tissue tester, an indentator with a linear variable differential transformer (LVDT) and load cell (Figure 1.7) which measured applied displacement and a resulting force simultaneously. A chair was built to hold the lower leg motionless (Figure 1.8) with an adjustable arm to hold the tissue tester. The indentor was defined to have seated when the measured force exceeded 0.2 N. The indentor was threaded to a given position; then that position was held for 60 seconds before the resulting force was recorded.

A typical displacement-force response (Figure 1.9) was nonlinear [8]. The muscle belly appeared to exhibit repeatable behavior without "preconditioning". Also they noted minimum slope of the curve at 2 mm (at low deformation) is one-fifth of that at 20 mm. The changes in posture and muscle contraction strategies by the subject caused variations in the shape and the stiffness of the muscle belly. In a multisubject test the stiffness at 7.0 N reaction force averaged 0.519 N/mm relaxed, and 0.769 N/mm (mild exertion).

They concluded the load-deformation response for this composite tissue always exhibited hysteresis. The composite tissue relaxed less then 10 percent under stress in time

period between 5 and 1,200 seconds after indentation. Also they concluded that the preconditioning was not necessary to observe a repeatable load-deformation response.

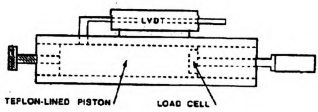

Figure 1.7 Tissue Tester

Figure 1.8 Testing Chair was Built to Hold the Lower Leg Motionless with an Adjustable Arm To Hold The Tissue Tester [8].

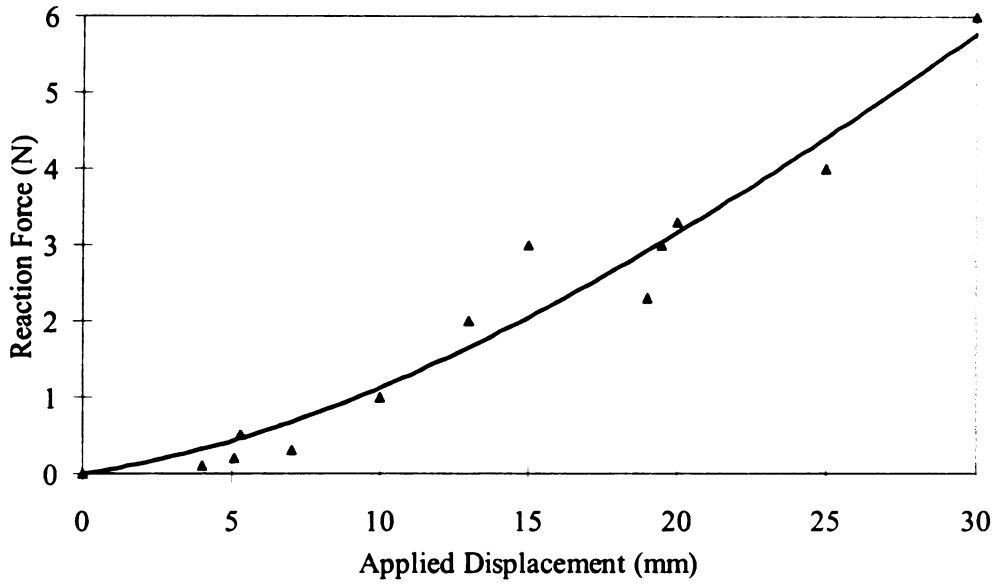

Figure 1.9 A Typical Load-Deformation Response of the Calf (Posterior Muscle Belly) of the Lower Leg of Living Human Subjects [8].

Deng [9] studied the load-deformation responses of the hamstring regions of human thighs in seated postures for ten subjects. A chair with load cells and electronic gauges was built to support people in variety of seated postures. The chair was adjusted according to each subject's body size, the subject sat in this chair with the hands dropped to the sides of the chair. Based on the thigh circumferences, the subjects were divided into small female, average male, and large male.

A rigid flat plate (254 X 138 mm) was pushed in a stepwise manner into the back of subject's thigh. The rigid flat plate could rotate about a lateral axis to align with the back of the thigh. The load-deformation data were collected after a ten second wait after each deformation step to allow load relaxation and to approach a quasi-static condition. The tests were performed for different knee angles at 90, 120, 150, and 165 degree. The knee

angle was defined as the angle between two vectors, one from the greater trochanter of the femur to the lateral condyle of the femur, another from the lateral condyle to the lateral malleolus of the ankle.

The vertical deformation versus lateral deformation of the mid-thigh was plotted to reflect the geometry change of the mid-thigh (Figure 1.10). A typical nonlinear load-deformation relationship for a soft tissues under compression with increasing contact area is shown in Figure 1.11. The load-deformation curves became stiffer as the knee angle straightened and the knee angle increased. These experiments were conducts to provide thigh geometry and structure properties for the finite element modeling. The result of Deng's computer model agreed with the experimental results.

As part of the development of a deformable computer model for human thigh, the present study provided experiment data that describe foam mechanical properties, thigh structure properties, load-deformation of the thigh-foam interaction, and the thigh geometry for seven human subjects. Also this study focused on the variation of thigh deformation with different foam thicknesses and densities. More specifically the objectives for this thesis are to measure:

1. Foam mechanical stress-stain properties.
2. Thigh geometry including thigh dimensions and femur location.
3. Thigh structure load-deformation responses.
4. Thigh-foam interaction responses, load-deformation relationships of the thigh interacting with foams of different thicknesses and densities.

This study is a continuation of a previous study [9]. In the present study, seven subjects were tested to measure the load-deformation response of their thighs with a rigid plate and with foams. The testing chair of previous study [9] was modified and used for this research.

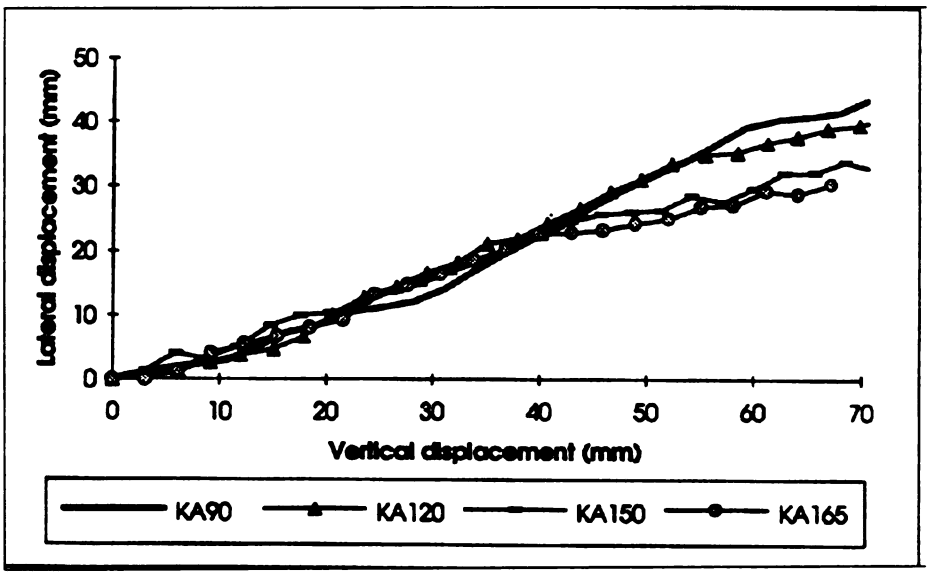

Figure 1.10 Lateral-Vertical Deformation Relationship of Mid-Thigh [9]

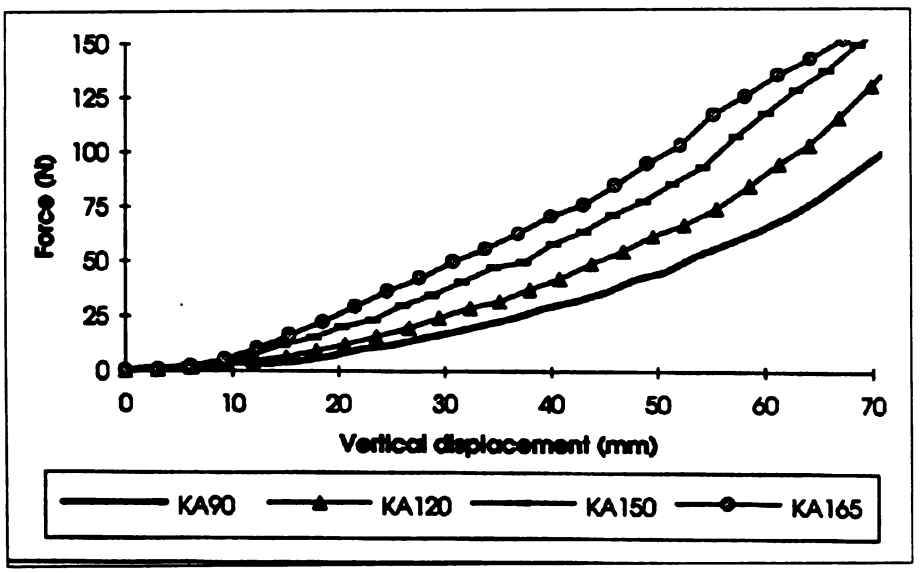

Figure 1.11 Force-Displacement Relationship of Mid-Thigh [9].

CHAPTER 2

SUBJECT ANTHROPOMETRY METHODS AND RESULTS

2.1 PHYSICAL CHARACTERISTICS OF SUBJECTS

Different foam densities and thicknesses were used to study the interaction between automotive foam cushion materials and human thighs with two knee angles. Seven volunteers were tested for the thigh and seat cushions interactions in seated posture experiments. The standing heights of the subjects ranged from 1651 mm to 1930 mm, the weights ranged from 489 N to 1245 N, and their ages ranged from 18 to 36 years old, and the thigh circumferences ranged from 447 mm to 695 mm. These physical characteristics of these subjects are summarized in Table 2.1. A written consent form was obtained from each subject prior to testing. The consent form used in this project can be found in Appendix 1.

Based on an anthropometric study [10], the subjects were divided into three categories according to the circumference of their mid-thigh, small female (5th percentile), mid-sized male (50 percentile), and large-male (95 percentile). These thigh measurements were taken an in erect seated position. The mid-thigh circumference measurements are summarized in Table 2.2.

An initial study was conducted with one subject; four different foam densities (51, 49, 44, 43 kg/m^3) and three thicknesses (25, 50, 100 mm) were tested with different knee angles of 100° and 130°. The purpose of this initial study was to identify the important

variables for further study. The results for the initial study will be discussed in Chapter Four along with the results of the full scale study on all subjects.

Two different foam stiffnesses (51 and 43 kg/m^3) and two thicknesses (25 and 100 mm) with knee angles of 100° and 130° were the test conditions for the thigh-foam interaction tests for the remaining six subjects. In addition, a test in which the thigh was loaded with a rigid flat plate was done for each subject. The thigh-rigid plate test was conducted to provide load-deformation responses of the subject's thighs for the finite element modeling. Table 2.3 shows the test conditions that were used and the group definition for each subject.

Table 2.1 Subject Physical Data

Subject No.	Gender	Age (Years)	Height (mm)	Weight (N)	Mid-Thigh Circumference (mm)
1	Male	18	1930	778	520
2	Female	23	1702	600	531
3	Male	19	1829	689	510
4	Male	21	1803	600	462
5	Male	36	1778	912	608
6	Male	26	1930	1245	695
7	Female	29	1651	489	447

Table 2.2 Thigh Circumferences for Small Female (5th Percentile) , Mid-Male (50th Percentile), and Large-Male (95th Percentile) [8].

Subjects	Minimum (mm)	Mean (mm)	maximum (mm)
small female	370	427	472
mid-male	442	504	550
large-male	485	559	635

Table 2.3 Subject Test Conditions And Group Definitions.

Subject No.	Group Definition	Knee angle (Degree)		Rigid Plate	Foam						
					Thickness (mm)			Densities (kg/ m^3)			
		100	130		25	50	100	43	44	49	51
1	mid-male	X	X	X	X		X	X			
		X	X		X	X	X		X		
		X	X		X		X			X	
		X	X		X	X	X				X
2	mid-female	X	X	X			X	X			
		X	X				X				X
			X		X			X			
3	mid-male	X	X	X			X	X			
		X	X				X				X
			X		X			X			
4	small male	X	X	X			X	X			
		X	X				X				X
			X		X			X			
5	large male	X	X	X			X	X			
		X	X				X				X
			X		X			X			
6	large male	X	X	X			X	X			
		X	X				X				X
			X		X			X			
7	small female	X	X	X			X	X			
		X	X				X				X
			X		X			X			

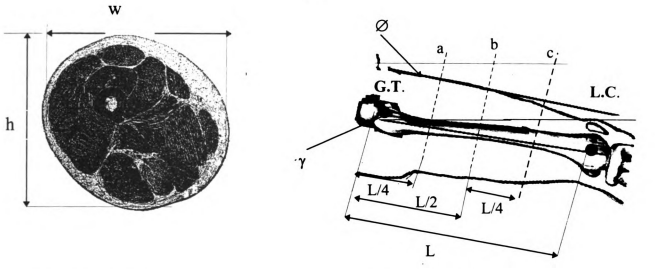

(A) Thigh Cross section (B) Thigh Side View

Figure 2.1 Thigh Measurement [11].

2.2 THIGH MEASUREMENT

Anthropometric measurements for the right thigh were taken with the subjects in a erect seating posture with two knee angles of 100° and 130°. The measurements were used to draw the thigh geometry for finite element modeling. The subject was seated in an adjustable chair designed to support a person in variety of seated postures. The chair was adjusted according to each subject's body size. The backrest was adjusted to allow the subject to be seated in erect posture. The pivots of the moveable footrest were aligned with lateral condyle to keep the femur in the same position when the knee angle changed from 100 to 130 degrees. These (Figure 2.1) measurements include:

1. Hip to knee length (L): the distance between the greater trochanter (G.T.) and lateral Condyle (L.C.) of femur, measured by using a measuring tape and defined as thigh length

(L). Middle thigh section b = L/2, section a= L/4 toward hip, and section c= L/4 toward knee were marked on the right thigh.

2. Thigh circumference: measured by a measuring tape in the plane perpendicular to the long axis of the thigh at sections a, b, and c.
3. Thigh side to side width (w) and thigh anterior to posterior thickness (h): Measured by a digital caliper placed on the plane perpendicular to the axis of the thigh at sections a, b, c.
4. Thigh angle (∅): Measured by placing an angle finder on the top of the thigh in section a.
5. Femur angle (γ): Measured by placing an angle finder on line connected between greater trochander (G.T.) and lateral condyle (L.C.).
6. Knee angle (α): Defined as the angle between two vectors: one from the femur greater trochanter to the lateral condyle of femur, and another from the lateral condyle of femur to the lateral malleolus.

These measurements are summarized in Table (2.4).

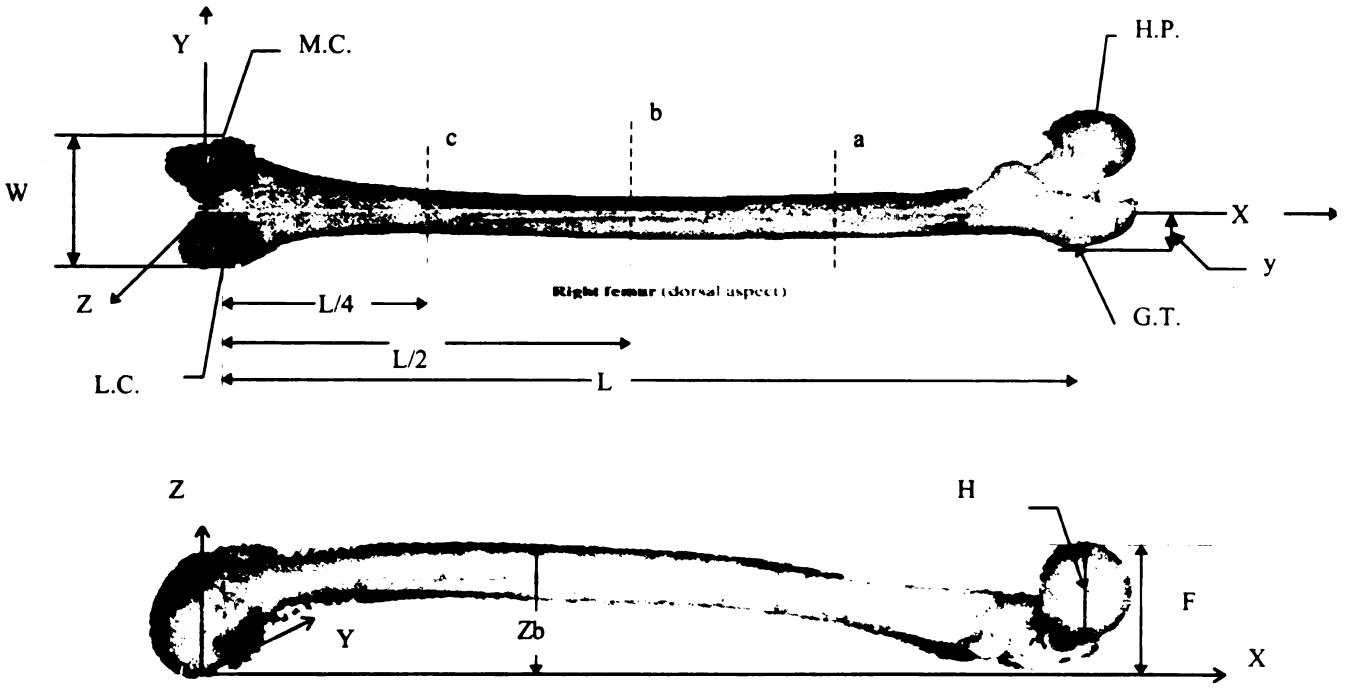

Figure 2.2 The Coordinate System Used to Measure the Femur Dimensions [11].

2.3 FEMUR MEASUREMENT

The femur measurements were needed to estimate the dimensions and the location of the femur relative to the external measurements of the subject's thigh. This internal location was also used to draw and to locate the femur in the finite element model. Six femurs that varied in size were selected from fifty femurs stored in the MSU Gross Anatomy laboratory. Measurements were taken (Figure 2.2) to estimate the femur dimensions of human subject based on the femur length (L) (distance between the greater trochanter to lateral condyle) and the femur width (distance between the lateral condyle and medial condyle) using the following procedure:

1. Femur alignment and securing.

a. A center line (X axis) was drawn on flat board (360 mm X 510 mm). Figure 2.2 shows the coordinate system were used in this measurement.

b. The intercondylar groove was aligned at the origin (0,0,0) the center line (X axis).

c. Proximal shaft was placed at section on the center line (X axis).

Tape was applied to secure the femur to the board

2. The greater trochanter (G.T.), medial condyle (M.C.), and the lateral condyle (L.C.) coordinate points were measured with respect to the origin (0,0,0) point. These measurements are summarized in Table 2.5
3. Middle femur sections b = L/2 (L = length between L.C. and GT. = $X_{G.T.} - X_{L.T.}$), section a = L/4 toward hip, and section c = L/4 toward knee were marked to measure the length of the sections a (L_a), b (L_b), and c (L_c) (Figure 2.2). These measurements summarized in Table 2.6. The X coordinates for section a, b, and c were measured form the marks of sections a, b, and c to the origin point (0,0,0). The Y coordinates for section a, b, and c were measured from the medial of the femur to the center line (X axis). The Z coordinates were measured from the top point of the femur to board. These measurements are summarized in Table 2.7.
4. The diameters of sections a, b, and c were measured in Z and Y directions because the cross section of the femur shaft is not symmetric in the Z and Y directions. These diameters were measured by a digital caliper. These measurement were summarized in Table 2.8.
5. The X, Y, and Z coordinates for the hip point (H.P.) were measured by the following procedure:

a. First, four points were marked around femur head. These points were projected on the board

b. By using a circle template, a circle was selected to best fits four points.

c. The center of the circle was located and defined as hip point (H.P.).

6. The $X_{H.P.}$ and $Y_{H.P.}$ coordinates were measured from the center of this circle to the origin point (0,0,0). The distance from the board to the top of femur head was measured and defined as dimension F. The diameter in Z direction of the femur head was measured and defined as dimension H. The Z coordinate of the hip joint $Z_{H.P.}$ was calculated from F and Z dimensions by the following equation

$$Z_{H.P.} = F - H/2.$$

These measurements are summarized in Table 2.9.

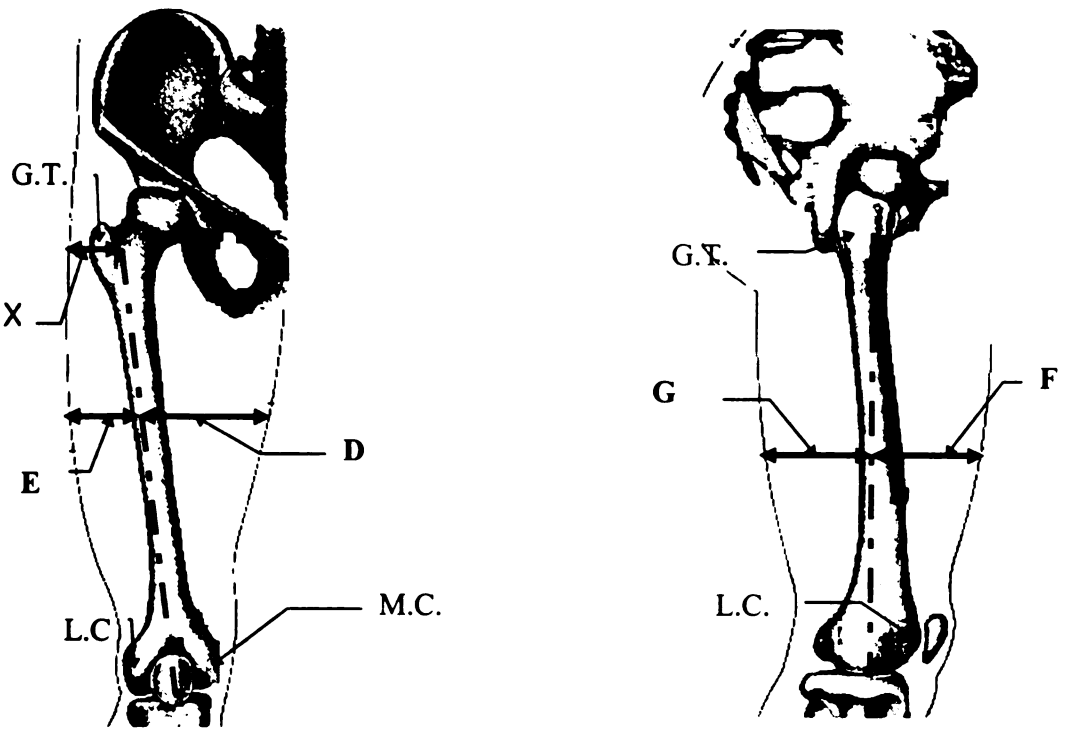

Thigh Top View

Thigh Side View

Figure 2.3 Top View and Side View for the Right Thigh [11].

2.4 ESTIMATE FEMUR LOCATION IN THE SUBJECT THIGH

The femur location in the subject's thigh was estimated by calculating the approximate femur center line in the top and side views for subject's thigh. To find the femur location, three bony landmarks located on the subject thigh by palpating; lateral condyle, medial condyle, and greater trochanter (Figure 2.3).

On the top view of the thigh, two points were marked on the thigh of each subject to estimate the proximal femur center line. The first point was located by estimating the distance from the greater trochanter landmark to femur center (X), calculated by the following equations:

$$X = \frac{a}{2} + y$$

a: the skin thickness at greater trochanter landmark, measured by pinching the skin (Figure 2.3).

y: the distance from the greater trochanter to femur center, calculated by the simple linear regression model (equation No. 1, see section 2.7).

The second point was located by estimating the mid point of the distance between lateral condyle and medial condyle landmarks.

To estimate the femur center line in the side view, two landmarks, greater trochanter and the lateral condyle landmarks were found by palpating on each subject's thigh. The femur center line was drawn on top and side view of each subject's thigh. A digital caliper placed on the plane perpendicular to the long axis of the thigh at sections a, b, and c (Figure 2.3) was used to take the following measurements for each subject with two knee angles 100 and 130 (Figure 2.3):

1. D the distance between the thigh medial side and femur center line on thigh top view.
2. E the distance between the thigh lateral side and femur center line on thigh top view.
3. F the distance between the thigh superior side and femur center line on thigh side view.
4. G the distance between the thigh inferior side and femur center line on thigh side view.

Table 2.10 shows the these measurement for each subject. The femur centers at the thigh front view of sections a, b, and c were located by superposition the top and side views of the thigh dimensions at sections a, b, and c (E, D, G, and F Dimensions).

2.5 THIGH AND FOAM CONTACT SURFACE LOCATIONS

Both the subject's thigh and the contact surface of the foam were located in the seat fixture space. The thigh was located by the X, Y, Z coordinates of two landmarks(the lateral condyle and the greater trochanter of the femur). The contact surface of the foam was located by the X, Y, Z coordinates of the contact surface corners. The lateral condyle of the femur landmark was chosen as the origin point 0,0,0 (Figure 2.4). These coordinates were measured by a ruler. The results can be found in Table 2.11

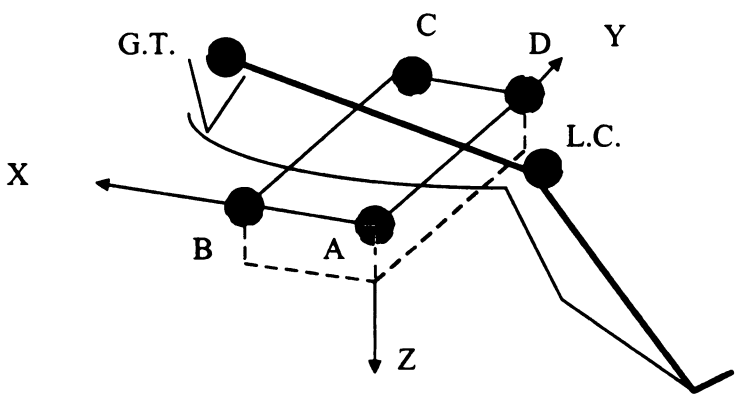

Figure 2.4 Coordinate System of the Thigh and the Contact Surface.

2.6 ANTHROPOMETRIC RESULTS

Table 2.4 shows the thigh measurements for each subject with two knee angles 100 and 130 degree.

Table 2.4 Subject Thigh Measurements

Subject No./ Knee angle α	Thigh Circumference (mm)	Thigh Side to side Width (W) (mm)	Thigh Anterior to Posterior Thickness (h) (mm)	Thigh Angle(ϕ) (degree)	Femur Angle (γ) (degree)	Hip to Knee (L) (mm)	Group Definition
1/100°	a=545 b=520 c=430	a=163 b=149 c=127	a=184 b=177 c=142	14	16	490	Mid-Male.
1/130°	a=555 b=522 c=425	a=170 b=152 c=125	a=177 b=174 c=149	12	15	490	Mid-Male
2/100°	a=545 b=510 c=415	a=165 b=145 c=120	a=173 b=170 c=137	11	13	430	Mid- Female
2/130°	a=562 b=515 c=420	a=168 b=148 c=122	a=167 b=163 c=130	14	15	430	Mid- Female
3/100°	a=530 b=495 c=395	a=155 b=145 c=110	a=168 b=156 c=126	8	10	470	Mid-Male

Table 2.4 Continued, Subject Thigh Measurements

Subject No./ Knee angle α	Thigh Circumference (mm)	Thigh Side to side Width (W) (mm)	Thigh Anterior to Posterior Thickness (h) (mm)	Thigh Angle(ϕ) (degree)	Femur Angle (γ) (degree)	Hip to Knee (L) (mm)	Group Definition
3/130°	a=530 b=498 c=385	a=160 b=150 c=112	a=159 b=153 c=120	9	11	470	Mid-Male
4/100°	a=489 b=468 c=375	a=146 b=138 c=112	a=151 b=153 c=124	10	13	449	Small-Male
4/130°	a=488 b=475 c=382	a=148 b=140 c=109	a=147 b=149 c=124	9	13	449	Small-Male
5/100°	a=625 b=608 c=525	a=180 b=162 c=142	a=206 b=210 c=172	10	15	465	Large-Male
5/130°	a=627 b=614 c=530	a=180 b=170 c=144	a=210 b=200 c=172	12	14	465	Large-Male
6/100°	a=762 b=695 c=580	a=193 b=195 c=157	a=248 b=230 c=197	16	17	522	Large-Male

Table 2.4 Continued, Subject Thigh Measurements

Subject No./ Knee angle α	Thigh Circumference (mm)	Thigh Side to Side Width (W) (mm)	Thigh Anterior to Posterior Thickness (h) (mm)	Thigh Angle(ϕ) (degree)	Femur Angle (γ) (degree)	Hip to Knee (L) (mm)	Group Definition
6/130°	a=761 b=688 c=580	a=197 b=200 c=159	a=250 b=220 c=187	18	18	522	Large-Male
7/ 100°	a=485 b=447 c=385	a=164 b=131 c=110	a=134 b=146 c=120	12	12	420	Small-Female
7/130°	a=492 b=455 c=390	a=166 b=146 c=112	a=133 b=135 c=120	11	12	420	Small-Female

The following tables summarized the femur measurements:

Table 2.5 Greater Trochanter (G.T.), Medial Condyle (M.C.), and Lateral Condyle (L.C.) Coordinate Points

Femur No. 1	X(mm)	Y(mm)	Z(mm)
L.C.	20	34	19.05
M.C.	20	34.5	25.08
GT.	400	25	22.61
Femur No. 2			
L.C.	17	39	23.4
M.C.	13	41.6	25.4
G.T.	382	21	18.7
Femur No. 3			
L.C.	19	32.6	24.3
M.C.	19	41	23.5
GT.	282	16	17.67
Femur No. 4			
L.C.	19	32	19
M.C.	19	44	23.6
GT.	370	24	16.9
Femur No. 5			
L.C.	20	33	22
M.C.	20	42	24.8
GT.	396	25	19
Femur No. 7			
L.C.	20	33	25
M.C.	20	43	23
GT.	368	25	20

Table 2.6 Femurs Length L And The Lengths Of The Sections A (L_a), B (L_b), And C (L_c) Measurements

Femur No.	L (mm)	L_b (mm)	L_a& L_c (mm)
Femur 1	380	190	95
Femur 2	363	181.5	90.75
Femur 3	263	131.5	65.75
Femur 4	351	175.5	87.75
Femur 5	375	188	94
Femur 6	348	174	87

Table 2.7 Coordinate Points For Sections A, B, And C

Femur 1	X (mm)	Y (mm)	Z (mm)
a	305	20	45.19
b	210	19.5	57.32
c	115	21	58.84

Table 2.7 Continued, Coordinate Points For Sections A, B, And

Femur 2	X (mm)	Y (mm)	Z (mm)
a	289	14	40
b	200	13	51
c	108	13	56.3
Femur 3			
a	217	13	54.2
b	151	15	65.3
c	85	16	64.8
Femur 4			
a	282	14	44.2
b	195	14	52.5
c	108	16	55
Femur 5			
a	302	14	45.7
b	208	14	56
c	114	19	61.5
Femur 6			
a	281	13	45
b	194	10	57.6
c	107	13	60.4

Table 2.8 Femurs Diameters In Z And Y Directions For Sections A, B, And C

	diameter in Y directions (mm)			diameter in Z directions (mm)		
Femur No.	a	d	c	a	b	c
Femur 1	25.72	23.67	29.39	25.2	28.2	28.08
Femur 2	28	26	28.8	26	26.4	27.2
Femur 3	27	25.6	28	25.2	28	29.6
Femur 4	24.5	23.5	23.9	21.7	20.9	22.5
Femur 5	27.3	26.9	33.2	25	27.7	31.2
Femur 6	25.9	23.5	26	25	26.8	26.7

Table 2.9 X, Y, and Z coordinates for H.P. (Hip joint).

Femur No.	F [mm]	H [mm]	$X_{H.P.}$ [mm]	$Y_{H.P.}$[mm]	$Z_{H.P.}$[mm]
Femur 1	58	44.18	426	39	35.91
Femur 2	52.3	41.5	401	43	31.55
Femur 3	62.7	42.8	315	49	41.3
Femur 4	61.7	41.17	385	34	41.115
Femur 5	67.6	44.6	420	48	45.3
Femur 6	58.1	43.8	391	33	36.2

Table 2.10 Thigh Measurements to Estimate Femur Location in Subject's Thigh

	Knee angle 100,			Knee angle 130		
	A (mm)	B (mm)	C (mm)	A (mm)	B (mm)	C (mm)
Subject No. 1						
D	115	89	81	112	102	77
E	40	50	47	45	52	48
F	50	58	61	48	59	65
G	126	110	73	121	106	80
Subject No. 2						
D	105	89	74	108	88	73
E	46	43	40	47	46	44
F	61	62	57	53	61	57
G	108	105	69	105	86	64
Subject No. 3						
D	107	90	70	113	95	79
E	41	43	37	36	45	30
F	69	70	65	66	67	68
G	98	83	62	83	76	56
Subject No. 4						
D	113	80	61	102	83	53
E	41	44	46	36	43	43
F	45	62	65	46	58	62
G	89	80	48	88	77	46
Subject No. 5						
D	120	108	90	117	113	88
E	50	50	45	51	50	46
F	68	83	90	82	93	98
G	133	121	80	123	99	68
Subject No. 6						
D	128	126	96	131	134	101
E	65	69	61	66	66	58
F	68	66	74	72	70	73
G	180	164	123	178	150	114
Subject No. 7						
D	105	105	70	109	98	78
E	50	38	35	41	41	39
F	30	43	51	35	45	50
G	105	103	67	110	96	69

Table 2.11 the Coordinate Points of the Thigh and the Foam Contact Surface for the Subjects

subject No. 1	X (mm)	Y (mm)	Z (mm)	Subject No. 4	X (mm)	Y (mm)	Z (mm)
L.C.	0	0	0	L.C.	0	0	0
G.T.	510	-10	-140	G.T.	444	-25	-110
A	143	-25	48	A	112	-33	75
B	357	-25	48	B	327	-33	75
C	357	242	48	C	327	237	75
D	243	242	48	D	112	237	75
subject No. 2				subject No. 5			
L.C.	0	0	0	L.C.	0	0	0
G.T.	475	-14	-157	G.T.	460	-21	-83
A	102	-80	90	A	120	-70	75
B	318	-80	90	B	335	-70	75
C	318	190	90	C	335	195	75
D	102	190	90	D	120	195	75
Subject No. 3				Subject No. 6			
L.C.	0	0	0	L.C.	0	0	0
G.T.	460	-15	-120	G.T.	515	-39	-130
A	120	-84	75	A	148	-40	100
B	335	-84	75	B	362	-40	100
C	120	181	75	C	362	230	100
D	355	181	75	D	148	230	100

subject No. 7	X (mm)	Y (mm)	Z (mm)
L.C.	0	0	0
G.T.	418	-12	-80
A	100	-20	75
B	315	-20	75
C	315	245	75
D	100	245	75

2.7 FEMUR MEASUREMENT ANALYSIS

Statistical methods [12] were used to estimate the femur dimensions for each subject. The standard deviation (STDV) was calculated to measure the variability of the measurement (femur dimensions) about their mean. The coefficients of determination R^2 were calculated to measure the degree of linear relationship between the independent variable: the femurs length and the femur width and the dependent variables: femur diameters, the distance from the greater trochanter to femur center, and the X, Y, Z coordinates for sections a, b, c, and H.P., as reflected in the simple linear regression model. The result of these analysis are given in Table 2.12.

As can be seen in Table 2.11, the mean of the femur length for this sample was 347 mm and the standard deviation was 43 mm. The linear regression model between the femurs length and other femur dimensions (except the dimension $Y_{G.T.}$ (the distance from the greater trochanter to femur center), and X coordinate for H.P.) can not be used to estimate the femur dimensions by knowing the femur length for the subject because the coefficients of determination were small, possibly becouse the femurs that were chosen belonged to people of different races or genders [13]. The coefficient of determination R^2 between the femur lengths and the dimension $Y_{G.T.}$ was 0.78, so the simple linear regression model can be used to estimate this variable.

$$y = 0.0741L - 3.0182 \qquad \text{Equation (1)}$$

y: The distance from the greater trochanter to femur center.

L: The femur length

The linear regression model between the femur dimensions and the femur width can not be used to estimate the femur dimensions by knowing the femur width of the subject because the coefficients of determination were small. However, based on statistical analysis [13] of femur measurements of 35 females and 50 male skeletons, the diameters of the mid-shaft femurs were estimated according to subject gender (Table 2.7.1).

Table 2.7.1. The Circumference and Diameters of the Femur [13]

gender	Circumference (mm)	Antero-posterior diameter (mm)	Transverse diameter (mm)
Male	90	29	28
Female	82	27	25

Table 2.12 Femurs Data analysis

	Femur 1 mm	Femur 2 mm	Femur 3 mm	Femur 4 mm	Femur 5 mm	Femur 6 mm	Average mm	STDV mm	R^2 (femur length)	R^2 (LC-M.C.)
Femur length	380	363	263	351	376	348	347	43	1.00	0.50
distance between L.C - M.C	82	75	73	76	77	78	77	3	0.50	1.00
X Section a	305	289	216	282	302	281	279	32	1.00	0.52
Y Section a	20	14	13	14	14	13	15	3	0.24	0.68
Z Section a	45	51	54	44	46	45	48	4	0.55	0.51
X Section b	210	199	151	195	208	194	193	22	1.00	0.54
Y Section b	20	13	15	14	14	10	14	3	0.01	0.21
Z Section b	57	51	65	53	56	58	57	5	0.59	0.04
X Section c	115	108	85	107	114	107	106	11	0.99	0.57
Y Section c	21	13	16	16	19	13	16	3	0.09	0.33
Z Section c	59	56	65	55	62	60	59	4	0.39	0.05
diameter Ya	26	28	27	25	17	26	25	4	0.15	0.02
diameter Za	25	26	26	22	25	25	25	2	0.02	0.00
Average diameter a	25	27	26	23	21	25	25	2	0.15	0.02
diameter Yb	24	26	25	24	27	24	25	1	0.00	0.19
diameter Zb	28	26	28	21	28	27	26	3	0.01	0.04
Average diameter b	26	26	27	22	27	25	26	2	0.01	0.00
diameter Yc	29	29	28	24	33	26	28	3	0.08	0.03
diameter Zc	28	27	30	23	31	27	28	3	0.01	0.00
Average diameter c	29	28	29	23	32	26	28	3	0.01	0.01
Y Greater trochanter to femur center	25	21	16	24	25	25	23	4	0.78	0.59
X Greater trochanter to femur center	400	382	282	370	396	368	366	43	1.00	0.51
ZGreater trochanter to femur center	23	19	18	17	19	20	19	2	0.25	0.78
X H.P.	426	401	315	385	420	391	390	40	0.98	0.58
Y H.P.	39	43	49	34	48	33	41	7	0.13	0.20
Z H.P.	36	31	41	41	45	36	38	5	0.04	0.03

CHAPTER 3

LOAD-DEFORMATION MEASUREMENT METHODS

To measure the load-deformation characteristics of the posterior sides of human thighs, an experimental chair was used to support a person in a variety of seated postures. This chair was first contracted and used by Deng [9] to measure the load-deformation responses of people's thighs by loading their thigh's with a flat rigid plate. The movement of this chair allowed changes in knee angle to affect the length and tension in the hamstring muscles in the back of the thigh. This chair provided a backrest, a pelvis support, and a movable footrest to change knee angle from 90 to 180 degrees (Figure 3.1). The knee angle was defined as the angle between two vectors: one from the greater trochanter to the lateral condyle of femur, and another from the lateral condyle of the femur to the lateral malleolus of the ankle. The knee angle was 180° when the leg was completely extended. The backrest had a pivot that allowed rotation about the lateral axes to comfortably accommodate the subjects. The chair dimensions were adjustable to correspond to each individual's body size. The backrest was adjustable both vertically and horizontally and supported the subject's torso in the rib cage.

A plate supported the back of the pelvis, and two plates supported the right and left buttocks. A load cell was put under each plate to measure the force under the buttocks [7]. The load cell specifications were given in Appendix C.

A hydraulic jack with a 254 mm stroke was positioned under the right thigh. The contour measurement system (described in the next section) was placed on the jack. A load cell was installed between the contour measurement system and the jack. The load

cell measured the reaction force in the vertical direction under the thigh. A digital caliper was attached between on the jack and the contour measurement system and was used to measure the vertical displacement of the system. The digital caliper specifications were given in Appendix C. Figure 3.1 shows the experimental method set up.

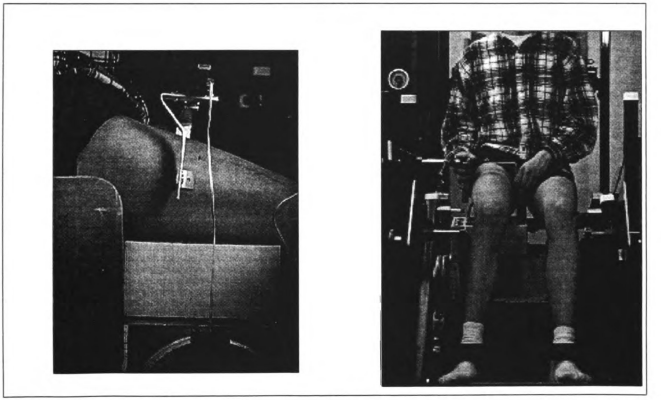

Figure 3.1 Experiment Method Set up

3.1 THE CONTOUR MEASUREMENT SYSTEM.

The contour measurement system (Figure 3.2) consisted of an aluminum box 213 mm × 533 mm × 165 mm, 2.56 mm diameter plastic tubes, 1.5 mm diameter steel wires, a clear plastic plate to align the wires, and an alignment plate to align the tubes . Twenty four holes were drilled on the top face of the box. The ends of plastic tubes passed inside the box and were fixed in these holes. The other ends were fixed into the alignment plate of the tubes. The alignment plate for the wires was clear plastic plate with 24 semicircular slits was attached to the alignment plate of the tubes. A video camera was aligned perpendicular to the bottom face of the box so it was facing the clear plastic plate. Florescent lights were behind the clear plastic plate so the image of the wires could be captured with the video camera (Figure 3.3). A foam block with 24 holes and adjustable spacer were on the top of the box. The holes were drilled through the foam face in a matrix of four rows by six columns as shown in Figure 3.4. The hole numbers represent the row and column (e.g. node 3,4 represent row 3 and column 4). Steel wires with a flat button on one of their ends, were passed through the foam holes, tubes, alignment plate, and into the slits of the clear plastic plate. When the foam deformed, the wires were displaced with foam deformation. The video camera captured an image for each wire displacement. These displacement images were digitized using a computer connected to the camera.

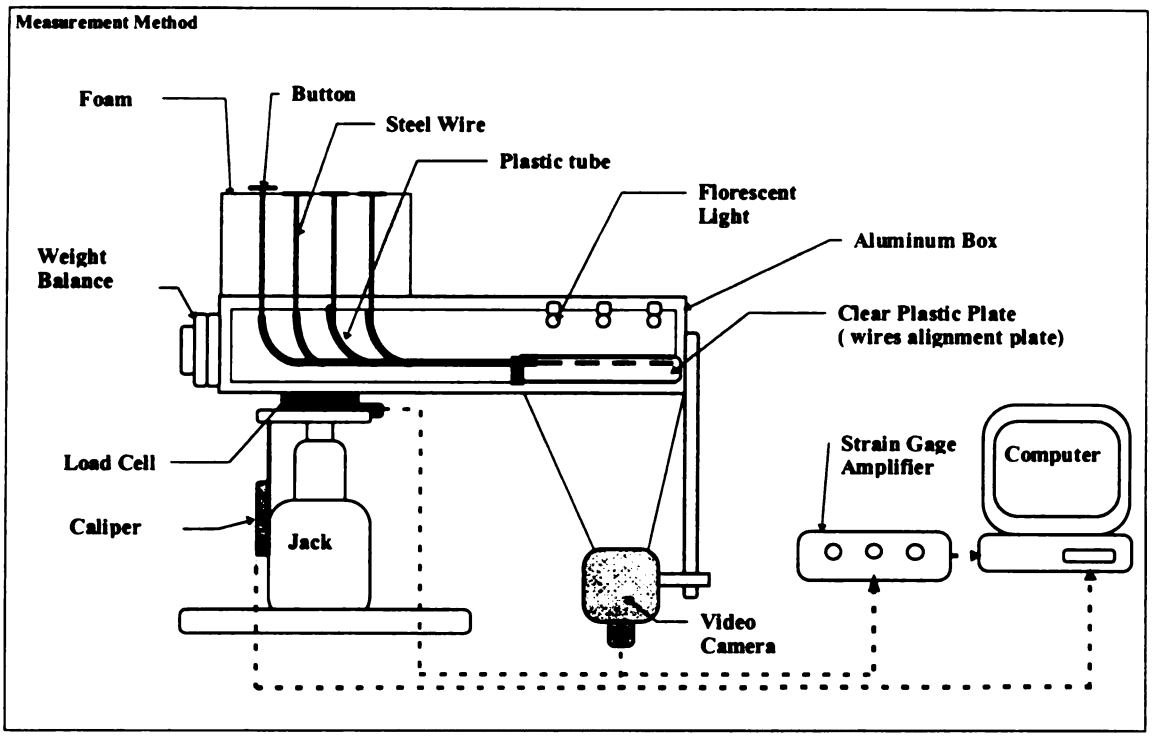

Figure 3.2 Contour Measurement System

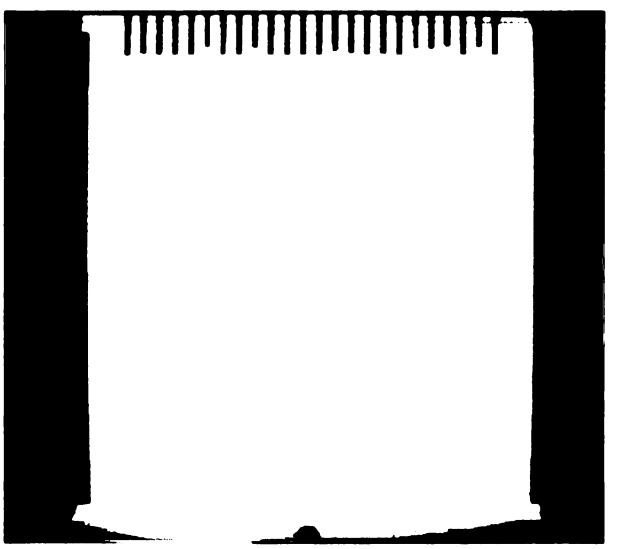

Figure 3.3 A Wire Images Captured by the Video Camera

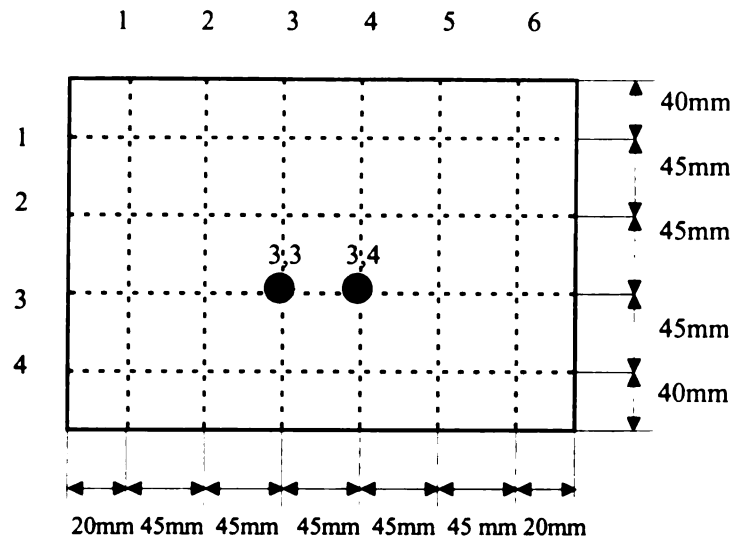

Figure 3.4 Grid System Used on the Foam Face.

3.2 TESTING STIFFNESS OF THE FOAMS WITH AND WITHOUT WIRES

To check how much the friction force between the wires and the system affected the foam stiffness, force-compression tests were done on the foam with and with out the wires.

3.2.1. Compression Test of Foam With Wires

The foam was placed on the top of the contour measurement system with wires passing through the foam, plastic tubes, and the alignment plates. A flat rigid plate (300 mm X 360 mm) was fixed on the seating fixture and horizontal to the foam testing surface (265 mm X 215 mm). The testing surface was raised to contact the rigid plate. Contact of the loading plate was chosen to be a small initial value of 0.22 N. The digital caliper attached to contour measurement system recorded the vertical deformation of the foam. The testing surface was raised in a stepwise manner typically 5 mm. The reaction forces and the

deformations were recorded after 20 seconds to allow stress relaxation of the foam, which approached a quasi-static test condition.

3.2.2. Compression Test of Foam Without Wires

The wires were taken out of the foam. The test procedure used for the foam with wires were repeated. These tests were conducted on 43 kg/m^3 and 51 kg/m^3 foam densities and 100 mm. foam thickness. The data were processed and plotted using Microsoft Excel. Figure 3.5 show the effect of the friction force on load-deformation responses of the foam samples.

3.3 THIGH LOAD-DEFORMATION TESTS

3.3.1 Thigh-Foam Interaction Test

The chair was adjusted according to the subject's body size. The subject sat in the seating fixture with the feet placed firmly on the footrest plate, the head and body were in a relaxed posture with hands dropped to the sides of the chair. All subjects wore shorts during testing, so that clothing was not a variable. The foam was raised against the back of the thigh and displaced in a quasi-static manner. Contact was identified when the measurement force exceeded 0.22 N. As the foam block was pushed into the back of the thigh, the digital caliper, that was attached to contour measurement system, recorded the total vertical deformation of the thigh and the foam. The foam surface (265 mm x 215 mm) was raised into the thigh in displacement steps of approximately 5 mm. Each displacement step was held for 20 to 30 seconds before the resulting force was recorded. A rest time of 20 to 30 seconds was chosen in order to allow for short-term stress relaxation of the thigh and foam; after this time, the forces were stable.

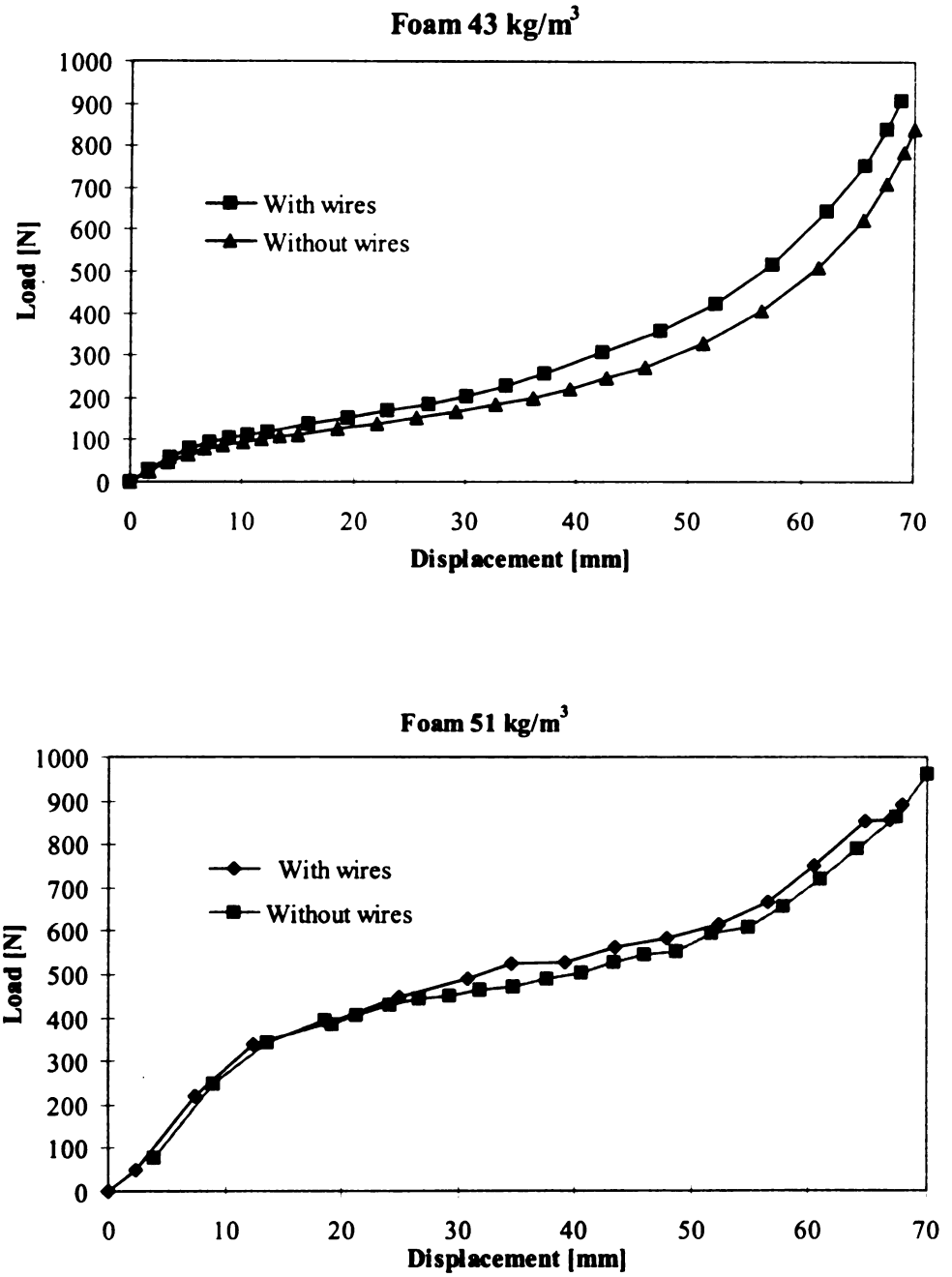

Figure 3.5 The Effect Friction Force of the Wires on the Foam Stiffness

The contour measurement system was displaced until the elevated foam block lifted the subject's leg and the foot from the footrest plate. The lateral deformation of the thigh was recorded by placing a digital caliper across the middle section of the thigh and adjusted by the subject. As the forces were being recorded, the foam deformation was recorded by a video camera that captured the wire displacement images for each increment of movement. This image was digitized by the computer.

The thigh deformation on the contact area with the foam was calculated by subtracting the foam deformation from the total deformation. Both the subject's thigh and the contact surface of the foam were located in the seat fixture space (see Chapter 2.5 for more details).

3.3.2 Thigh-Flat, Rigid Plate Test

Tests in which the thigh was loaded and deformed with a flat, rigid plate test were needed to measure the thigh stiffness for the finite element model. The foam specimen on top of the contour measurement system was replaced by a rigid flat plate (138 mm X 252 mm). The rigid flat pate could rotate on the lateral axis to align with the thigh posterior. With knee angles at 100° and 130° and leg muscles relaxed, the testing surface was raised to contact the back of the thigh. The system was defined to have contacted the thigh when the measurement force exceeded 0.22 N. The digital caliper attached to contour measurement system recorded the vertical deformation of the thigh. The thigh lateral deformation was recorded by placing a digital caliper on middle section of the thigh and adjusted for each reaction force by the subject. The testing surface was raised in stepwise manner of 5 mm for each step. The reaction force and the deformations were recorded

after 20 to 30 seconds wait for short-term stress relaxation to approach a quasi-static test condition.

3.4 UNIAXIAL COMPRESSION TEST OF FOAM SAMPLES.

In seating design most foam properties are based upon static test methods [3]. Compression tests for the foam were conducted to provide foam mechanical properties for finite element model. The American Society for Testing and Materials [14] (ASTM D3674-C) testing method was used to measure the force necessary to produce a 60% compressive strain by loading over the entire area of the foams specimen. These tests were obtained by using an Instron machine.

3.4.1 Test Specimens

The foam test specimens had parallel top and bottom surfaces and vertical sides. Their thicknesses were 25.4 mm, 50.8 mm, and 101.6 mm. The other dimension were 382 mm by 382 mm. These samples had different densities 41 kg/m^3, 44 kg/m^3, 49 kg/m^3 and 51 kg/m^3 that were determined from measuring their separate weights and volumes.

3.4.2 Procedure

1. Using a compression platen (flat plate 508 by 508 mm. with 6 mm holes on 20 mm centers to allow for rapid escape of air during the test), each specimen was precompressed twice to 60% of its original thickness at 4 mm/s.
2. Then the specimen rested for a period of 6 min.
3. An initial load of 5 N was applied to the specimen area.
4. After the application of the initial load, the specimen was compressed 60% of the foam thickness at 0.83 mm/s. The final position was held for 60 seconds.

Figure 3.6 shows the stress-strain curve obtained for all foam samples by using the ASTM D3674-C testing method. Table 3.1 lists the different foam stiffnesses, thicknesses and suppliers of foam samples were used in this study.

Table 3.1 Densities, Thicknesses and Suppliers of foams test samples.

Density (kg/m^3)	Thickness (mm)	Supplier (Company Name)
43	25.4	Atoma
43	101.6	Atoma
44	101.6	Johnson Controls, Inc.
44	50.8	Johnson Controls, Inc.
44	25.4	Johnson Controls, Inc.
49	101.6	Johnson Controls, Inc.
49	50.8	Johnson Controls, Inc.
49	25.4	Johnson Controls, Inc.
51	101.6	Johnson Controls, Inc.
51	50.8	Johnson Controls, Inc.
51	25.4	Johnson Controls, Inc.

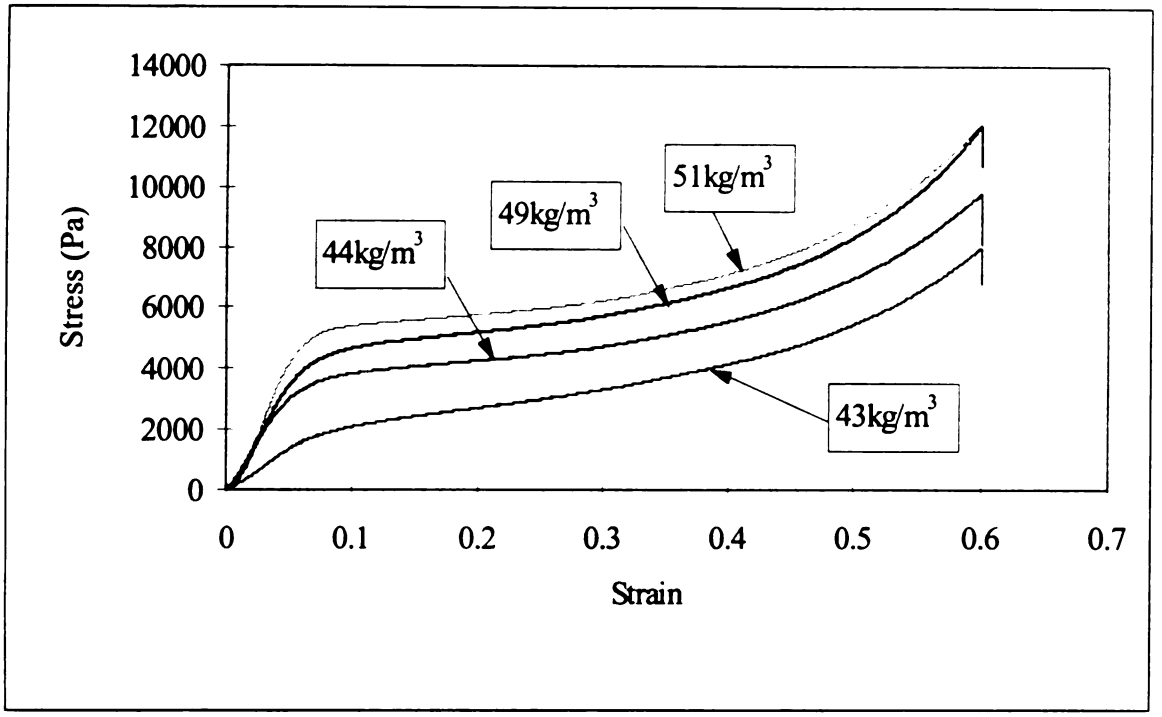

Figure 3.6. Stress-Strain Curve for 43 kg/m^3, 44 kg/m^3, 49 kg/m^3, and 51 kg/m^3 foams.

CHAPTER 4

THIGH AND FOAM DEFORMATIONS RESULTS AND DISCUSSION

The load and deformation responses of any material or structure depends on many factors including the magnitude and direction of the applied load, the material that constitutes the body, and the size and shape of the body. In discussing the thigh and the foam interaction, it is important to distinguish between the structural and mechanical properties. Structural properties reflect the mechanical behavior of the body as a whole, including both material and geometric contributions of the load-deformation response (i.e., thigh). The mechanical properties describe the intrinsic characteristics of the material itself, and depend on its composition, molecular structure, and ultrastructure (i.e., foam, bone tissue, or skeletal muscle tissue) [15].

Two trials of loading and unloading the thigh and the foam with a rigid plate were conducted to check the test repeatability. Figure 4.1 shows the difference between the load-deformation both of loading and unloading the foam 43 kg/m^3 with rigid plate for two trials were small. Figure 4.2 shows the difference between the load-deformation both of loading and unloading the thigh with rigid plate for two test trials was small. The hysteresis curves (Figures 4.1, 4.2) were one of the evidence of the viscolastic behavior of the soft tissue and foam material [7]. The thigh-foam interaction test was repeated twice on the same subject under the same test conditions (foam stiffness, thickness, and knee angle) (Figure 4.3). The graphs of these tests (Figures 4.1,4.2, 4.3) show that the differences between the results of the two trials were small, therefore the tests were considered repeatable without having to be "preconditioned" [7,8].

4.1 FOAM MECHANICAL PROPERTIES

The load-deformation responses of the foam were measured using two methods of uniaxial compression tests. The tests were conducted by ASTM D3674-C [14] testing method with an Instron machine (refer to Chapter 3 for more details). This test provided foam mechanical properties for the finite element modeling. Tests were conducted by quasi-static method with contour measurement system to evaluate the effect on the foam mechanical properties of the friction between the wires and contour measurement system.

A typical stress-strain nonlinear relationships for cellular materials (Figure 4.4) were obtained from the load-deformation relationship for the uniaxial compression foam tests [16, 17, 18]. Also, the foams exhibited compressible behavior and zero Poisson (ν) effect in compression (the lateral deformation was very small compared to the large vertical deformation, ν = -lateral strain/axial strain)[16].

The stress-strain relationship (Figure 4.4) exhibited three different phases [19]. At low strains, the foam showed a linear response followed by continuing deformation at almost constant stress. Finally the stress increased rapidly. These three phases can be explained in terms of the individual cells that made up the bulk foam material. When the foam was loaded in compression, the first type of deformation which occurred is due to bending of the cell walls (beams). This initial phase was limited to small strains (typically 5% in compression for a static test) [19]. The phase two was initiated when the critical buckling stress for individual beams was reached. Once the beams begin to buckle, deformation increased at almost constant load accompanied by an increase in the strain

energy of the deformed structure. As the cell walls continue buckling, they crush together causing a sharp increase in stress with small change in strain [16].

A best-fit lines were developed to obtain first modulus for phase one and the second modulus of phase two (Figures 4.5, E.1 to E.6) of quasi-static and ASTM tests for 43 kg/m^3 and 51 kg/m^3 foam densities (Throughout the remainder of Chapter 4, results will be shown with a typical Figure, like Figure 4.5, that was representative of the results from all similar conditions, like Figure E.1 to E.6 in Appendix E). These modulii were calculated to find the effect of the stress relaxation between the ASTM and quasi-static tests due to different strain rates. The strain rate of ASTM tests was 0.83 mm/s, however the quasi-static tests were performed in stepwise manner with 20 seconds wait between each step for stress relaxation. Also, the first and second modulii were calculated to find the effect of friction force between the wires and the contour measurement system on the foam material properties. Phases one and two were considered for this analysis because the foam samples were loaded in these regions in thigh-foam interaction tests, discussed later in this chapter.

The first and second modulus of quasi-static tests of the foam with and without wires were considered to find the friction force effect on the foam material properties. These tests were considered because they have the same strain rate. Therefore, the stress relaxation effects were eliminated as a variable between these tests. The results (Table 4.1) showed that the friction forces increased the value of the first and second modulus by 9% and 18%, respectively, for 51 kg/m^3 foam density, and by 17% and 16%, respectively, for 43 kg/m^3 foam density.

The first and the second modulus of quasi-static test and the ASTM test were considered to find the stress relaxation effect on the foam material properties. The results (Table 4.1) showed that the relaxation stress effect decreased the first and second modulus for by 50% and 21% , respectively, for 51 kg/m^3 foam density, and by 17% and 16%, respectively, for 43 kg/m^3 foam density.

Table 4.1 First and Second Modulus of 43 kg/m^3 and 52 kg/m^3 Foam Densities For ASTM and Quasi-Static Tests

Foam Density 51 kg/m^3	Phase I modulus (Pa)	Phase II modulus (Pa)	Foam Density 43 kg/m^3	Phase I modulus (Pa)	Phase II modulus (Pa)
ASTM test	91832	12512	ASTM test	27007	8995
With wire	50405	12149	With wire test	26897	8983
Without wire test	45779	9916	Without wire test	22385	7573
Friction effect %	9	18	Friction effect %	17	16
Relaxation Stress effect %	-50	-21	Relaxation Stress effect %	-17	-16

4. 2 THIGH STRUCTURAL PROPERTIES

The load-deformation response of the thighs of seven subjects with two knees angles 100° and 130°, were measured using a thigh-rigid plate test to provided structure properties for finite element modeling (Figures 4.6, E.7 to E. 13). Both the material (a composite of veins, skin, fat, and muscles) and geometry (thigh shape and femur location with respect to soft tissue) of the thigh contributed to the load-deformation response. The load-deformation (vertical deformation) relationship exhibited low stiffness in the beginning with large deformation at small initial load. This response became stiffer as the thigh deformation and contact area of the thigh increased. This is a typical nonlinear load-

deformation relationship for a bulk soft tissue under compression with increasing in contact area [8, 9, 20].

This behavior of the thigh tissue under compression load can be represented by splitting the load-deformation curve into two parts (Figures 4.7, E.14 to E.20), the first part started from zero load to a load of approximately 30 N, the second part started at 30 N to the load of approximately 120 N. The load readings were different between the tests, so the closest values for the 30 N and 120 N were selected for these calculations. The second part of the curve represented the working region of the thigh stiffness when the thigh typically interacts with a seat in seated posture. This working region of 30 N to 120 N ranged from 7% of body weight of small female (the 5th percentiles of population weight distribution) to 12% of body weight of large male (the 95th percentiles of population weight distribution). The working region was based on the contact pressure of the thigh-seat interaction from the results of pressure mat for various people in the seated postures [21]. Some automotive seat manufactures recommend that the pressure distributed under the thigh in a typical automotive seat should range from 9% to 11% of body weight, which was contained in the second part of the curve. Best-fit lines were developed for each part and these lines were highly correlated to the data (R^2 values of 0.93 to 0.99). The slopes of fitting lines were calculated from their equations to estimate the thigh stiffnesses for each subject with different knee angles and to find the variance and the average of the thigh stiffnesses for the seven subjects. Table 4.2 shows the slopes for the first and the second parts of each subject with two different knee angles. The average slope (Table 4.2) for the seven subjects of the best-fit lines in the first part was 0.92 N/mm

for the 100° knee angle and 1.30 N/mm for the 130° knee angle. The average slopes of second part increased to 2.58 N/mm for the 100° knee angle and 2.96 N/mm for the 130° knee angle. The thigh stiffness increased from the first part to the second part by 65 % for knee angle 100° and 55 % for knee angle 130°, due to the increasing in the thigh-rigid plate contact area and to the effect of thigh soft tissue properties.

The graphs in Figures 4.6, E.7 to E. 13 and the slope of the fitting lines for first and second parts (Figures 4.7, E.14 to E.20) showed that human thighs become stiffer as the knee angle was straightened. The average thigh stiffness of seven subjects (Table 4.2) (except the second part for subject number seven due to negative value which could be due to the subject movement) increased by 14% for the first part and 11% for the second part as the knee angle increased from 100° to 130°. These results indicated that the tension of the hamstring muscles increased as the knee angle increased.

The variances and the average of the thigh stiffness for seven subjects with two knee angles were calculated from the slope of the second part in deformation-load relationship (Figure 4.8). The variances in the thigh stiffness due to the subject's characteristic (subject thigh circumference, height, sex, age) were 0.12 $(N/mm)^2$ for knee angle 100° and 0.59 $(N/mm)^2$ for knee angle 130° with average thigh stiffnesses 2.60 N/mm and 2.96 N/mm, respectively (Table 4.2). The correlation between the thigh stiffness and circumference was 0.22 (Figure 4.9) for knee angle 130° and 0.024 for knee angle 100°. These results indicated that the thigh stiffness varies from person to person and did not depend on the their size. Also, these results indicted that, when the knee angle was 100° variation in the thigh stiffnesses was small (5%) between the subjects and did not depended on the thigh

size. But when the knee increased to 130° (the tension of the hamstring muscles increased) the variation in the thigh stiffnesses increased (from 5% to 20%) and the size dependence increased from 0.024 to 0.22. Figure 2.10 shows the distributions of the thigh stiffnesses from their mean for knee angle 100° and 130°.

The average of the thigh stiffness for this study was compared with a previous study by Deng [9]. Figure 4.11 shows the data sets and the averages for both studies. Also, the average slopes of the thigh working region (second part for the load-deformation relationship) for both studies (Figure 4.12) were calculated to determine the variance from their mean. The average slopes were 2.6 N/mm for this study (sample number one) and 2.3 N/mm for previous study (sample number two). The variance between these studies was 0.045 $(N/mm)^2$. This result indicated the variance of the averages stiffness was small (1.8%) and the average of this study was stiffer by 12% for the previous study. This difference between the thigh stiffnesses of these studies could be due to differences in sample size and the knee angle.

To demonstrate the change of the thigh geometry during the tests, the lateral versus the vertical deformations of the thigh was plotted for each subject (Figure 4.13). The lateral-vertical deformation relationship (Figure 4.13) was nonlinear and exhibited a larger lateral deformation with larger vertical deformation. The muscle layers slide over one another and flow away from the area of immediate pressure, producing the lateral deformation.

Table 4. 2 Slope of the Fitting Lines for the First and the Second Part

	Knee angle 100°			Knee angle 130°			The Effect of the Change in knee Angle on thigh Stiffness (Percent)	
Subject No.	Slope Part I N/mm	Slope Part II N/mm	The Differ. in Thigh Stiffness between Part I & II (Percent)	Slope Part I N/mm	Slope Part II N/mm	The Differ. in Thigh Stiffness between Part I & II (Percent)	Part I	Part II
1	0.91	2.94	69	1.32	3.03	56	13.95	2.97
2	0.60	2.02	70	1.03	2.14	52	21.29	5.61
3	1.14	2.92	66	1.90	3.05	52	22.55	14.68
4	0.86	2.73	68	1.47	2.84	48	22.34	3.87
5	0.89	2.27	61	1.09	2.56	57	8.81	11.33
6	1.21	2.83	57	1.24	4.02	69	1.06	29.60
7	0.81	2.53	71	1.04	2.19	53	8.19	-15.51*
Average	0.92	2.60	65	1.30	2.96	56	14.03	11.34
Standard Deviation	0.20	0.35	5	0.31	0.77	7	8.41	10.03
Variance $(N/mm)^2$	0.04	0.12		0.10	0.59			

* The negative value indicated that there were errors in the data. This could be due to the subject movement, so this value was not considered in the average and standard deviation calculation for the slope for the second part.

4.3 THIGH-FOAM INTERACTIONS RESPONSE

The load and deformation responses of the thigh-foam interactions depend on many factors including, materials properties, geometric properties, and the magnitude and direction of the interaction forces. There are two components of interaction forces: (1) normal forces that are perpendicular to the thigh-foam interfaces, (2) shear forces that are tangent to the thigh-foam interface. These shear forces result from the relative motion between the thigh and foam. The magnitudes and distributions of the normal and shear on the thigh-foam interaction surface determine the magnitudes and direction of the resultant

force components acting on the interaction surface and determine the deformation of the soft tissue and foam.

In the thigh-foam interaction, the thigh-foam contact surface deforms relative to the foam support structure and the subject's thigh soft tissues deform relative to the femur. An assumption that the femur did not move during the test was made to calculate the thigh deformation from the total foam deformations. Figure 4.14 shows the determination of total, thigh, and foam deformation boundaries.

The total deformation of the thigh and foam (δ_{Total}) in the vertical direction was measured by the displacement of the contour measurement system. The foam deformation (δ_{Foam}) in vertical direction was calculated by digitizing the wire displacement images using a computer software program [23]. The rigid flat plate test of the foam with wires was used to obtain the calibration slope (D_{cal}) by plotting the reading of the digital caliper (Figure 3.2) (in millimeter units) with corresponding digitized wires displacement (in Pixel units) for each displacement step (Figure 4.15). The foam deformation was calculated as follow:

$$\delta_{Foam}(mm) = [\, d^{*}(Pixel) - d(Pixel)] \times D_{cal}\,(mm/Pixel) \qquad \text{Equation (2)}$$

d^{*} : The position of the wires before the foam deformation.

d : The position of the wires after the deformation.

The vertical deformation of the thigh at the contact area with the foam was calculated by subtracting the foam deformation from the total deformation δ_{Total}

$$\delta_{Total} = \delta_{Foam} + \delta_{Thigh} \Rightarrow \delta_{Thigh} = \delta_{Total} - \delta_{Foam} \qquad \text{Equation (3)}$$

Figure 4.16 shows the total, thigh, and the foam deformations for a typical test.

Two locations of foam deformation (3,3 and 3,4 nodes) were considered for the above calculation (Figure 3.4). These nodes were chosen because they were the first contact nodes between the thigh and the foam, and they were located at mid-thigh section. The deformation of the mid-thigh was selected because this region deformed more compared with other regions of the thigh.

The load-deformation responses of the thigh-foam interactions in seated postures were studied to determine the structural behavior of thigh's tissue with different thicknesses and densities of foam seat cushions. The experimental data collected also provided quantitative information for a finite element model.

A test series was conducted to estimate the variation in thigh deformation using different variables including seven subjects, the thigh-foam contact nodes, three foam thicknesses, four foam densities, and two knee angles. The initial number of possible variables were 336 (Table 4.3).

Table 4.3 Initial Variables of the Thigh Stiffnesses

Subject Numbers	Thigh-Foam Contact Points	Foam Thicknesses (mm)	Foam Densities (Kg/m^3)	Knee angles (degree)
7	3,3 and 3,4 Nodes	25, 50, and 100	43, 44, 49, and 51	100° and 130°

An initial study was conducted with subject number one to find the variation in mid-thigh deformation with different foam thicknesses and densities. Four different foam densities (51, 49, 44, 43 Kg/M^3) and three foam thicknesses (25, 50, 100 mm) were tested with thigh of subject number one and with two different knee angles (100°, 130°).

4.3.1 THIGH INTERACTION WITH DIFFERENT FOAM THICKNESSES.

The thigh deformations versus load for subject number one were plotted individually for each foam density and each knee angle for all foam thicknesses (Figures 4.17, E.21 to E.27). The deformations of the mid-thigh (node 3,4) at 90 N load were calculated from these graphs (Figure 4.17, E.21 to E.27). The deformation at 90 N load was chosen based on two facts: (1) all test ranges reached this limit of 90 N load and (2) the 90 N load located in the working range (discussed previously in Section 4.2) of the thigh. Table 4.4 shows the mid-thigh deformation at 90 N load with all densities and thicknesses of the foam for 100° knee angle.

Table 4.4 Thigh Deformations at 90 N Load with Different Foam Thicknesses and Densities, Subject No. 1, Knee angle 100°

		Thigh Deformation (mm)				Thigh-different Foam Density	
Foam Thickness (mm)		51 kg/m^3 Foam Density	49 kg/m^3 Foam Density	44 kg/m^3 Foam Density	43 kg/m^3 Foam Density	Average (mm)	Standard Deviation (mm)
100		39	46.5	43.5	42.5	42.9	3
50		42	42	45		43	1.7
25		46.5	46.5	43	42	44.5	2.3
Thigh-different Foam Thickness	Average (mm)	42.5	45	43.8	42.3	43*	2*
	Standard Deviation (mm)	3.7	2.6	1	0.4	2*	

* The means of averages and standard deviations of the thigh interacting with different foam thicknesses and densities

The average of the thigh deformation and the standard deviation were calculated for the thigh interacting with different foam thicknesses. Table 4.4 shows the average and the standard deviation of the thigh deformation at 90 N for different foam thicknesses with

knee angle 100°. The means of averages and standard deviations were 43 mm and 2 mm, respectively, of the thigh interacting with different foam thicknesses. Figure 4.17 shows small variation in the thigh deformation of subject number one due to different foam thickness for 43 kg/m^3 foam density with knee angle 100°.

The deformations of the mid-thigh (node 3,4) with knee angle 130° at 90 N load were calculated from the graphs in Figures 4.18, E.25 to E.27. Table 4.5 shows the mid-thigh deformation of subject number one with 130° knee angle at 90 N load for 100 mm, 50 mm, 25 mm foam thicknesses and 51 kg/m^3,44 kg/m^3, and 43 kg/m^3 foam densities.

Table 4.5 Thigh Deformations at 90 N Load for Different Foam Thicknesses and Densities, Subject No. 1, Knee angle 130°

		Thigh Deformation (mm)			Thigh-different Foam Density	
Foam Thickness (mm)		51 kg/m^3 Foam Density	44 kg/m^3 Foam Density	43 kg/m^3 Foam Density	Average (mm)	Standard Deviation (mm)
100		44.5	47	44	45	1.6
50		42	48		45	4
25		46	46	44	45	1.2
Thigh-different Foam Thickness	Average (mm)	44	47	44	*45	*2
	Standard Deviation (mm)	2	1	0	*1	

* The mean of averages and standard deviations of the thigh interacting with different foam thicknesses and densities

The average of the thigh deformation and the standard deviation were calculated for the thigh interacting with different foam thicknesses and with knee angle 130°. Table 4.5 shows the average and the standard deviation of the thigh deformation at 90 N for different foam thicknesses with knee angle 130°. The means of averages and standard deviations were 45 mm and 1 mm, respectively, of the thigh interacting with different

foam thicknesses. Figure 4.18 shows small variation in the thigh deformation of subject number one due to different foam thickness for 44 kg/m^3 foam density with knee angle 130°.

These results from subject number one indicated that the thigh deformation did not vary significantly (3%) with different foam thicknesses. Eliminating the foam thickness as a variable reduced the possible variable combinations of the thigh deformation from 336 to 112. In the same time, when the foam thicknesses increased (Figure 4.19), the foam stiffnesses decreased significantly. The 100 mm and 25 mm foam thicknesses were chosen for further analysis because they represented the softer and the stiffer foams, respectively, for each foam density.

4.3.2 THIGH INTERACTION WITH DIFFERENT FOAM DENSITIES

The interaction effect of different foam densities with the thigh of subject number one was determined by plotting the thigh vertical deformations versus the load for 100 mm and 25 mm foam thickness with all foam densities (Figures 4.20, 21, 22, 23). Table 4.4 shows the thigh deformation at 90 N load with knee angle 100° for these graphs. The average and the standard deviation were calculated to estimate the variability in the thigh deformations for different foam densities (Table 4.4). The means of averages and standard deviations were 43 mm and 2 mm, respectively, of the thigh interacting with different foam densities. Figures 4.20, and 4.21 show small variation in the thigh deformation of subject number one due to different foam densities for 100 mm, and 25 mm foam thicknesses with knee angle 100°.

The average of the thigh deformation and the standard deviation were calculated for the thigh interacting with different foam densities and with knee angle 130°. Table 4.5 shows the average and the standard deviation of the thigh deformation at 90 N for different foam thicknesses with knee angle 130°. The means of averages and standard deviations were 45 mm and 2 mm, respectively, of the thigh interacting with different foam densities. Figures 4.22 and 4.23 show small variation in the thigh deformation of subject number one due to different foam densities for 100 mm, and 25 mm foam thicknesses with knee angle 130°. Figure 4.24 displays a large difference in foam stiffnesses due to the different in the foam densities.

These results from the first subject showed that thigh deformation did not vary substantially (4%) with different foam densities. Since this thesis was primarily concurred with what was occurred in the thigh, the possible variable combinations were reduced from 112 to 28 by eliminating the foam density.

4.3.3 THIGH AND FOAM INTERACTIONS FOR ALL SUBJECTS

Eliminating foam thickness and foam density as variables was extremely helpful in reducing the number of tests run on subjects 2 through 7. However, two foams densities, foam density (43 Kg/m^3) with thickness 100 mm and 25 mm and foam density (51 kg/m^3) thickness 100 mm were chosen in the further tests to evaluate the thigh behavior with these variables. The 43 kg/m^3 and 51 kg/m3 were chosen because they represent the softest and the stiffest foams in this study.

The total, thigh, and foam load-deformation relationship (Figures 4.25, E.32 to E.38) for the thigh interaction with two different foam densities (43 kg/m^3 and 51 kg/m^3) were

plotted for the each subject with two knee angles 100° and 130°. These graphs (Figures 4.25, E.32 to E.38) show that the thigh deformed more than the foams and the thigh became stiffer as the displacement and contact region increased with both foam densities. Also, they show there was a large difference in the foam deformation due to the different foam densities. The difference in foam deformations increased as the displacement and contact area increased. The deformations of the mid-thigh (node 3,4) at 70 N load were calculated from these graphs. The deformation at 70 N load was chosen because some test ranges did not exceed this limit of 70 N load and it was located in the working range of the thigh. Table 4.6 shows the mid-thigh deformation with 100° and 130° knee angle at 70 N load for 100 mm foam thickness and 51 kg/m^3 and 43 kg/m^3 foam densities.

Table 4.6 Thigh and Foam Deformations at 70 N. Load for Thigh Interacting with Two Different foam Densities.

	Knee angle 100				Knee angle 130			
	Foam Deform. (mm)		Thigh Deform. (mm)		Foam Deform. (mm)		Thigh Deform. (mm)	
Subject No.	43 kg/m^3	51 kg/m^3	43 kg/m^3	51 kg/m^3	43 kg/m^3	51 kg/m^3	43 kg/m^3	51 kg/m^3
1	8	2	35	37	8	2	35	36
2	12	2	45	50	10	2	45	47
3	5	1	40	40.5	7	1	35	36
4	8	1	50	51	9	1	46	47
5	4	1	51	52	5	1	43	43
6	8	2	35	37	8	1	30	31
7	4	0.5	45	47	4	4	42	43
Average (mm)	**7**	**1**	**43**	**45**	**7**	**2**	**39**	**40**

The average foam deformations at 70 N load of the 43 kg/m^3 foam was 80% larger than 51 kg/m^3 foam. However, the thigh deformation did not vary significantly due to this variable. The average of the thigh deformations at 70 N with foam 43 kg/m^3 was smaller

by 3% than with 51 kg/m^3. These results indicated that the load was distributed on the larger contact area with softer foam and constrained the thigh so it became stiffer. Also, these graphs (Figure 4.25) show a large difference in the total deformations. That was contributed by a large difference in foam deformations due to the difference in foam densities. These results indicate a repeatable behavior of the thigh with different foam stiffnesses.

The total, thigh, and foam load-deformation relationships (Figures 4.26, E.39 to E.45) for the thigh interaction with two different foam thicknesses (100 mm and 25 mm) were plotted for the each subject with 130° knee angle. These graphs (Figures 4.26, E.39 to E.45) show that the thigh deformed more than the foams and the thigh became stiffer as the displacement and contact region increased. Also, these graphs show there was a large difference in the foam stiffness due to the difference in foam thicknesses. This difference increased as the displacement and the contact area increased. The deformations of the mid-thigh (node 3,4) at 70 N load were calculated from these graphs (Figures 4.26, E.39 to E.45) Table 4.7 shows the mid-thigh deformation with 130° knee angle at 70 N load for 100 mm and 25 mm foam thicknesses and 43 kg/m^3 foam density. The average of the thigh deformations with 100 mm foam thickness was smaller by 3% than with 25 mm foam thickness. The average foam deformations at 70 N load of the 100 mm foam was 50% larger than the 25 mm foam. These results indicated that the load was distributed on the larger contact area with the thick foam and constrained the thigh so it became stiffer.

Table 4.7 Thigh and Foam Deformations at 70 N Load for Thigh Interacting with Two Different foam Thicknesses.

Subject No.	Foam Deformation (mm)		Thigh Deformation (mm)	
	100 mm	25 mm	100 mm	25 mm
1	6	3	36	38
2	8	8	42	42
3	6	3	33	33
4	5	1	49	50
5	4	1	41	43
6	11	4	29	31
7	4	1	42	43
Average	6	3	39	40

The total, thigh, and foam load-deformation relationships (Figure 4.27, E.46 to E.60) for the foam interaction with thighs at two different knee angles (100° and 130°) were plotted for the each subject with 43 kg/m^3 and 51 kg/m^3 foam densities. The graphs in Figure 4.27, E.46 to E.60 show the thigh deformations decreased as the tensions of the hamstring muscle increased as the knee angle increased from 100° to 130°, but the changes in the foam deformations were small. This can be explained by the thigh-foam contact area that did not change considerably due to change in knee angle. In this case, most of the difference in total deformation was due to the difference in the thigh deformation.

Two locations of foam deformation (3,3 and 3,4 nodes) were considered for analysis (Figure 2.8). These nodes were chosen because they were the first contact nodes between the thigh and the foam, and they were located at mid-thigh section. To determine the variation in thigh deformation at the contact points (3,3 and 3,4), the load versus the vertical deformation of the thigh at these contact points (Figure 4.28, E.61 to E.67) were plotted in one graph for each subject and for each knee angle (100° and 130°). These graphs show that the thigh stiffnesses did not vary considerably (the difference in the thigh

deformation at 70 N was 1%) between these two contact points. This result indicated that the femur location respect to the thigh soft tissue did not effect the deformation in these nodes. Therefore, the possible variable combinations (variation in the thigh stiffnesses with different foam thicknesses and densities, contact nodes, knee angle, and subject thigh circumference) reduced from 28 to 14. The contact point 3,4 was selected for study. These fourteen variables in the thigh deformation (the subject thigh circumference and knee angles) were discussed earlier in this chapter (Section 4.2).

To summarize the thigh-foam interaction response, the non-linear load-deformation curve of the thigh and foam was split into two parts. The first part was from 0 to 46 N. This splitting point at 46 N load of thigh-foam tests (the width of testing surface was 215 mm) was equivalent to the splitting point at 30 N load of thigh-rigid plate test (the width of testing surface was 137 mm, 30 x 215/138 = 46). The second part ranged from 46 to 120 N. The second part of this curve represented the working region of the thigh stiffness when the thigh interacts with seat cushion in seated posture. The working region was defined base on the contact pressure of the thigh-seat interaction from the results of pressure mat for various people in the seated posture. The softest foam in this study (43 kg/m^3 foam density with 100 mm thickness) was chosen for this analyses due to its large deformations. The thigh with 100° knee angle was chosen for this analyses because it was deformed more than with knee angle 130° (Figure 4.29). These test conditions (100° knee angle with 43 kg/m^3) presented the largest range of deformation that occurred in the thigh and the foam in this study. A best-fit line was obtained for each part (part I and II for the load-deformation curves of thigh and foam). The best-fit lines for the thigh (Figure 4.29,

E.68 to E.74) were highly correlated to the data with correlation coefficients at least 0.92. The average slopes for the seven subjects of the best-fit lines of the thigh deformation in the first and second parts were 1.10 N/mm and 3.6 N/mm with standard deviation 0.27 N/mm and 1.17 N/mm (Table 4.8), respectively. The stiffness of the second part increased from the first part by 69%, meaning that the thighs became stiffer as the displacement and contact region increased. This amount of the increase in thigh stiffness is close to the increasing in thigh stiffness when the thigh interacted with rigid plate (65%). The small difference in the increase of thigh stiffness in second part was probably due to load distributed on the larger contact area in thigh-foam interaction with the large deformation that occurred in the foam.

The average slopes of the best-fit lines of the foam deformation in the first and second parts were 20.58 N/mm and 5.20 N/mm (Table 4.10), respectively. The stiffness of the foam in the second part was smaller than the first part by 278%. This decrease in the stiffness was the foam response to the increasing in the compression, shear, and tension forces on the foam-thigh contact area. The compression force produced by the reaction force on the foam-thigh contact area, the shear force produced by the friction force between the thigh and foam, and the tension force produced by the differences in the foam deformation at the contact surface.

Table 4.8 The Slope of the Fitting Lines for the First and the Second Part of Thigh-Foam Interactions.

	thigh			foam		
Subject No.	Slope Part I N/mm	Slope Part II N/mm	The Differ. in Thigh Stiffness between Part I & II %100	Slope Part I N/mm	Slope Part II N/mm	The Differ. in Foam Stiffness between Part I & II %100
1	1.44	4.30	66.51	12.53	4.69	-167.16
2	0.78	3.33	76.56	10.12	3.49	-189.97
3	1.29	4.35	70.34	11.14	3.73	-198.66
4	0.77	2.27	66.08	28.80	5.46	-427.47
5	1.23	2.82	56.34	33.21	5.99	-454.42
6	1.30	5.52	76.45	14.43	4.35	-231.72
7	0.92	2.61	64.75	33.85	8.66	-207.17
Average	1.10	3.60	68.71	20.58	5.20	-278.24
Standard deviation	0.27	1.17	7.60	10.83	1.77	128.01

4.4 NORMALIZATION OF LOAD-DEFORMATION RESPONSES OF THIGH-FOAM AND THIGH-RIGID PLATE TESTS.

The load-deformation responses of the thigh interaction with rigid plate and with the foam were normalized to determine the change in thigh stiffness when the thigh interacted with the foam. To normalize the load-deformation response of the thigh, the applied loads on the thigh were divided by the rigid plate width (138 mm) for thigh-rigid plate test and by the width of foam specimen (215 mm) for the thigh-foam interaction test. This normalization (Figure 4.30) of the load was based on the assumption that the load was distributed uniformly along the thigh-foam and thigh-rigid plate contact areas.

The graphs for subjects No. 1, 2, 3, 6, and 7 (Figures E.75, E.76, E.77, E.80, E.81) of the normalization load shows that the thigh deformed slightly less when the thigh

interacted with foam than when it interacted with flat rigid plate. That may be because the load in the thigh-foam interaction test was distributed on larger area due to foam deformation. However, the graphs for subjects number 4, and 5 (Figures E.78 and E.79) show that the thigh deformed less when it interacted with the rigid plate than when the thigh interacted with the foam. This result could be due to the load not being distributed uniformly (due to the thigh geometry) along the contact area. Which made the assumption of load normalization, loads were distributed uniformly along the thigh-foam and thigh-rigid plate contact areas, not valid for these two subjects (No. 4 and No. 5). Figure E.85 and E.86 show the foam contact areas with thigh for subjects 4 and 5 did not deform uniformly along the thigh axis. This non uniform deformation can be related to non uniform load distribution on the thigh-foam contact area, since magnitudes and distributions force components acting on interaction surface determine the deformation of the soft tissue and foam. To find the degree of the variation in the deformation along thigh-foam contour, the slopes between two contact points (points A and B, Figure 4.31) were calculated for each subject. Figures E.82 to E.88 show side view of thigh-foam interaction contour for each subject with contact points A and B. Table 4.11 show the slopes between these contact points for each subject that were calculated from Figures E.82 to E.88. The slopes for subjects 4 and 5 were 3.7 and 2.7, respectively. Which indicated that the deformations along the thigh-foam contact areas were not uniform for these two subjects.

Table 4.11 The Slopes between Two Contact Points of Thigh-Foam Contact Area.

Subject No.	1	2	3	4	5	6	7
Slope (degree)	1.8	1.3	0.5	3.7	2.7	0.26	1.03

4.5 THIGH-FOAM INTERACTION CONTOUR

The primary functions of the automotive seat cushion are to locate the occupant in a position where he can operate the vehicle with safely and comfort. Comfort is subjective and can be related to the objective data such as pressure distribution and posture. There are two extremes of seat stiffness, soft and firm. In soft seat, the cushion deforms to a level where the pressure distribution is essentially equilibrated over a larger area of the body. In the firm seat little deformation occurs. In the latter case, efforts to achieve proper pressure distributions on the body are incorporated into the contour of the seat cushion. Since all bodies are not of the same size and shape, an average contour that fits many people's bodies is important to equilibrate the pressure over a larger area. In the seated posture the maximum pressure occurs under the ischial tuberosities and can be minimize by distributing the pressure on a large area of the thigh.

The foam of 43 kg/m^3 density and 100 mm thickness loading the thigh for each subject at 11% of the subject's weight was chosen to find the average and the standard deviation contours. The 11% subject weight load was chosen because it was in thigh working region. This foam was chosen because it was the softest foam in this experiment and the load the distributed on largest area compared with the others foams. Figures 4.32 and 4.33 show the average contour of the seven subjects for knee angle 100° and 130°, respectively. The average contour represents a best fit thigh-foam contour for all subjects

and can be used to distribute the pressure on the larger thigh-foam contact area. These average contours fit the seven subjects with uniform standard deviations contours (Figures 4.34 and 4.35). This uniform variation in foam deformation indicated that the change in the thigh posterior contour between the subjects vary consistently due to the thigh geometry.

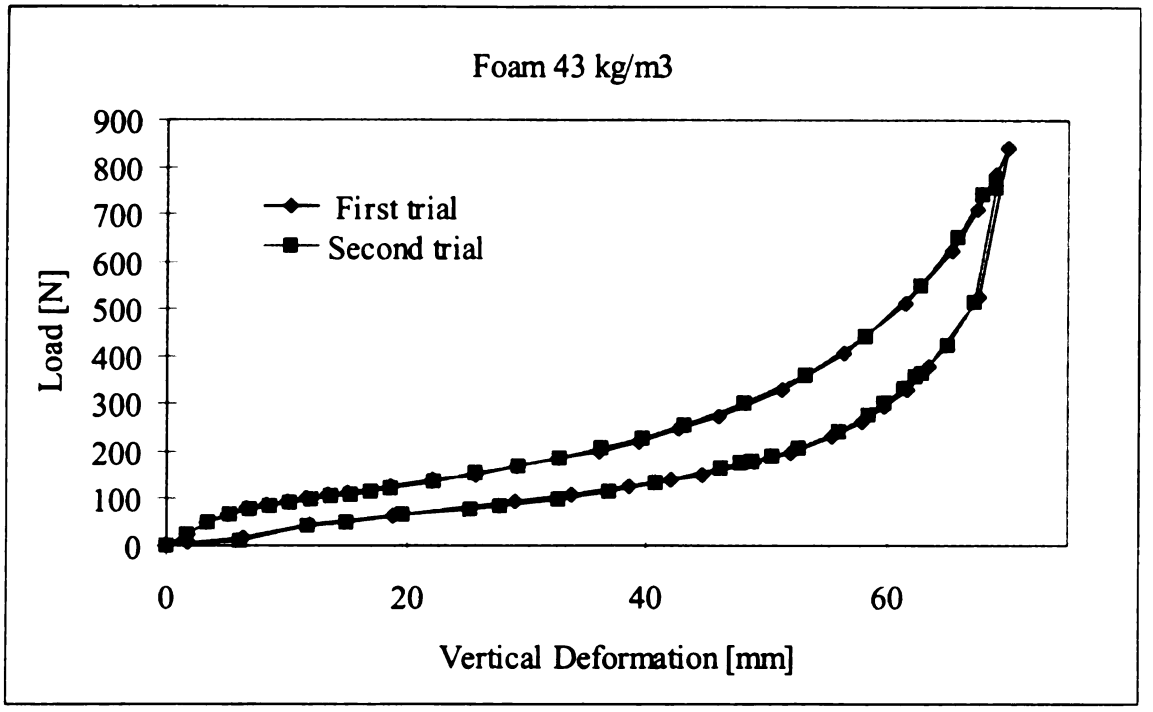

Figure 4.1 Hysteresis Curves Obtained From Loading and Unloading the M-4 (43 kg/m^3 Foam Density) Foam for Two Test Trials

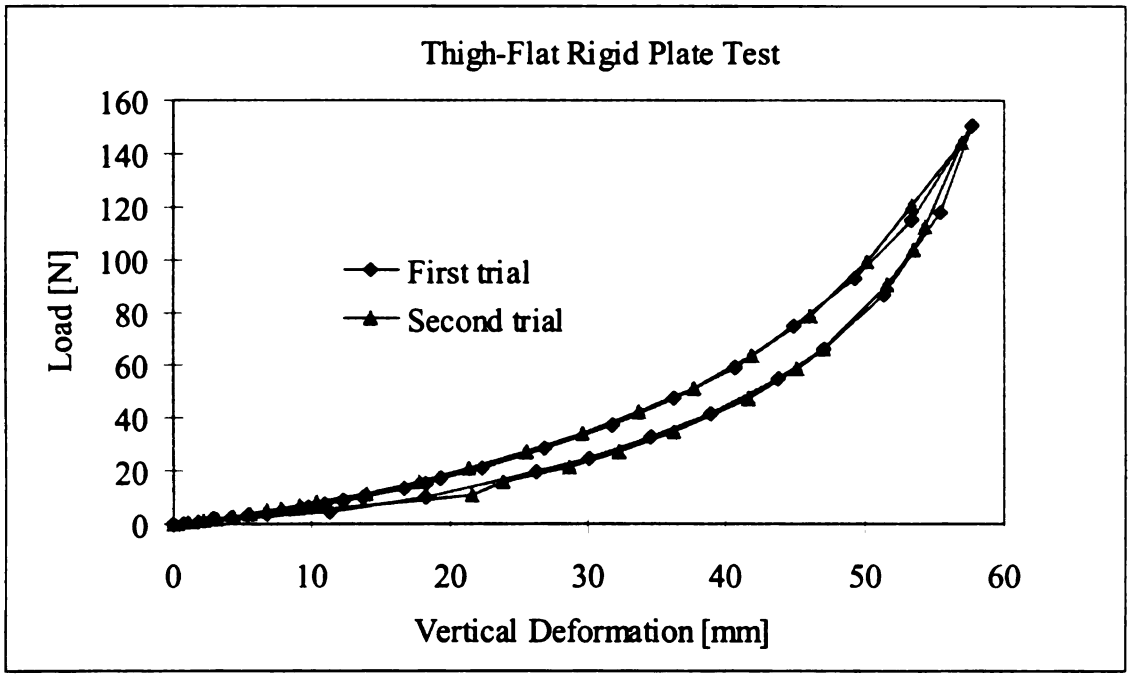

Figure 4.2 Hysteresis Curves Obtained From Loading and Unloading the Thigh for Two Test Trails

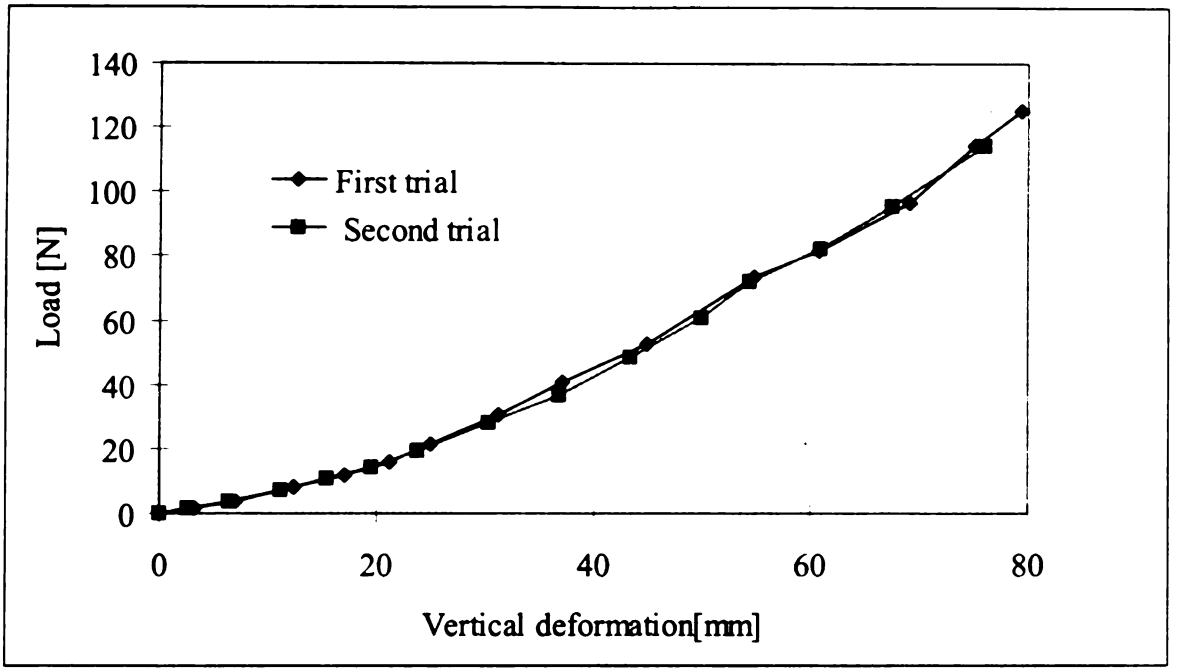

Figure 4.3 Total Deformation Versus Load Obtained from Thigh-Foam Interaction Test for Two trials.

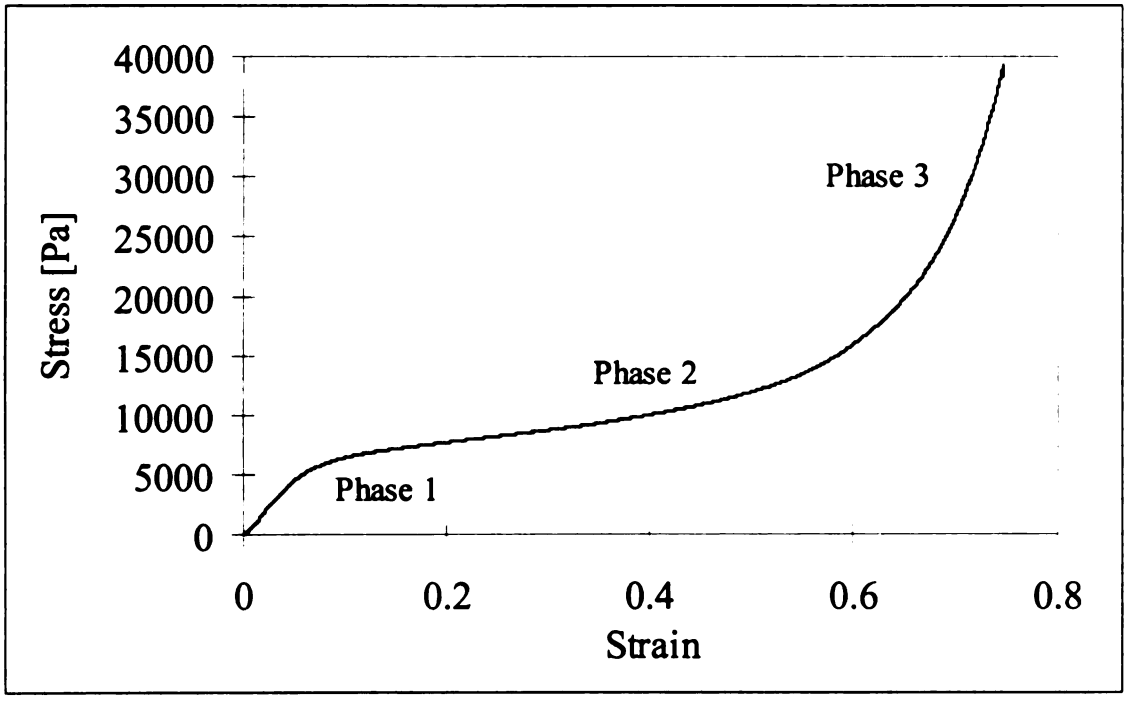

Figure 4.4 Typical Strain-Stress Curve for Cellular Materials Obtained from Uniaxial-Compression Foam Test.

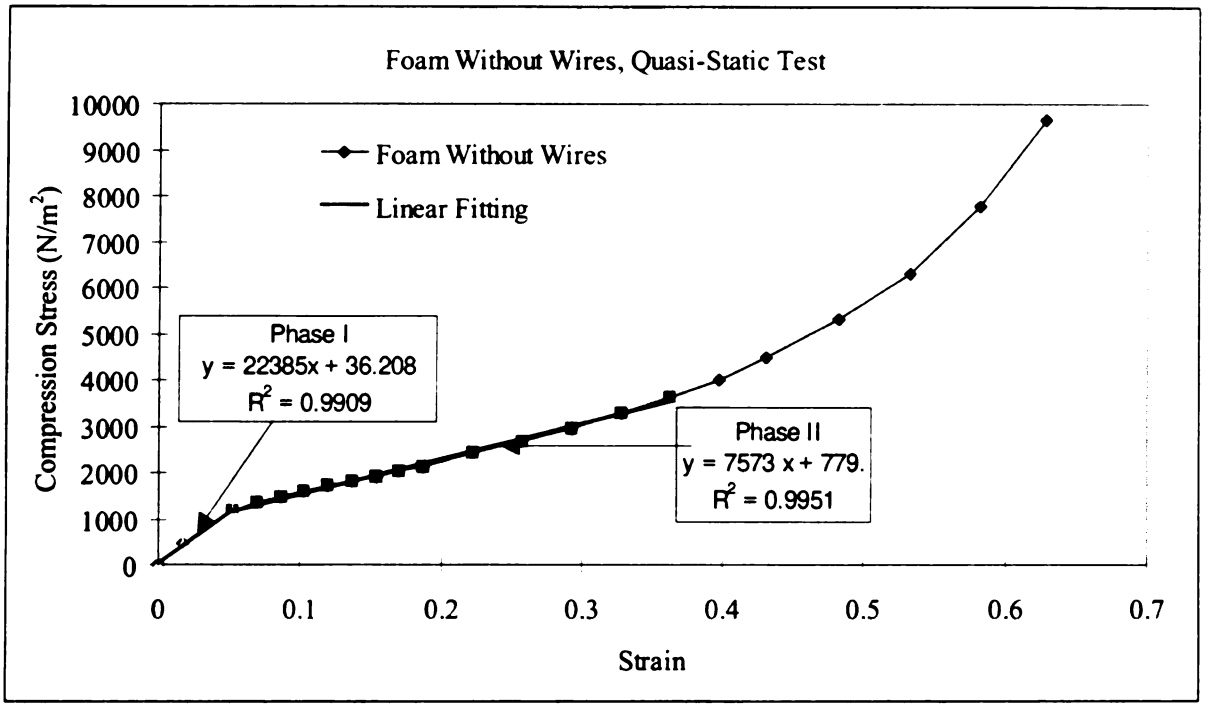

Figure 4.5 Typical Best-Fit Lines were Developed to Obtain Young's Modulus for Phase One and the Tangent Modulus for Phase Two of Compression, Quasi-Static Test.

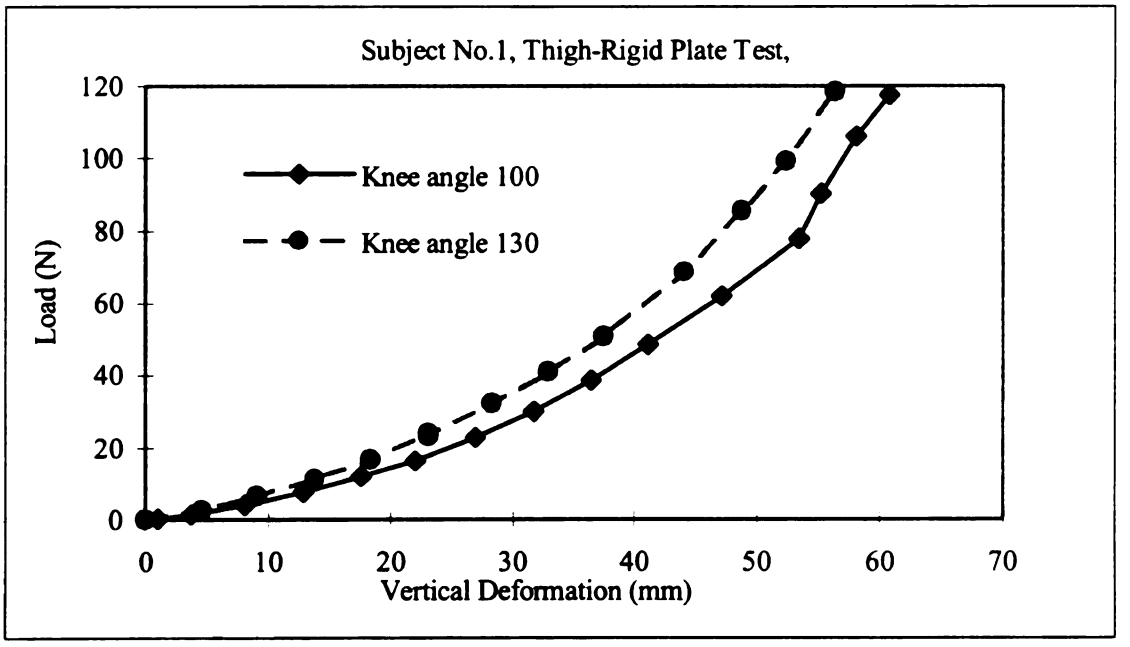

Figure 4.6 Typical Load-Deformation Relationship of Thigh Structure for Two Knee Angles.

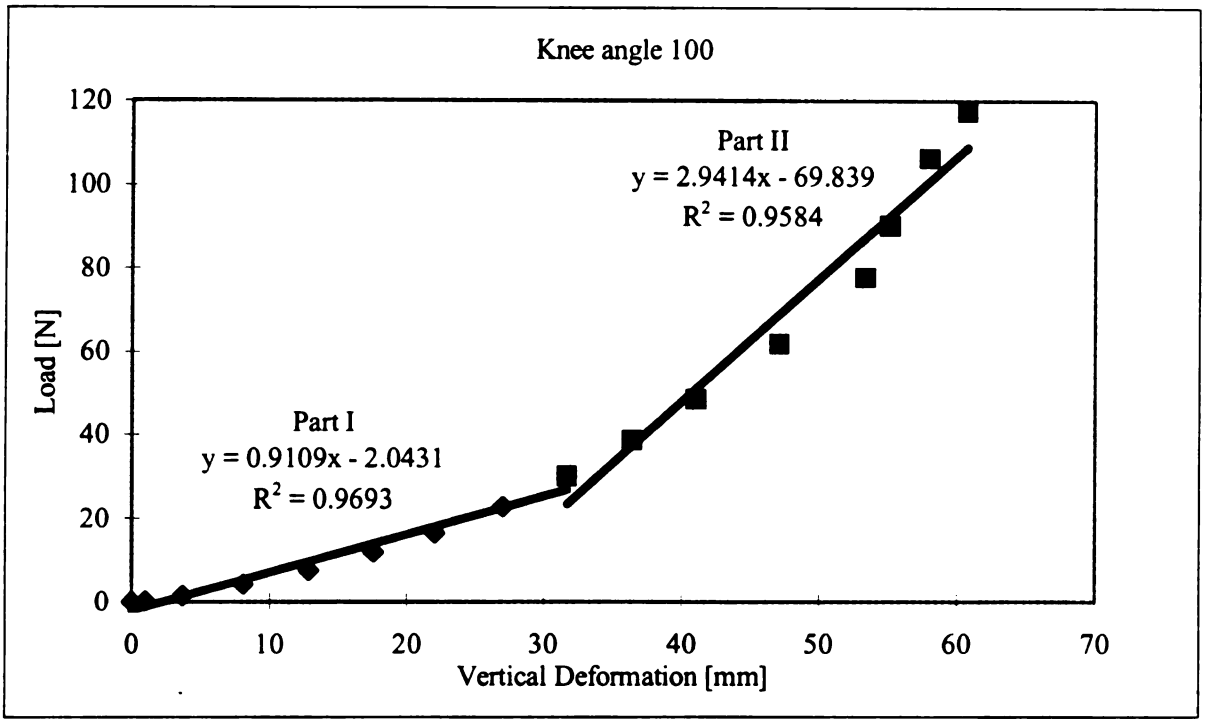

Figure 4.7 Typical Best-Fit Lines Developed for Load-Deformation Response of Thigh.

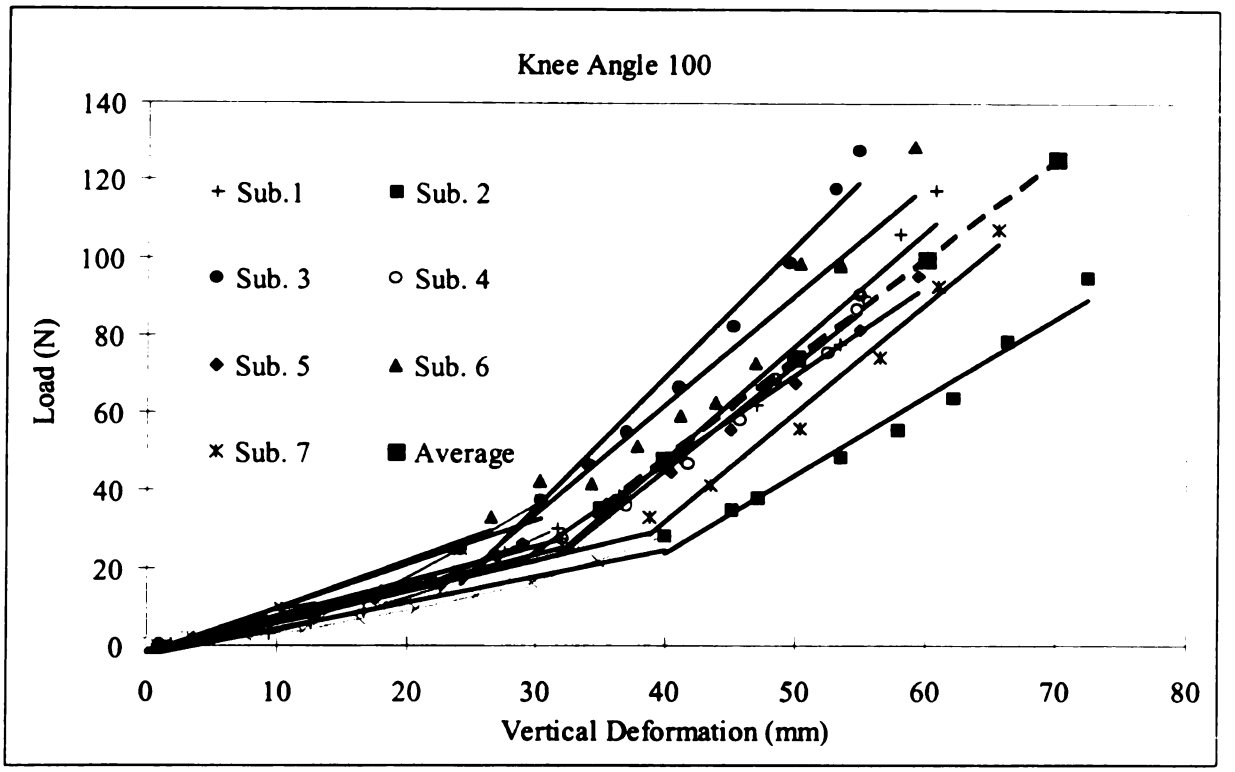

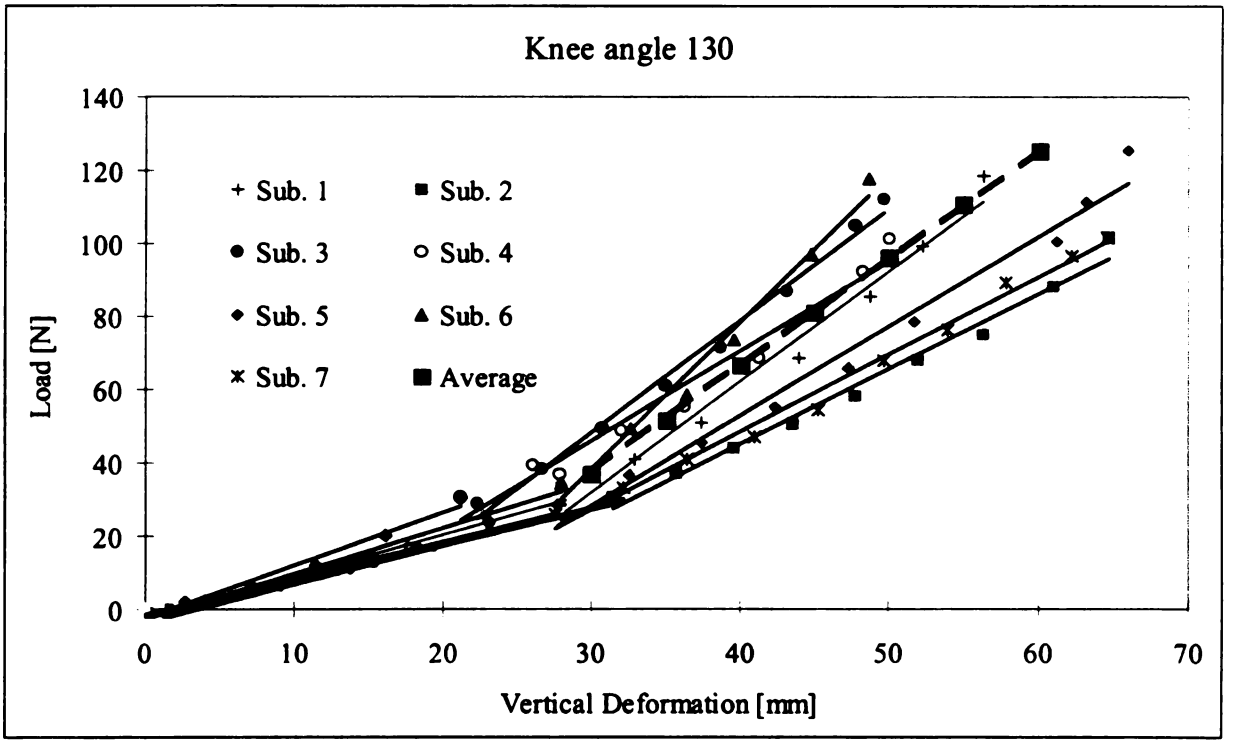

Figure 4.8 Lines Fit to Load-Deformation Relationship of the Subject Thighs with Average Thigh Stiffness

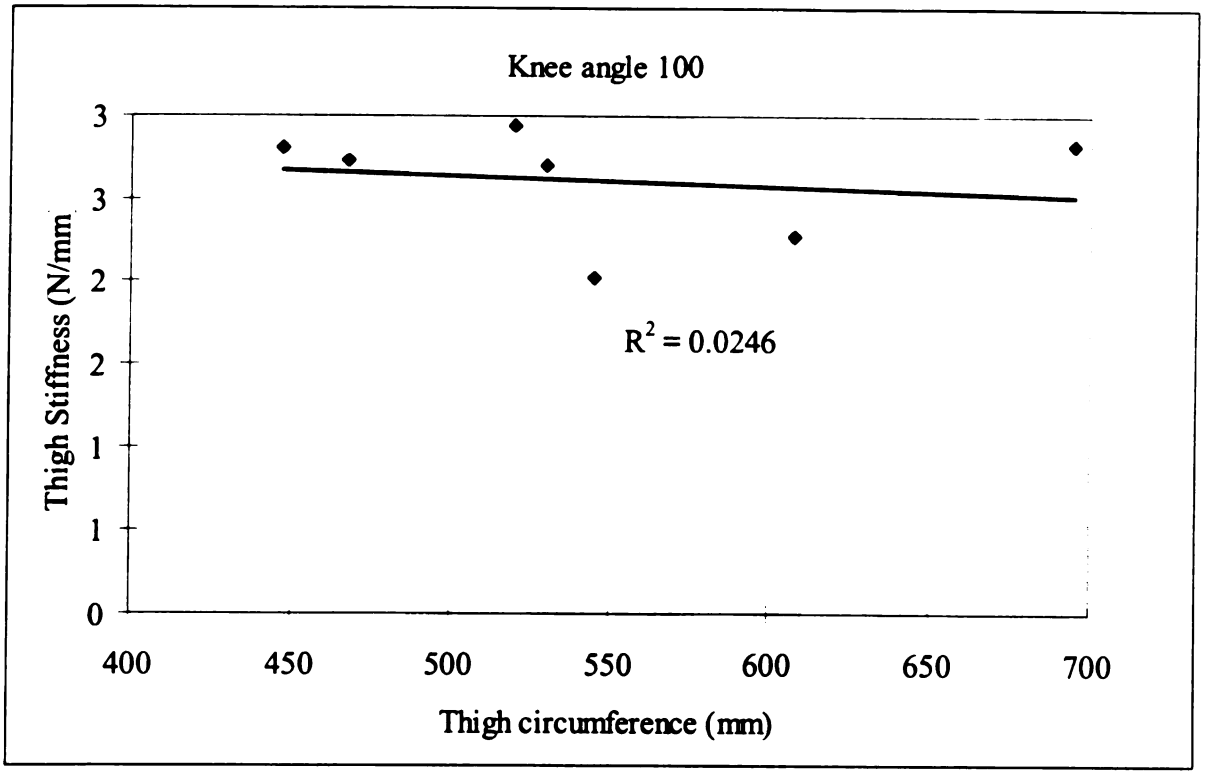

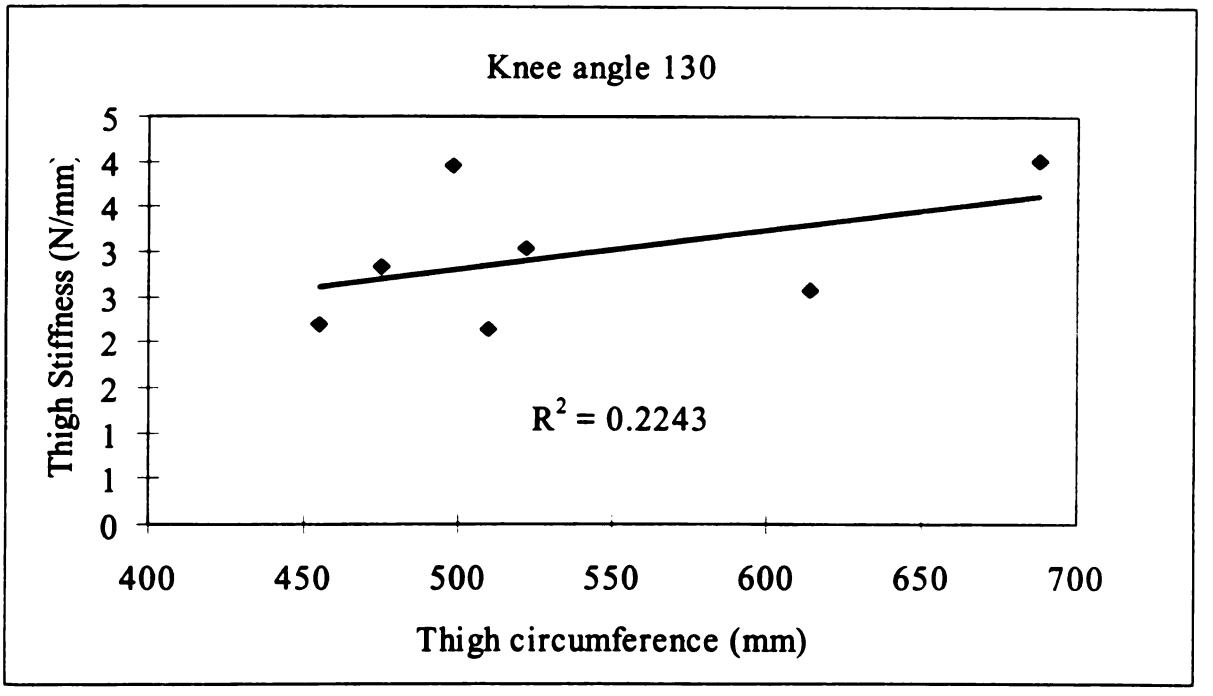

Figure 4.9 The Correlation Between the Circumference and Stiffnesses of Subject Thighs.

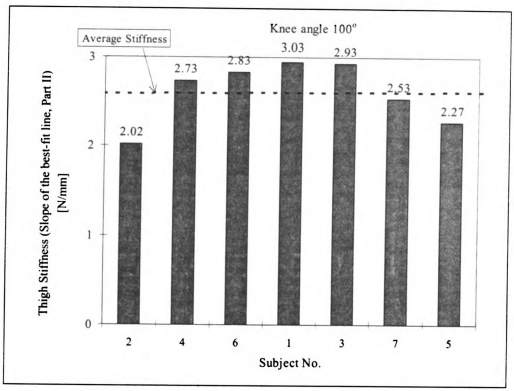

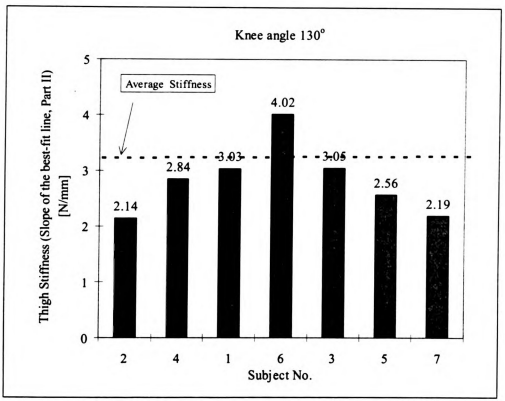

Figure 4.10 Stiffness of Subject Thighs Distributions from Their Mean.

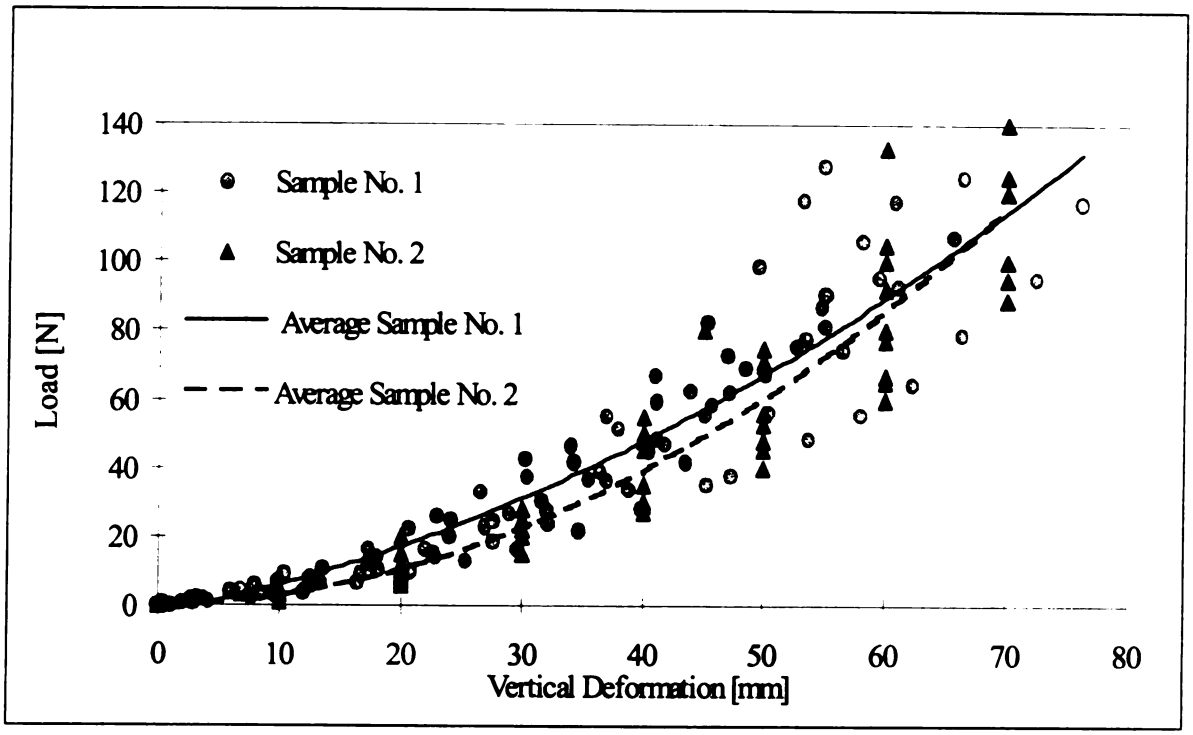

Figure 4.11 Comparison between the Thigh Stiffness Average of This Study (Sample No. 1) and Previous Study (Ref. No. 9) (Sample No. 2).

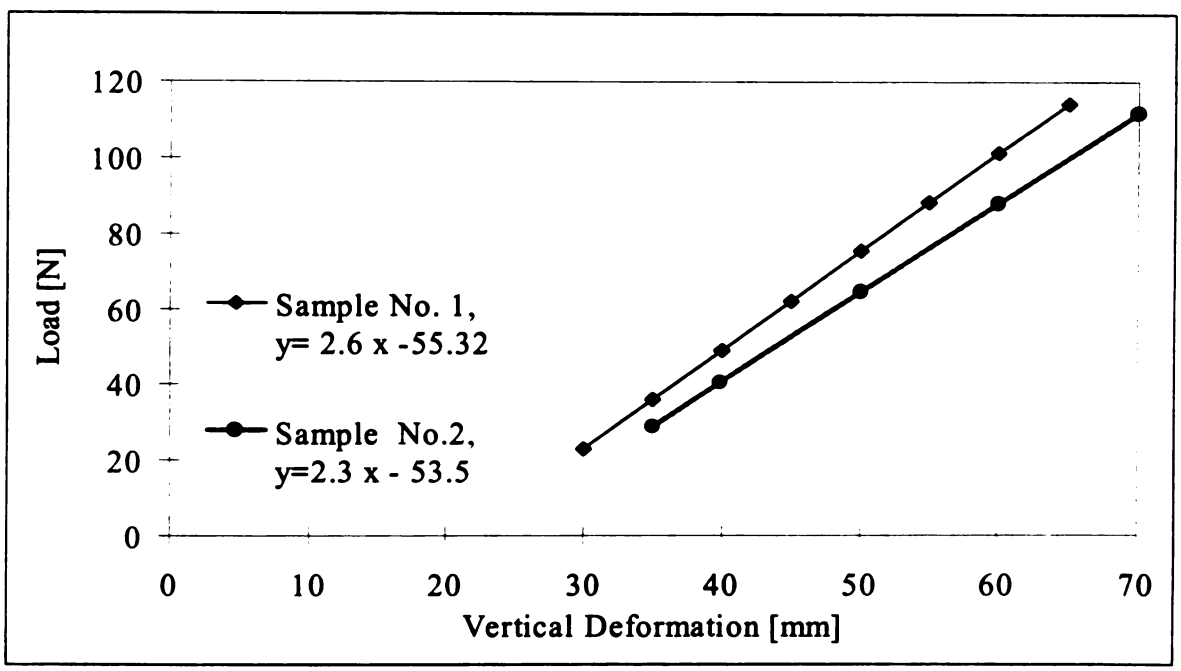

Figure 4.12 Comparison between the Average of Thigh Stiffness (Second Part) of This Study (Sample No. 1, Knee angle 100°) and Previous Study [5] (Sample No. 2, Knee angle 90°).

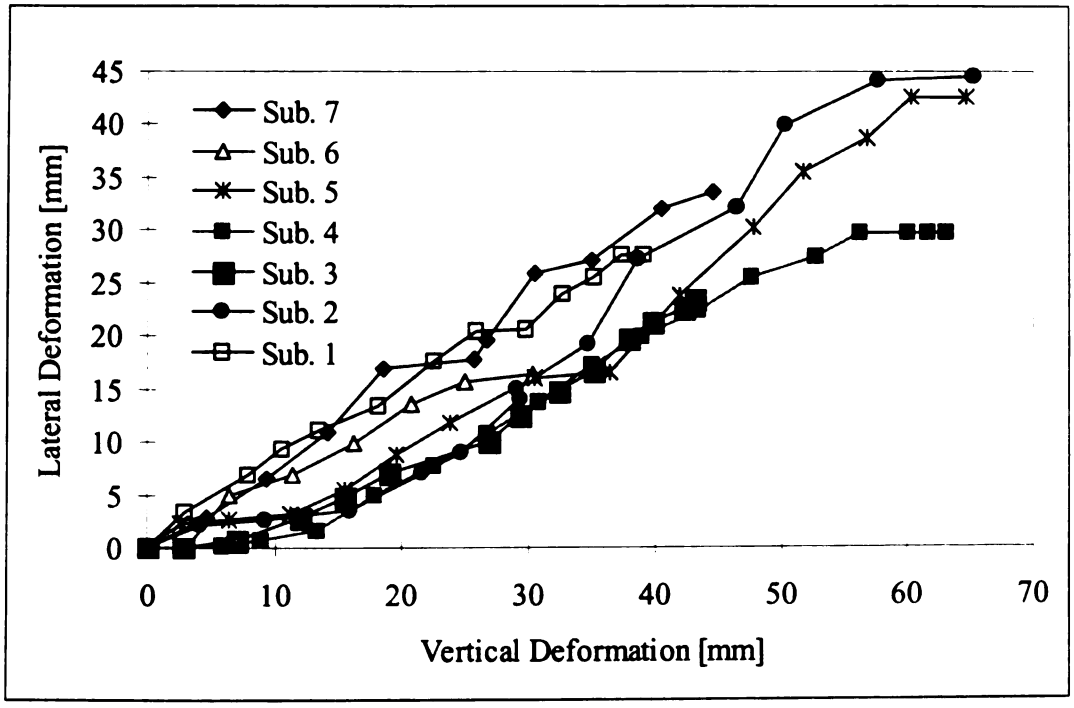

Figure 4.13 Lateral-Vertical Deformation Relationship of Thigh For Knee Angles 100°

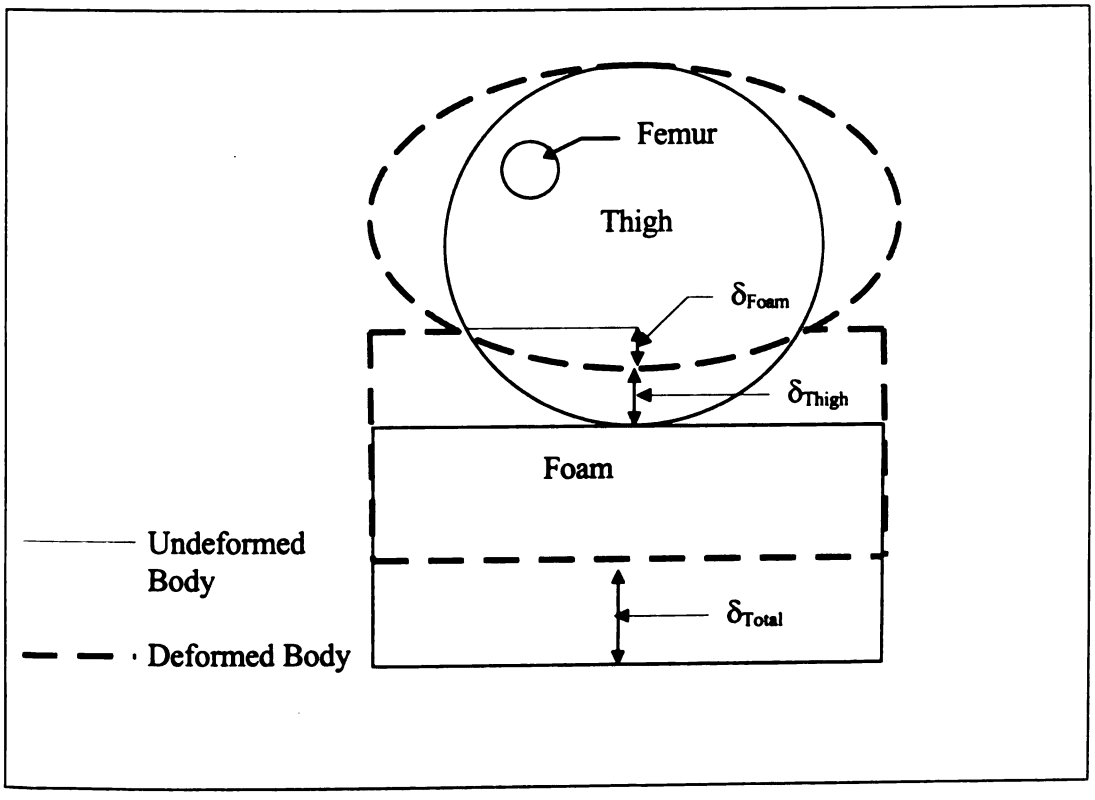

Figure 4.14 Total, Thigh, and Foam Deformations

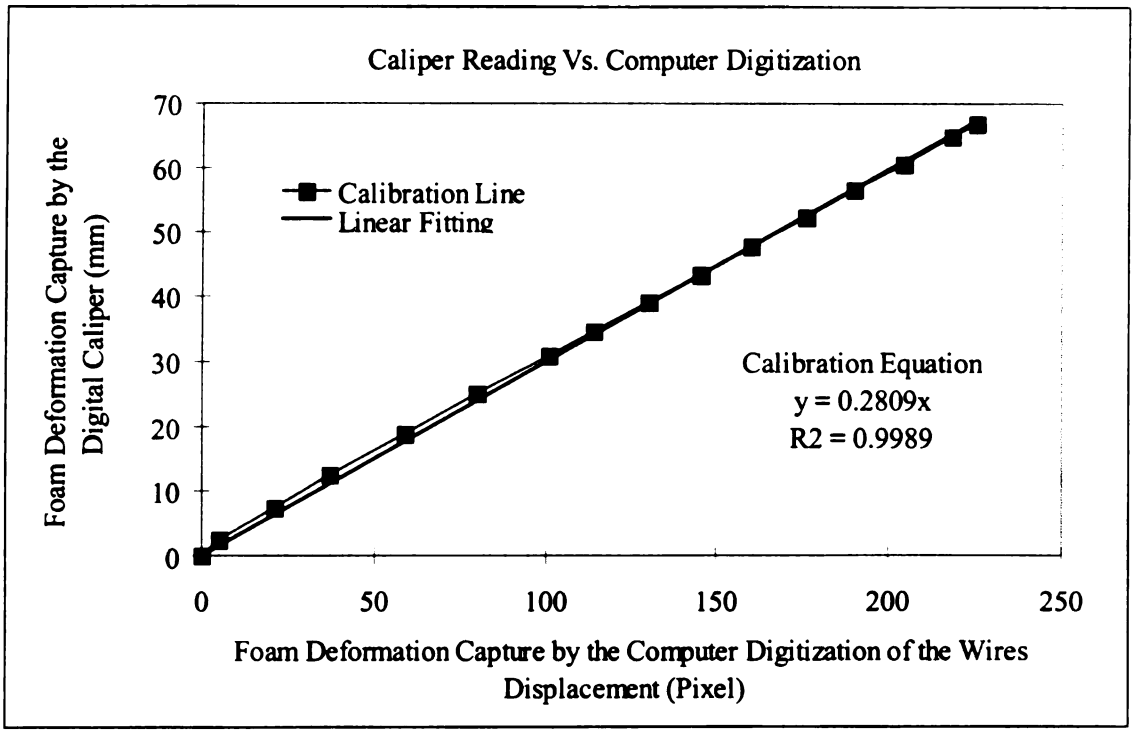

Figure 4.15 Calibration Line Between the Digital Caliper and the Digitized Wire Displacements.

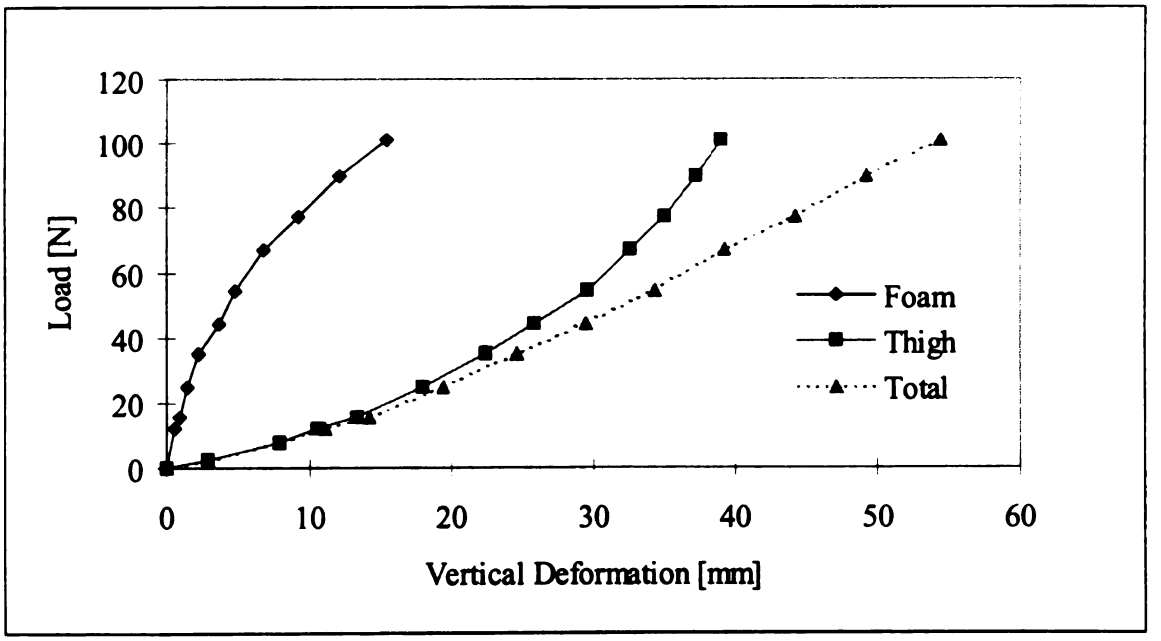

Figure 4.16 Typical Total, Foam, and Thigh Vertical Deformations at Node 3,4

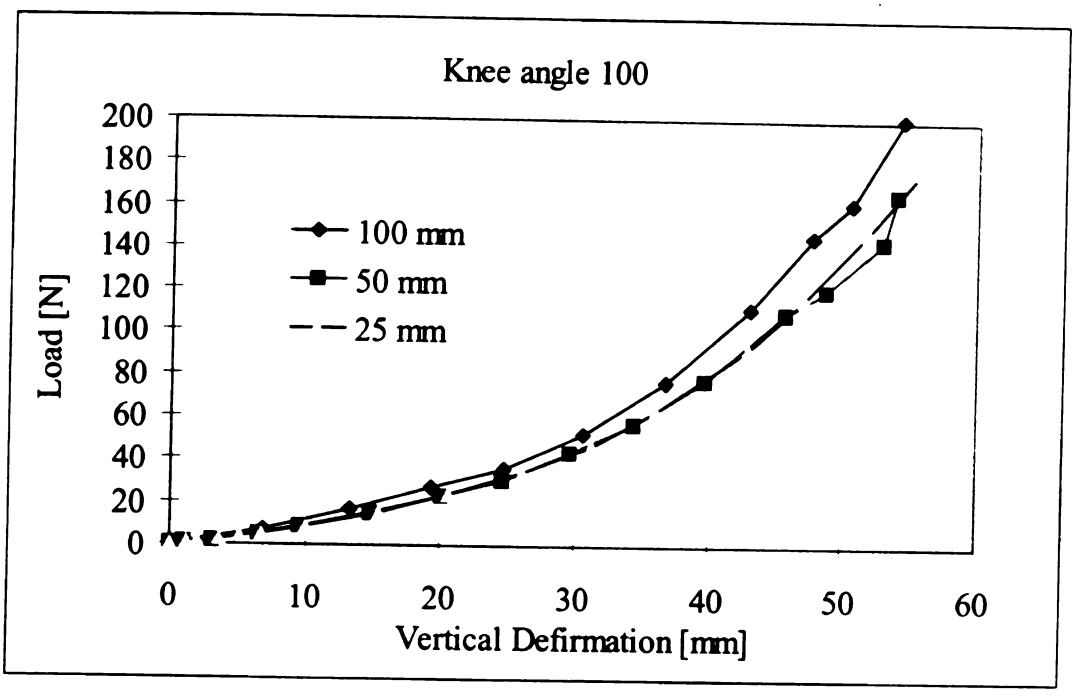

Figure 3. 17 Load-Deformation Relationship for the Thigh Interaction with 44 Kg/M^3 Foam Density, and with Three Different Thicknesses 25 mm, 50 mm And 100 mm. Knee Angle 100°.

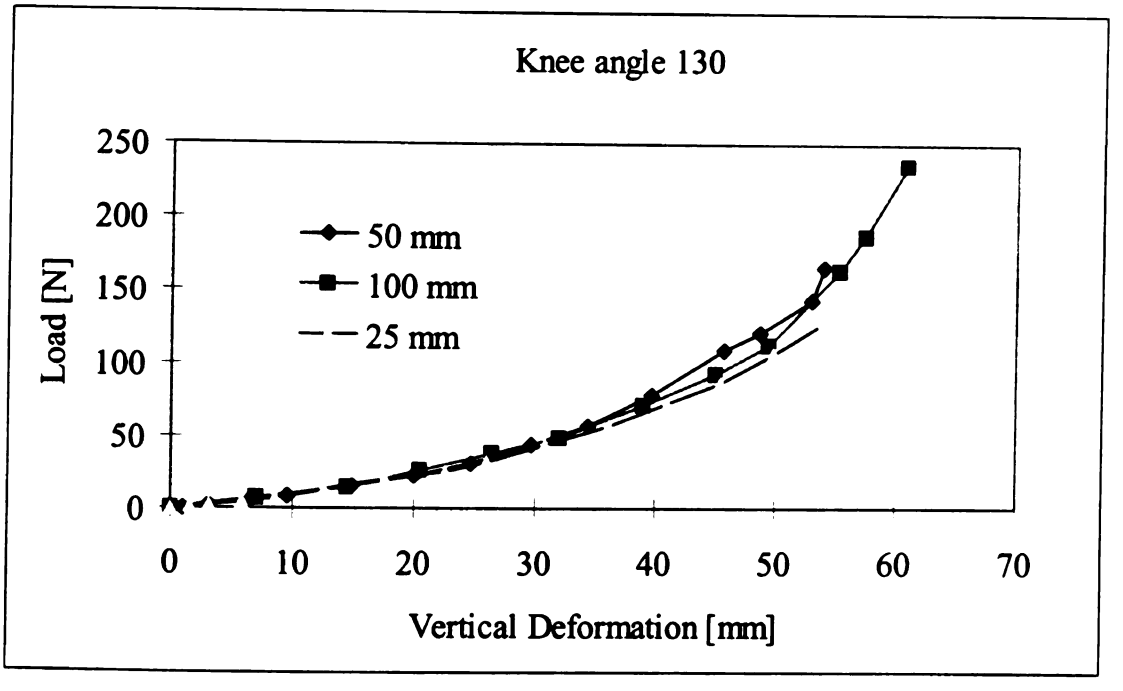

Figure 3. 18 Load-Deformation Relationship for the Thigh Interaction with 44 Kg/M^3 Foam Density, and with Three Different Thicknesses 25 mm, 50 mm and 100 mm. Knee Angle 130°.

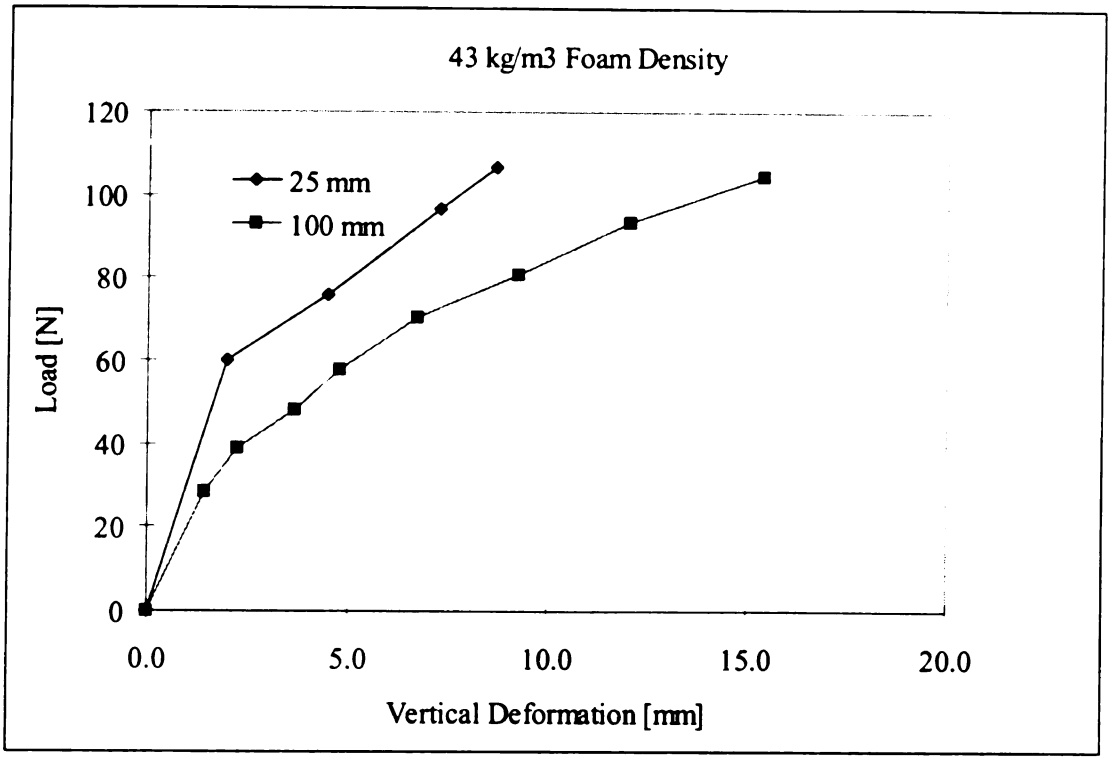

Figure 3. 19 Effect of The Foam Thickness on the Foam Stiffness in Thigh- Foam Interaction Test, Foam 43 kg/m^3.

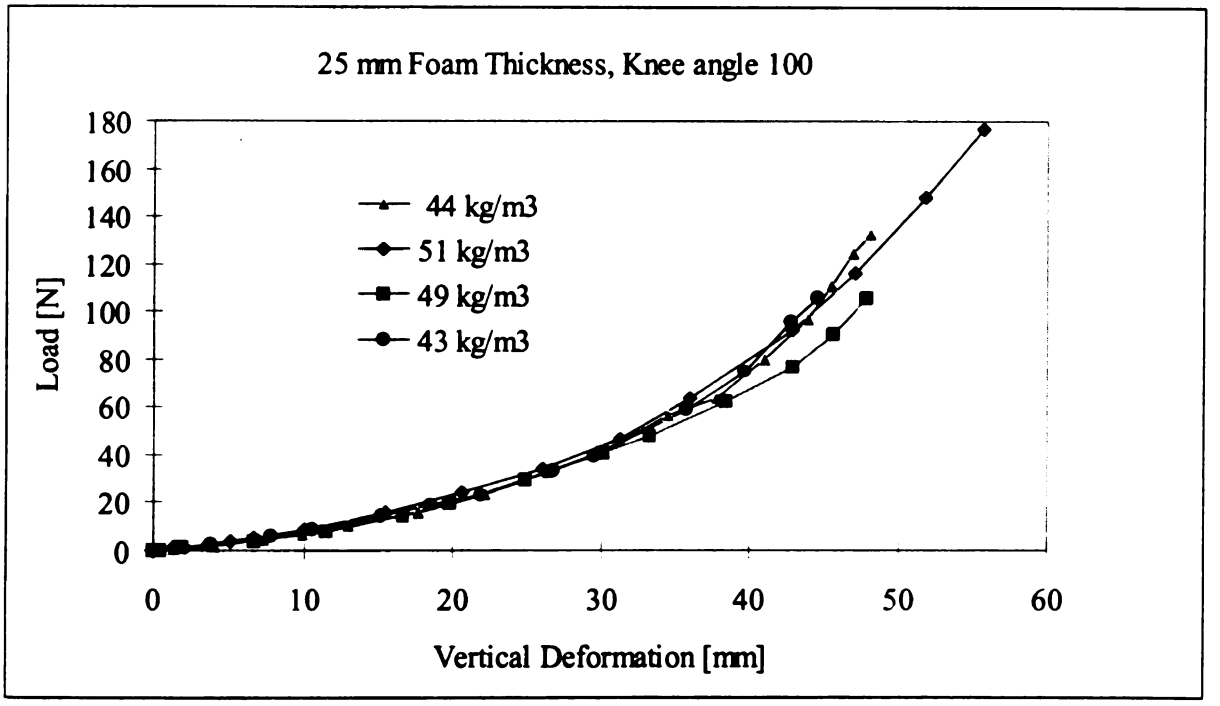

Figure 4. 20 Load-Deformation Relationship for the Thigh Interact with 25 mm Foam Thickness, and with Four Different Densities 43 kg/m^3, 44 kg/m^3 , 49 kg/m^3 and 51 kg/m^3. Knee Angle 100° Subject No. 1.

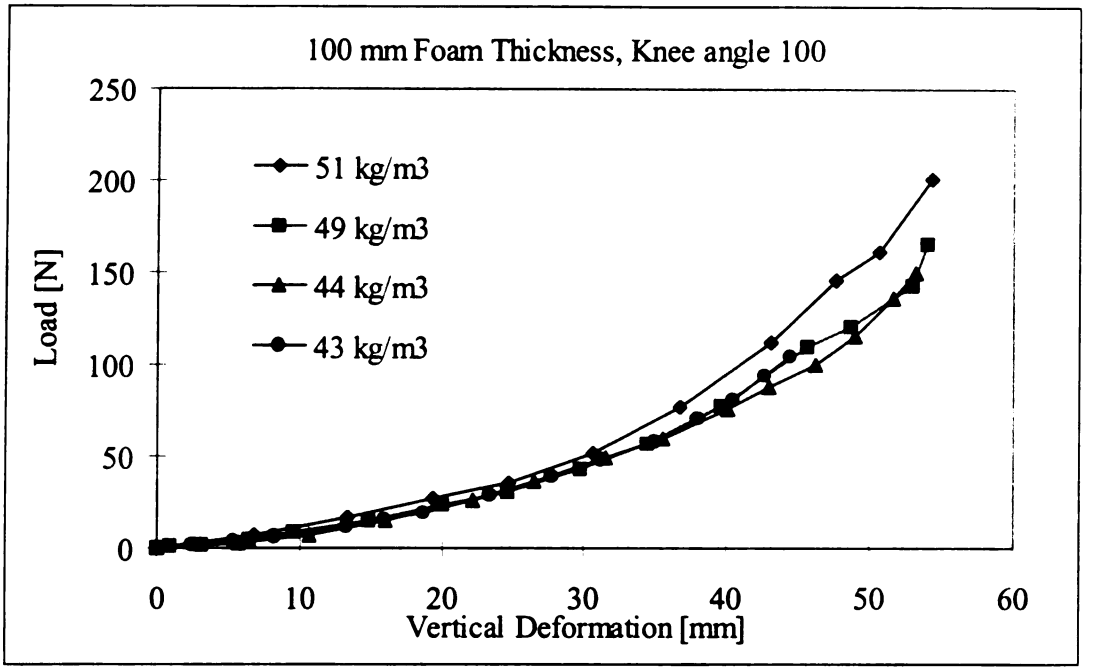

Figure 4. 21 Load-Deformation Relationship for the Thigh Interact with 100 mm Foam Thickness, and with Four Different Densities 43 kg/m^3, 44 kg/m^3 , 49 kg/m^3 and 51 kg/m^3. Knee Angle 100° Subject No. 1.

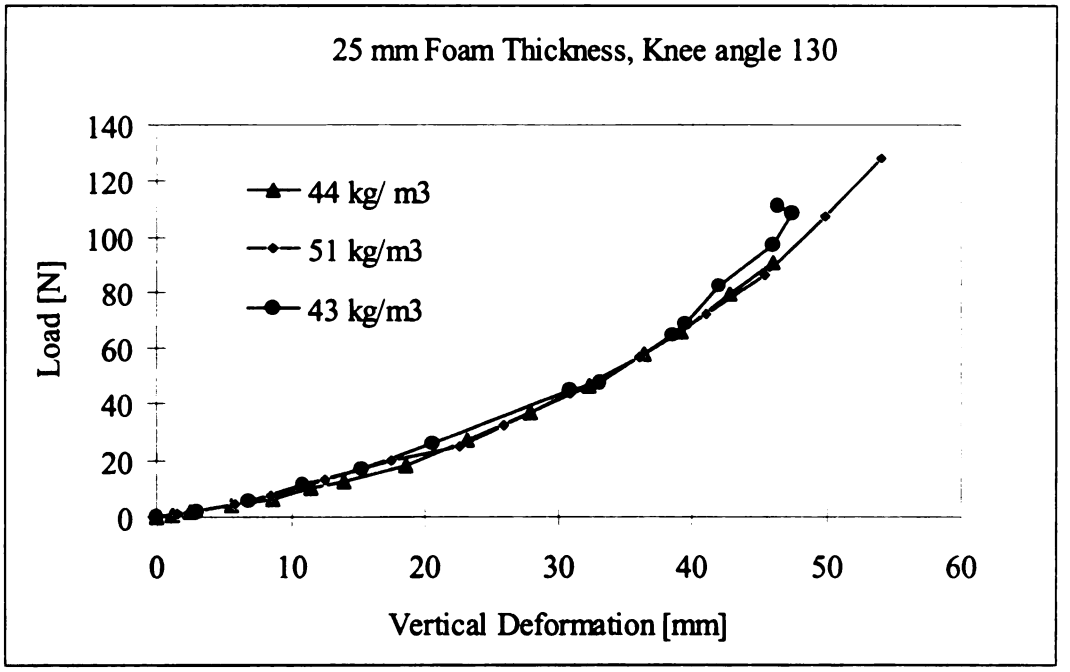

Figure 4. 22 Load-Deformation Relationship for the Thigh Interact with 25 mm Foam Thickness, and with Four Different Densities 43 kg/m^3, 44 kg/m^3 , 49 kg/m^3 and 51 kg/m^3. Knee Angle 130° Subject No. 1.

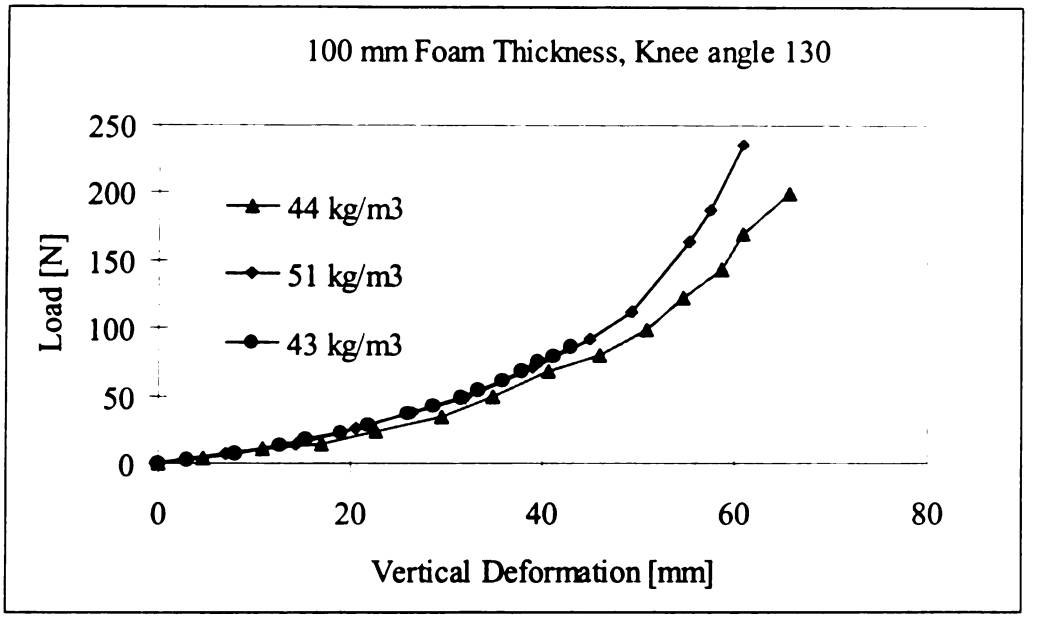

Figure 4. 23 Load-Deformation Relationship for the Thigh Interaction with 100 mm Foam Thickness, and with Four Different Densities 43 kg/m^3, 44 kg/m^3 , 49 kg/m^3 and 51 kg/m^3. Knee Angle 130° Subject No. 1.

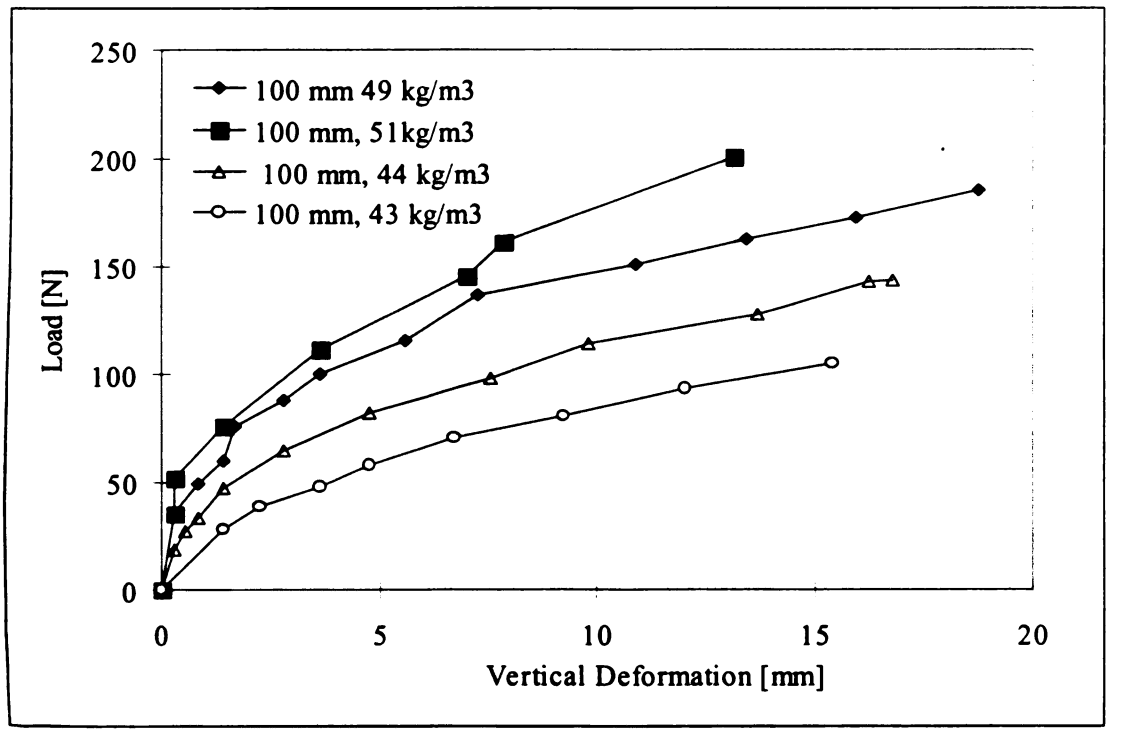

Figure 4.24 Effect of the Foam Densities on the Foam Stiffness in Thigh-Foam Interaction Test, Subject No. 1.

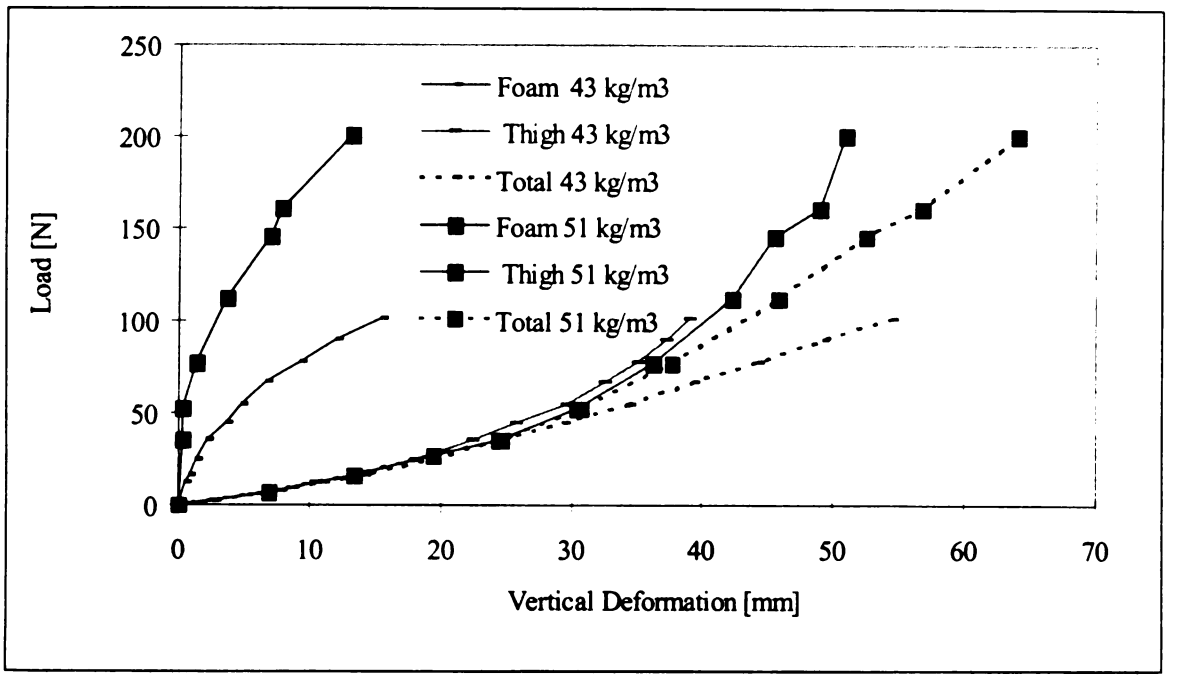

Figure 4.25 Typical Total, Thigh, and Foam Vertical Deformation versus Load for Thigh Interaction with Two Different Foam Density (43 kg/m^3 and 51 kg/m^3), 100 mm Foam Thickness

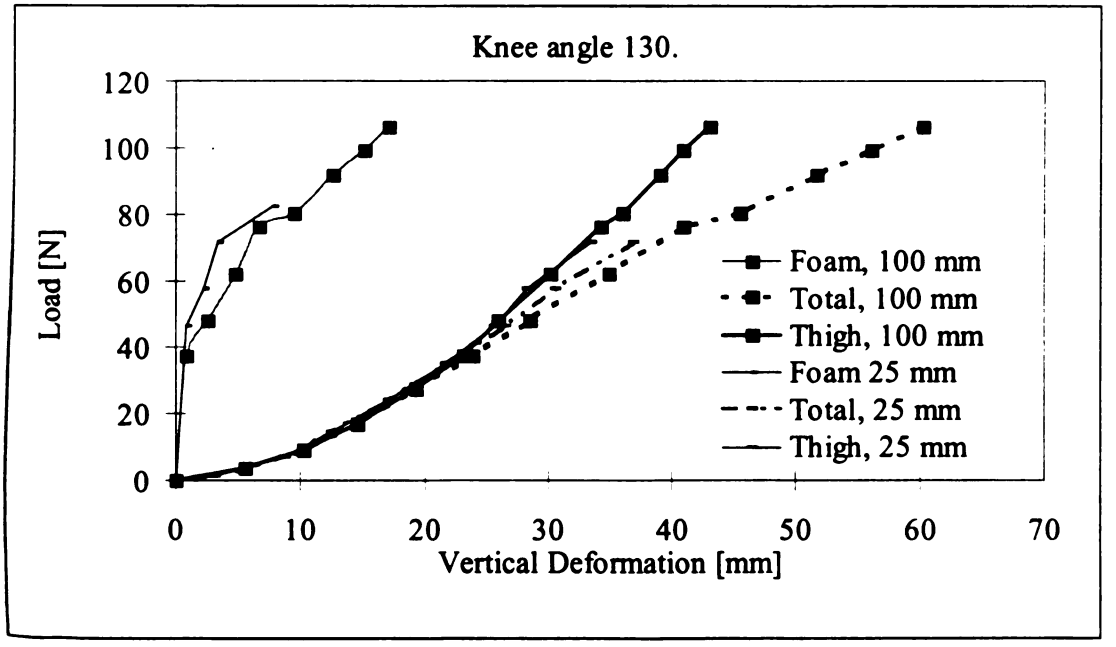

Figure 4.26 Typical Total, Thigh, and Foam Vertical Deformation Versus Load for Thigh Interaction with Two Different Foam Thickness (100 mm and 25 mm), and 43 kg/m^3 Foam Density

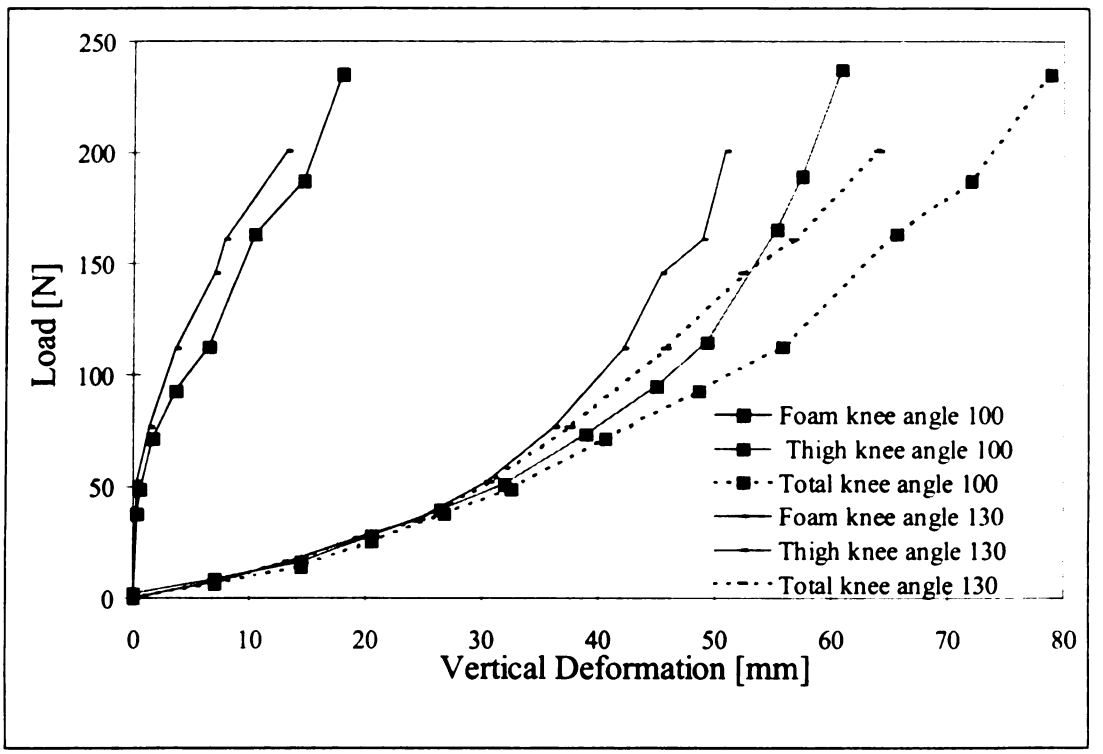

Figure 4.27 Typical Total, Thigh, and Foam Vertical Deformation Versus Load, Thigh with Two Knee Angle 100° and 130° Interaction with Foam (100 mm Thickness and 51 kg/m^3 Density)

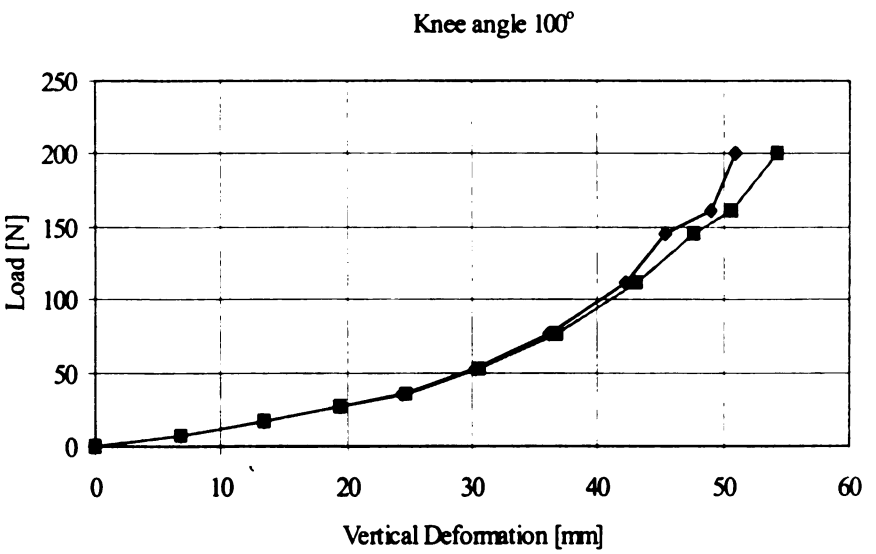

Figure 4.28 Typical Vertical Deformation of Thigh versus Load at Node 3,3 and 3,4.

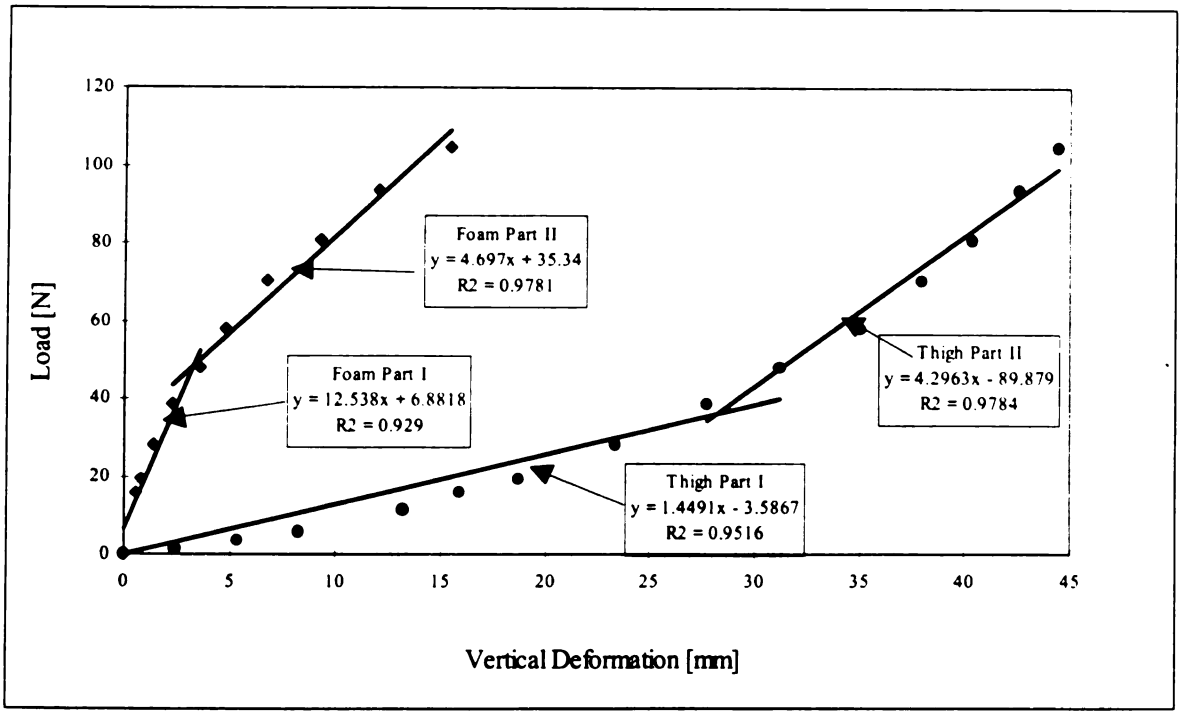

Figure 4.29 Linearization of Typical Load-Vertical Deformation Curves for the Thigh and Foam. Foam 43 kg/m^3, Knee Angle 100°.

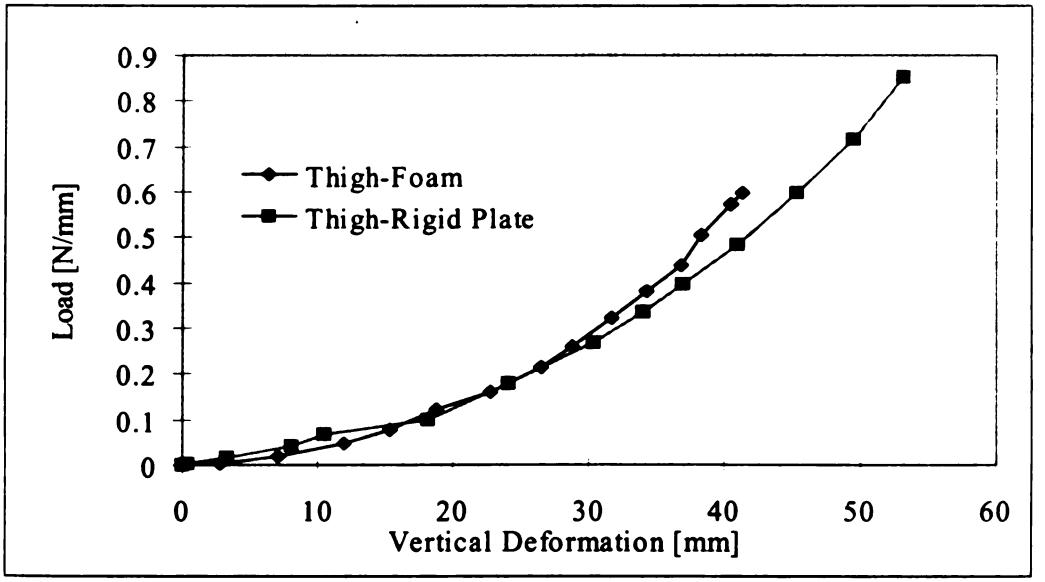

Figure 4.30 Typical Load Normalization for Thigh-Foam (43 kg/m^3 Foam Density) Interaction and Thigh-Rigid Plat Tests.

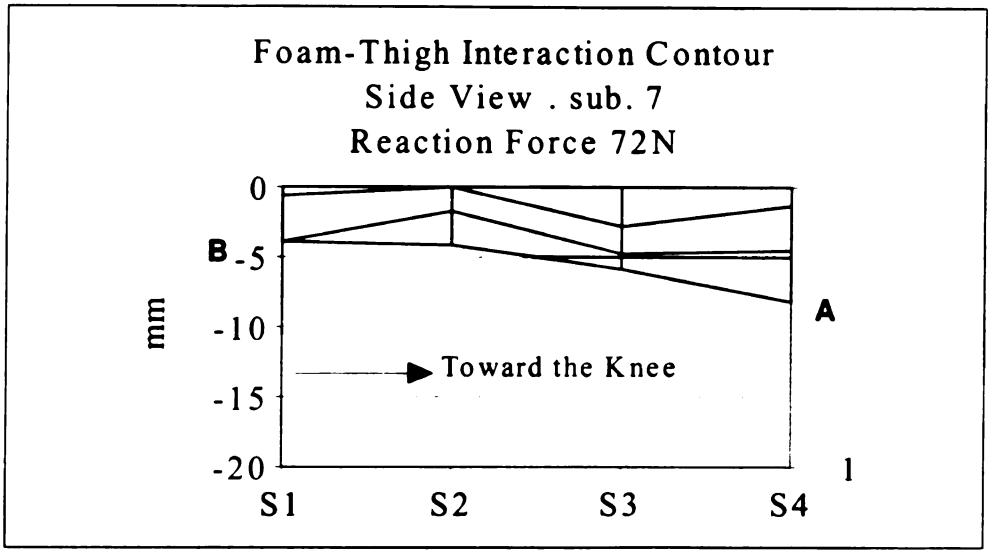

Figure 4.31 Typical Side View of Foam-Thigh Interaction Contour.

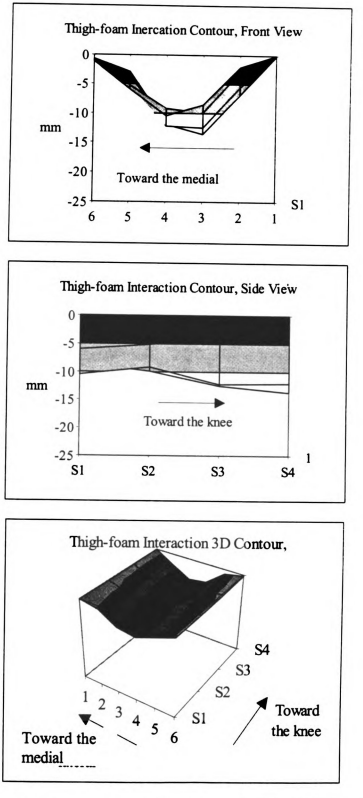

Figure 4.32 Average Contour of Thigh-Foam Interaction Contour, Knee angle 100°

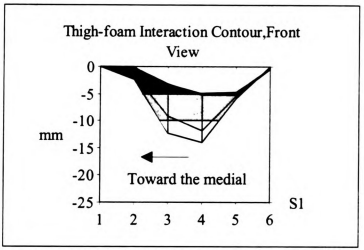

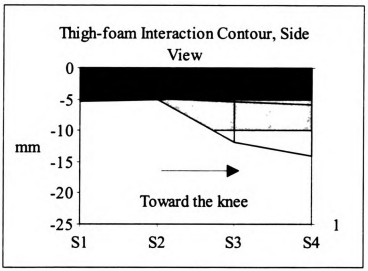

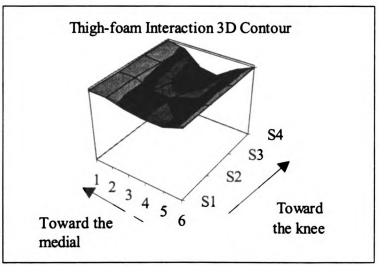

Figure 4.33 Average Contour of Thigh-Foam Interaction Contour, Knee angle 130°

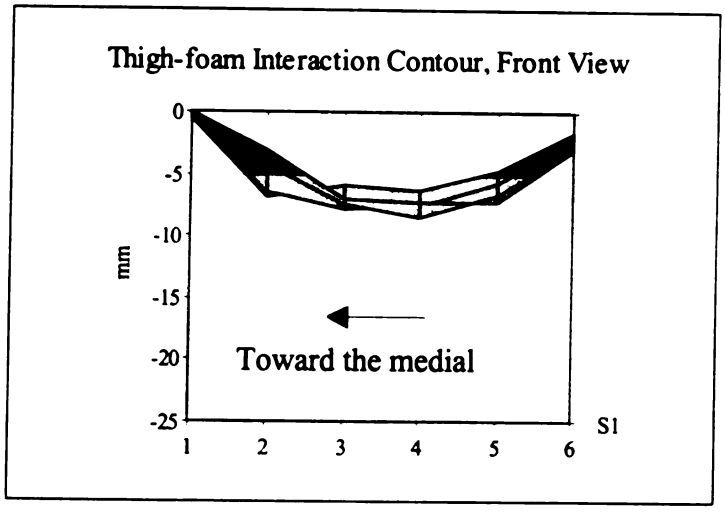

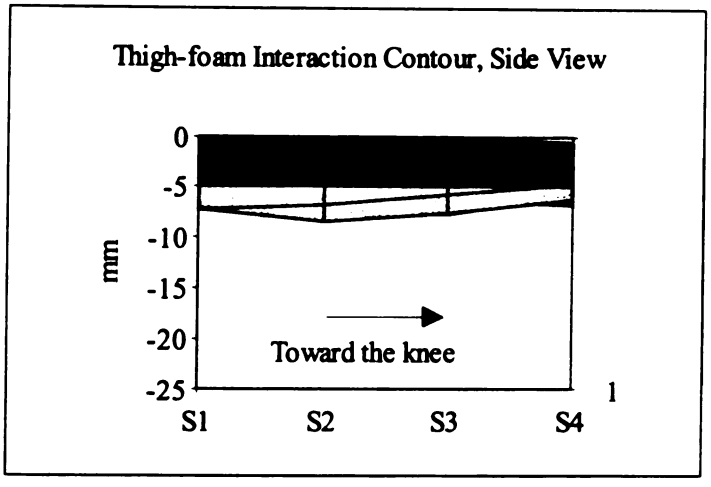

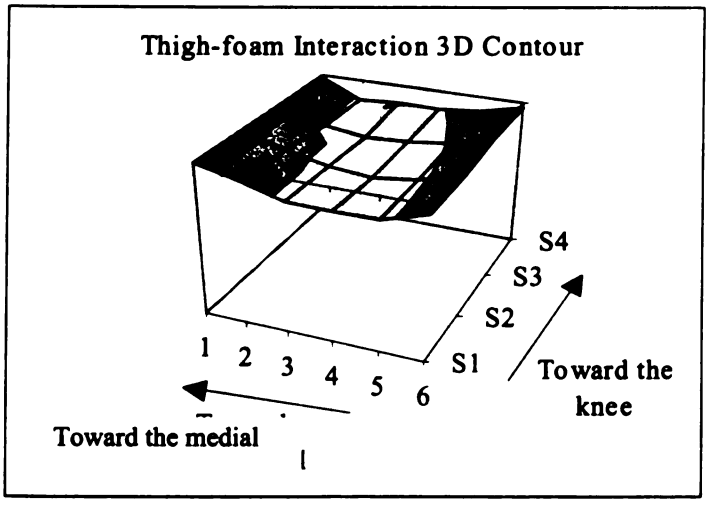

Figure 4.34 Standard Deviation Contour of Thigh-Foam Interaction Contour, Knee angle 100°

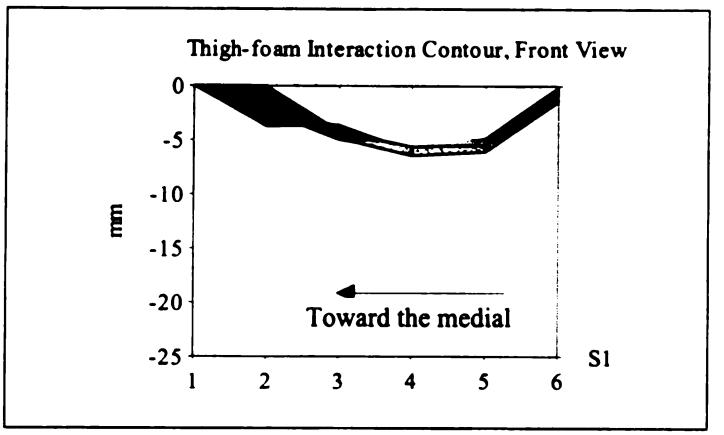

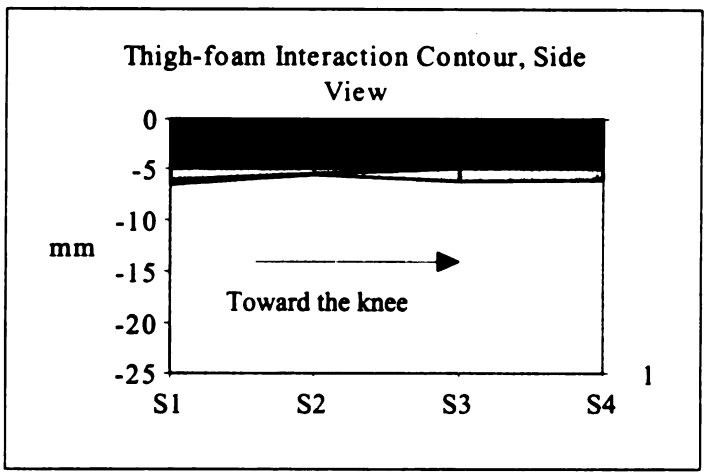

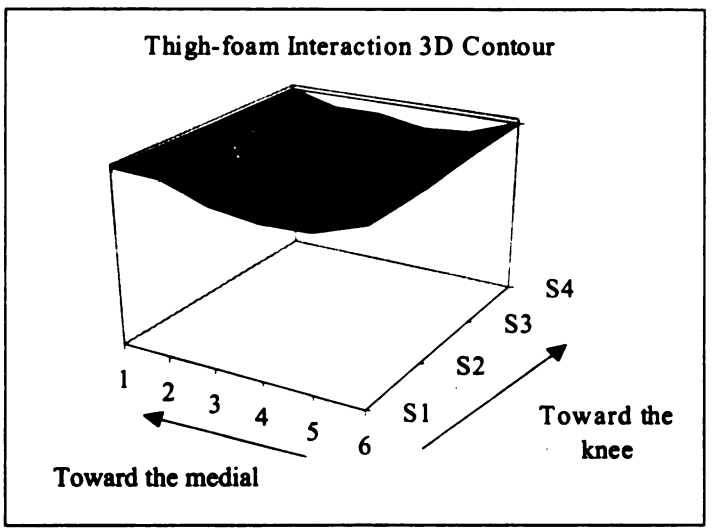

Figure 4.35 Standard Deviation Contour of Thigh-Foam Interaction Contour, Knee angle 130°

CHAPTER 5

CONCLUSIONS AND FUTURE WORK

The objectives of this study were to measure load-deformations responses of the human thigh with different foam thicknesses and densities and to provided thigh geometry, thigh structural properties and foam mechanical properties for finite element modeling.

Thigh dimensions for three sections were measured for seven subjects. Femur bone geometry was estimated from statistical analyses of six femurs measurements. The location of the femur in each subject's right thigh was estimated by locating three landmarks: lateral condyle, medial condyle, and greater trochanter.

The load-deformation responses of the thighs of seven subjects with two knees angles 100° and 130° were measured using a thigh-rigid plate test to provide structure properties for finite element modeling. The initial load to deformation ratio was very small. As the load increased, the soft tissues of the thigh at the contact region were deformed vertically and laterally, and the contact area increased greatly. As a result, the load to deformation ratio increased. This is a typical nonlinear load-deformation response for soft tissues under compression with increasing in contact area.

The behavior of the thigh tissue under compression load was represented by splitting the load-deformation curve into two linear parts. The second part of the curves represents the working region of the thigh stiffness when the thigh typically interacts with the seat in seated postures. Lines were fit by regression equations to estimate the thigh stiffness for each subject with different knee angles and to find the variance and the average of the

thigh stiffness for the seven subjects. Also the fitting lines for the second part could be used to linerearize the thigh structural behavior.

A typical nonlinear stress-strain relationship for cellular materials was obtained from the load-deformation for the uniaxial compression test of foam samples. The stress-strain relationship exhibited three different phases. At low strains, the foam showed a linear response followed by continuing deformation at almost constant stress. Finally the stress increased rapidly. The foam exhibited highly compressible behavior and zero Poisson (ν) effect in compression.

The thigh-foam interaction contour was accomplished by transferring the deformed shape of the foam surface to video images using wires through the foam. Deformation of the mid-thigh was selected for studying the large deformation of the soft-tissues with different foam thicknesses and densities. As the thighs and foams were loaded, the deformation of the thigh was relatively large and the initial stiffness was low. The initial deformations in the foam were smaller with stiffness that was greater than the thigh. As loading increased, the stiffness of the thigh increased and the stiffness of the foam decreased. The thigh deformations did not vary significantly with different foam thicknesses and densities but did vary with different knee angles. That means that changing the posture affects the thigh deformation more than the foam stiffnesses.

This study provided quantitative data to develop a deformable model and useful information for thigh-foam interaction behavior that can be used in seat cushion design.

Work is ongoing to measure the contour of the thighs, buttocks, and the backs for different people in different seated postures with different foam stiffnesses. The recommendations for future work are:

1. Relate thigh deformation to subjectively feel of comfort .
2. Study time-deformation responses of the thigh and buttock. This can be used to evaluate the change in the thigh-foam contour in time with seated posture.
3. Measure the corresponding load for each wire displacement to proved the finite element model load-displacement data for each node (wire). This can be measured by using pressure mat on the seat cushion.
4. Measure the three-dimensional contours of thighs and buttocks before and after deformation by using a combination of contour measurement system and motion analysis system. This will provide useful information to study the change in human contours due to the deformation in the soft tissue in seated posture.

APPENDICES

APPENDIX A

CONSENT FORM FOR THE NON-INVASIVE MEASUREMENT OF DEFORMATIONS AND LOADS IN THE HUMAN THIGHS OF SEATED POSTURES

INFORMED CONSENT STATEMENT

I,_____, consent to serve to an experimental subject in the research project, "Non-invasive measurement of deformation and load in the thighs and buttock of sitting people." The purpose of this research project is to study the deformation characteristics of the back of human thighs and buttocks as they are loaded by a deformable cushion like foam that is typical for seats in automobile seats or office chairs. You will be seated in a special chair that supports your back, pelvis, and feet, and a surface will be raised into contact with the back of your thigh for about half the area between your buttocks and knee. This surface will be either a flat plate or a padded cushion. This surface will be raised until the weight of your leg is fully supported. There is no restraint of your leg to upward movement and the limit of the load on the back of your thigh will be the weight of your leg. This procedure will be repeated with your foot supported in different positions to obtain information at various angles of your knee. The results from these measurements will be compared to the results from a theoretical computer model and used to improve the understanding of the interactions between people's bodies and the seats that support them.

I have been thoroughly informed of the purpose and procedures of this study in which I will participate.
I have been advised that all work will be conducted under the supervision of individuals who are experienced with measuring loads and deformations in the thighs of human subjects.
I have been given an opportunity to request that the experimenter be of my same gender.
I understand that the tests are non-invasive and that it will take twenty minutes to take anthropometric measurements, next it will take one hour to collect seated measurements of thigh deformation.
I have been assured that my participation remains confidential, and published experimental results will not reveal my identity.
My consent to serve as subject is given freely and without coercion.
Further, I understand that I may withdraw from this experiment at any time and reason of my choice.

_____ _____
SUBJECT SIGNATURE DATE

_____ _____
TYPED OR PRINTED NAME ADDRESS

_____
PHONE NUMBER

_____ _____
WITNESS DATE

_____
TYPED OR PRINTED WITNESS' NAME
If you have any questions, contact Prof. Robert Hubbard at 517-353-5013 or hubbard@msm.msu.edu

APPENDIX B

COPYRIGHT PERMISSION

IGAKU-SHOIN MEDICAL PUBLISHERS, INC.
ONE MADISON AVENUE, NEW YORK, NY 10010
(212) 779-0123 Fax (212) 779 0322

September 27, 1996

Mr Akram Ali
Biomechanics Department
E Fee Hall, Rm A-439
Michigan State University
College of Osteopathic Medicine
Department of Osteopathic Manipulative Medicine
East Lansing, Micigan 48824-1316

Dear Mr Ali

Please note that the request to reproduce the material quoted on the attached form(s) is granted

Also be advised that the credit line should read "Courtesy of Johannes W. Rohen, Dr med , Chihiro Yokochi, MD, in collaboration with E.C.B. Hall-Craggs from the book COLOR ATLAS OF ANATOMY· A PHOTOGRAPHIC STUDY OF THE HUMAN BODY, SECOND EDITION, Igaku-Shoin Medical Publishers, New York, NY, 1988 "

Please don't hesitate to contact me if you have any questions or if I can be of any further assistance

Sincerely,

Alina Cusati
Editorial Assistant

Enclosure

APPENDIX C

LOAD CELL SPECIFICATION

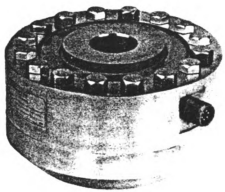

	Load Range	Static Error Band (+/-%) F.S.)*	Non-linearity (% F.S.)**
Model 45	200; 500; 1,000;	.05	.05
	2,000-10,000	.05	.05
	25,000; 50,000;	.05	.05
	100,000	.07	.05
Model 47	200; 500; 1,000; 2,000	.02	.02
	5,000; 10,000	.03	.03
	25,000; 50,000	.04	.03
	100,000	.06	.05
Output (std.)		2mv/v	
Fatigue life		10⁶, Fully reversed	
Symmetry		1%	
Resolution		Infinite	
Temperature, Operating		-65° to 200° F	
Temperature, Compensated		0° to 150° F	
Temperature Effect			
- Zero (max)		.10% F.S./100° F	
- Span (max)		.15% F.S./100° F	
Strain Gage Type		Bonded foil	
Excitation (calibration)		10VDC	
Excitation (acceptable)		Up to 15VDC or VAC	
Insulation Resistance		5000 megaohms @ 50VDC	
Bridge Resistance		350 ohms	
Shunt Calibration Data		Included	
Wiring Code		See Below	
Electrical Termination (std.)		PC02A-10-6P (cable optional with 1/4 NPT conduit connection)	
Mating Connector (not incl.)		PC06A-10-6S	
Static Overload Capacity		200%	
Deflection—Full Scale		.001" to .003"	
Material		17-4 PH stainless steel	
Outputs Available		+/- 5VDC, 4-20 mA	

APPENDIX D

DIGITAL CALIPER SPECIFICATION

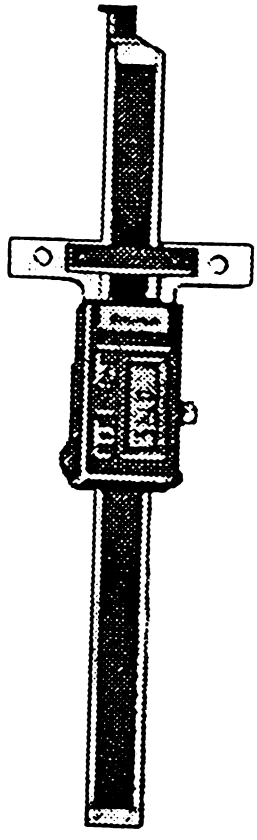

Mitutoyo and Starrett Electronic Depth Gauges

Sliding scale and LCD provide quick, easy-to-read depth measurements of holes, slots, and recesses.

Display features inch/mm conversion, zero setting, and SPC output. A knurled screw locks gauge on the hardened stainless steel bar. Battery and fitted case are included.

STARRETT 745 SERIES

0-6"/150mm	745Z-6	±0.001" (0.025mm)	**85945A66**	**236.60**
7" Extension	745E-7		**85945A67**	**26.25**
12" Extension	745E-12		**85945A68**	**44.80**
SPC Cable	22650		**8602A66**	**29.95**
Replacement Battery (requires 2)			**21105A169**	**1.14**

APPENDIX E

LOAD-DEFORMATION RESPONSES FOR THE FOAMS AND THE THIGHS

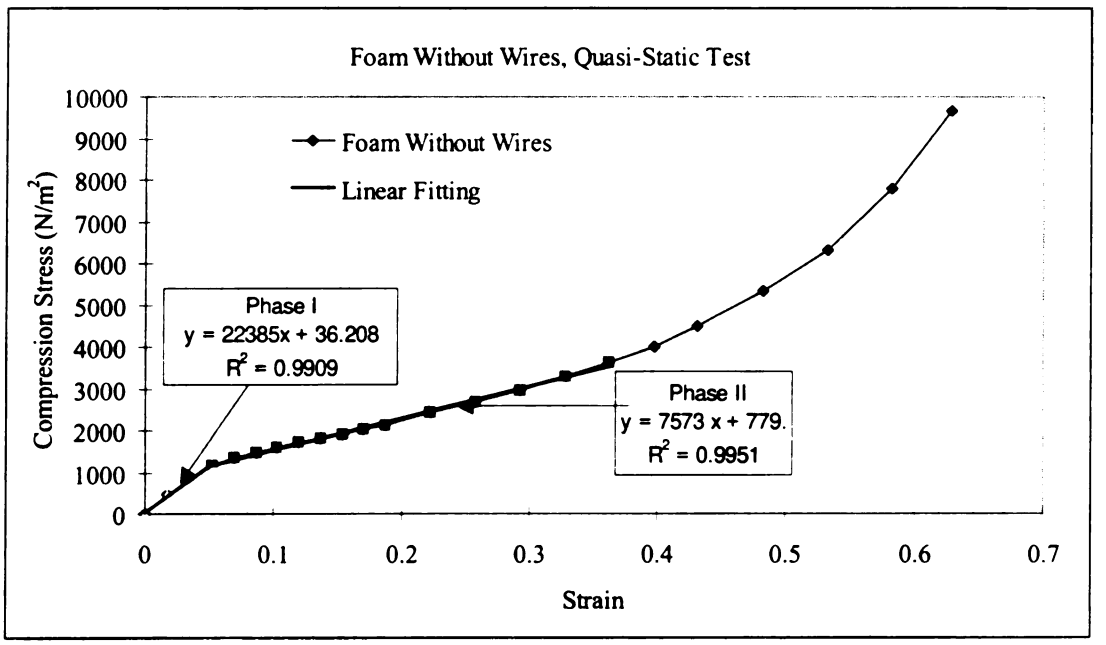

Figure E.1 Best-Fit Lines were Developed to Obtain Young's Modulus for Phase One and the Tangent Modulus for Phase Two of Compression, Quasi-Static Test for 43 Kg/M^3 Foam Density (Foam Without Wires).

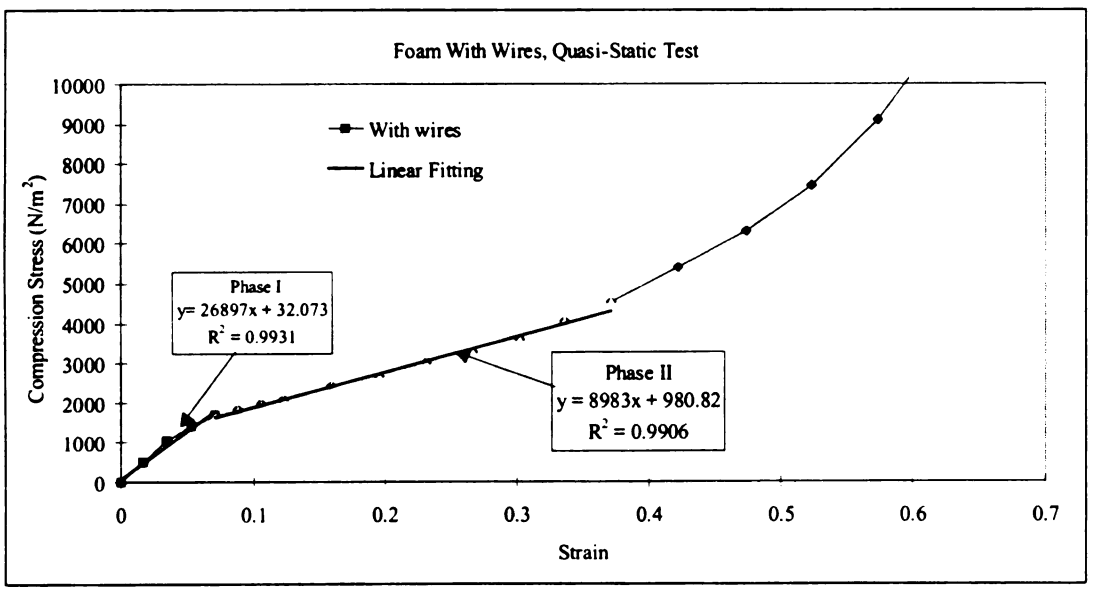

Figure E.2 Best-Fit Lines were Developed to Obtain Young's Modulus for Phase One and the Tangent Modulus for Phase Two of Compression, Quasi-Static Test for 43 Kg/m^3 Foam Density (Foam With Wires).

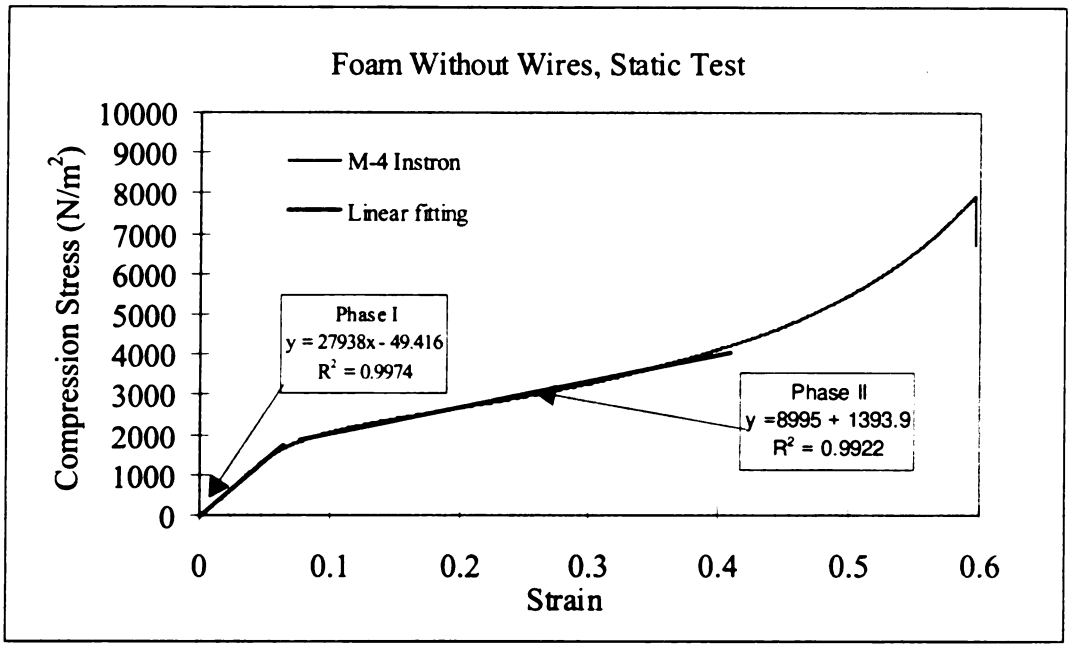

Figure E.3 Best-Fit Line were Developed to obtain Young's modulus for Phase One and the Tangent Modulus for Phase Two of Compression, Static Test (ASTM)for 43 Kg/m3 Foam Density.

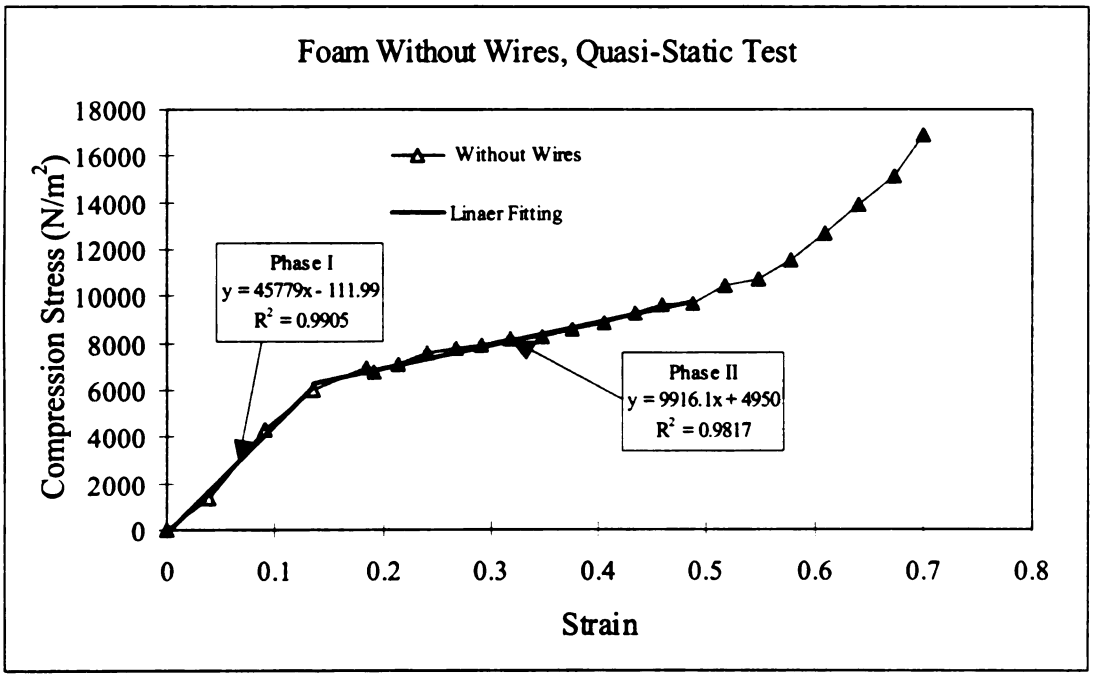

Figure E.4 Best-Fit Lines were Developed to Obtain Young's Modulus for Phase One and the Tangent Modulus for Phase Two of Compression, Quasi-Static Test For 51 Kg/m^3 Foam Density (Foam Without Wires).

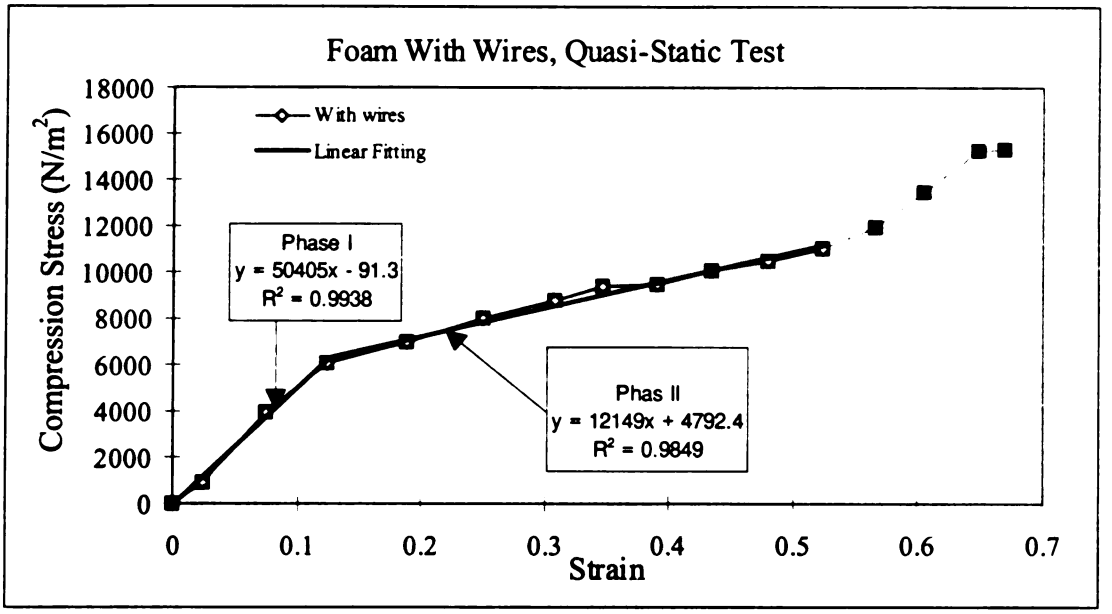

Figure E.5 Best-Fit Lines were Developed to Obtain Young's Modulus for Phase One and the Tangent Modulus for Phase Two of Compression, Quasi-Static Test for 51 Kg/m^3 Foam Density (Foam With Wires).

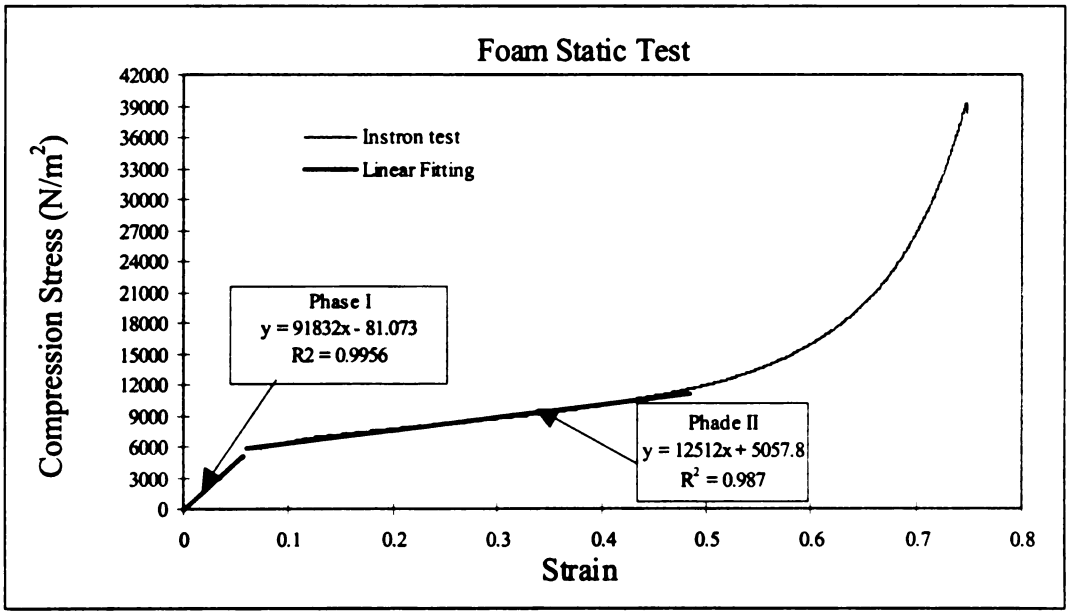

Figure E.6 Best-Fit Lines were Developed to Obtain Young's Modulus for Phase One and the Tangent Modulus for Phase Two of Compression Static Test (ASTM) for 51 Kg/m^3 Foam Density (Foam With Wires).

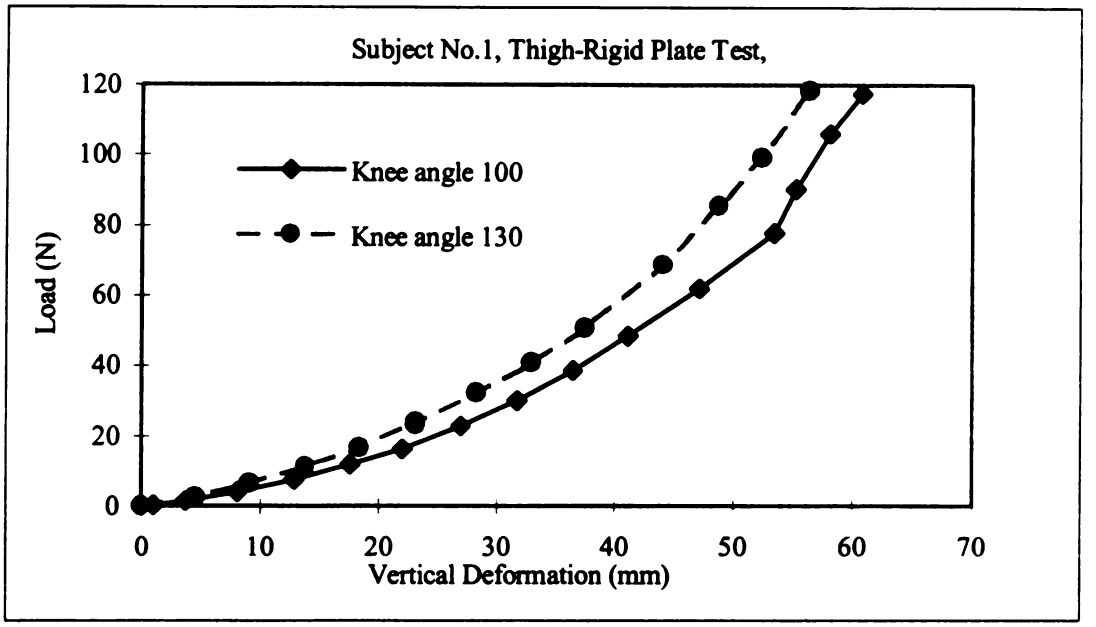

Figure E.7 Load- Deformation Relationship of Thigh Structure for Two Knee Angles, Subject No. 1

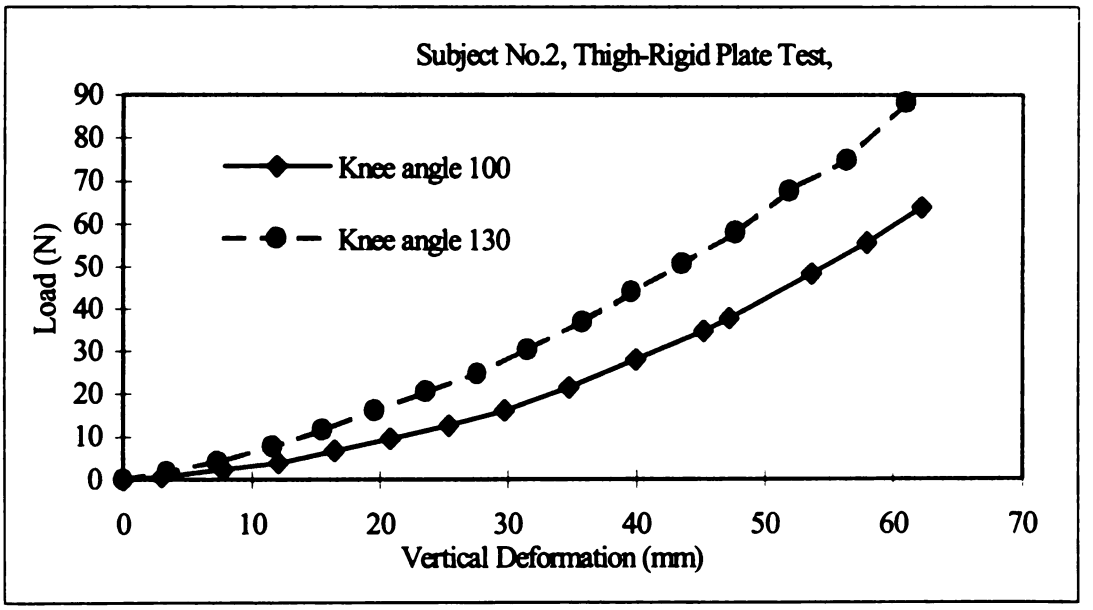

Figure E.8 Load- Deformation Relationship of Thigh Structure for Two Knee Angles, Subject No. 2

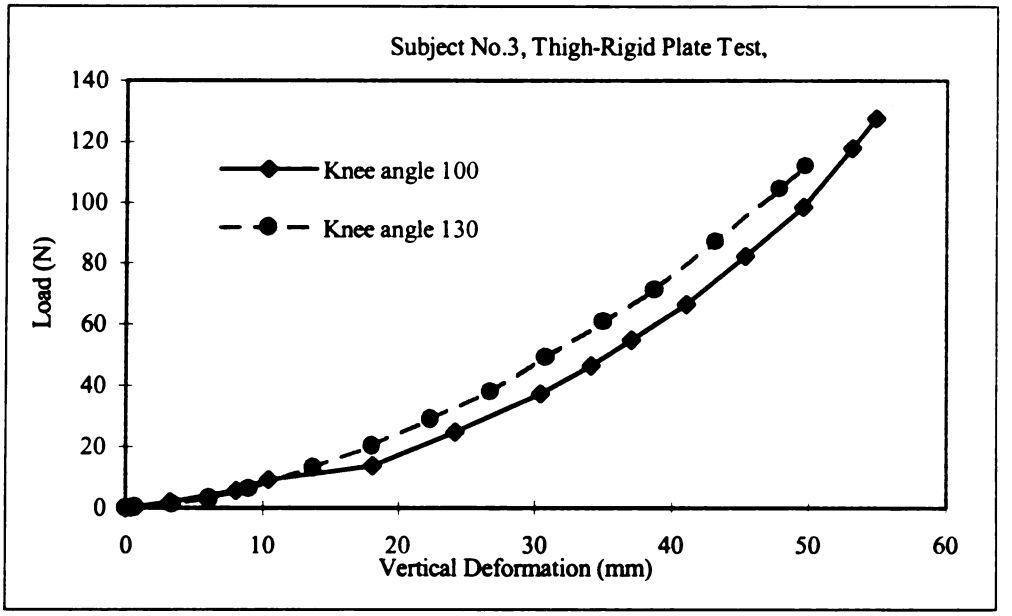

Figure E.9 Load- Deformation Relationship of Thigh Structure for Two Knee Angles, Subject No. 3

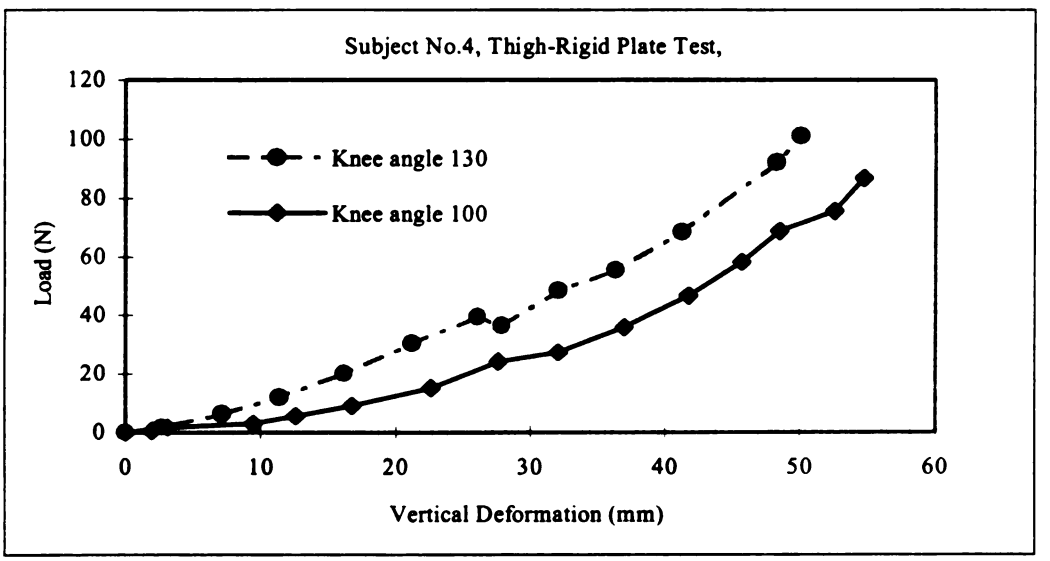

Figure E.10 Load- Deformation Relationship of Thigh Structure For Two Knee Angles, Subject No. 4

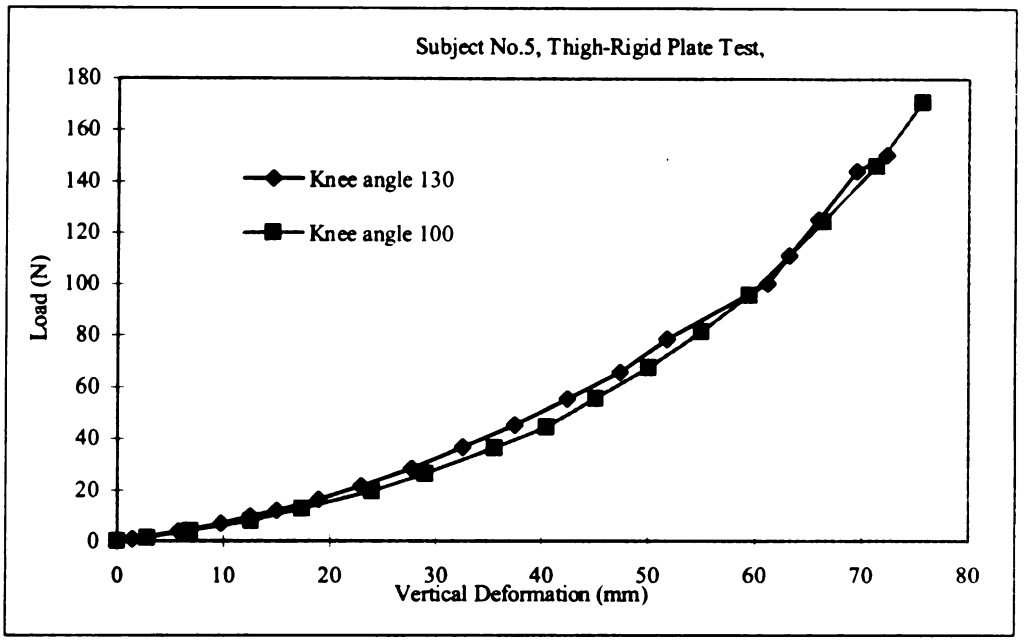

Figure E.11 Load- Deformation Relationship of Thigh Structure for Two Knee Angles, Subject No. 5

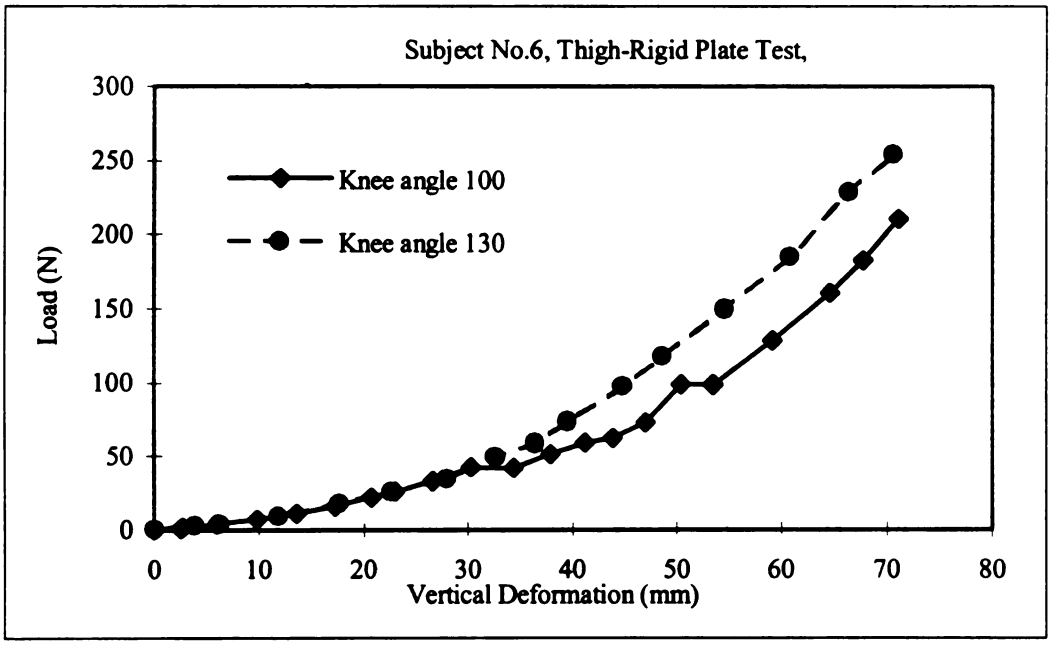

Figure E.12 Load- Deformation Relationship of Thigh Structure for Two Knee Angles, Subject No. 6

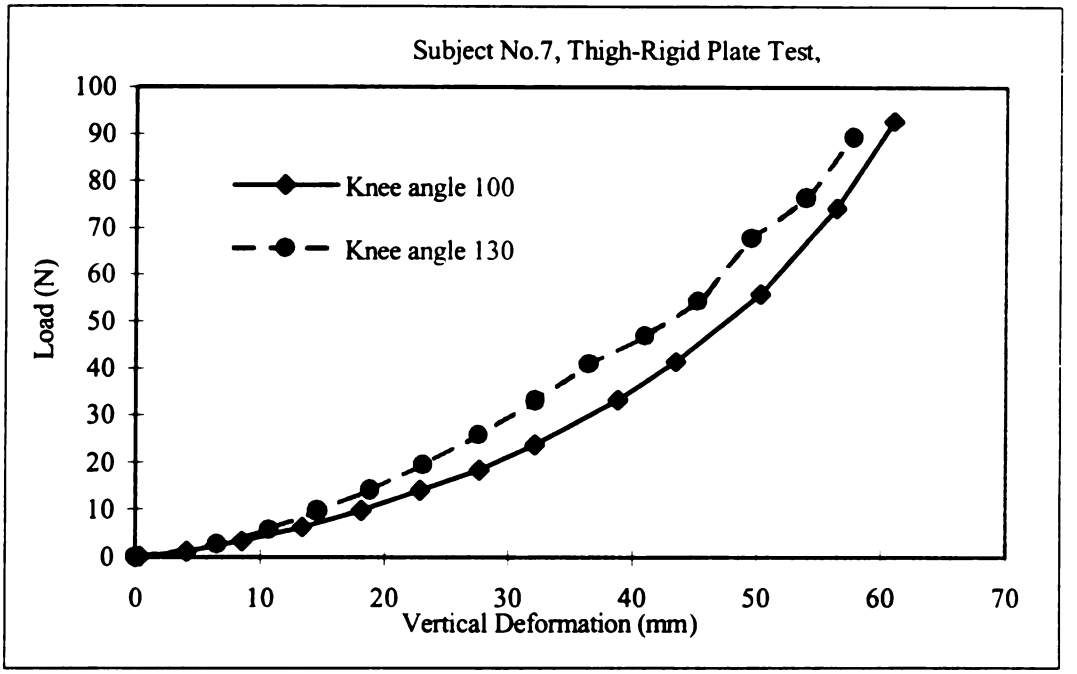

Figure E.13 Load- Deformation Relationship of Thigh Structure for Two Knee Angles, Subject No. 7

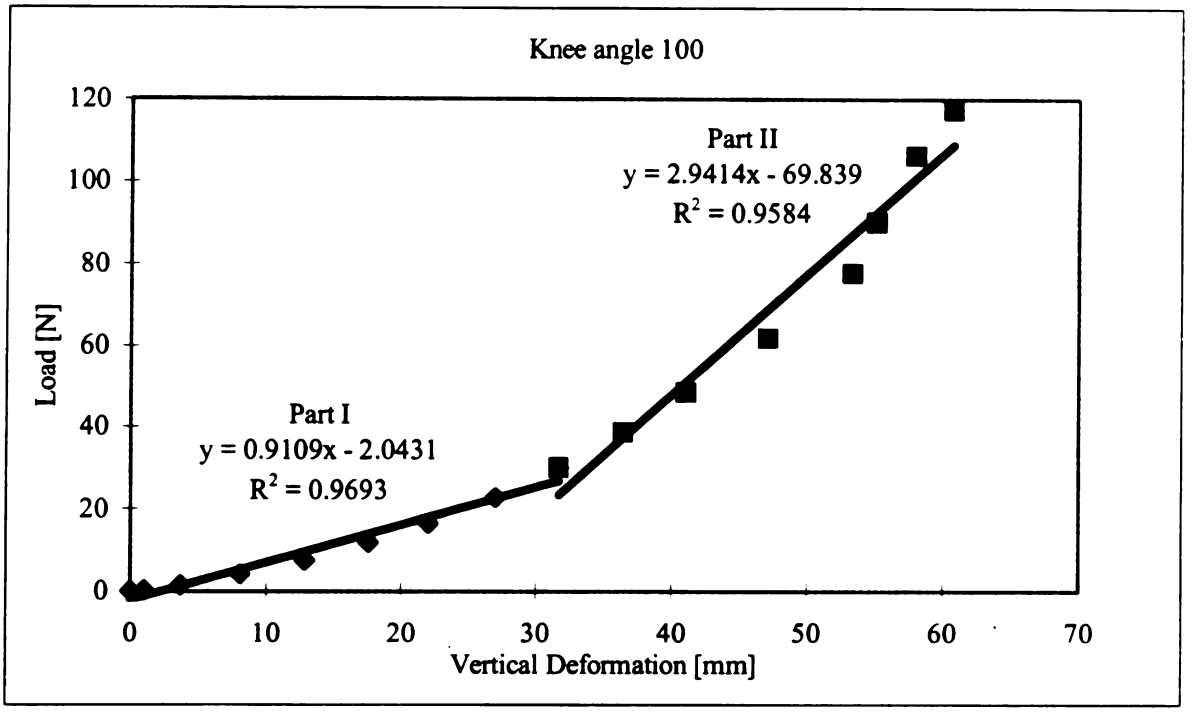

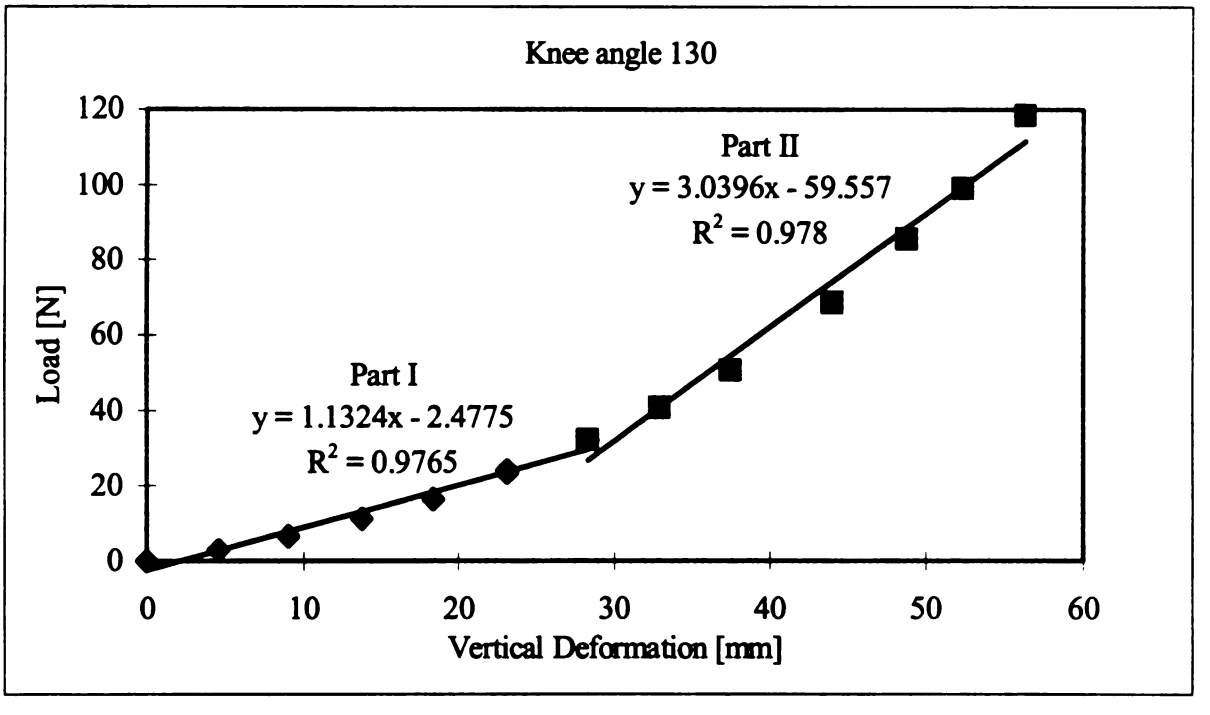

Figure E.14 Best-Fit Lines Were Developed for Load-Deformation Curve of Thigh, Subject No. 1

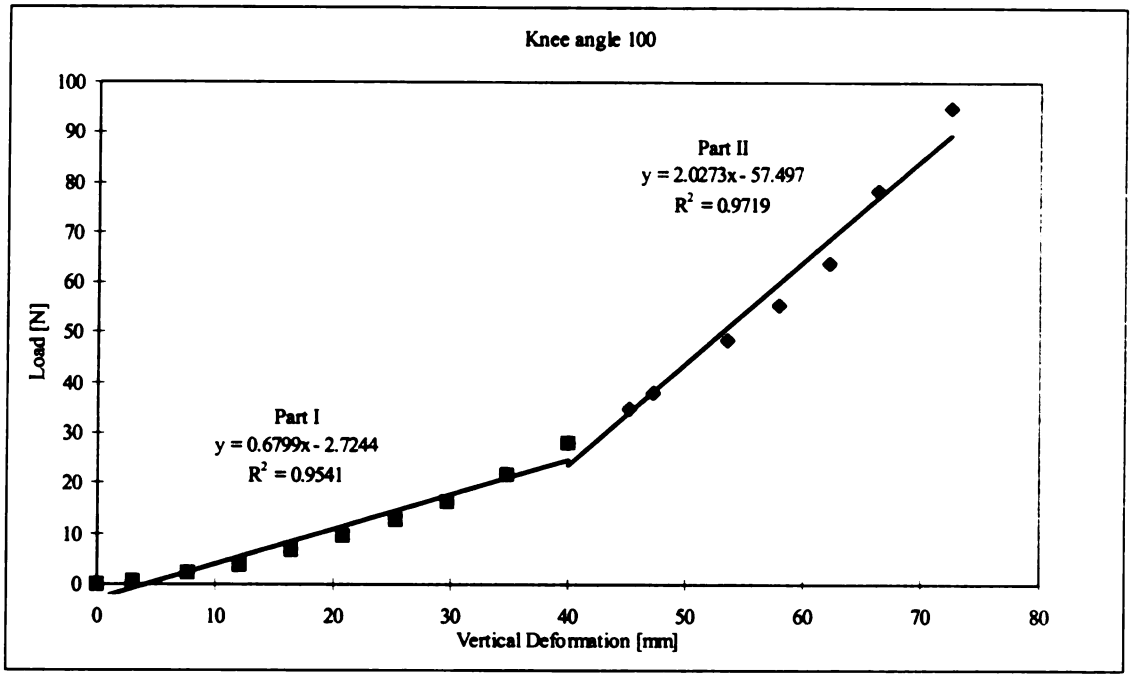

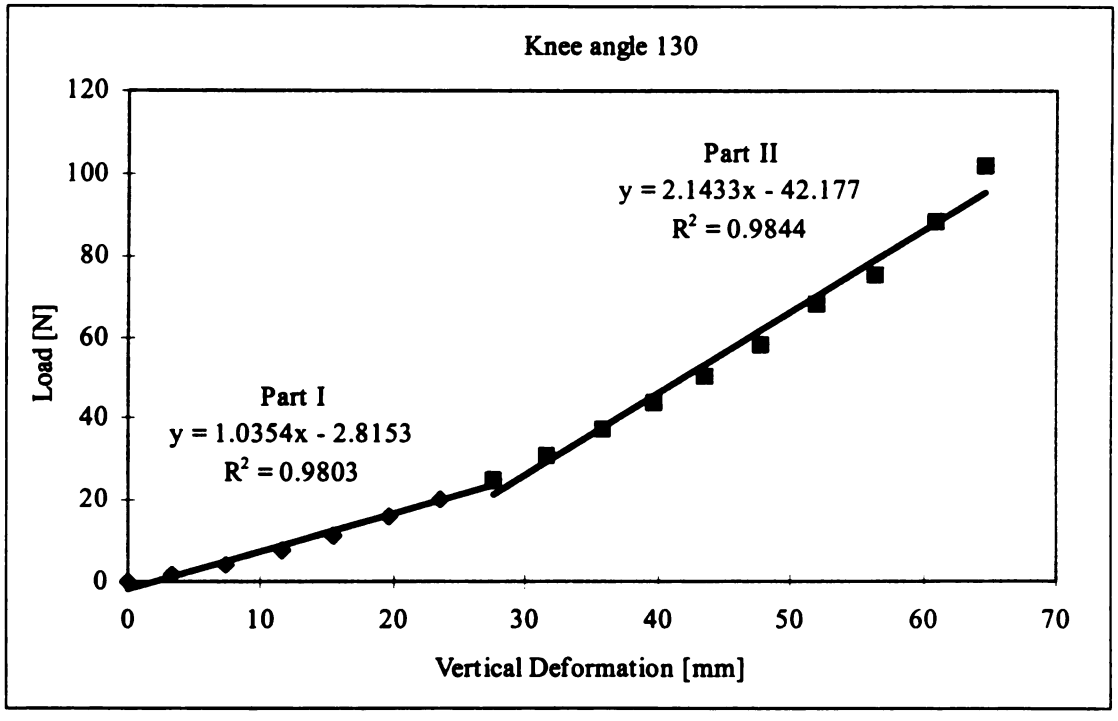

Figure E.15 Best-Fit Lines were Developed for the Load-Deformation Curve of Thigh, Subject No. 2

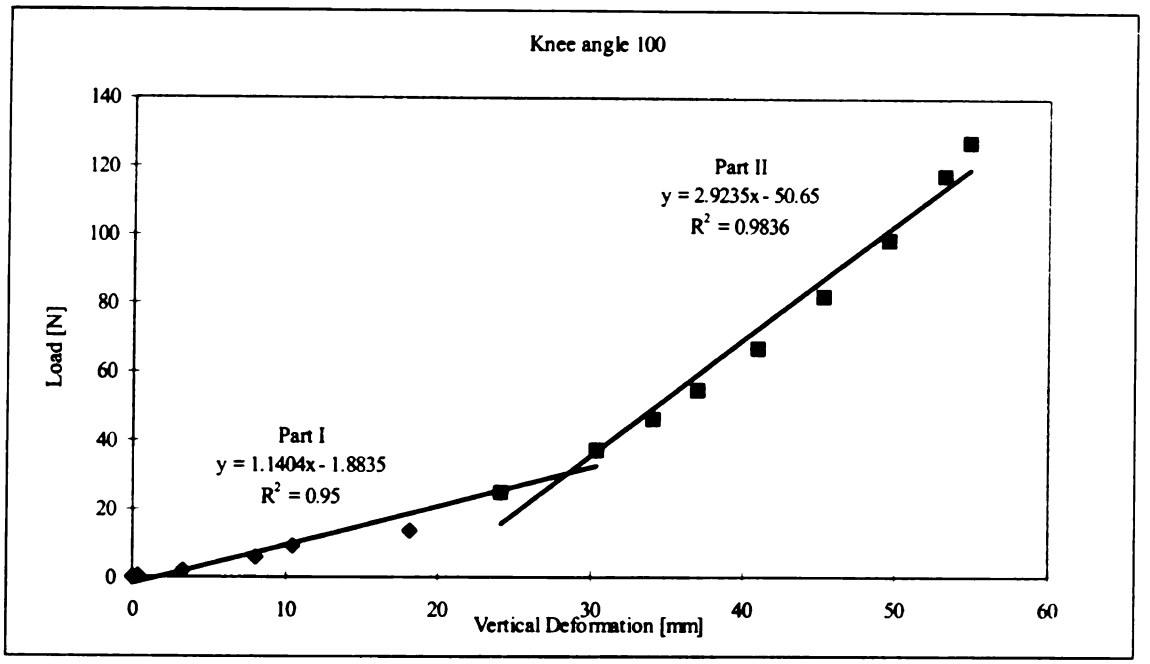

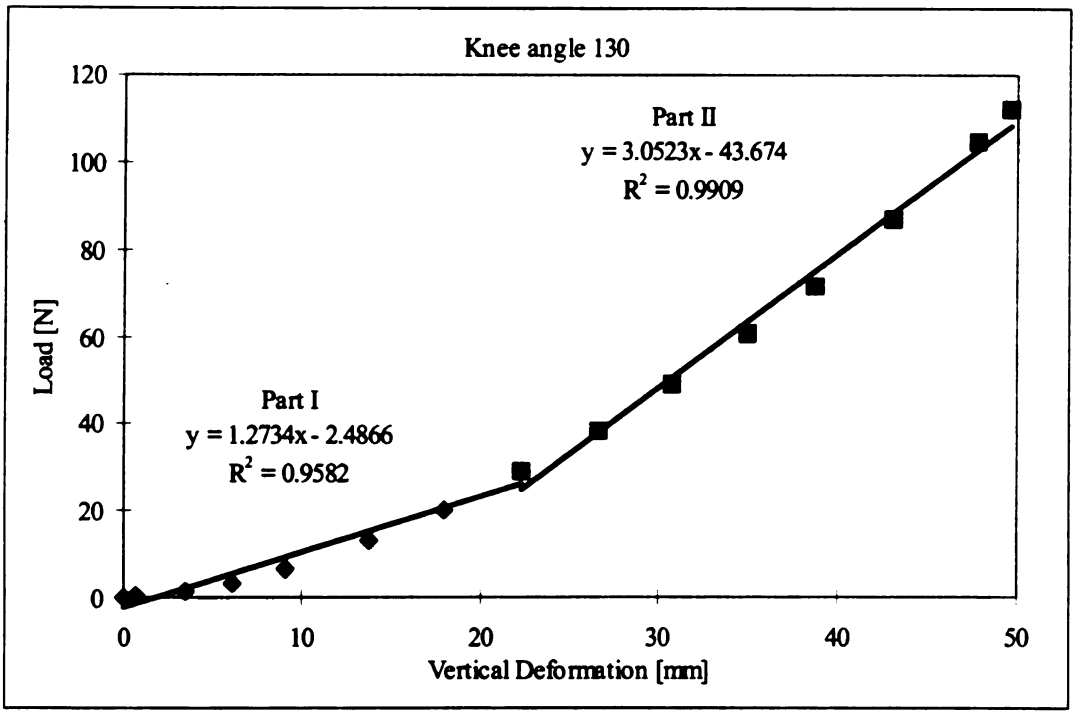

Figure E.16 Best-Fit Lines Were Developed for the Load-Deformation Curve of Thigh, Subject No. 3

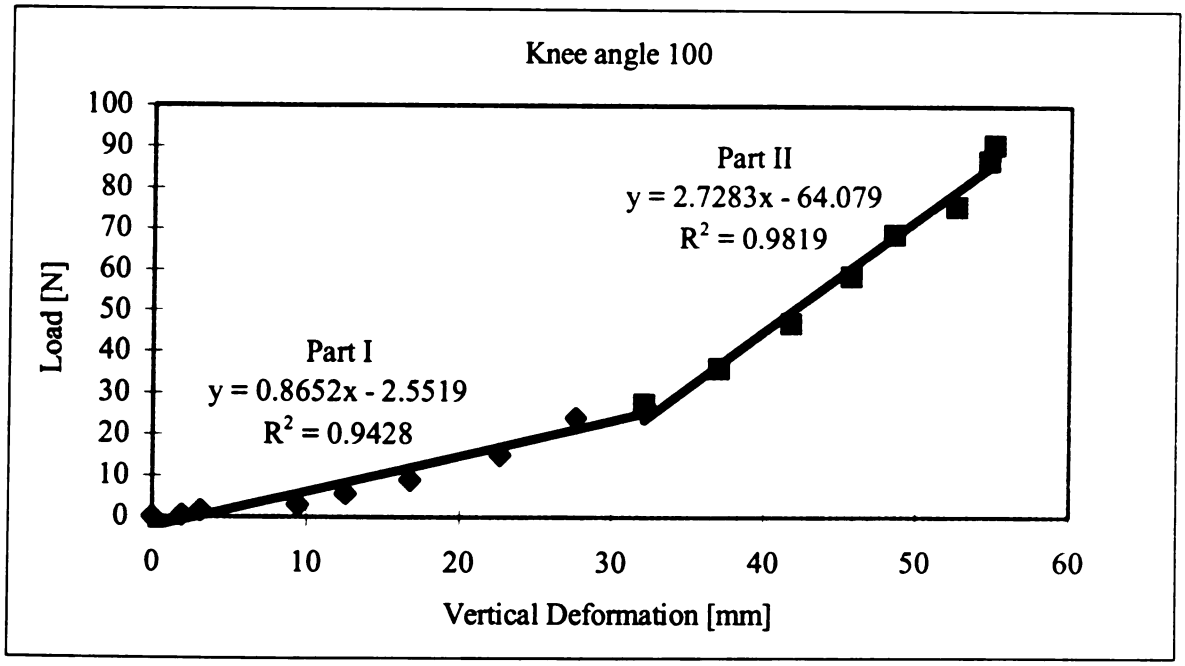

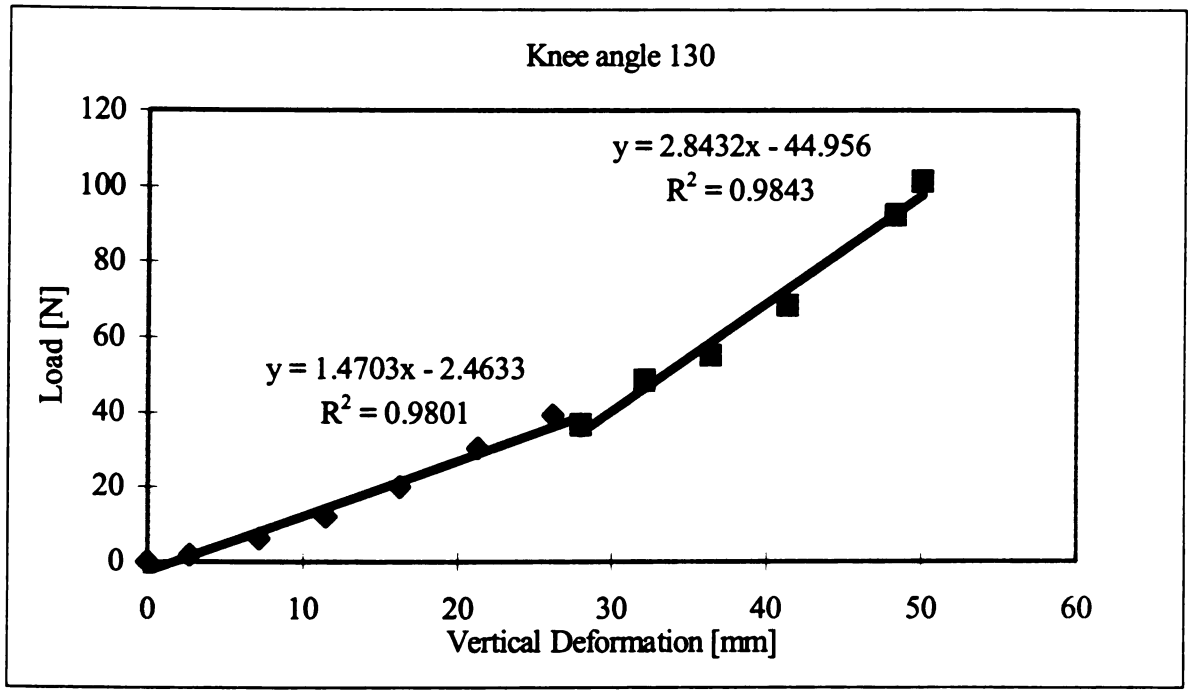

Figure E.17 Best-Fit Lines Were Developed for the Load-Deformation Curve of Thigh, Subject No. 4

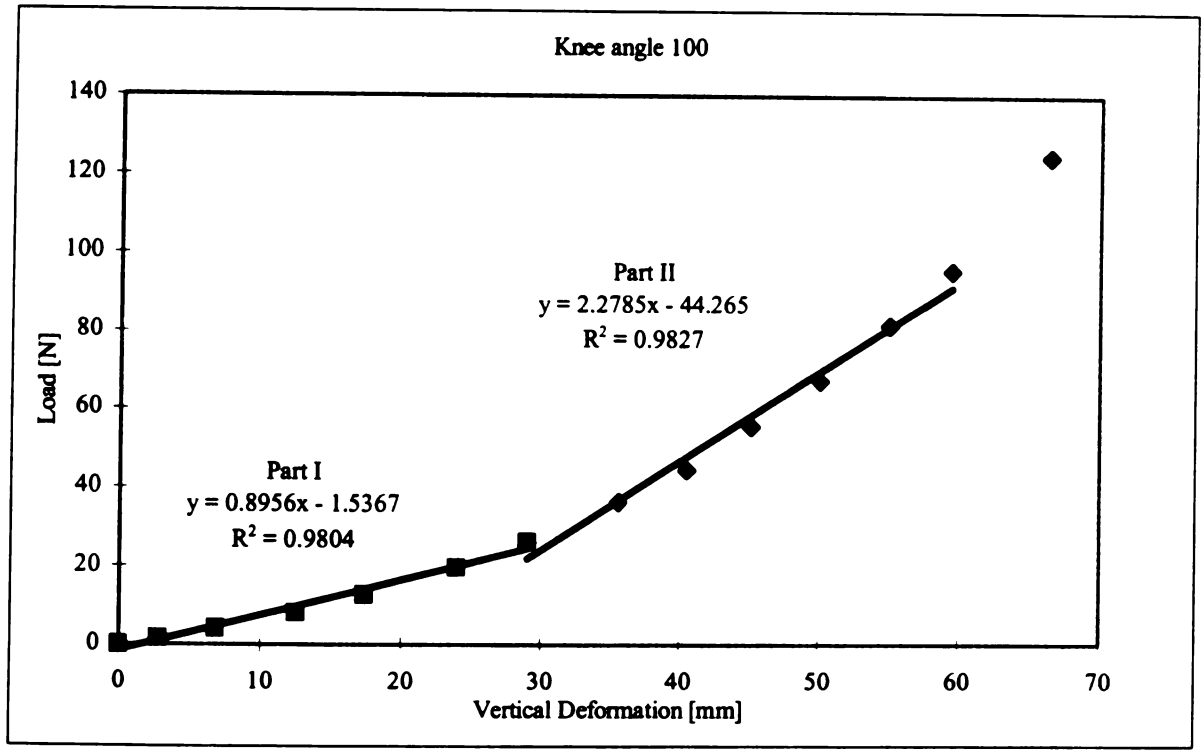

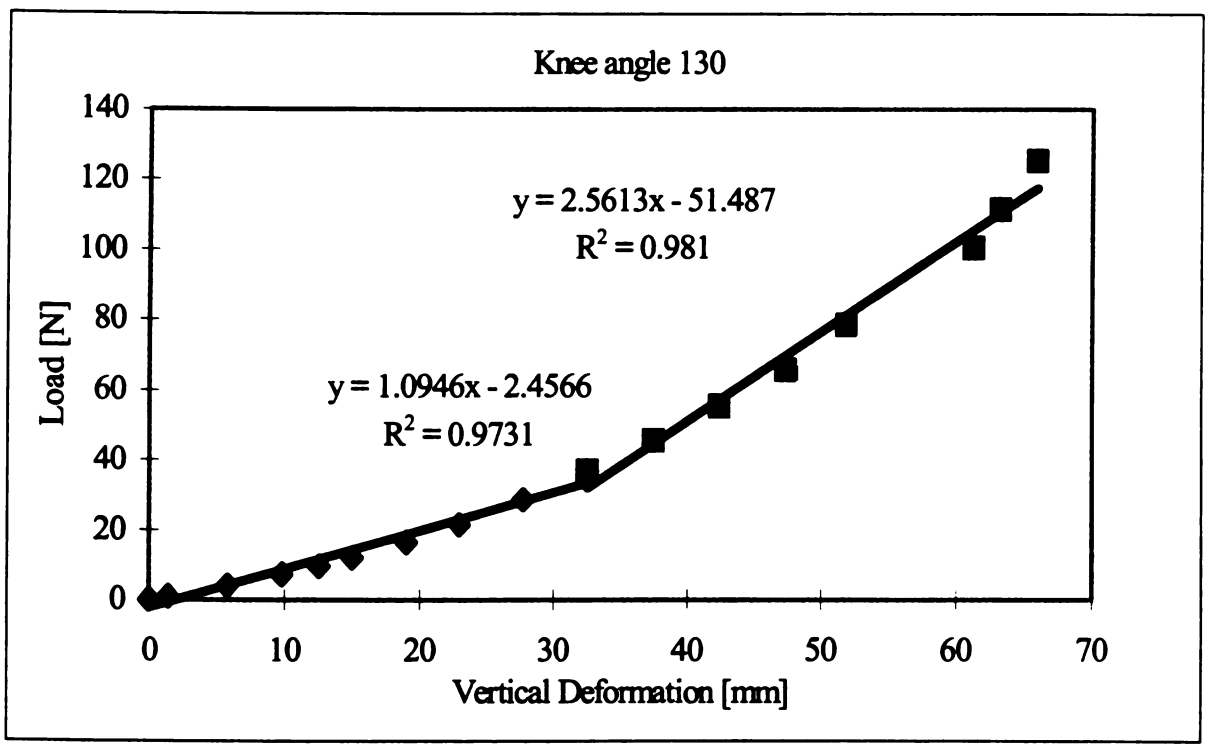

Figure E.18 Best-Fit Lines Were Developed for the Load-Deformation Curve of the Thigh, Subject No. 5

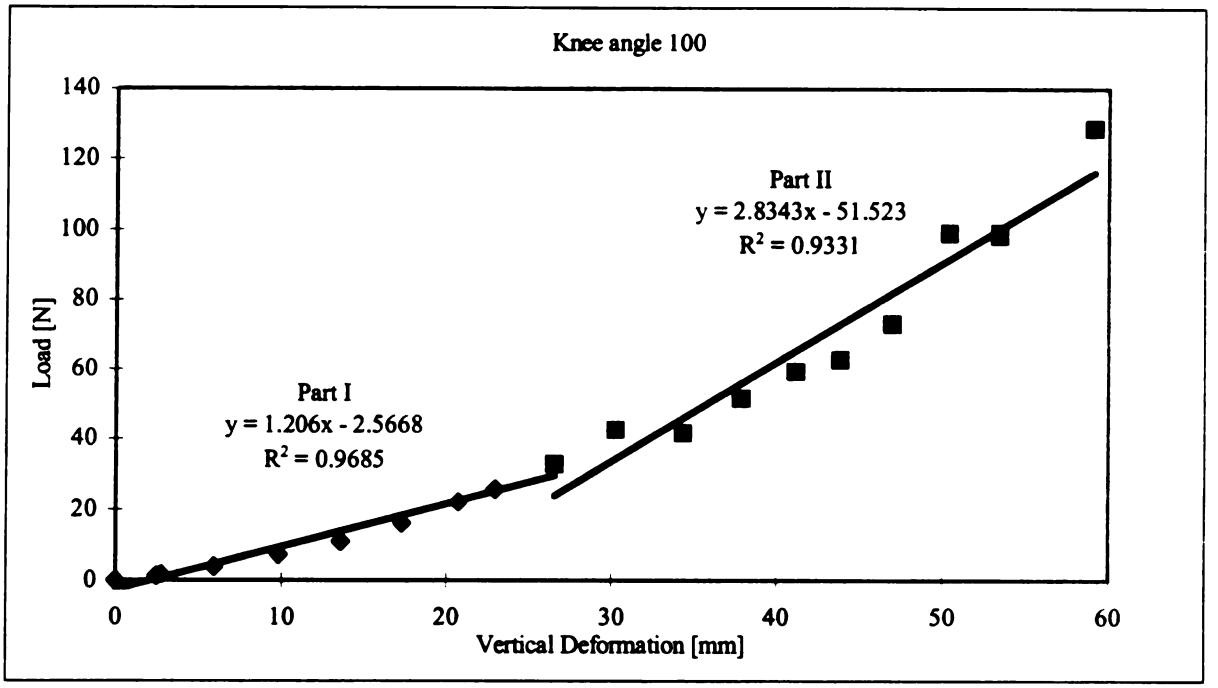

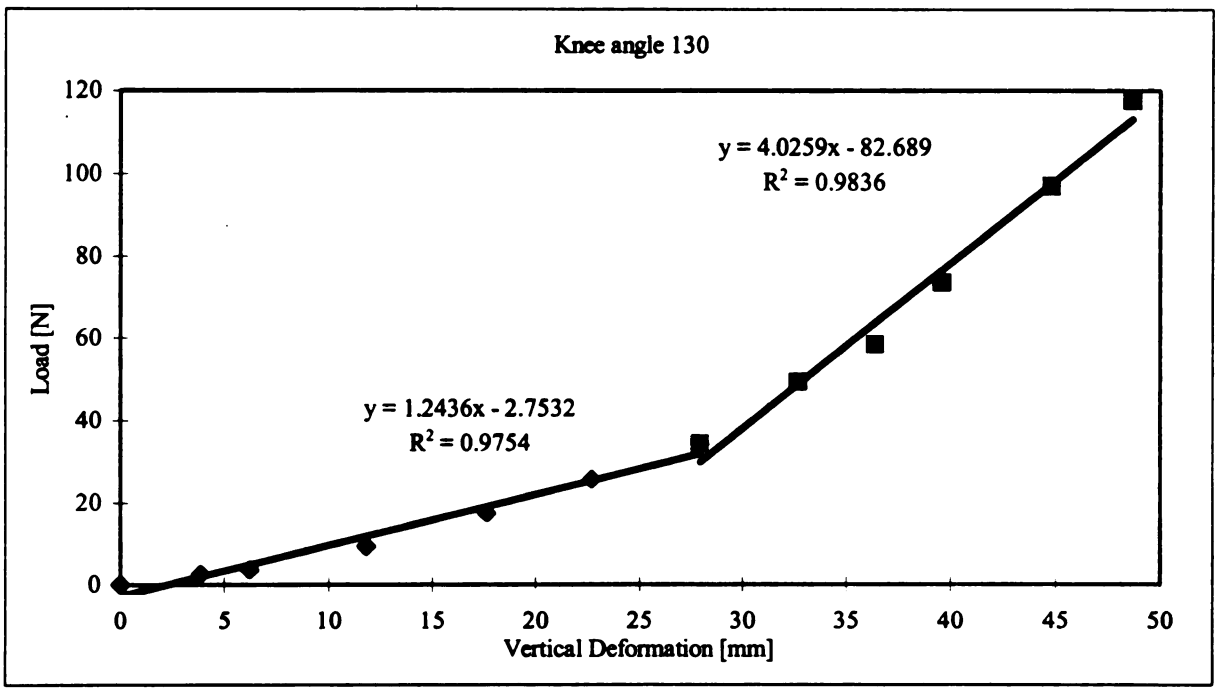

Figure E.19 Best-Fit Lines Were Developed for the Load-Deformation Curve of Thigh, Subject No. 6

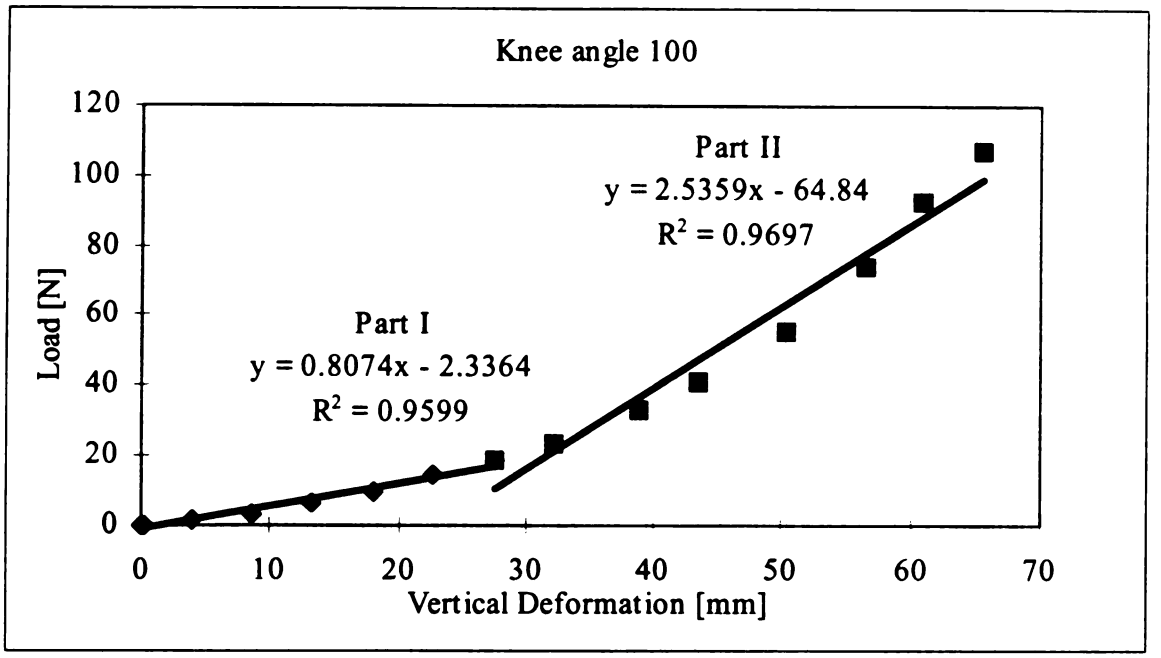

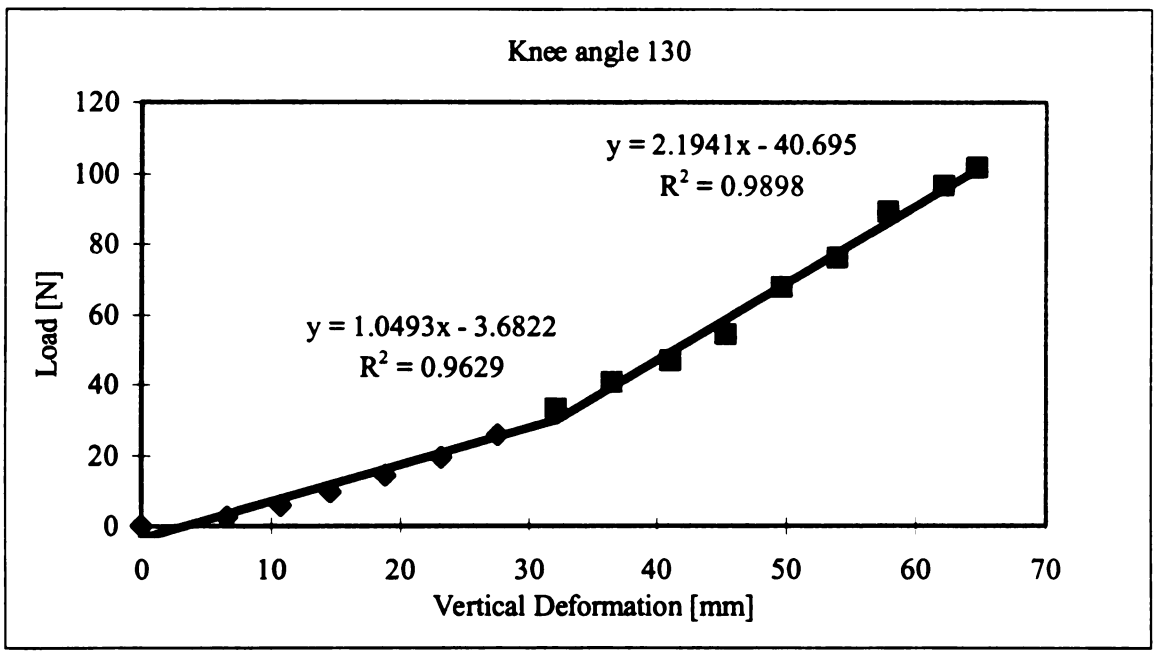

Figure E.20 Best-Fit Lines Were Developed for the Load-Deformation Curve of Thigh, Subject No. 7

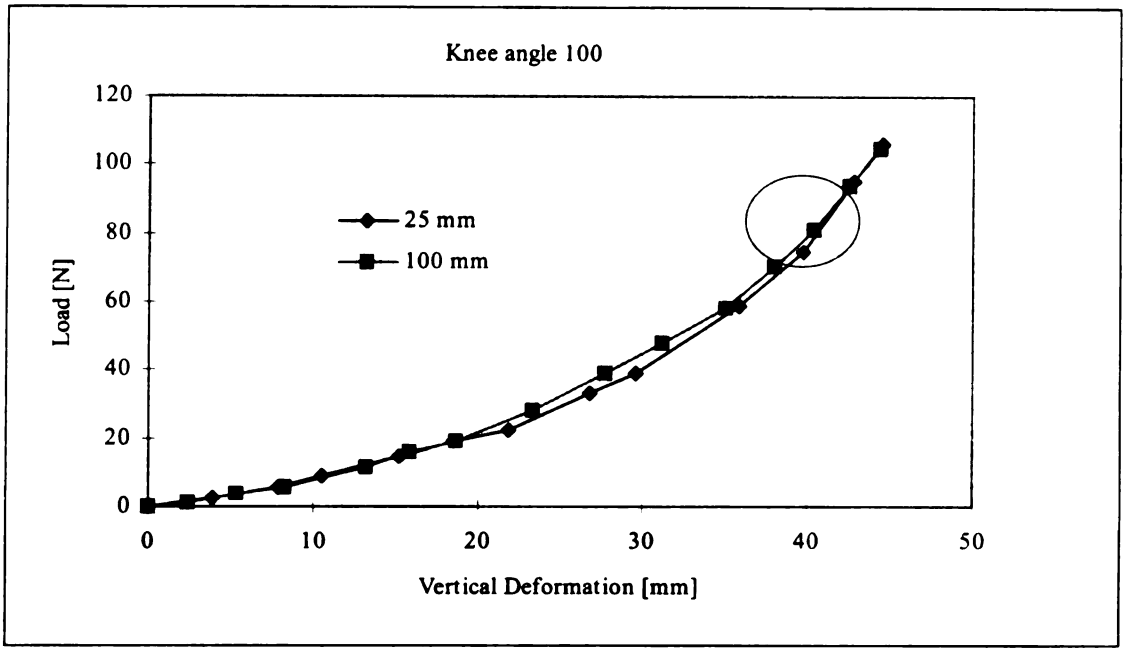

Figure E.21 Load-Deformation Relationship for the Thigh Interaction with 43 Kg/m^3 Foam Density, and with Two Different Thicknesses 25 mm and 100 mm, Knee angle 100°, Subject No.1.

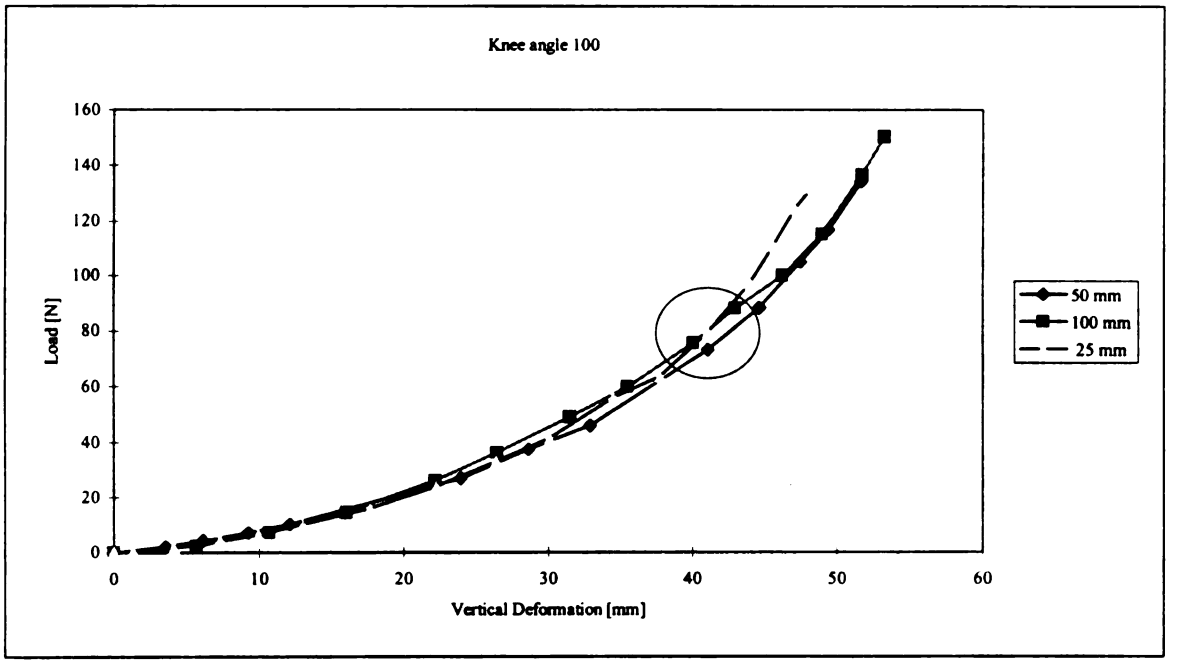

Figure E.22 Load-Deformation Relationship for the Thigh Interaction with 44 Kg/m^3 Foam Density, and with Three Different Thicknesses 25 mm, 50 mm and 100 mm, Knee angle 100° Subject No.1.

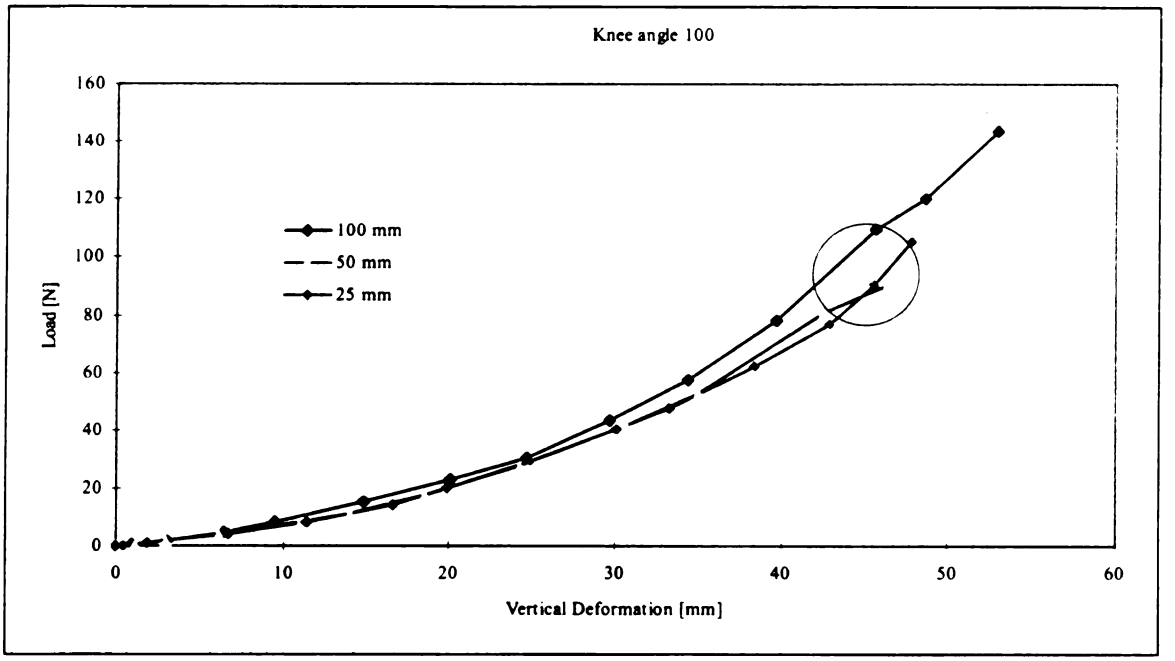

Figure E.23 Load-Deformation Relationship for the Thigh Interaction with 49 Kg/m^3 Foam Density, and with Three Different Thicknesses 25 mm, 50 mm and 100 mm, Knee angle 100° Subject No.1.

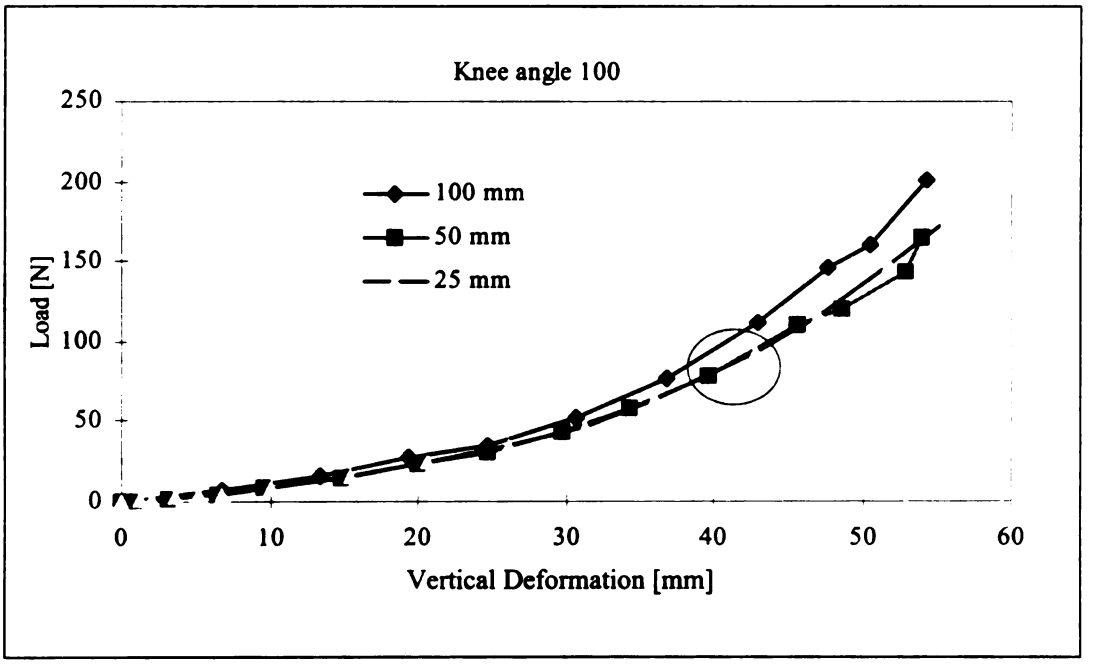

Figure E.24 Load-Deformation Relationship for the Thigh Interaction with 51 Kg/m^3 Foam Density, and with Three Different Thicknesses 25 mm, 50 mm and 100 mm, Knee angle 100°. Subject No.1.

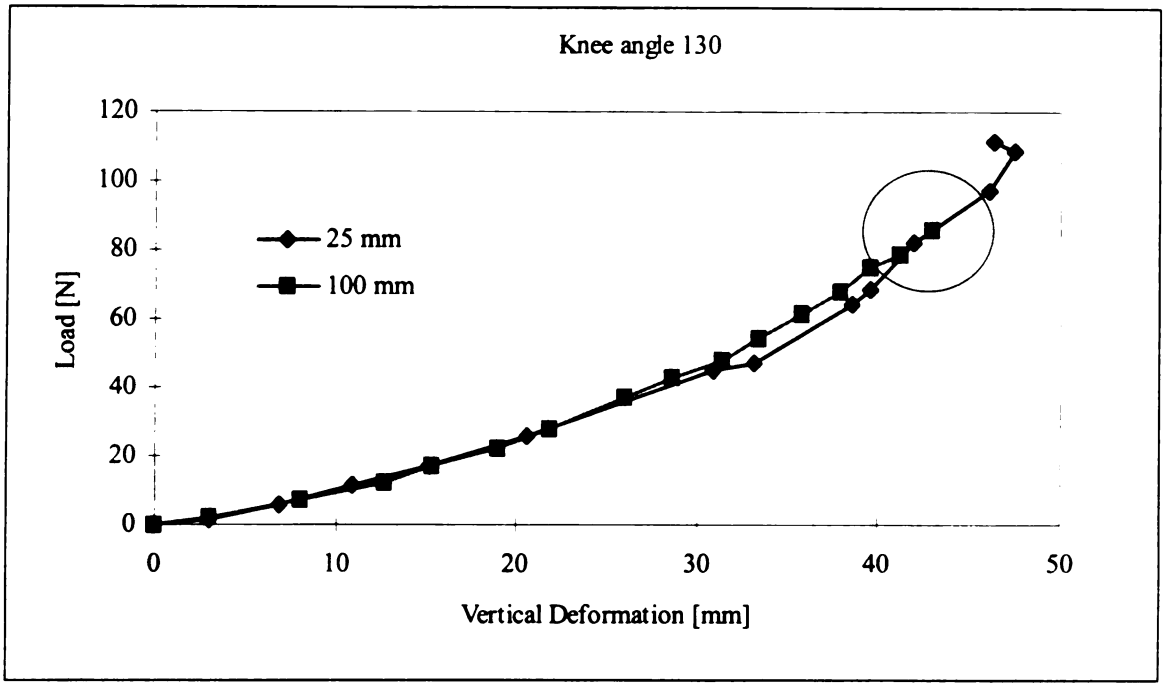

Figure E.25 Load-Deformation Relationship for the Thigh Interaction with 43 Kg/m^3 Foam Density, and with Two Different Thicknesses 25 mm and 100 mm, Knee angle 130° Subject No.1.

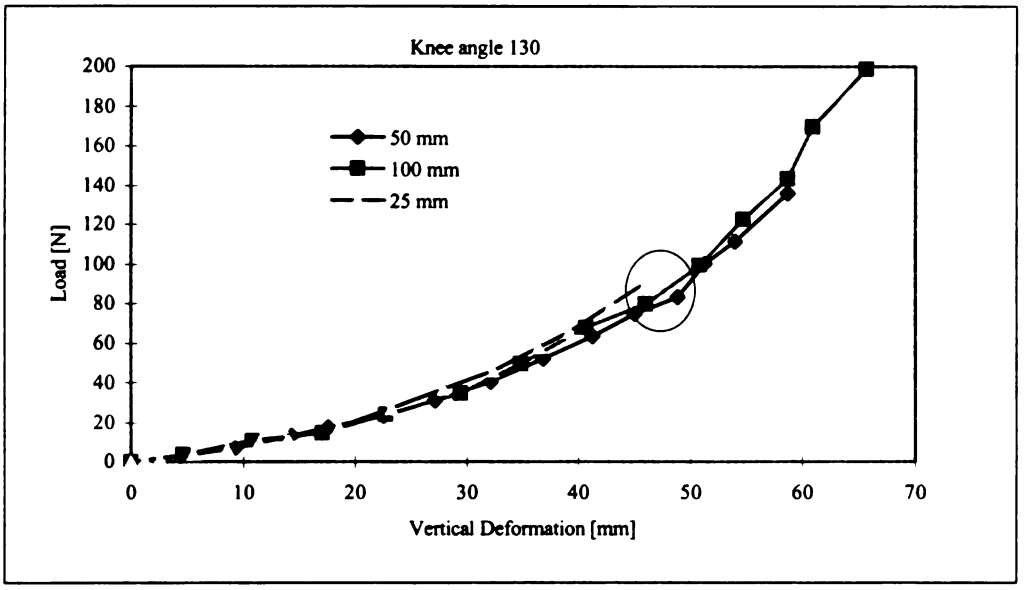

Figure E.26 Load-Deformation Relationship for the Thigh Interaction with 44 Kg/m^3 Foam Density, and with Three Different Thicknesses 25 mm, 50 mm and 100 mm, Knee angle 130° Subject No.1.

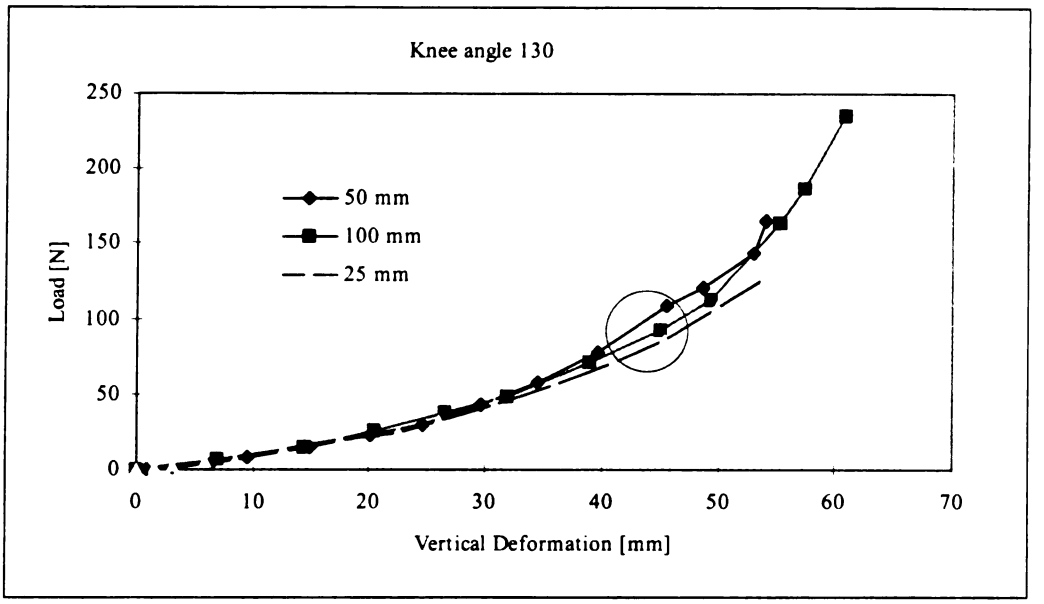

Figure E.27 Load-Deformation Relationship for the Thigh Interaction with 51 Kg/m^3 Foam Density, and with Three Different Thicknesses 25 mm, 50 mm and 100 mm, Knee angle 130° Subject No.1.

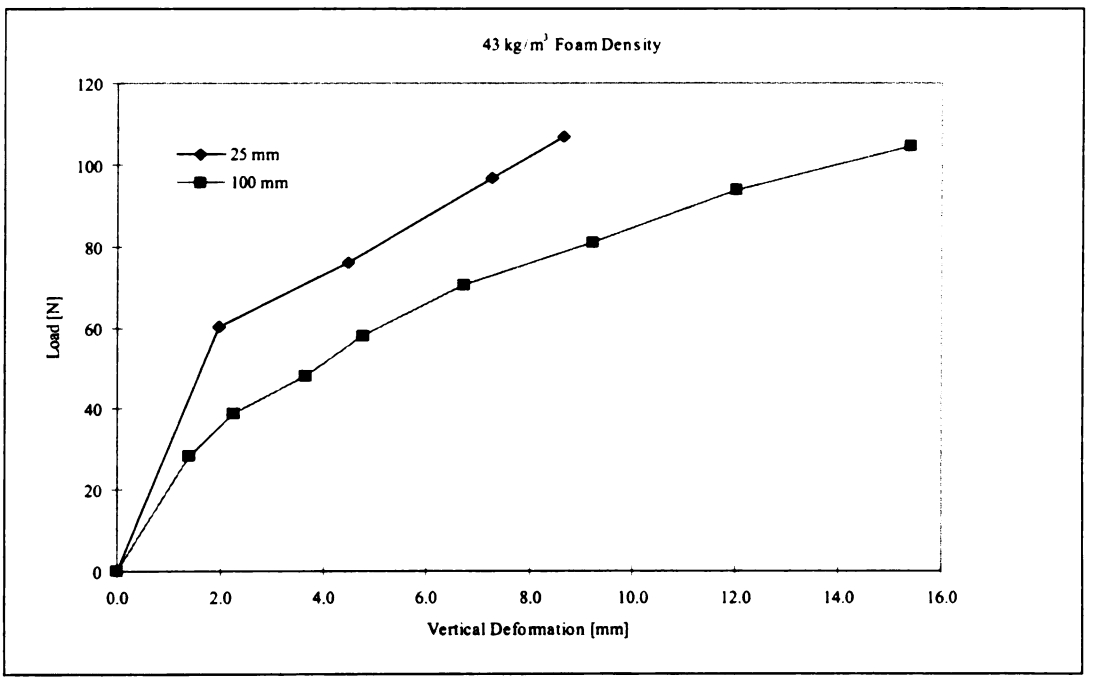

Figure E. 28 Effect of the Foam Thickness on the Foam Stiffness in Thigh-Foam Interaction Test, Foam 43 kg/m^3

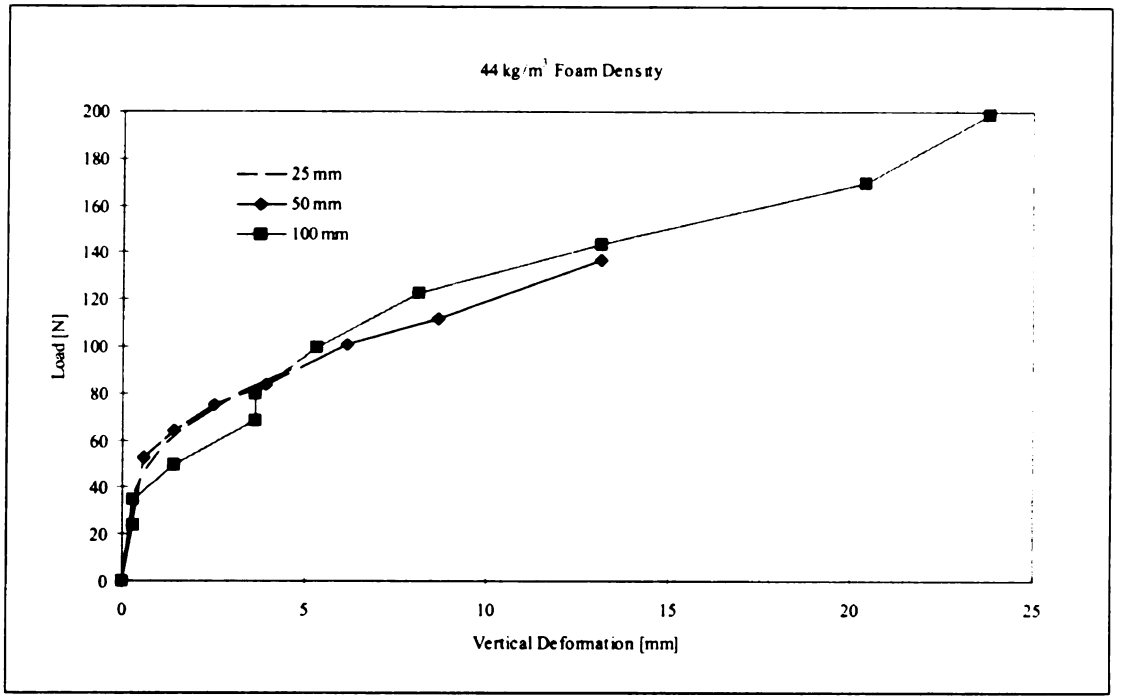

Figure E.29 Effect of the Foam Thickness on the Foam Stiffness in Thigh- Foam Interaction Test, Foam 44 kg/m^3 Subject No.1.

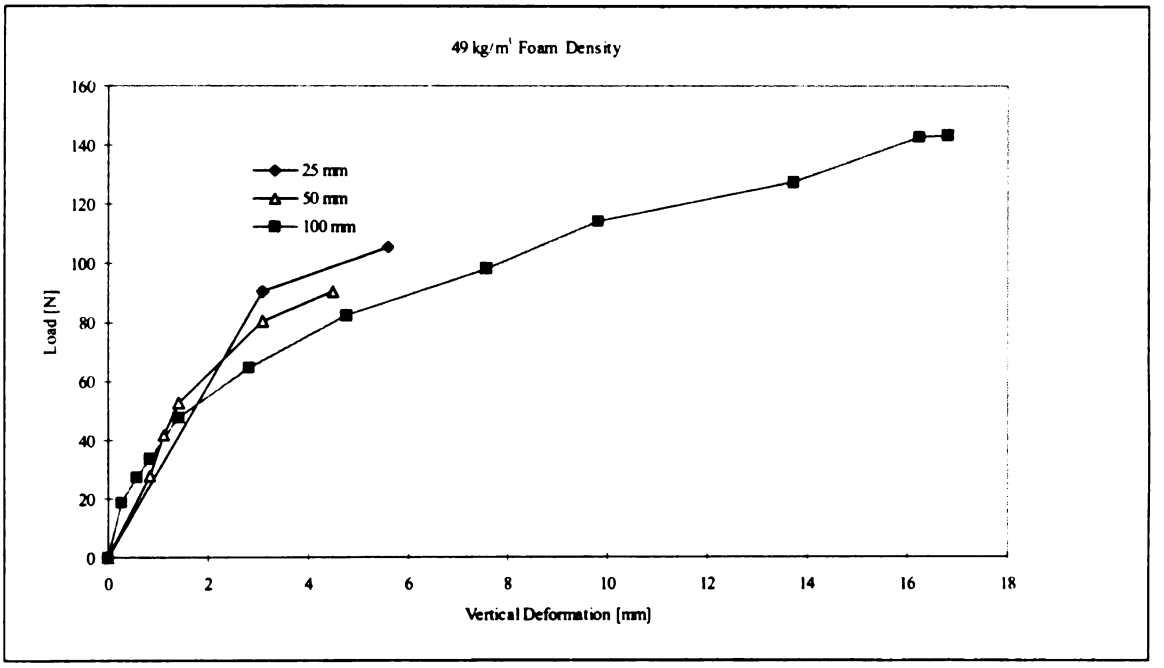

Figure E.30 Effect of the Foam Thickness on the Foam Stiffness in Thigh- Foam Interaction Test, Foam 49 kg/m^3 Subject No.1.

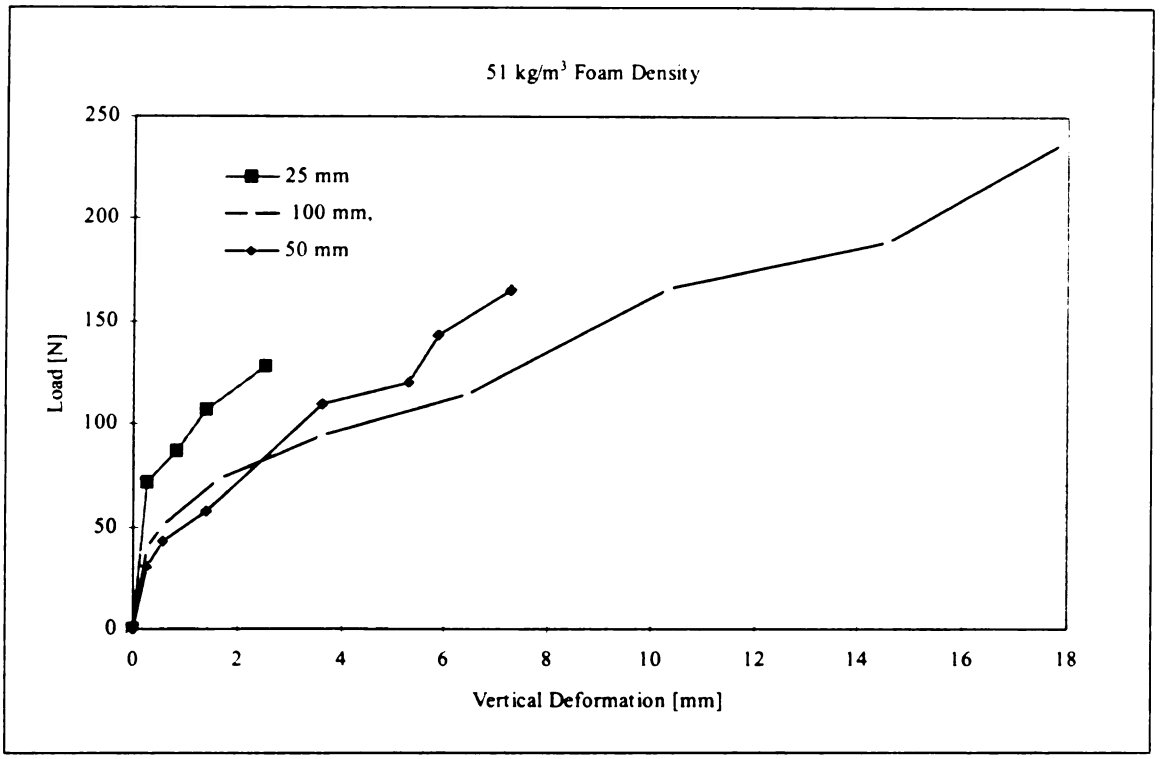

Figure E.31 Effect of the Foam Thickness on the Foam Stiffness in Thigh- Foam Interaction Test, Foam 51 kg/m^3, Subject No.1.

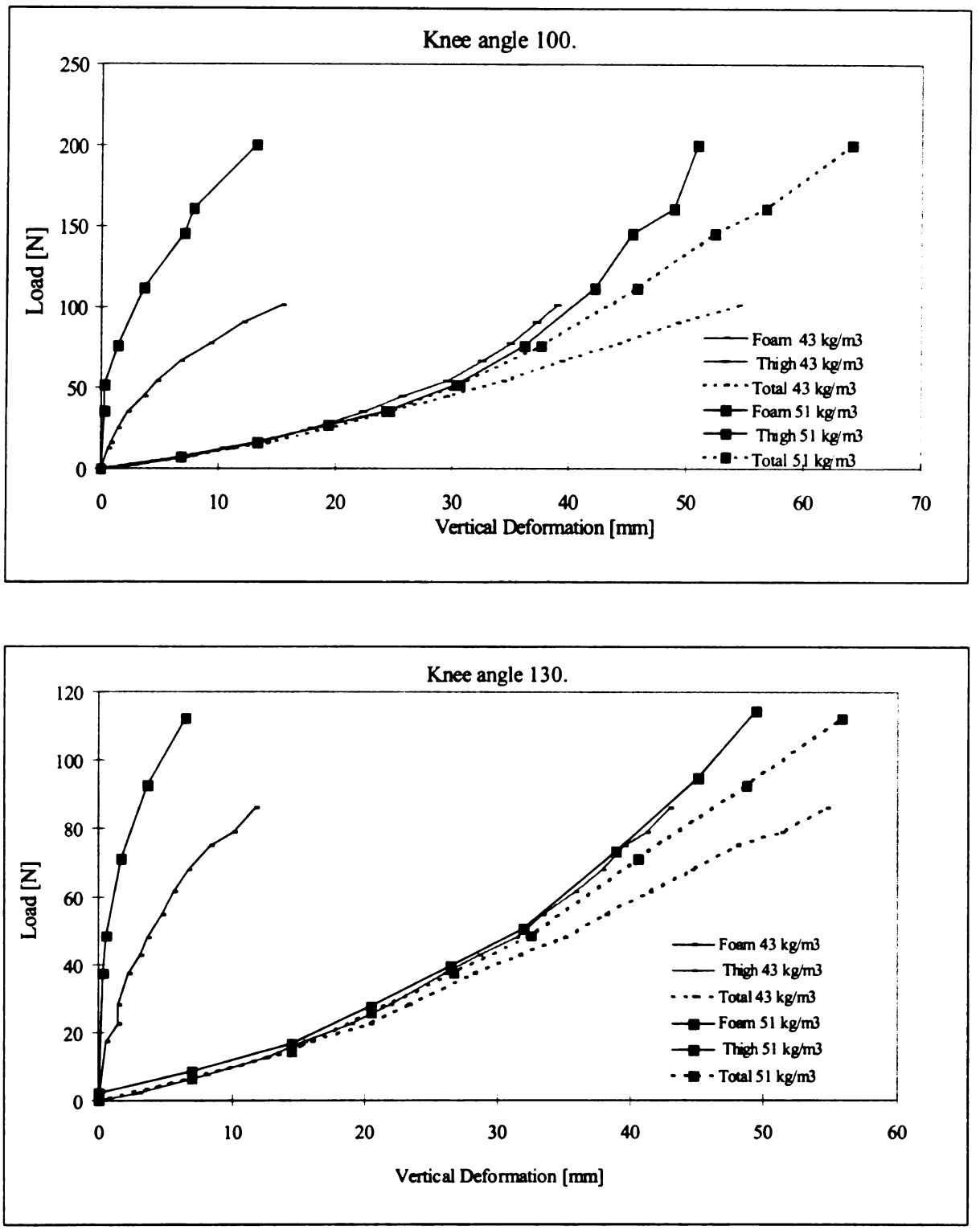

Figure E.32 Total, Thigh, and Foam Vertical Deformation versus Load, Subject No. 1 Thigh Interaction with Two Different Foam Density (43 kg/m^3 and 51 kg/m^3), 100 mm Foam Thickness

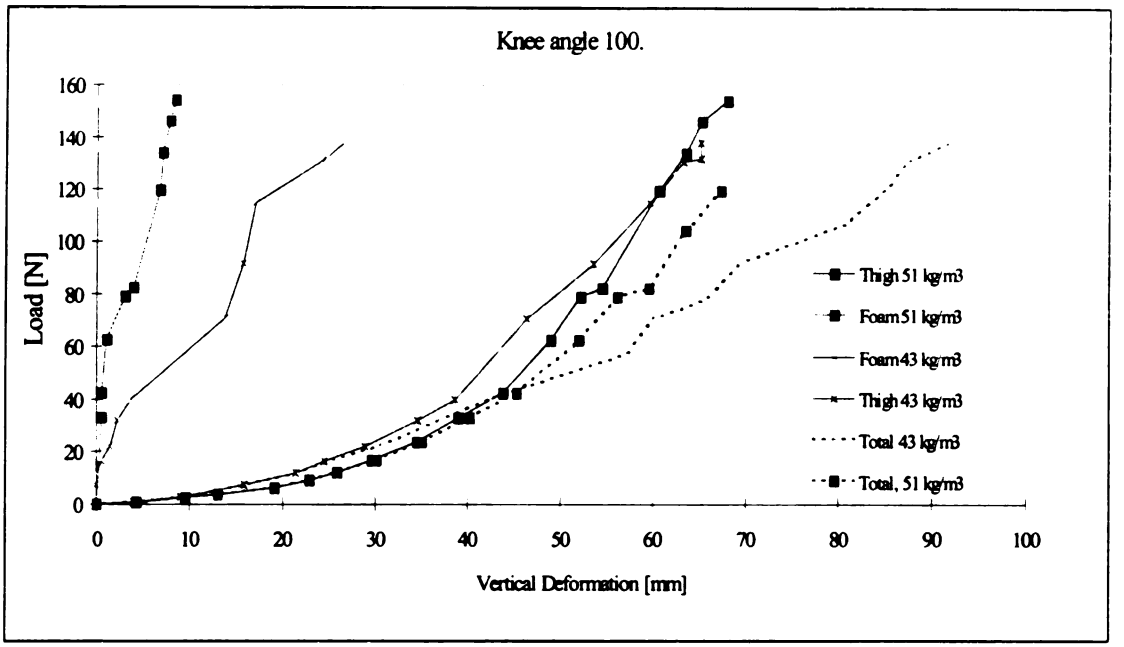

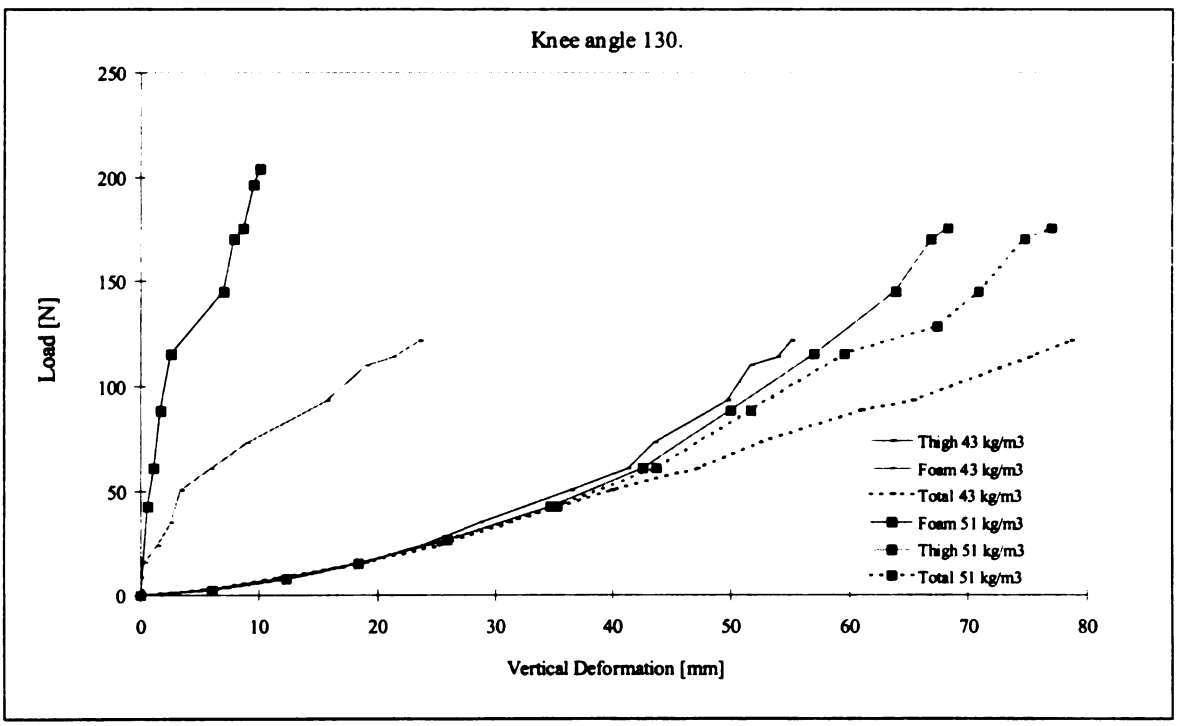

Figure E.33 Total, Thigh, and Foam Vertical Deformation versus Load, Subject No. 2 Thigh Interaction with Two Different Foam Density (43 kg/m^3 and 51 kg/m^3), 100 mm Foam Thickness

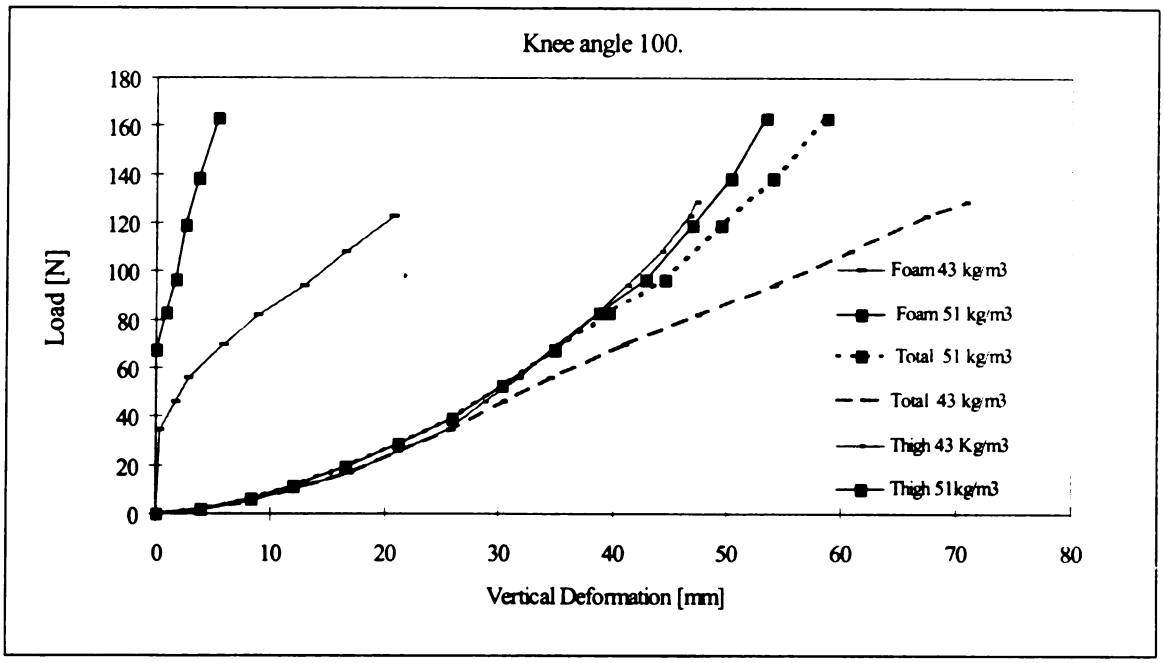

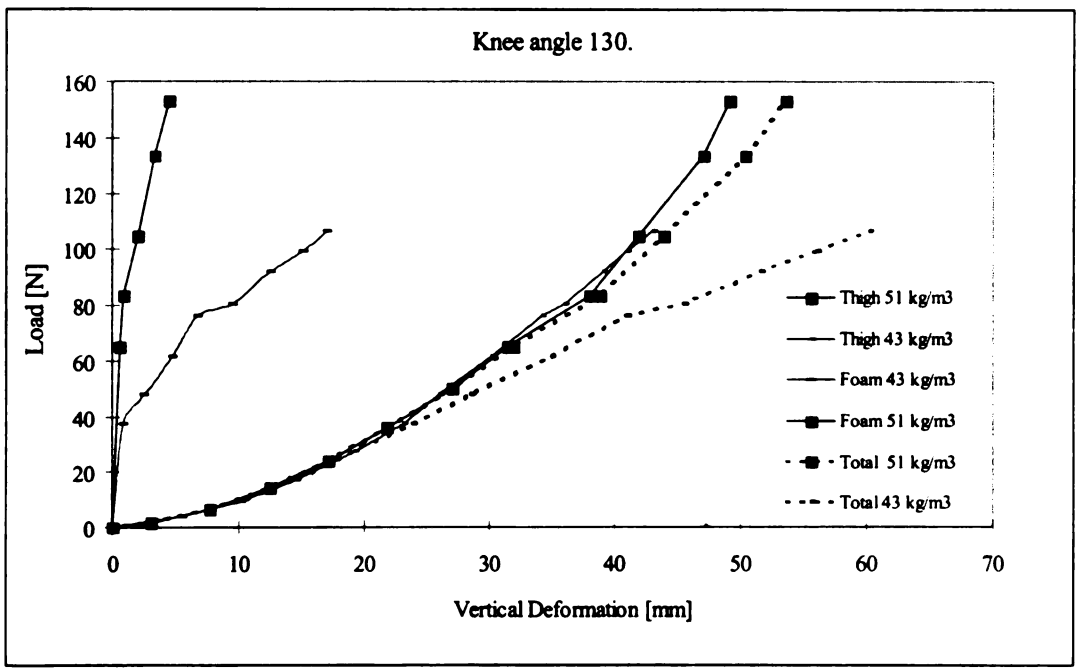

Figure E.34 Total, Thigh, and Foam Vertical Deformation versus Load, Subject No. 3 Thigh Interaction with Two Different Foam Density (43 kg/m^3 and 51 kg/m^3), 100 mm Foam Thickness

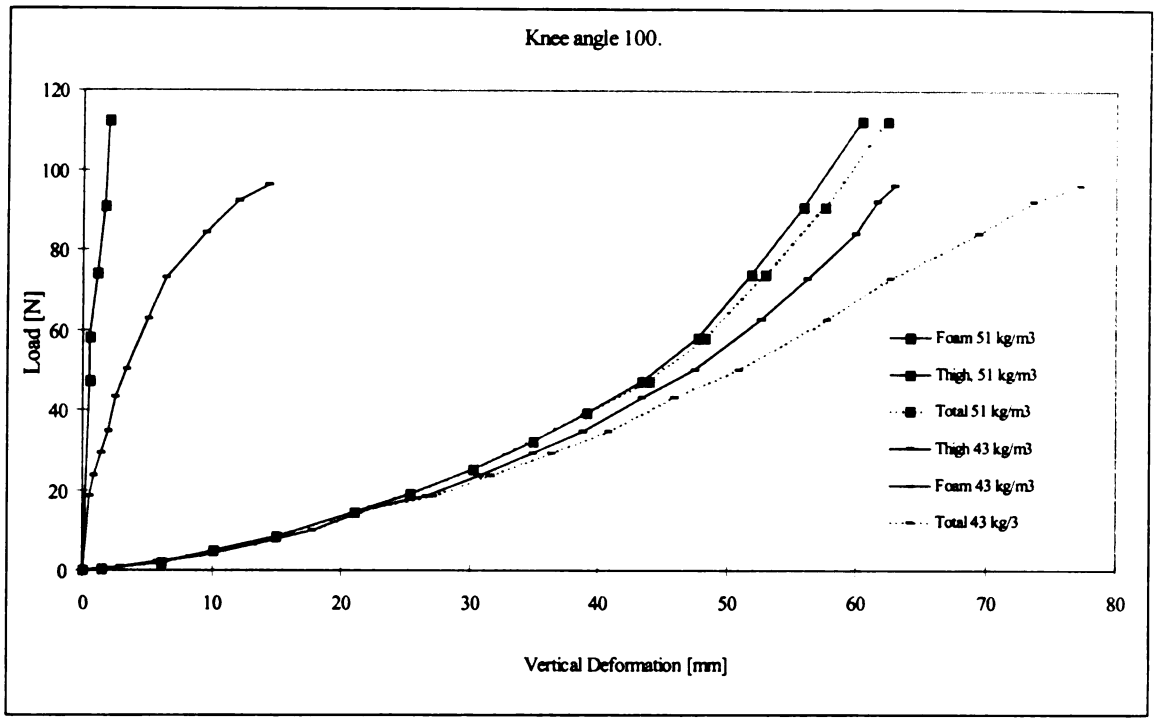

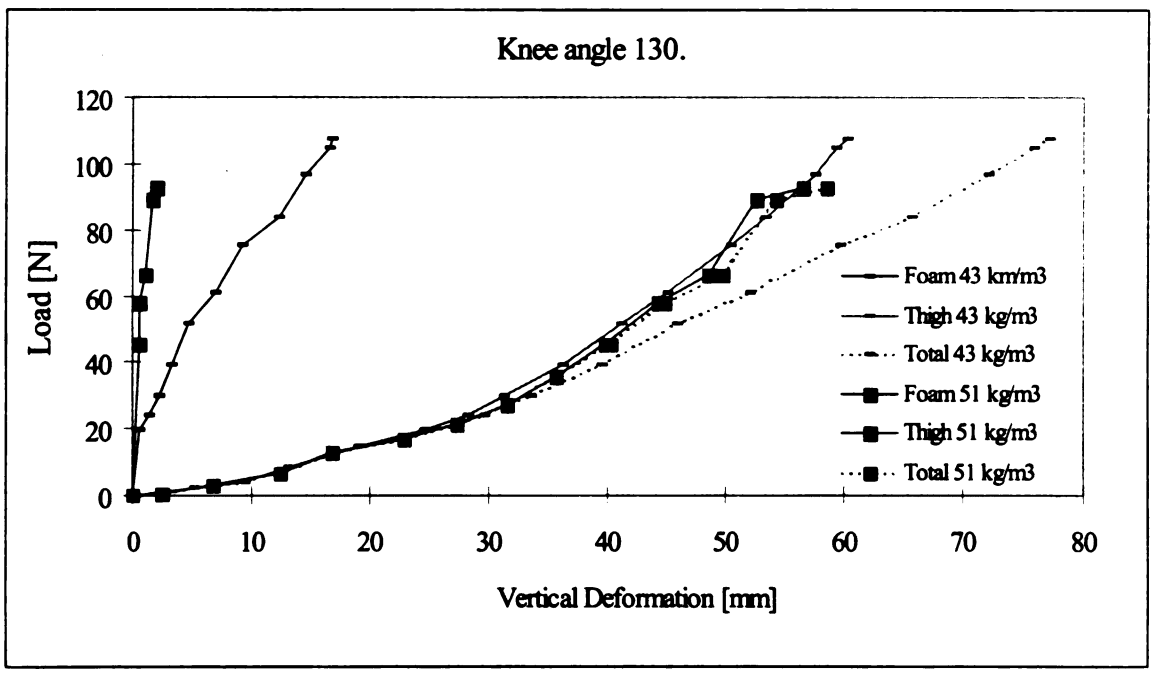

Figure E.35 Total, Thigh, and Foam Vertical Deformation versus Load, Subject No. 4 Thigh Interaction with Two Different Foam Density (43 kg/m^3 and 51 kg/m^3), 100 mm Foam Thickness

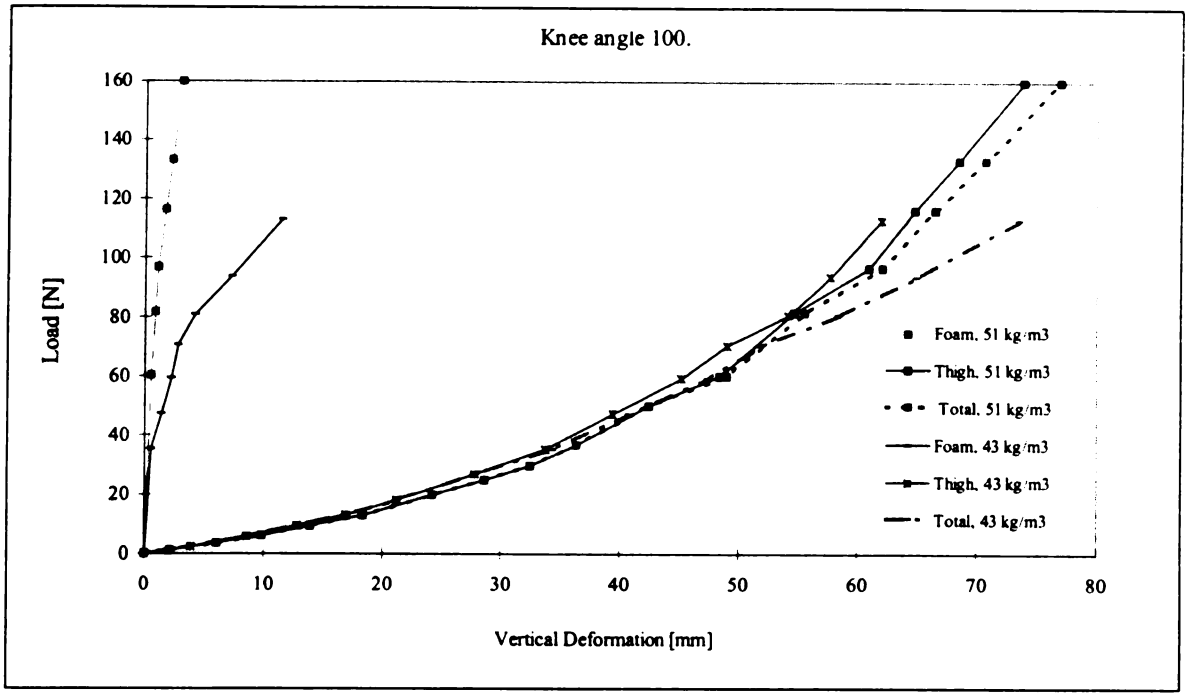

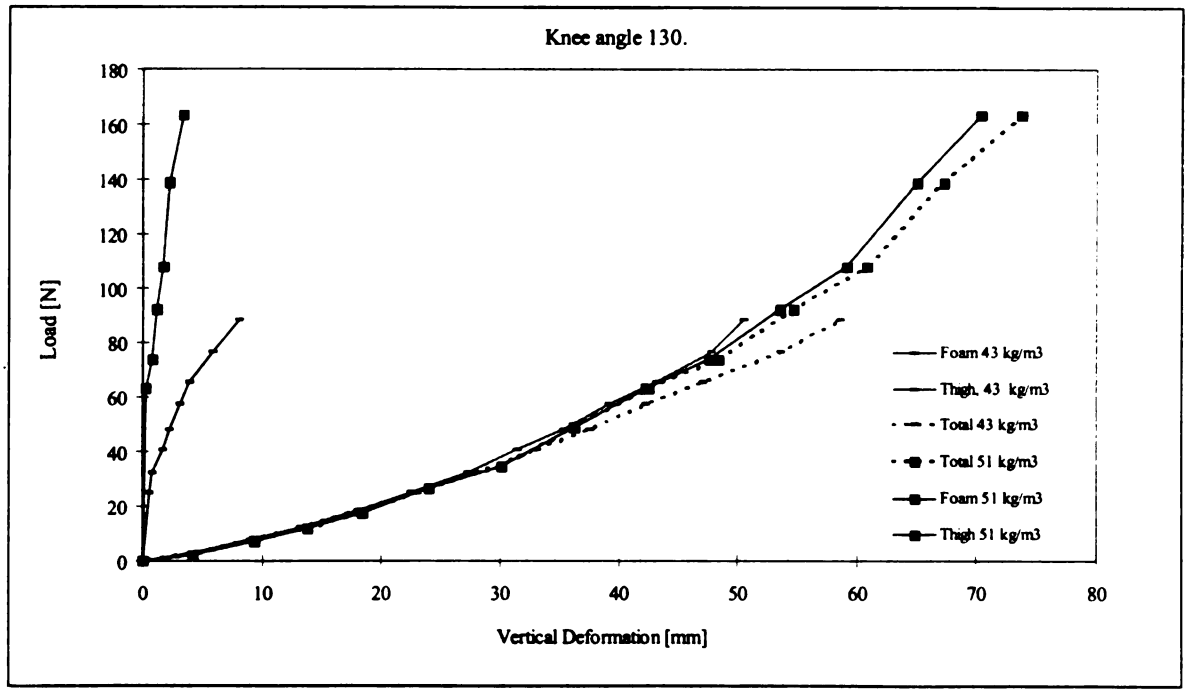

Figure E.36 Total, Thigh, and Foam Vertical Deformation versus Load, Subject No. 5 Thigh Interaction with Two Different Foam Density (43 kg/m^3 and 51 kg/m^3), 100 mm Foam Thickness

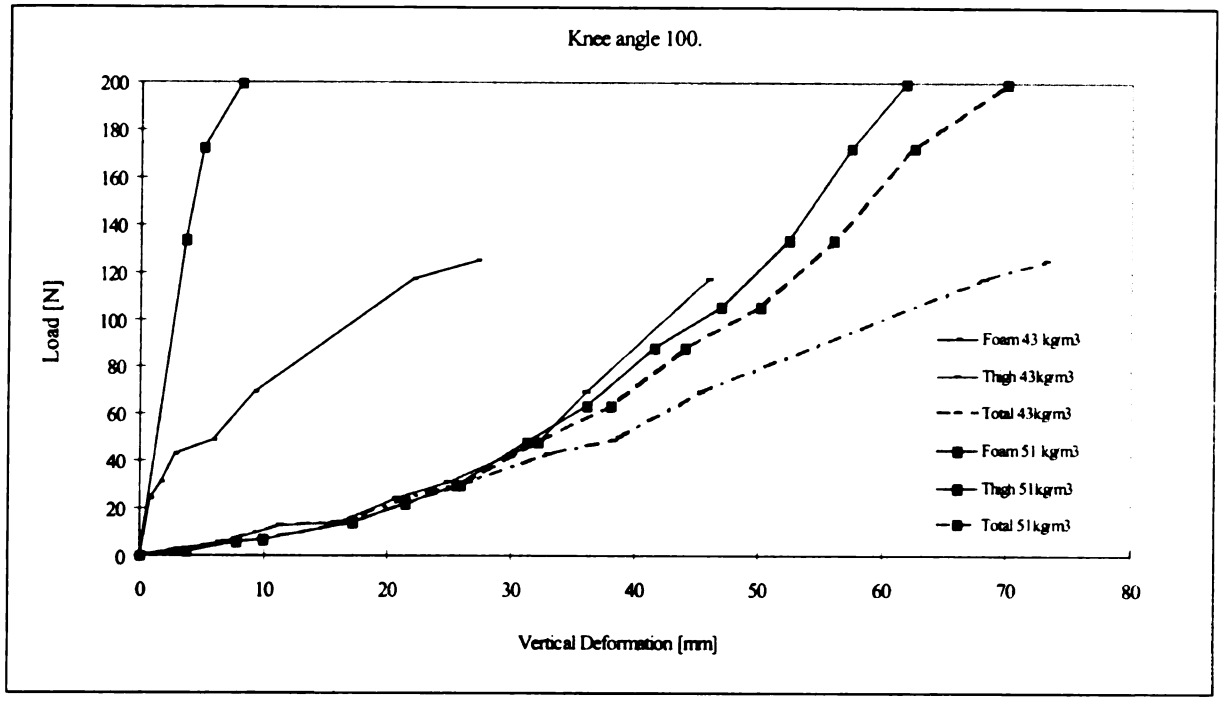

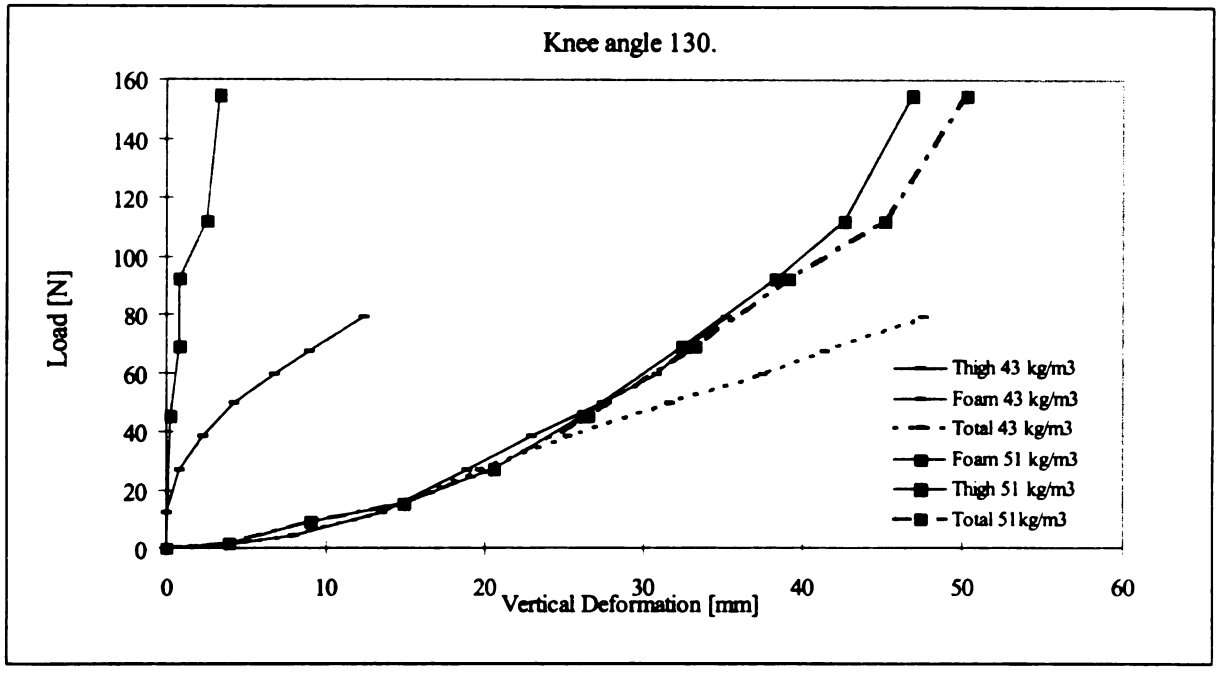

Figure E.37 Total, Thigh, and Foam Vertical Deformation versus Load, Subject No. 6 Thigh Interaction with Two Different Foam Density (43 kg/m^3 and 51 kg/m^3), 100 mm Foam Thickness

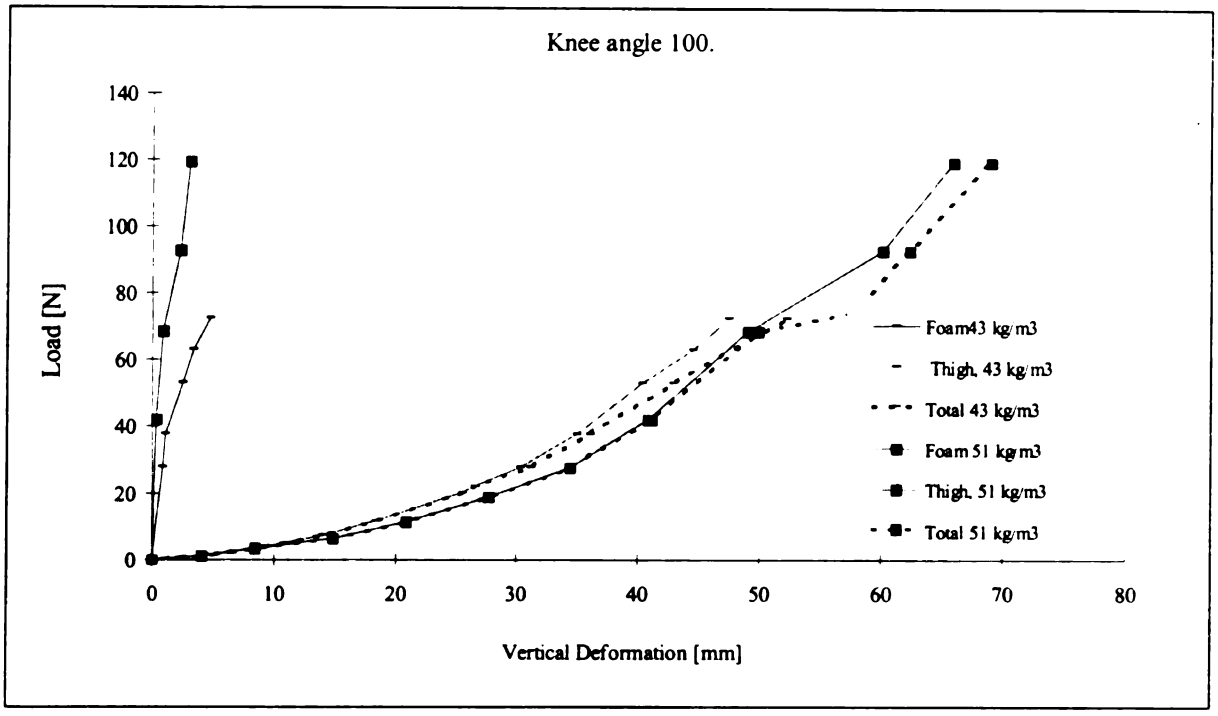

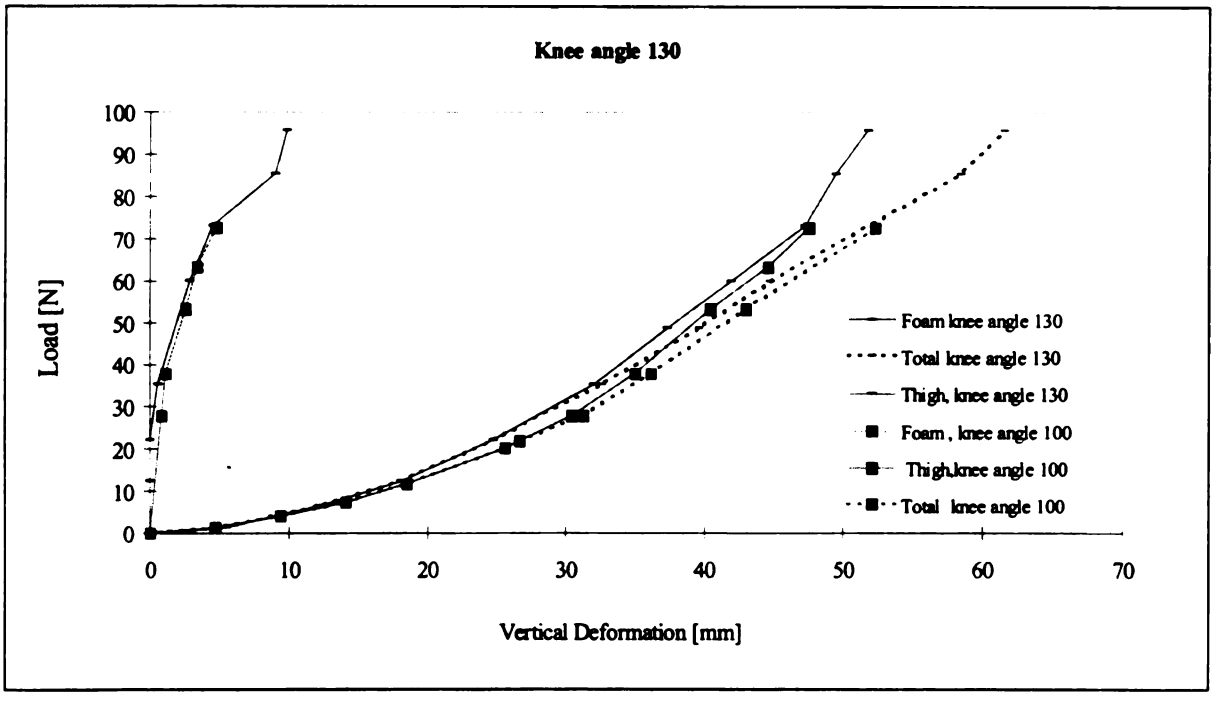

Figure E.38 Total, Thigh, and Foam Vertical Deformation Versus Load, Subject No. 7 Thigh Interaction with Two Different Foam Density (43 kg/m^3 and 51 kg/m^3), 100 mm Foam Thickness

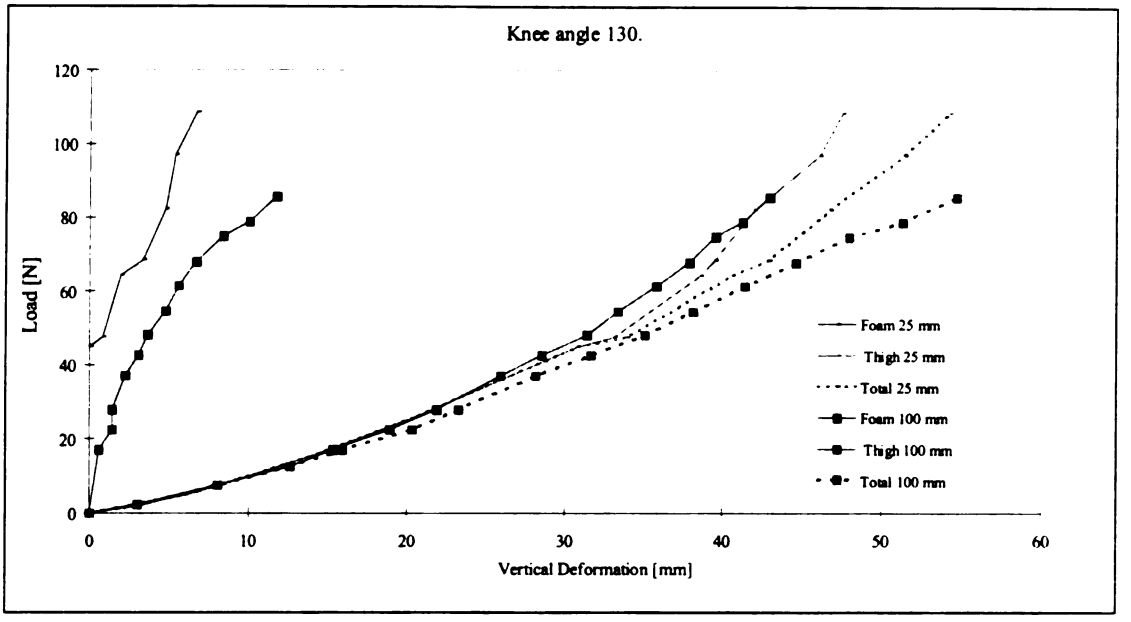

Figure E.39 Total, Thigh, and Foam Vertical Deformation Versus Load, Subject No. 1, Thigh Interaction with Two Different Foam Thickness (100 mm and 25 mm), and 43 kg/m^3 Foam Density

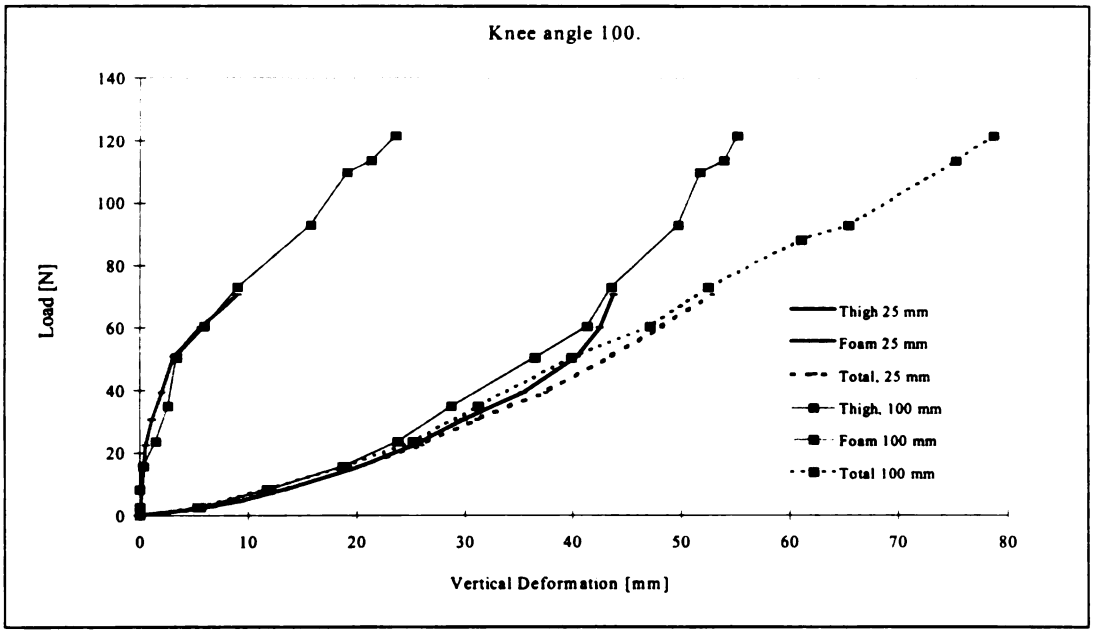

Figure E.40 Total, Thigh, and Foam Vertical Deformation Versus Load, Subject No. 2, Thigh Interaction with Two Different Foam Thickness (100 mm and 25 mm), and 43 kg/m^3 Foam Density

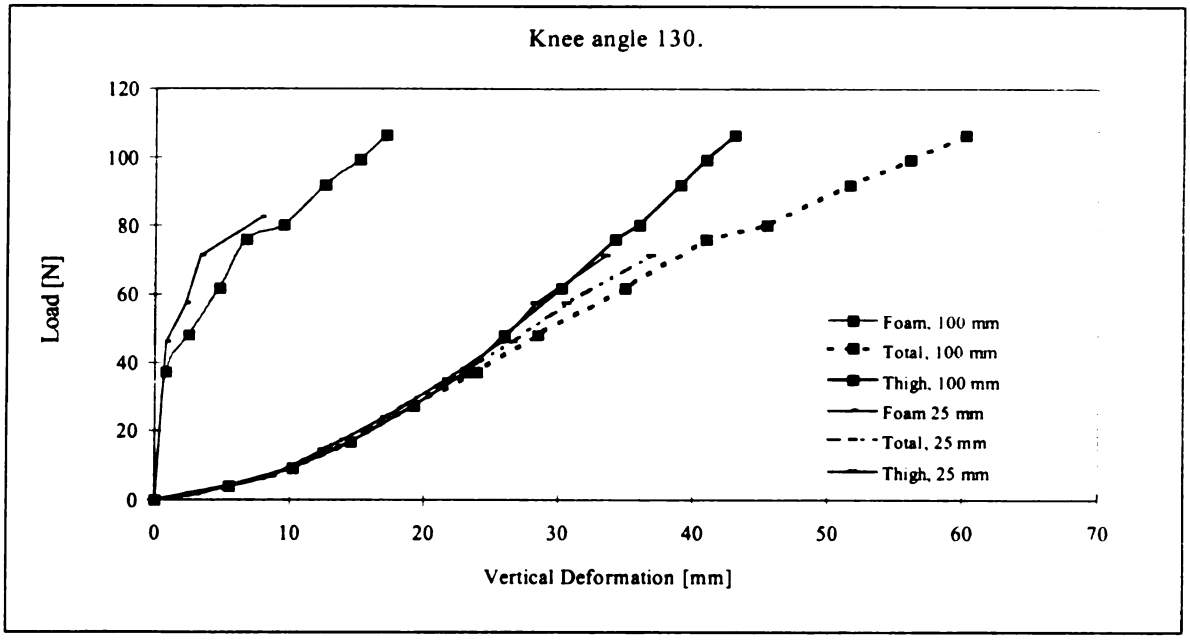

Figure E.41 Total, Thigh, and Foam Vertical Deformation Versus Load, Subject No. 3, Thigh Interaction with Two Different Foam Thickness (100 mm and 25 mm), and 43 kg/m^3 Foam Density

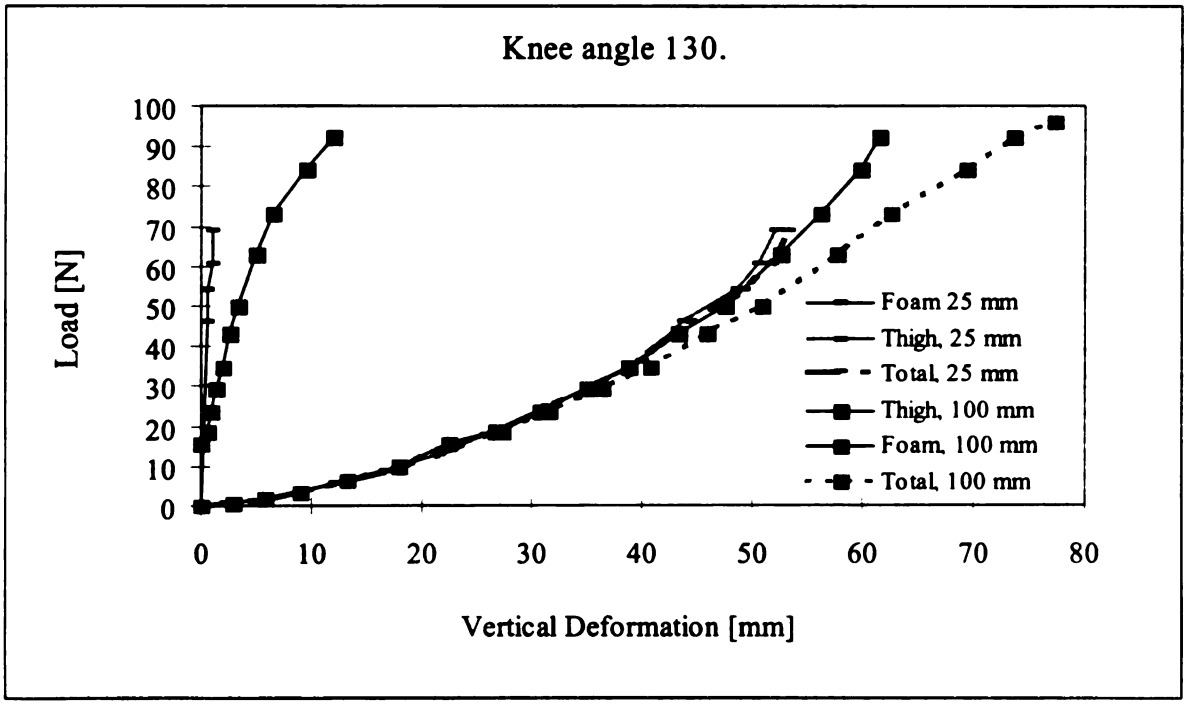

Figure E.42 Total, Thigh, and Foam Vertical Deformation Versus Load, Subject No. 4, Thigh Interaction with Two Different Foam Thickness (100 mm and 25 mm), and 43 kg/m^3 Foam Density

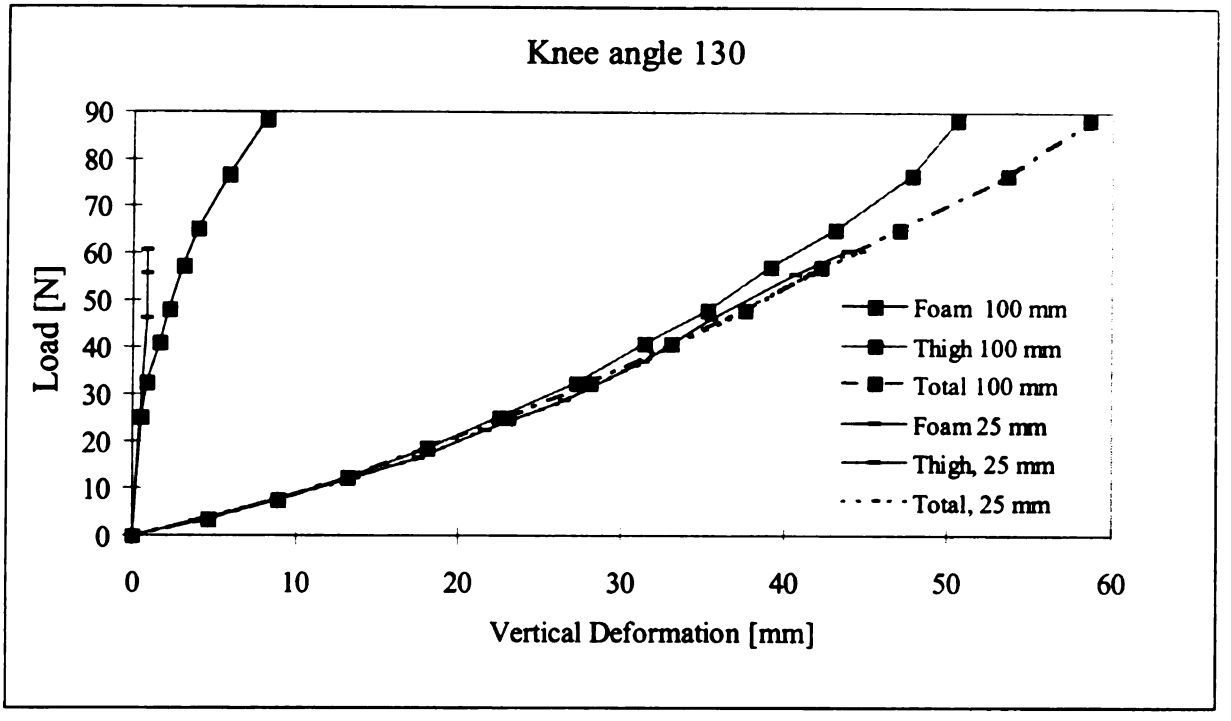

Figure E.43 Total, Thigh, and Foam Vertical Deformation Versus Load, Subject No. 5, Thigh Interaction with Two Different Foam Thickness (100 mm and 25 mm), and 43 kg/m^3 Foam Density

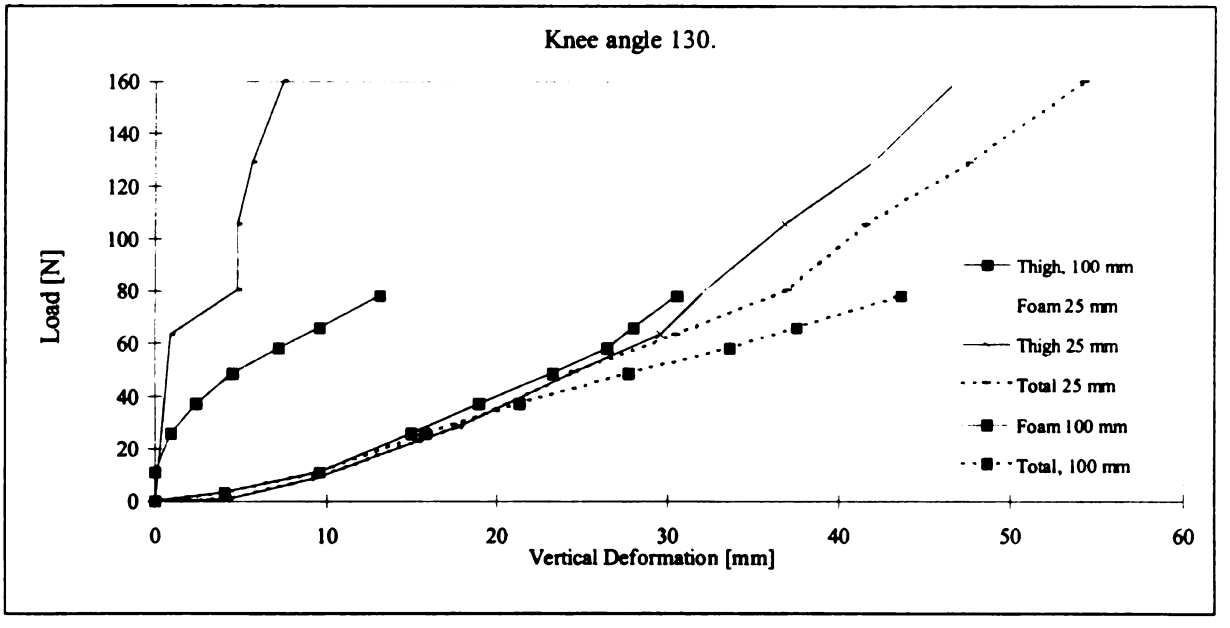

Figure E.44 Total, Thigh, and Foam Vertical Deformation Versus Load, Subject No. 6, Thigh Interaction with Two Different Foam Thickness (100 mm and 25 mm), and 43 kg/m^3 Foam Density

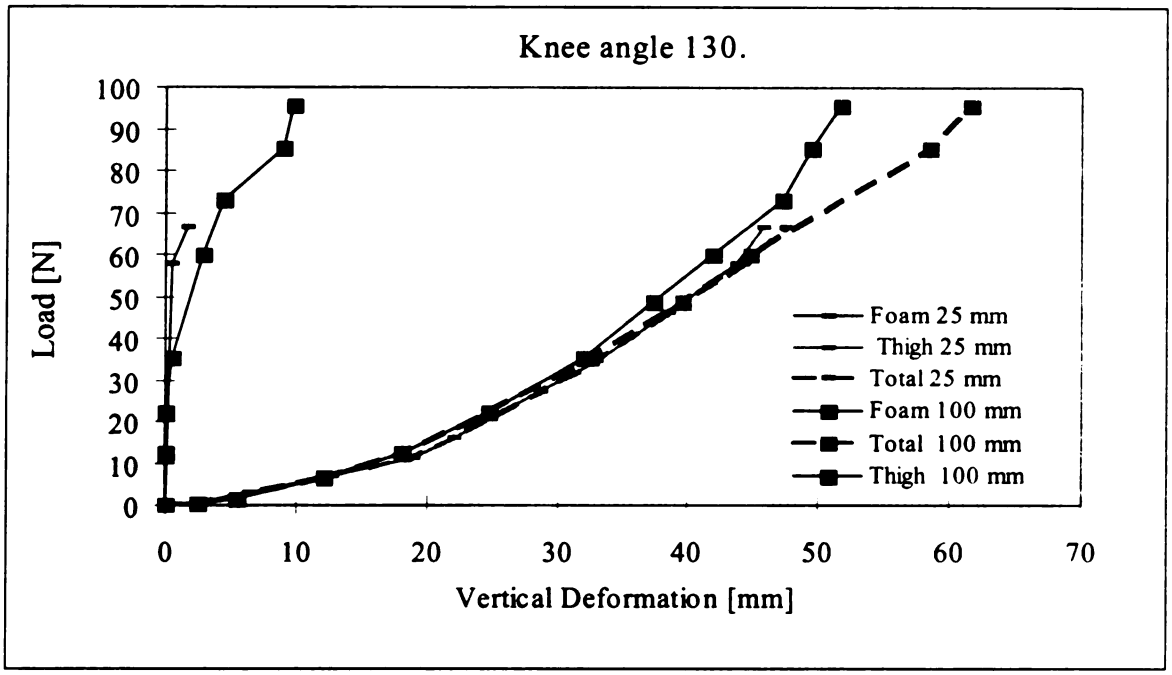

Figure E.45 Total, Thigh, and Foam Vertical Deformation Versus Load, Subject No.7, Thigh Interaction with Two Different Foam Thickness (100 mm and 25 mm), and 43 kg/m^3 Foam Density

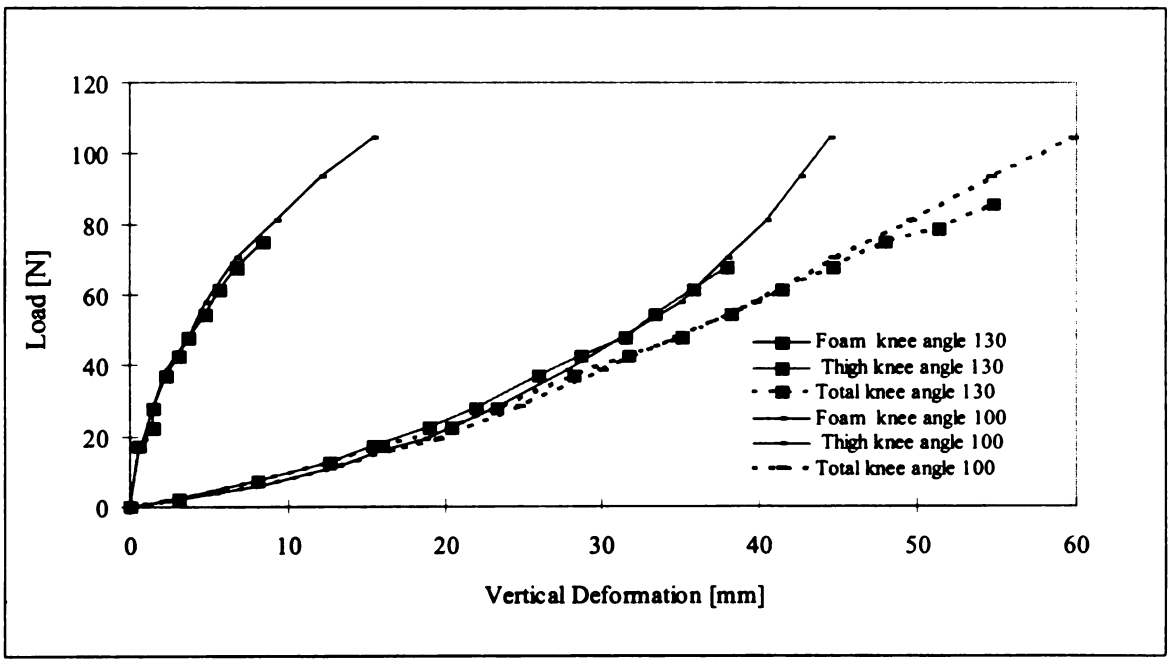

Figure E.46 Total, Thigh, and Foam Vertical Deformation Versus Load, Subject No. 1, Thigh With Two Knee Angle 100° and 130° Interaction with One Foam (100 mm Thickness and A3 kg/m^3 Density)

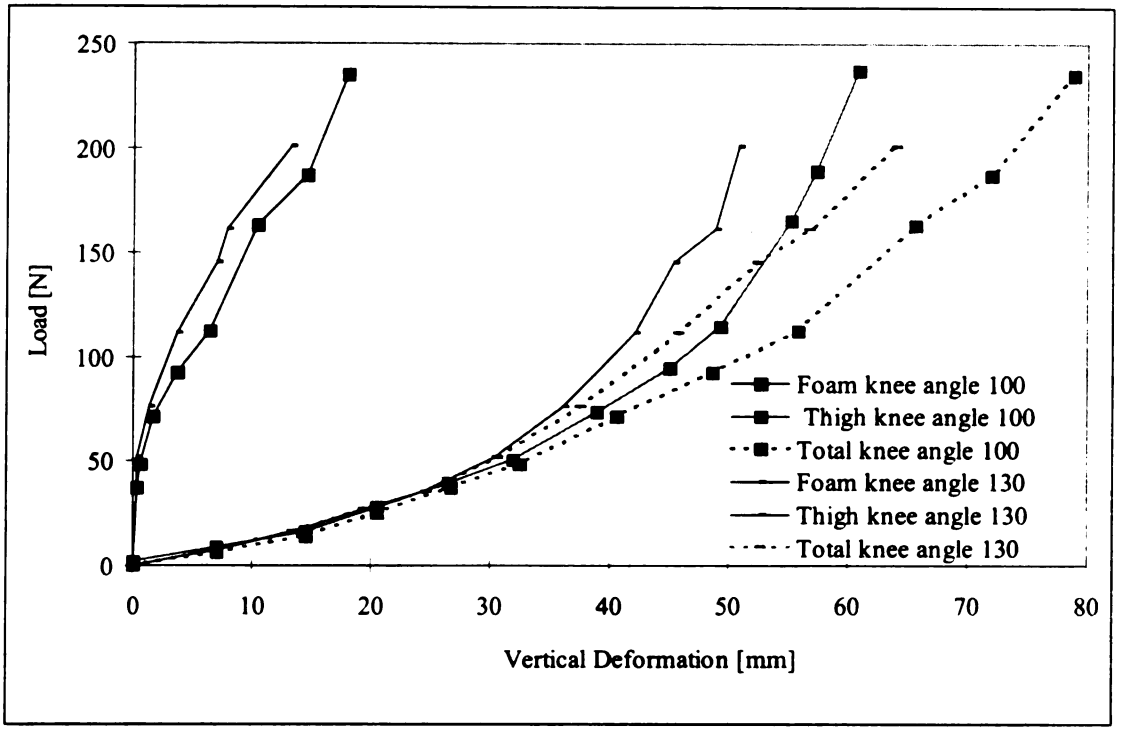

Figure 4.47 Total, Thigh, and Foam Vertical Deformation Versus Load, Subject No. 1, Thigh with Two Knee Angle 100° and 130° Interaction with One Foam (100 mm Thickness and 51 kg/m^3 Density)

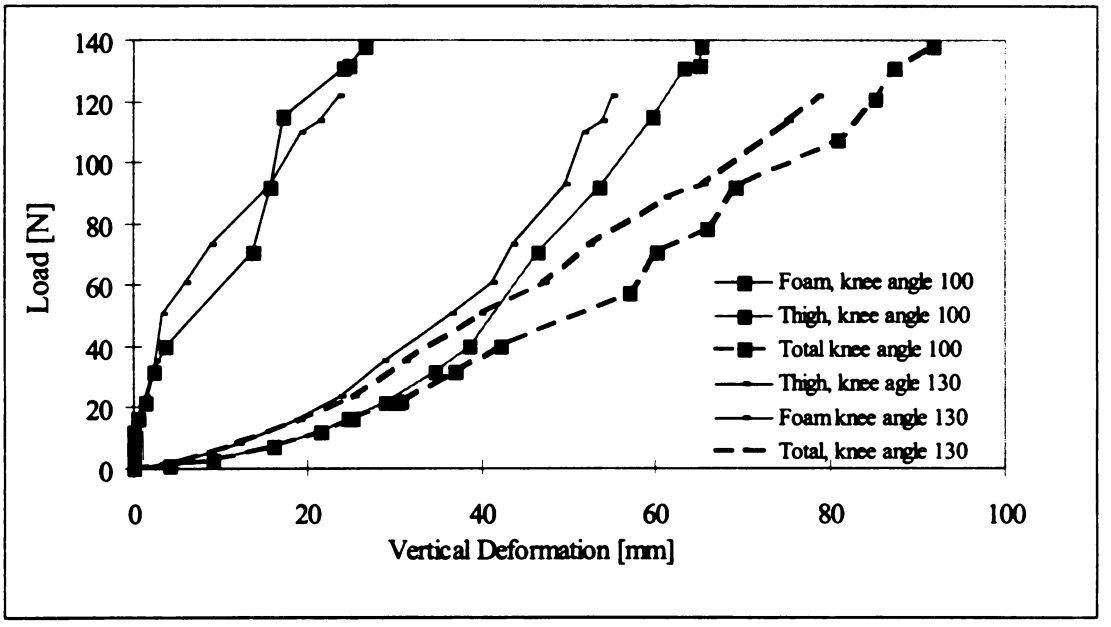

Figure E.48 Total, Thigh, and Foam Vertical Deformation Versus Load, Subject No. 2, Thigh with Two Knee Angle 100° and 130° Interaction with One Foam (100 mm Thickness and 43 kg/m^3 Density

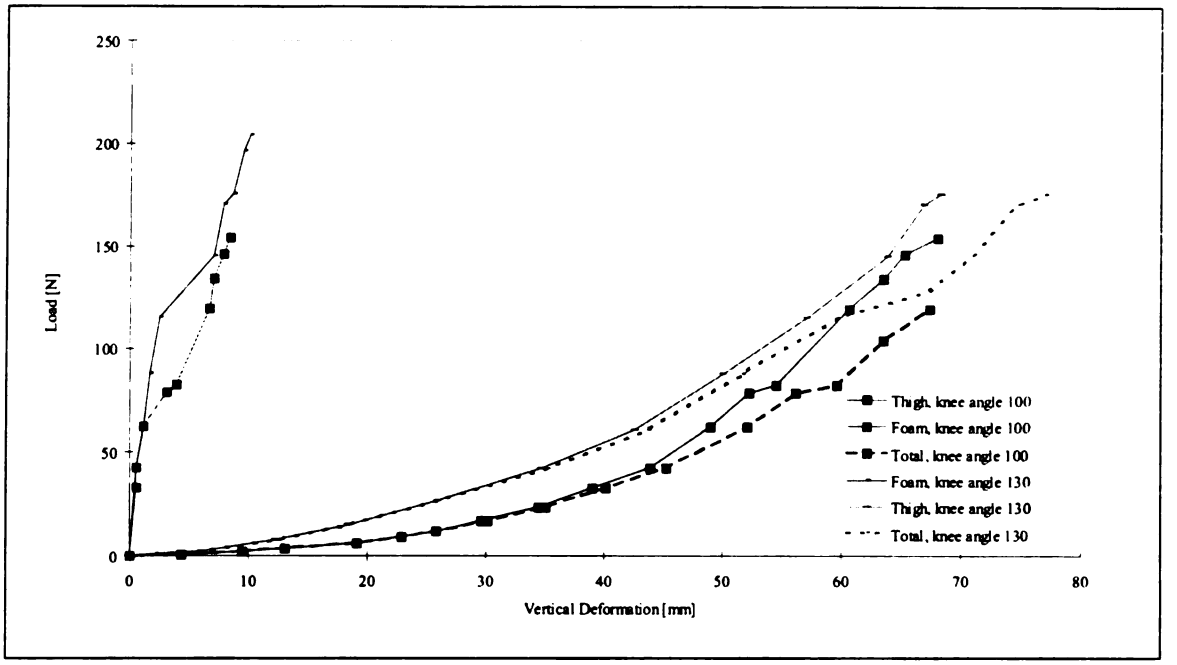

Figure E.49 Total, Thigh, and Foam Vertical Deformation Versus Load, Subject No. 2, Thigh with Two Knee Angle 100° and 130° Interaction with One Foam (100 mm Thickness and 51 kg/m^3 Density)

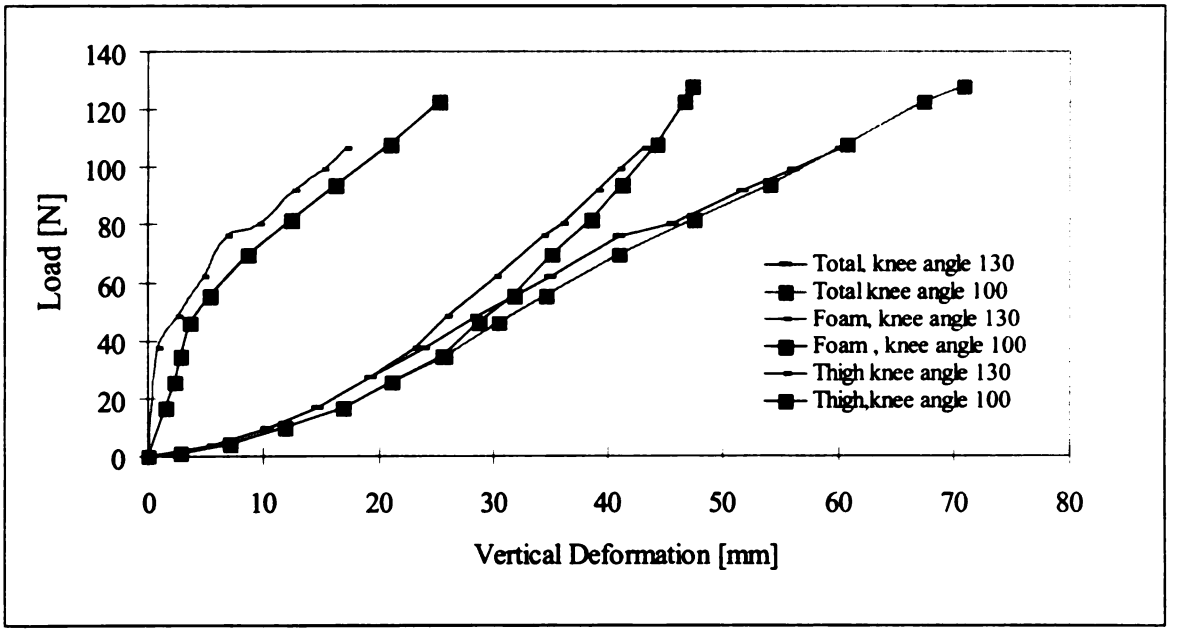

Figure E.50 Total, Thigh, and Foam Vertical Deformation Versus Load, Subject No. 3, Thigh with Two Knee Angle 100° and 130° Interaction with One Foam (100 mm Thickness and 43 kg/m^3 Density

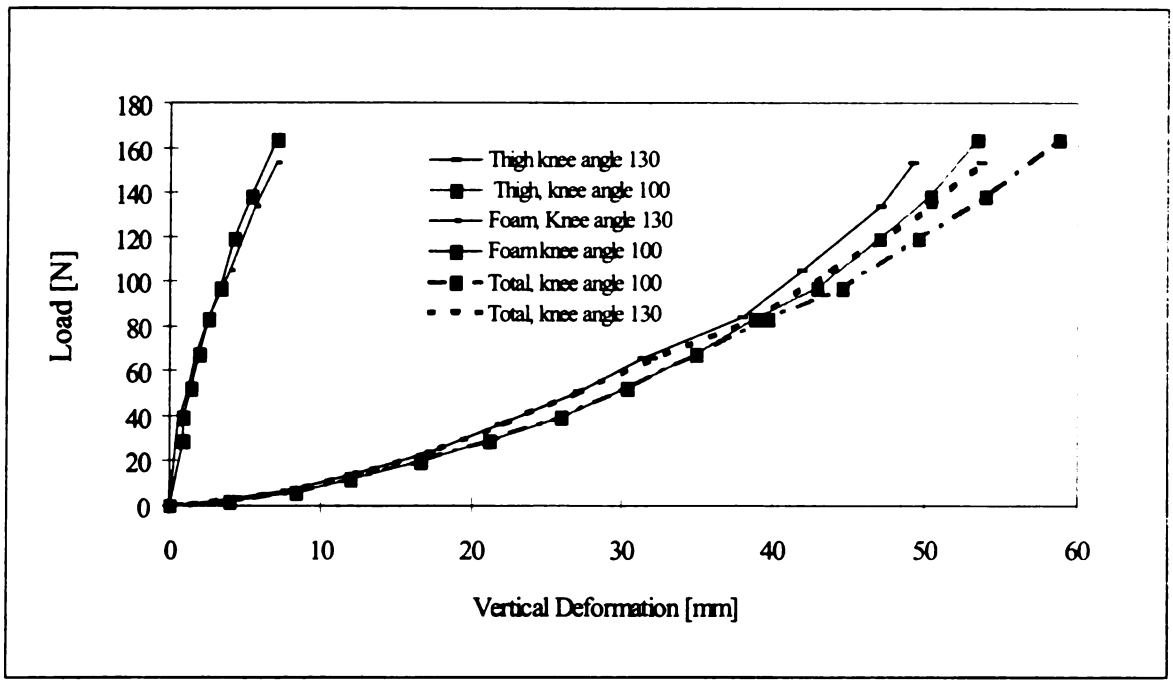

Figure E.51 Total, Thigh, and Foam Vertical Deformation Versus Load, Subject No. 3, Thigh with Two Knee Angle 100° and 130° Interaction with One Foam (100 mm Thickness and 51 kg/m^3 Density)

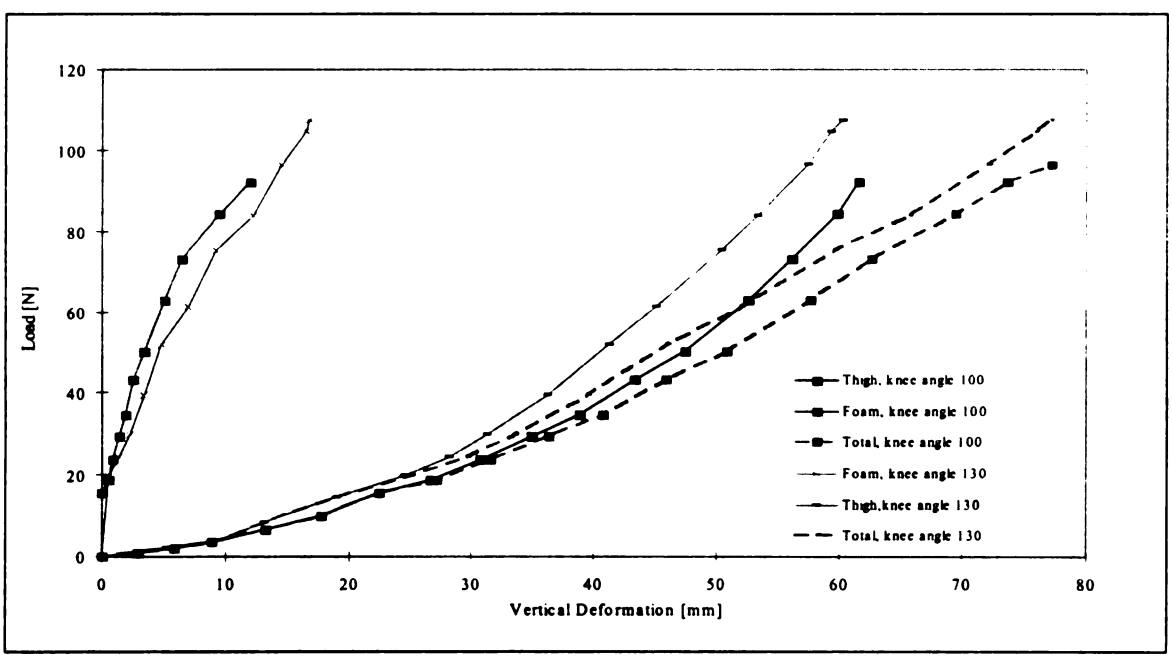

Figure E.52 Total, Thigh, and Foam Vertical Deformation Versus Load, Subject No. 4, Thigh with Two Knee Angle 100° and 130° Interaction with One Foam (100 mm Thickness and 43 kg/m^3 Density)

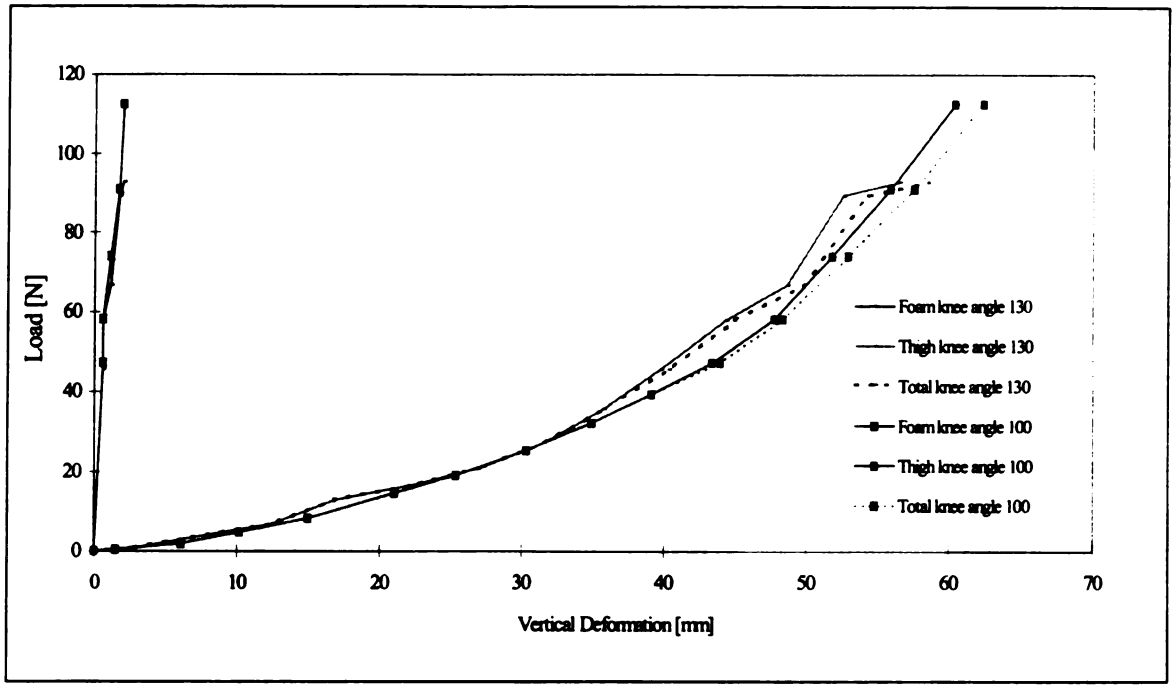

Figure E.53 Total, Thigh, and Foam Vertical Deformation Versus Load, Subject No. 4, Thigh with Two Knee Angle 100° and 130° Interaction with One Foam (100 mm Thickness and 43 kg/m^3 Density)

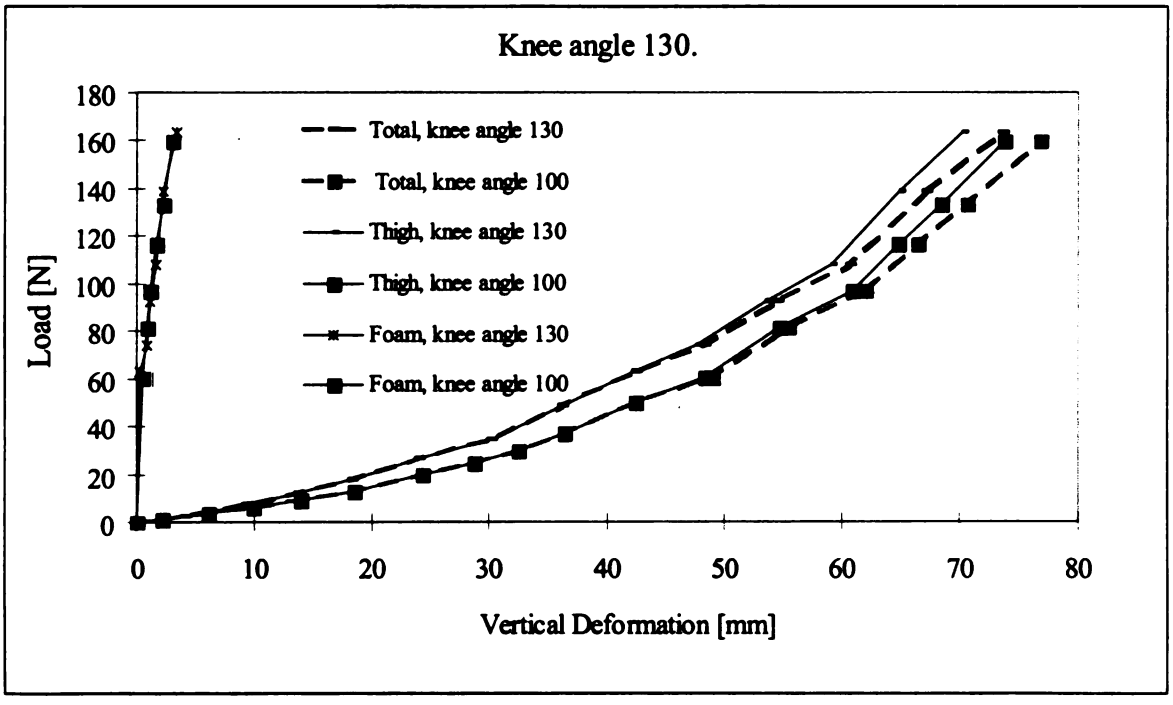

Figure E.54 Total, Thigh, and Foam Vertical Deformation Versus Load, Subject No. 5, Thigh with Two Knee Angle 100° and 130° Interaction with One Foam (100 mm Thickness and 51 kg/m^3

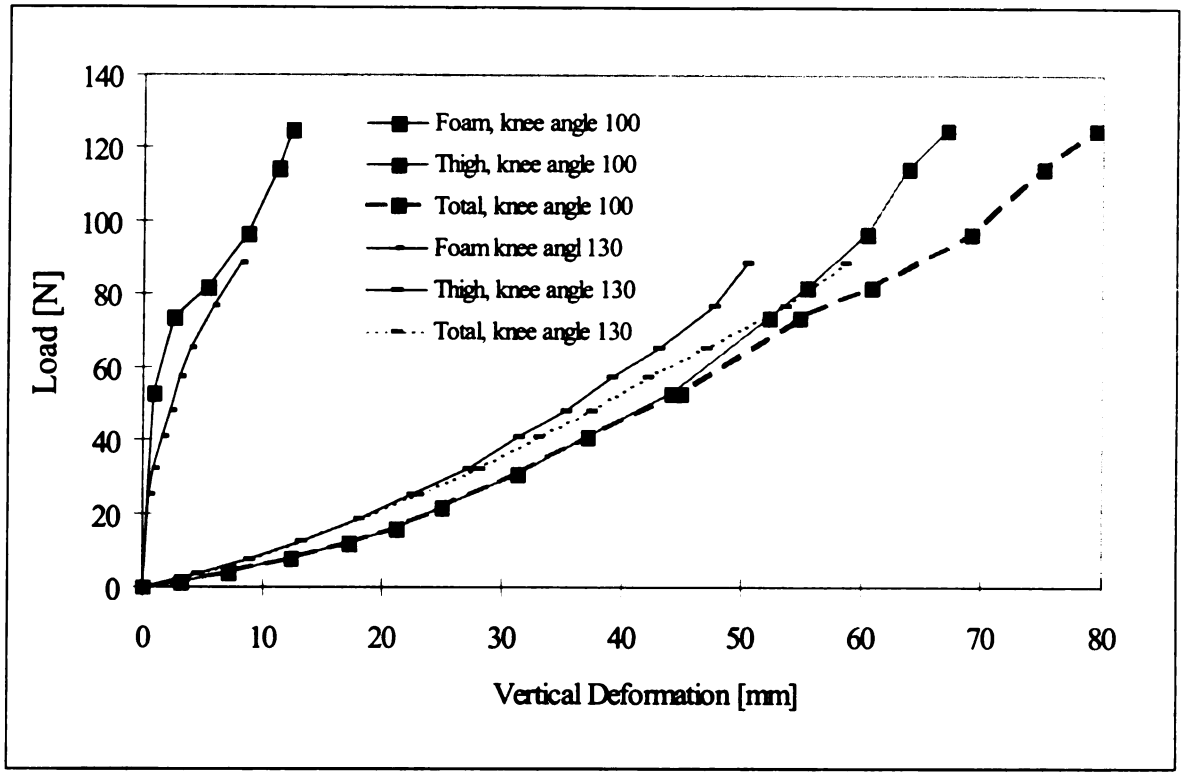

Figure E.56 Total, Thigh, and Foam Vertical Deformation Versus Load, Subject No. 5, Thigh with Two Knee Angle 100° and 130° Interaction with One Foam (100 mm Thickness and 43 kg/m^3 Density)

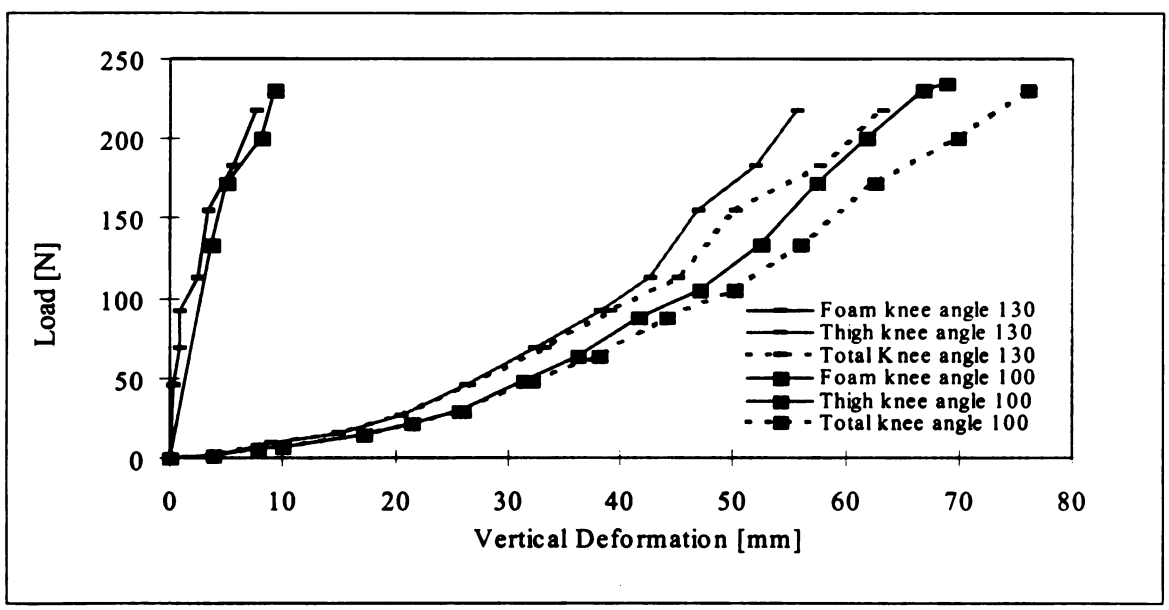

Figure E.57 Total, Thigh, and Foam Vertical Deformation Versus Load, Subject No. 6, Thigh with Two Knee Angle 100° and 130° Interaction with One Foam (100 mm Thickness and 51 kg/m^3 Density

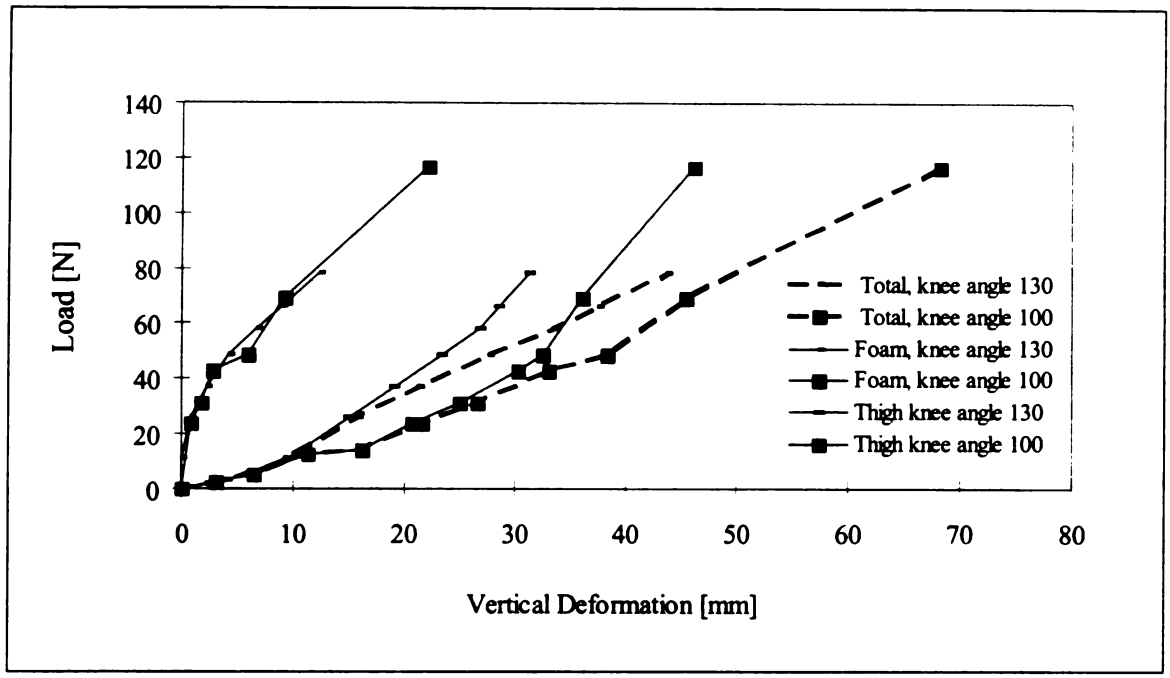

Figure E.58 Total, Thigh, and Foam Vertical Deformation Versus Load, Subject No. 6, Thigh with Two Knee Angle 100° and 130° Interaction with One Foam (100 mm Thickness and 43 kg/m^3 Density)

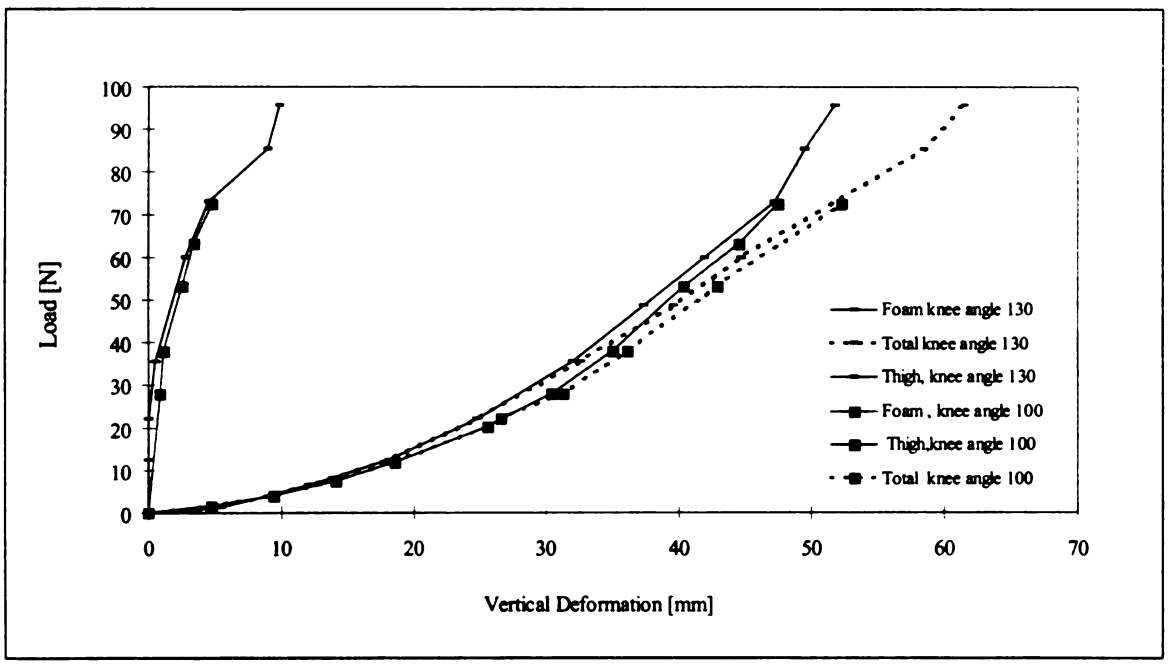

Figure E.59 Total, Thigh, and Foam Vertical Deformation Versus Load, Subject No. 7, Thigh with Two Knee Angle 100° and 130° Interaction with One Foam (100 mm Thickness and 43 kg/m^3 Density)

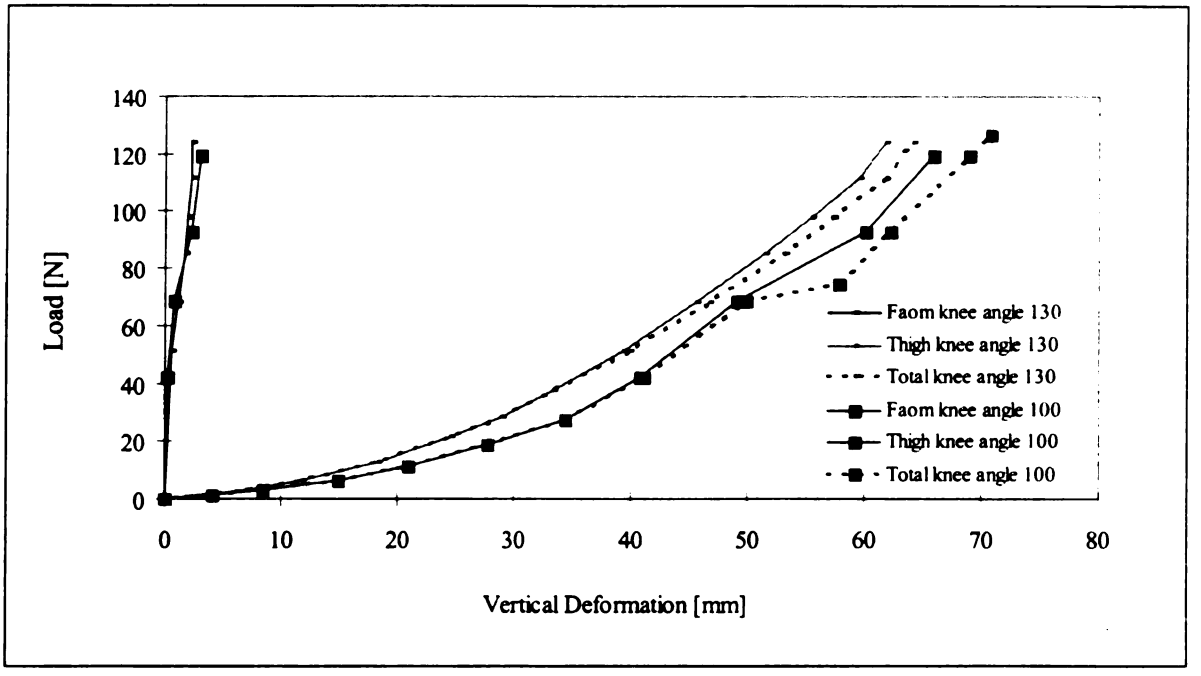

Figure E.60 Total, Thigh, and Foam Vertical Deformation Versus Load, Subject No. 7, Thigh with Two Knee Angle 100° and 130° Interaction with One Foam (100 mm Thickness and 51 kg/m^3 Density)

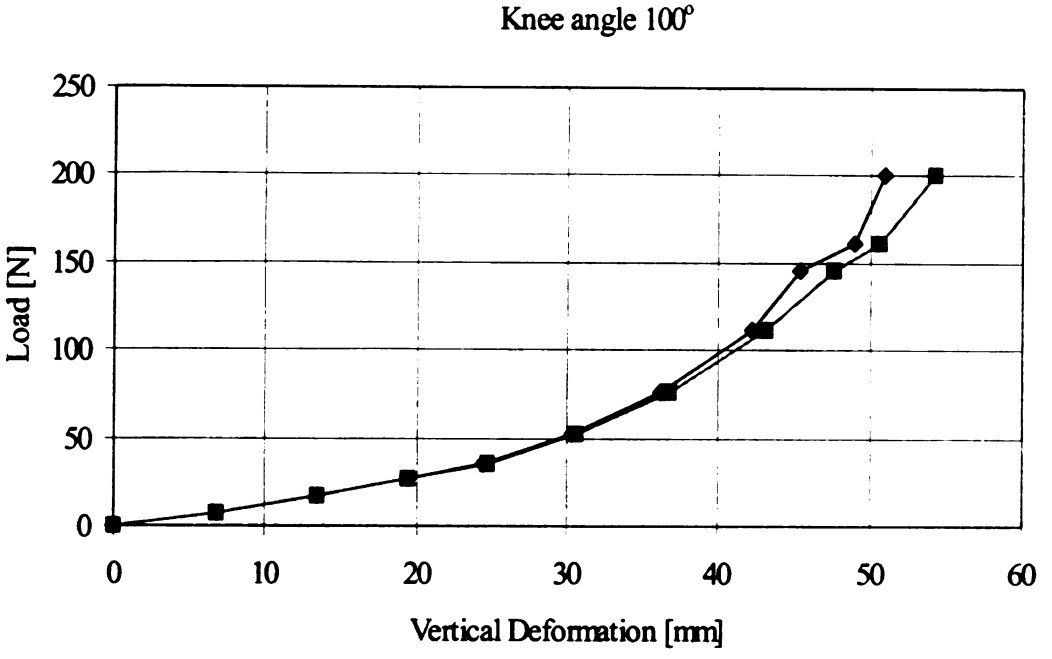

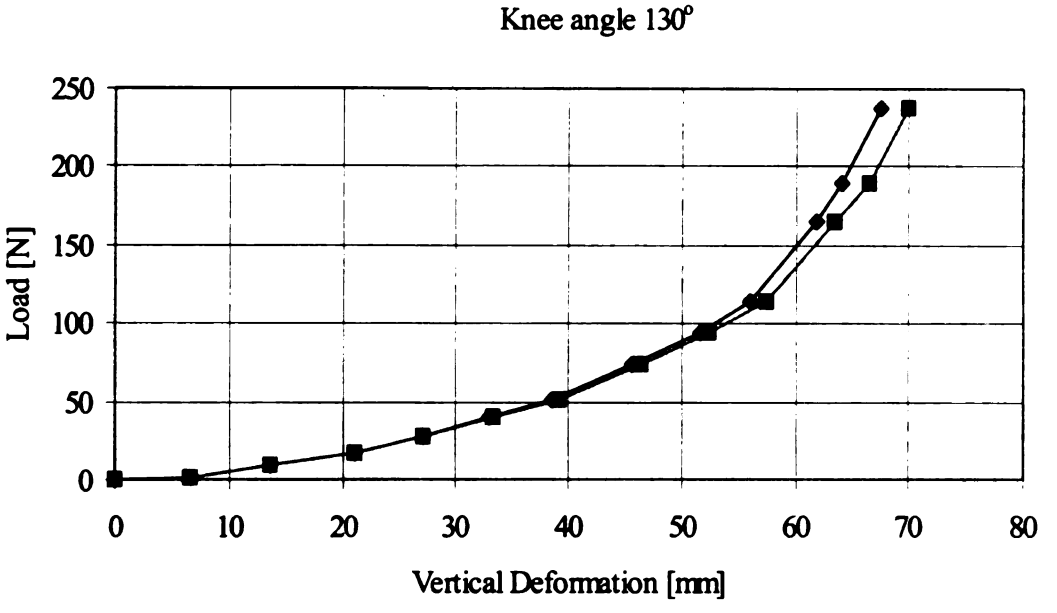

Figure E.61 Vertical Deformation of Thigh versus Load at Node 3,3 and 3,4, Subject No. 1, Foam 61, Thickness 100 mm. Knee angles 100° and 130°

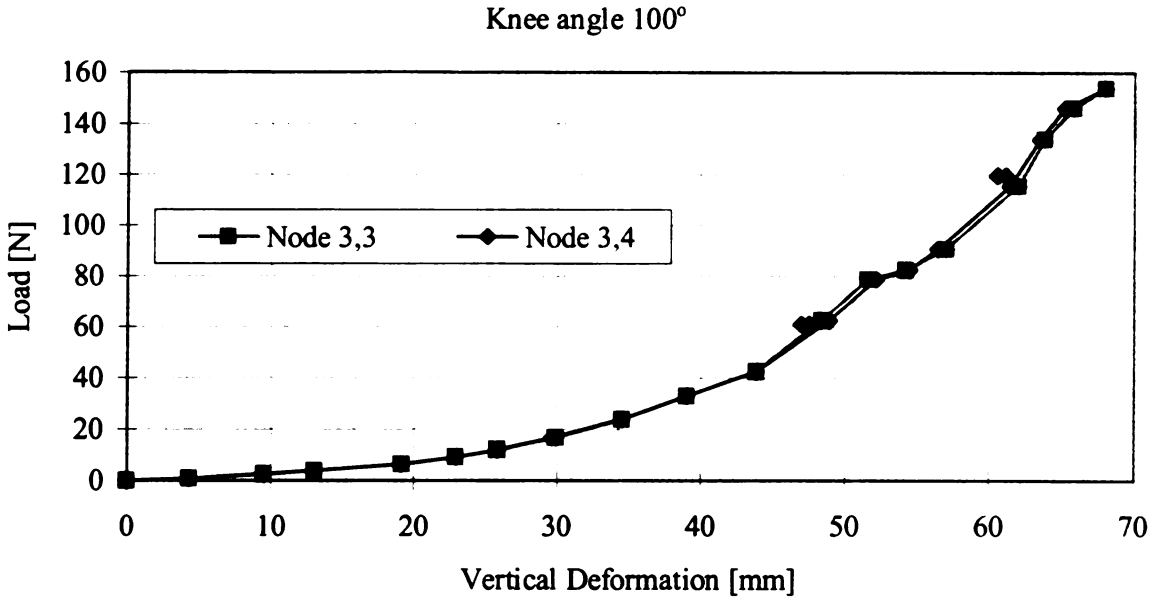

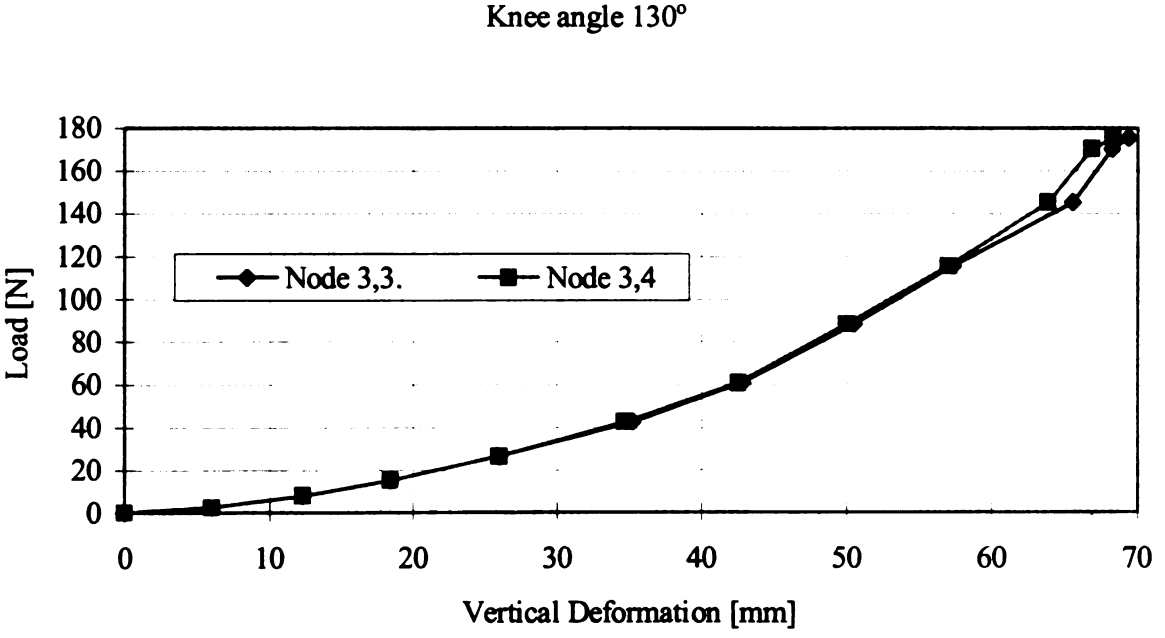

Figure E.62 Vertical Deformation of Thigh versus Load at Node 3,3 and 3,4, Subject No.2, Foam 61, Thickness 100 mm. Knee angles 100° and 130°

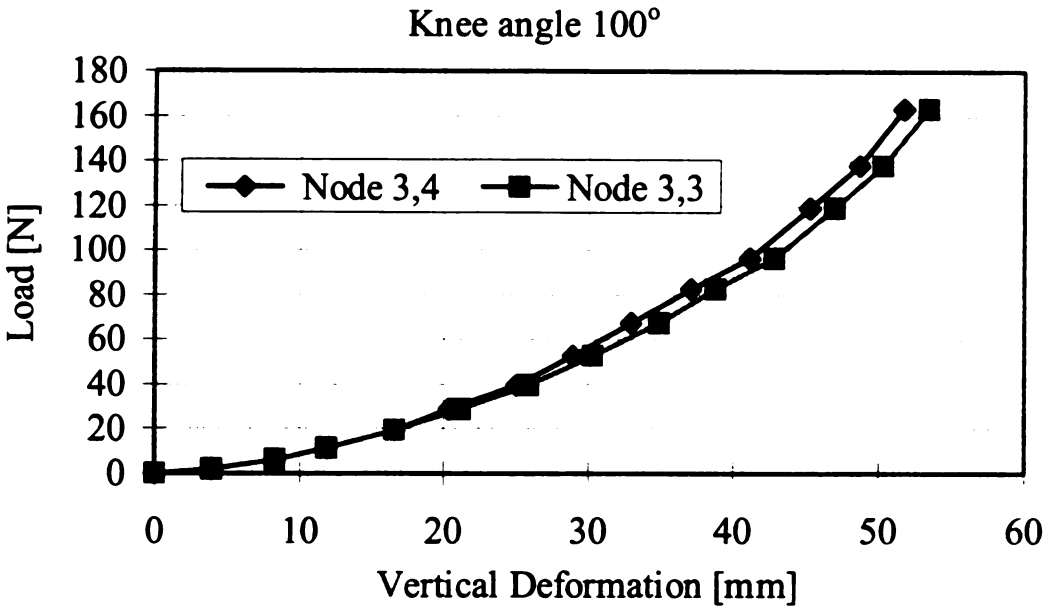

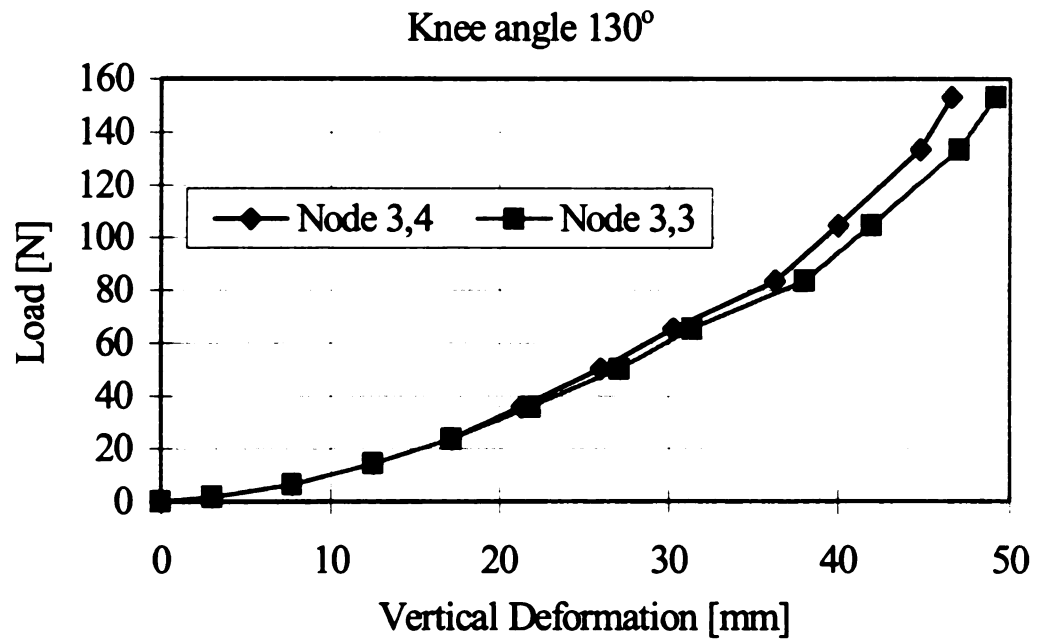

Figure E.63 Vertical Deformation of Thigh versus Load at Node 3,3 and 3,4, Subject No.3, Foam 61, Thickness 100 mm. Knee angles 100° and 130°

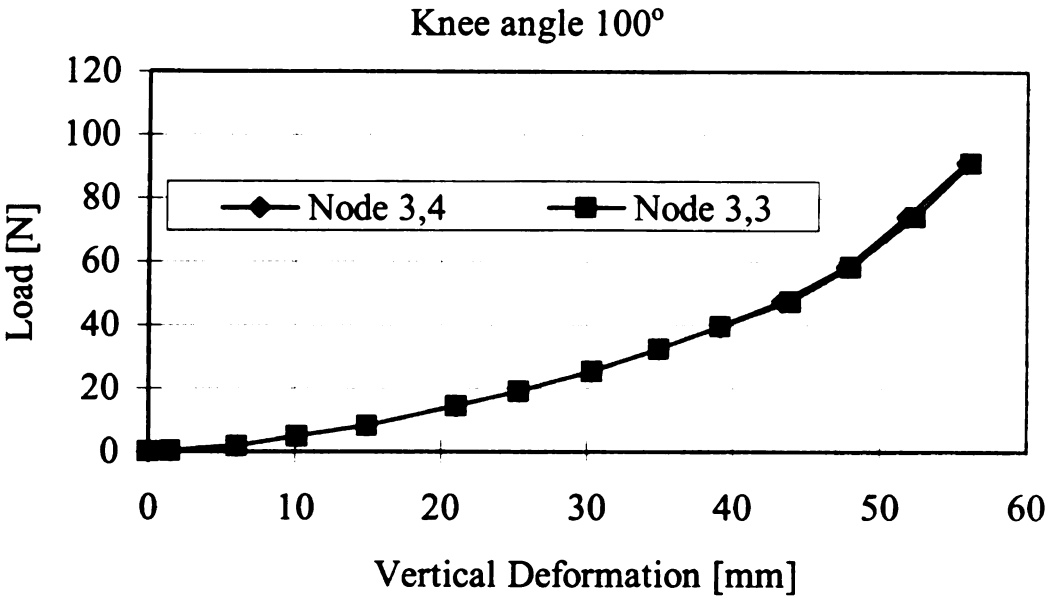

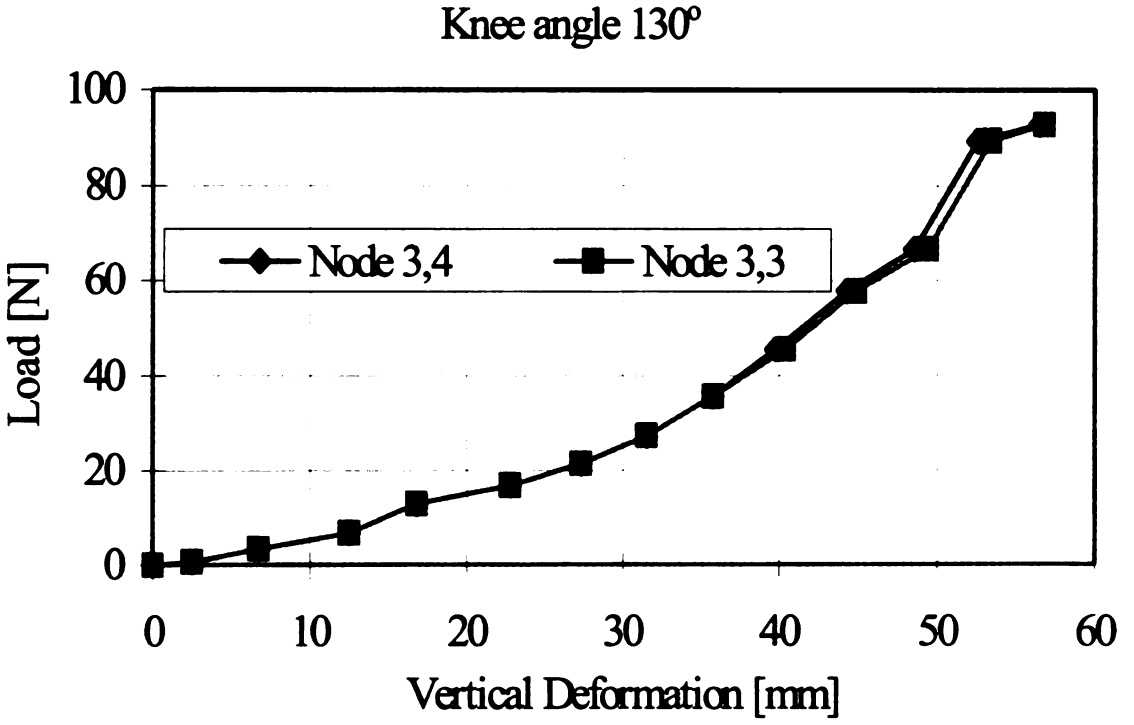

Figure E.64 Vertical Deformation of Thigh versus Load at Node 3,3 and 3,4, Subject No.4, Foam 61, Thickness 100 mm. Knee angles 100° and 130°

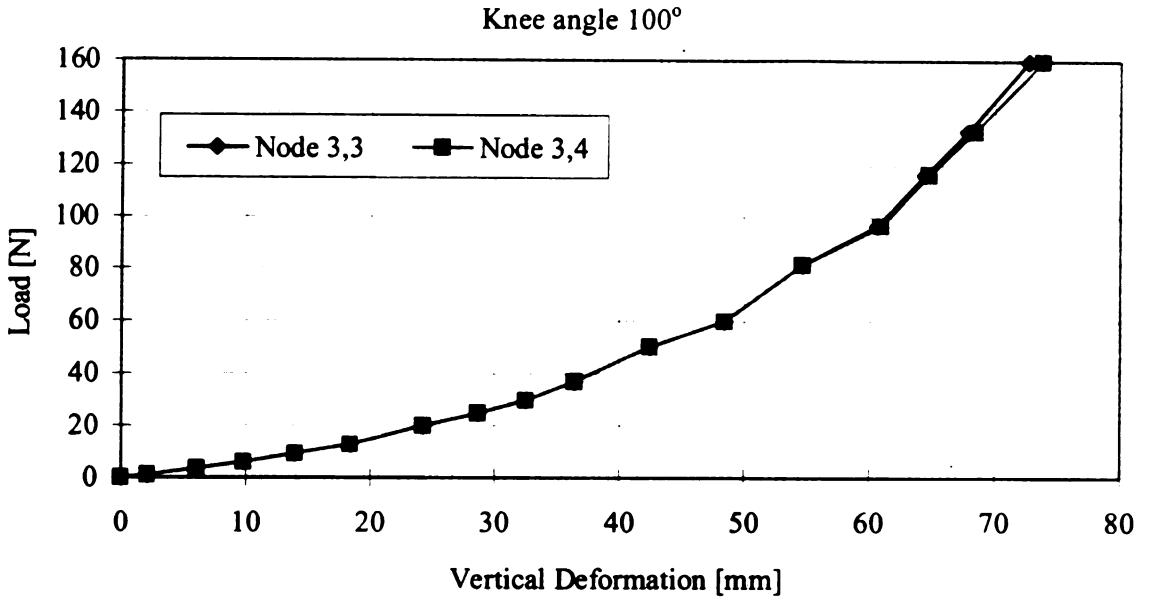

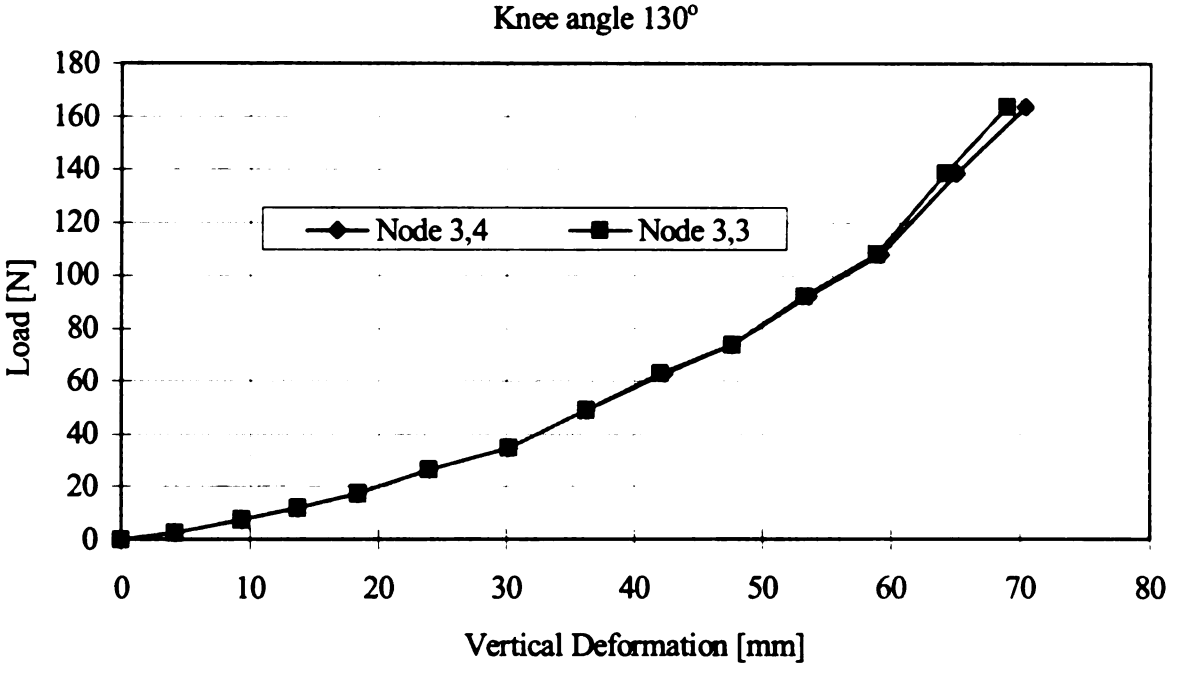

Figure E.65 Vertical Deformation of Thigh versus Load at Node 3,3 and 3,4, Subject No. 5, Foam 61, Thickness 100 mm. Knee angles 100° and 130°

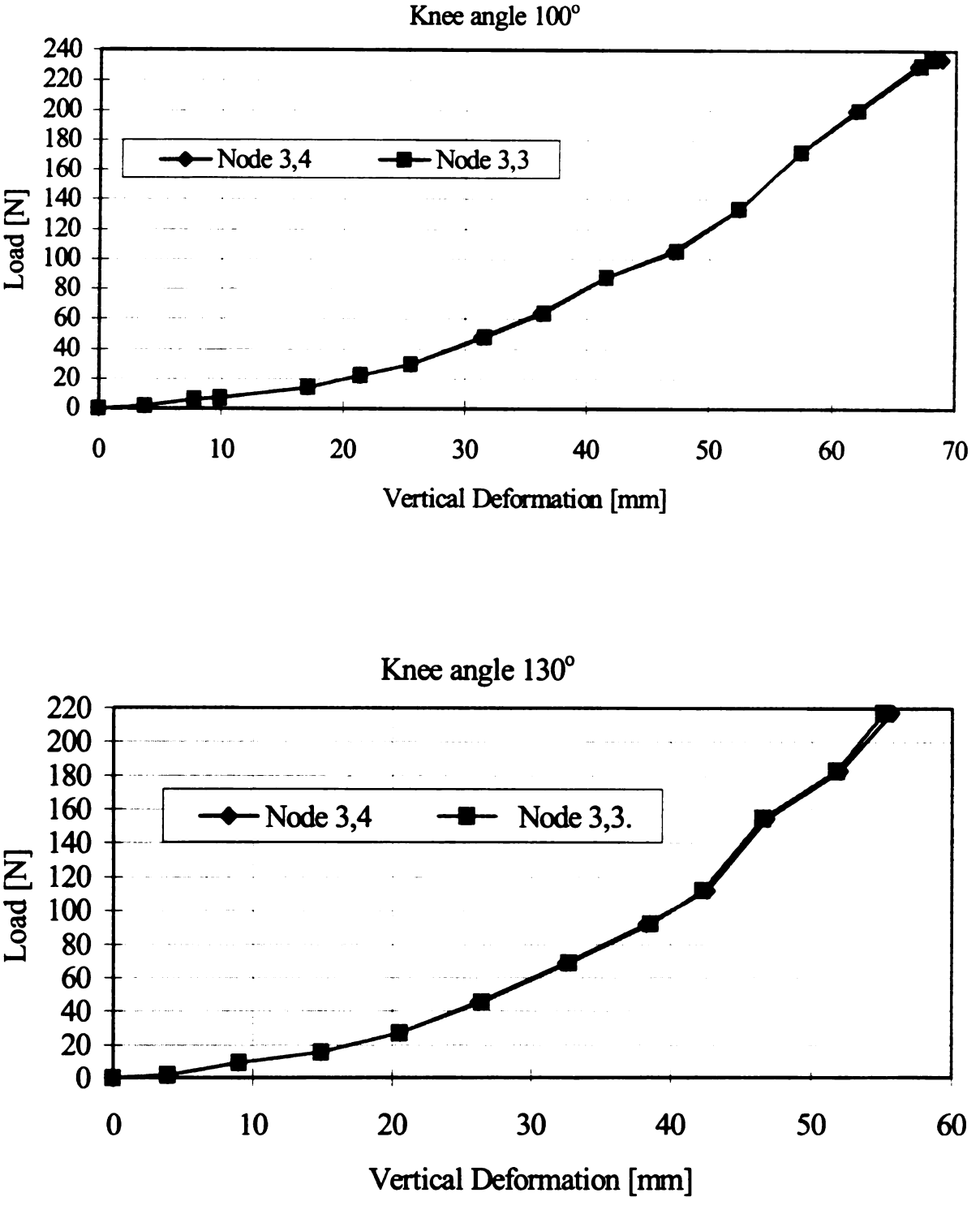

Figure E.66 Vertical Deformation of Thigh versus Load at Node 3,3 and 3,4, Subject No.6, Foam 61, Thickness 100 mm. Knee angles 100° and 130°

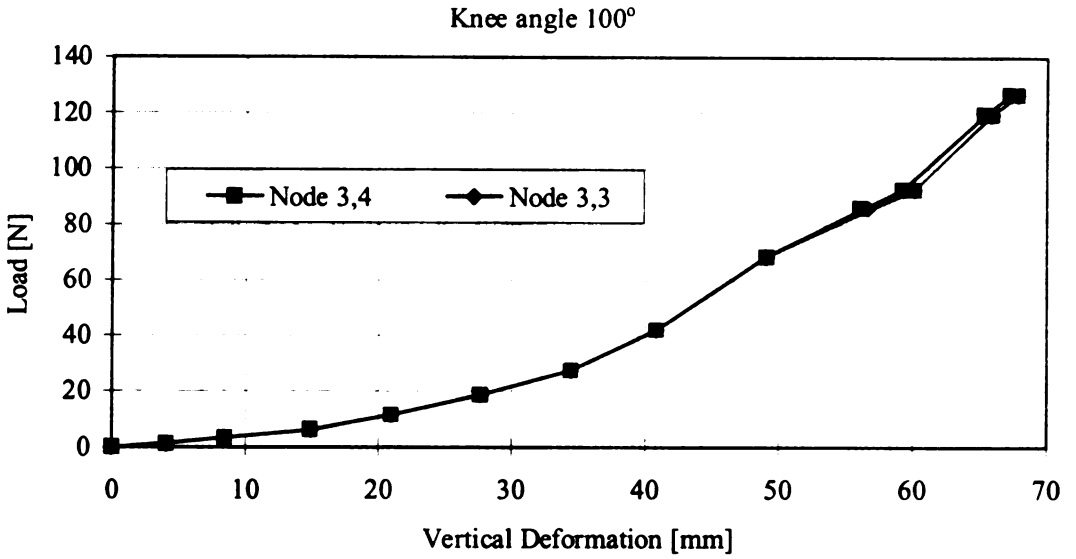

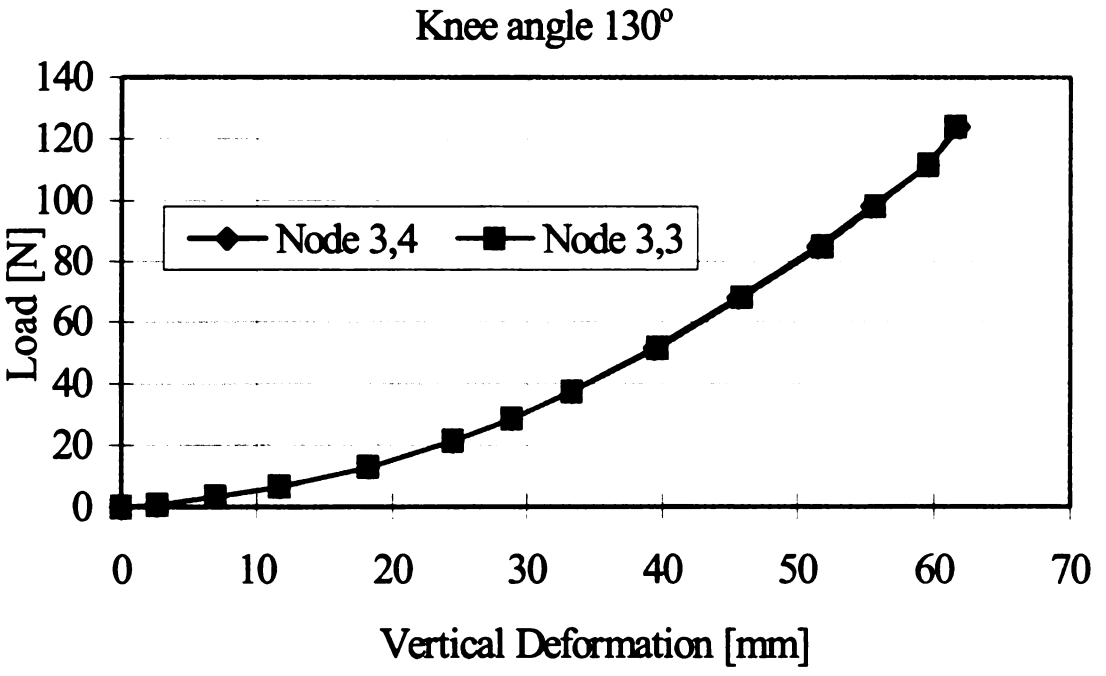

Figure E.67 Vertical Deformation of Thigh versus Load at Node 3,3 and 3,4, Subject No.7, Foam 61, Thickness 100 mm. Knee angles 100° and 130

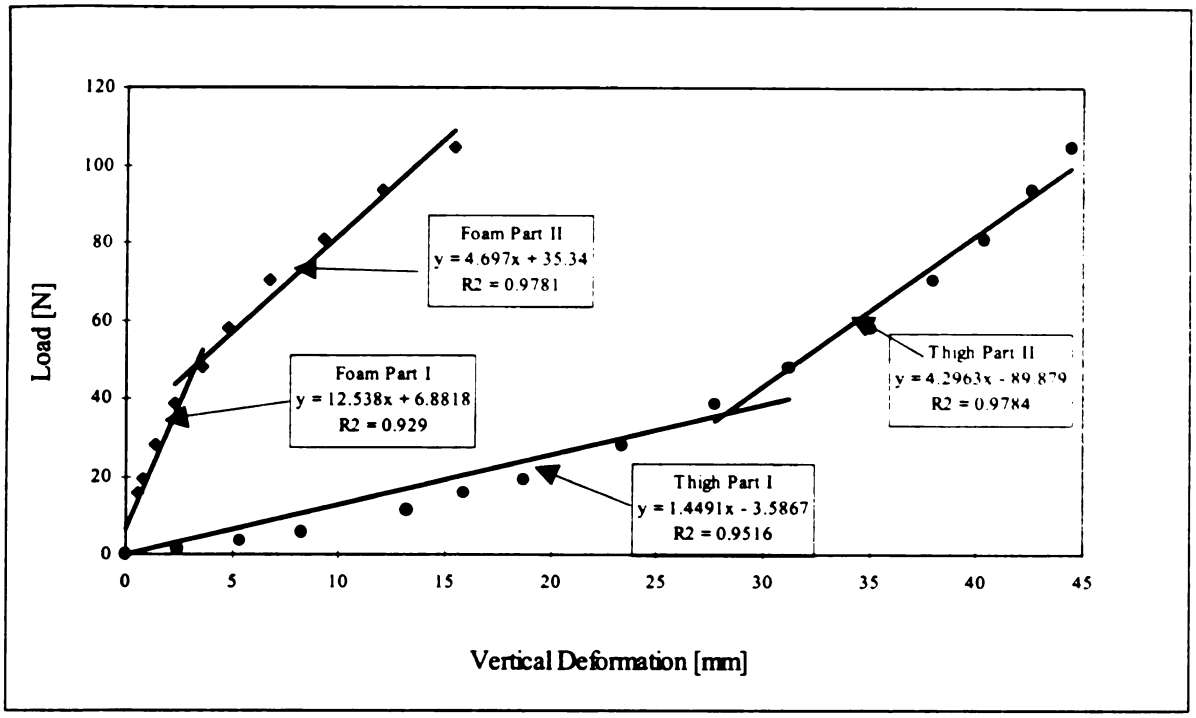

Figure E.68 Linearization of Load-Vertical Deformation Curves for the Thigh and Foam. Foam 43 kg/m^3, Knee Angle 100°, Subject No. 1

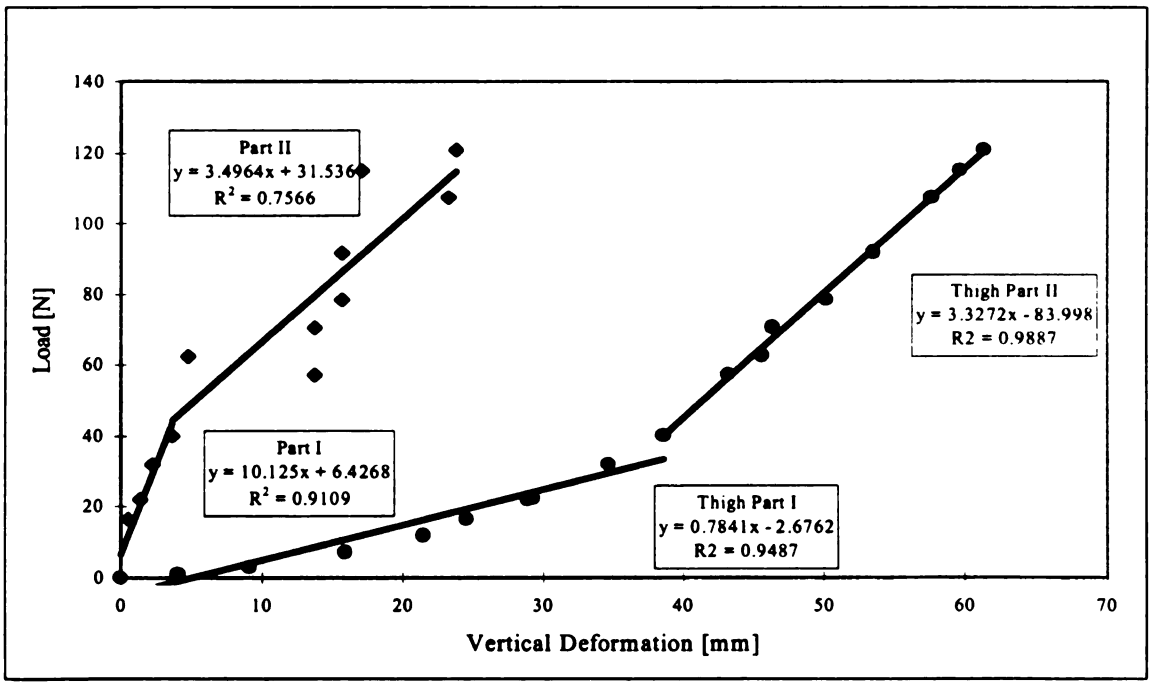

Figure E.69 Linearization of Load-Vertical Deformation Curves for the Thigh and Foam. Foam 43 kg/m^3, Knee Angle 100°, Subject No. 2

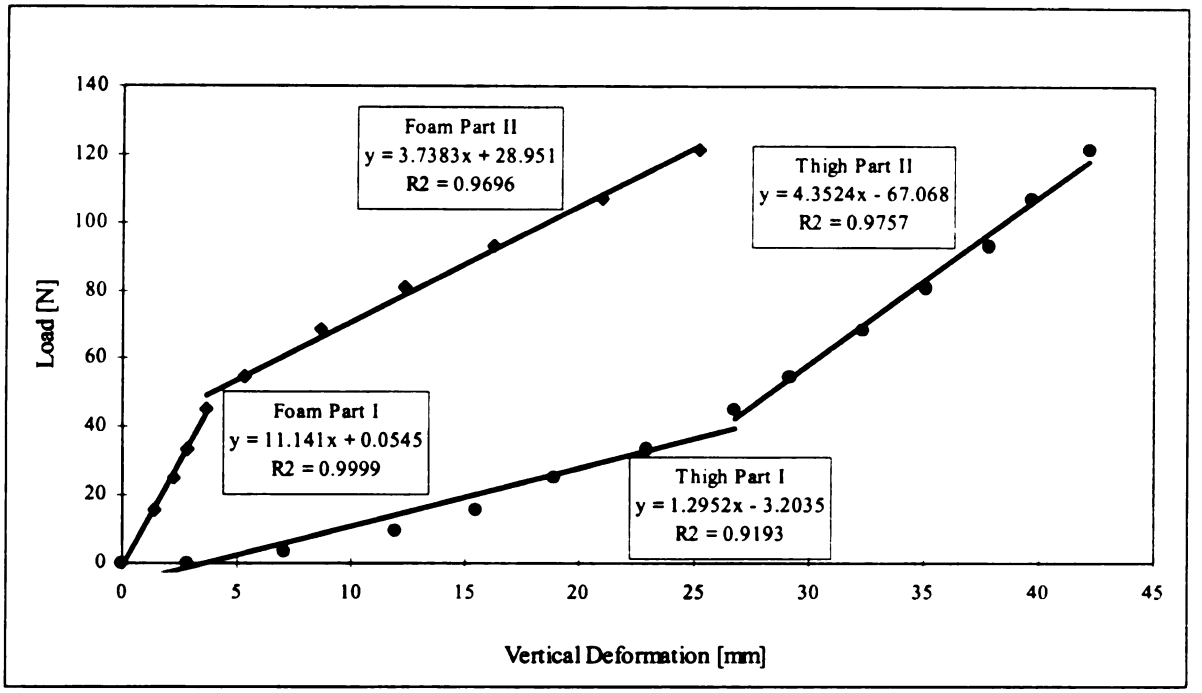

Figure E.70 Linearization of Load-Vertical Deformation Curves for the Thigh and Foam. Foam 43 kg/m^3, Knee Angle 100°, Subject No. 3

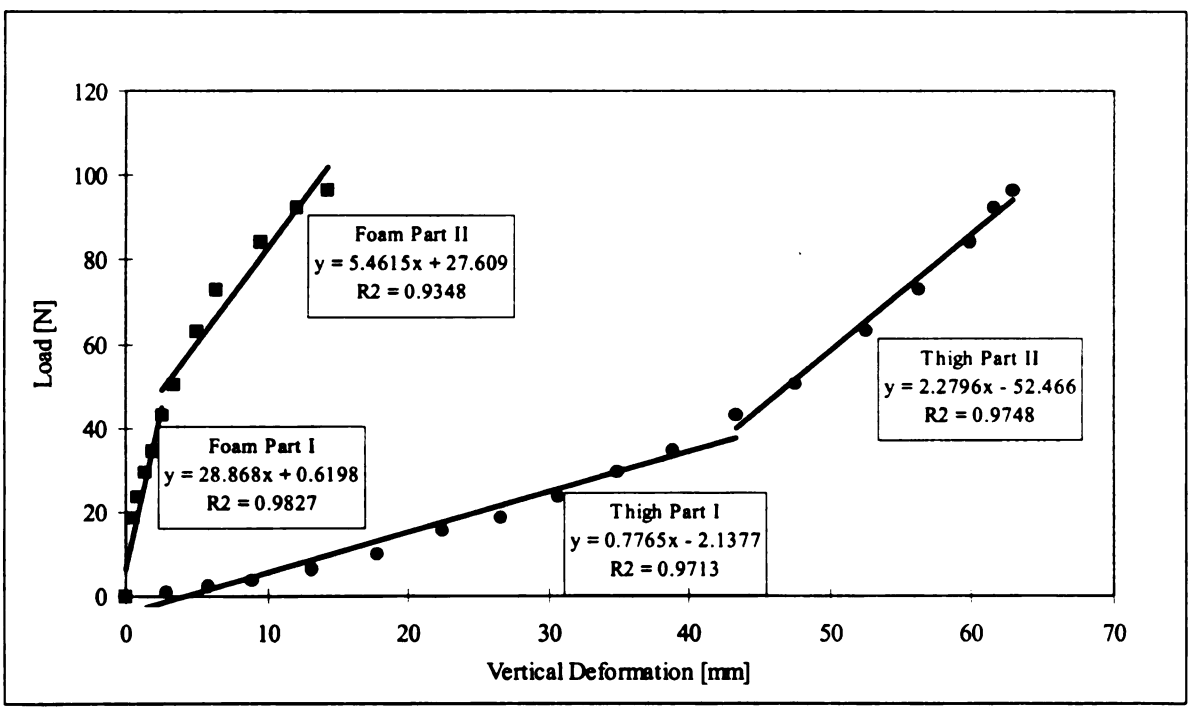

Figure E.71 Linearization of Load-Vertical Deformation Curves for the Thigh and Foam. Foam 43 kg/m^3, Knee Angle 100°, Subject No. 4

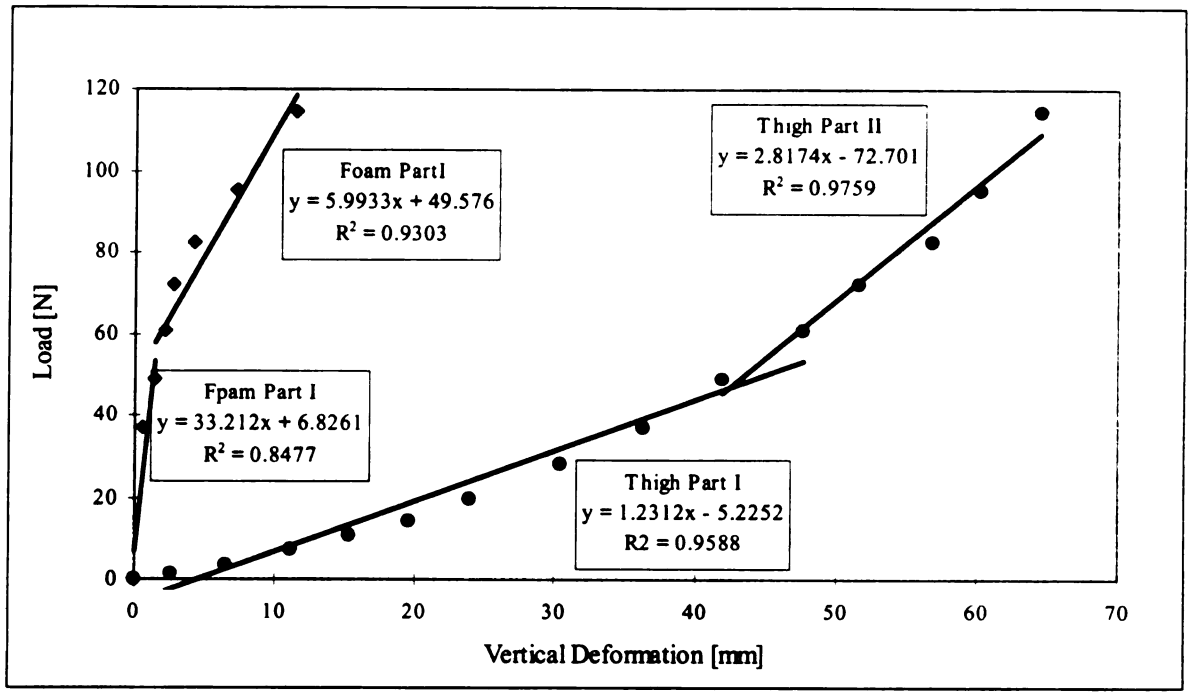

Figure E.72 Linearization of Load-Vertical Deformation Curves for the Thigh and Foam. Foam 43 kg/m^3, Knee Angle 100°, Subject No. 5

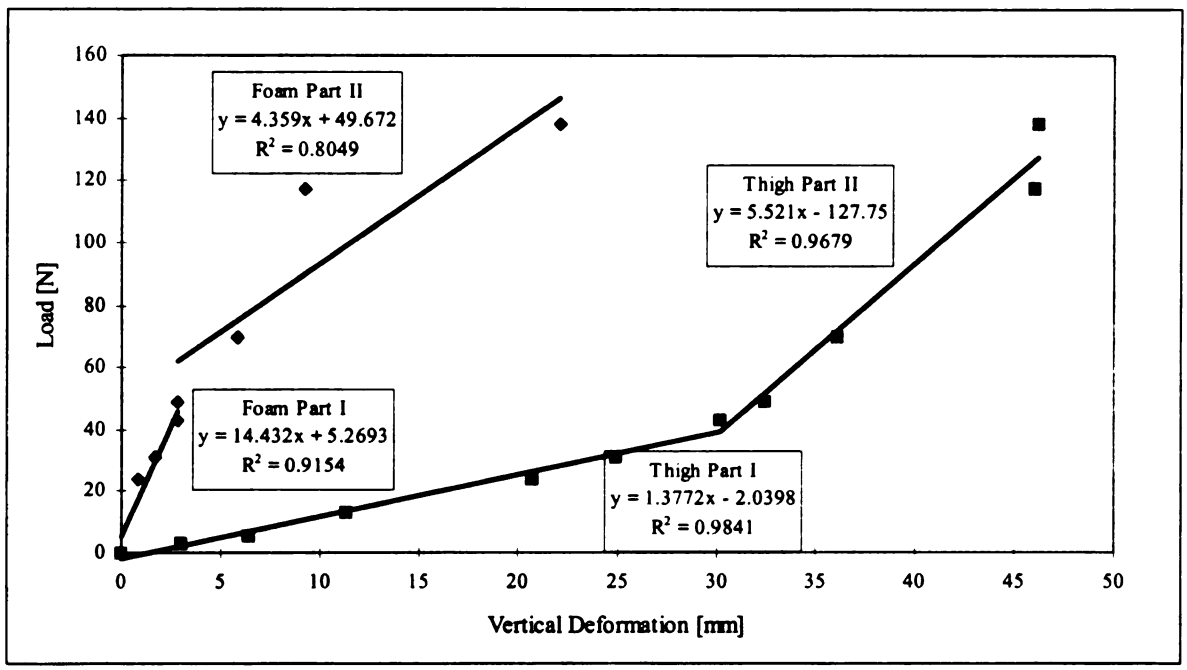

Figure E.73 Linearization of Load-Vertical Deformation Curves for the Thigh and Foam. Foam 43 kg/m^3, Knee Angle 100°, Subject No. 6

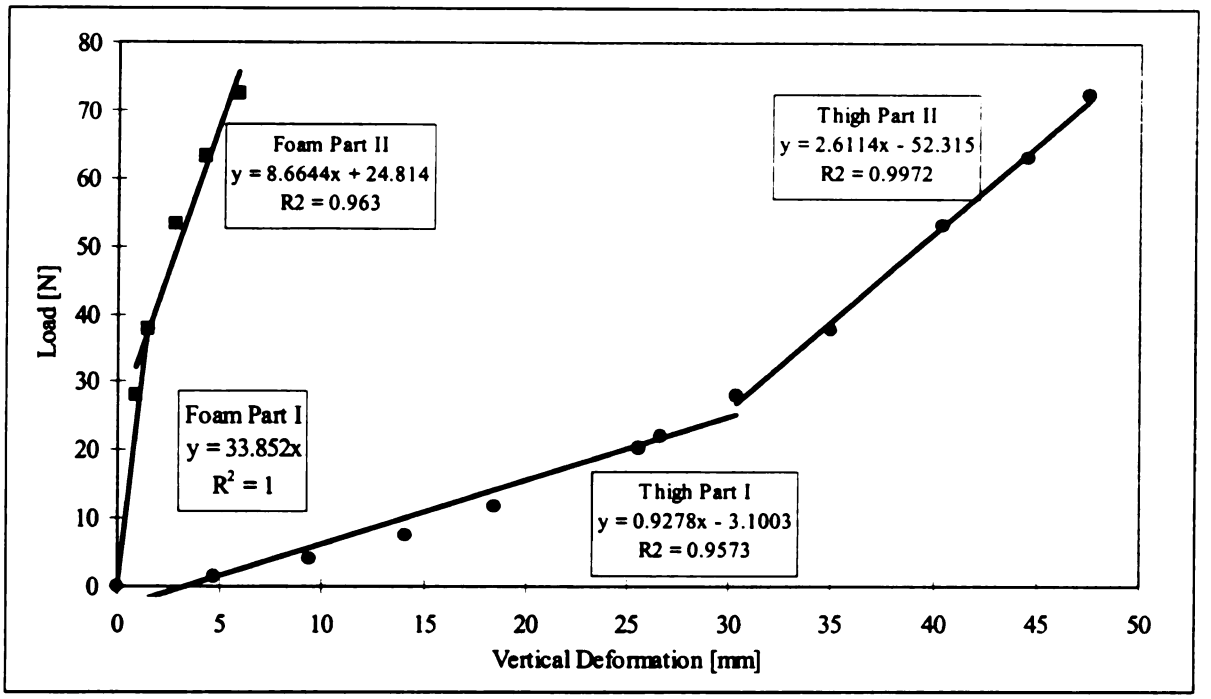

Figure E.74 Linearization of Load-Vertical Deformation Curves for the Thigh and Foam. Foam 43 kg/m^3, Knee Angle 100°, Subject No. 7

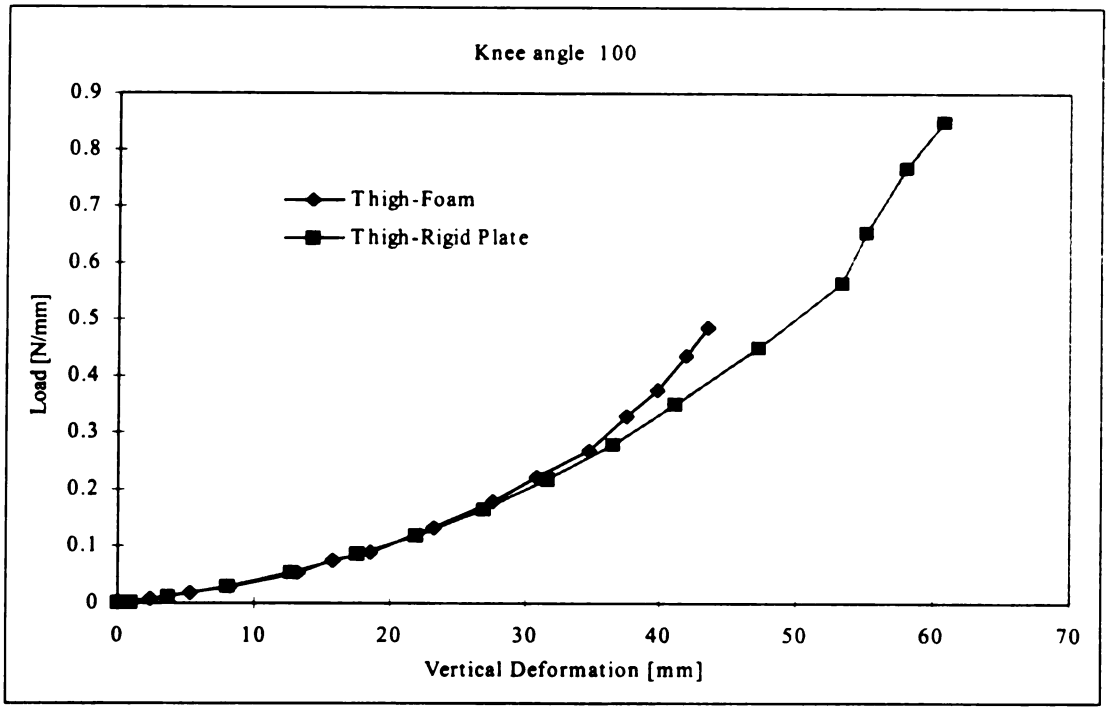

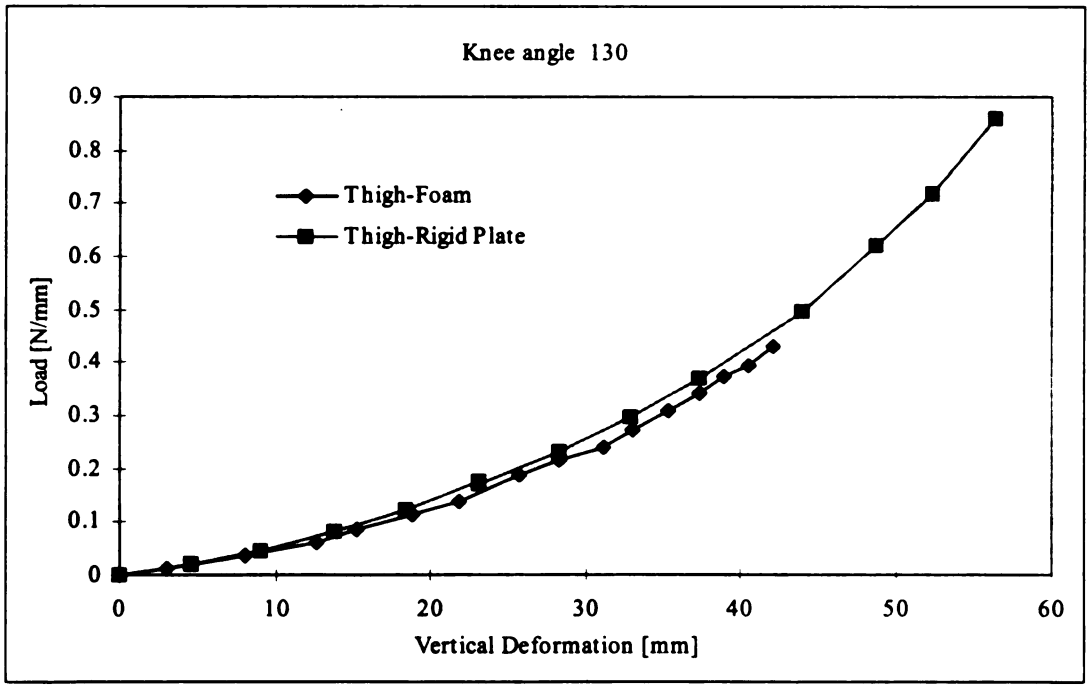

Figure A.75 Load Normalization for Thigh-Foam (43 kg/m^3 Foam Density) Interaction and Thigh-Rigid Plat Tests, Subject No. 1

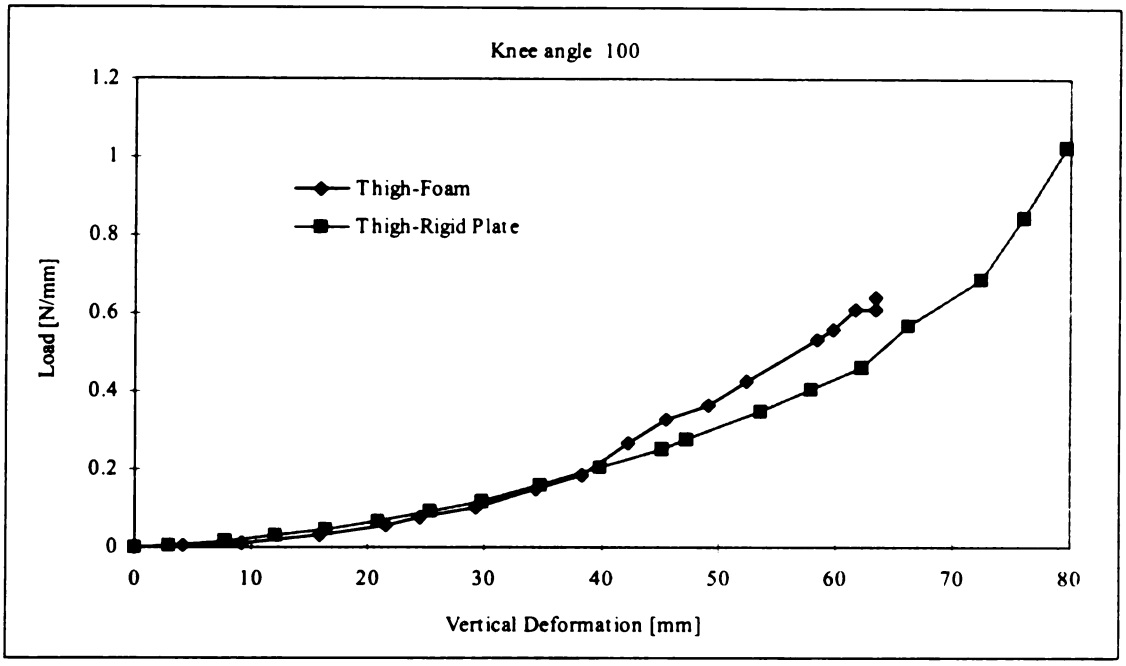

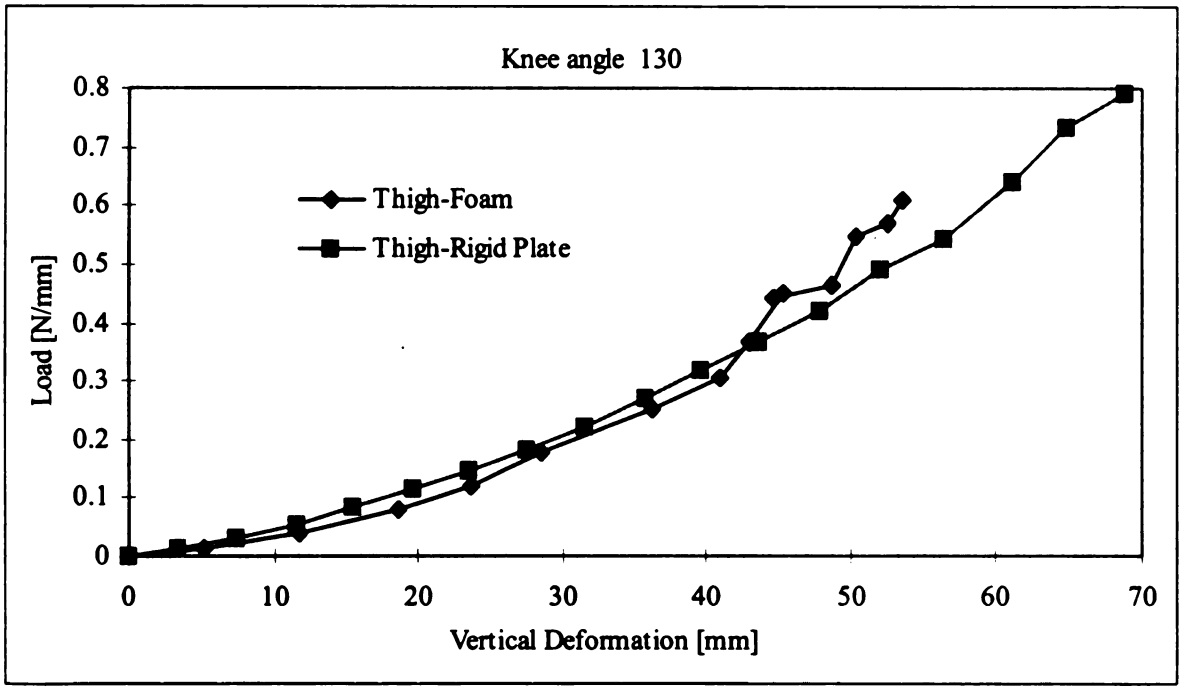

Figure A.76Load Normalization for Thigh-Foam (43 kg/m^3 Foam Density) Interaction and Thigh-Rigid Plat Tests, Subject No. 2

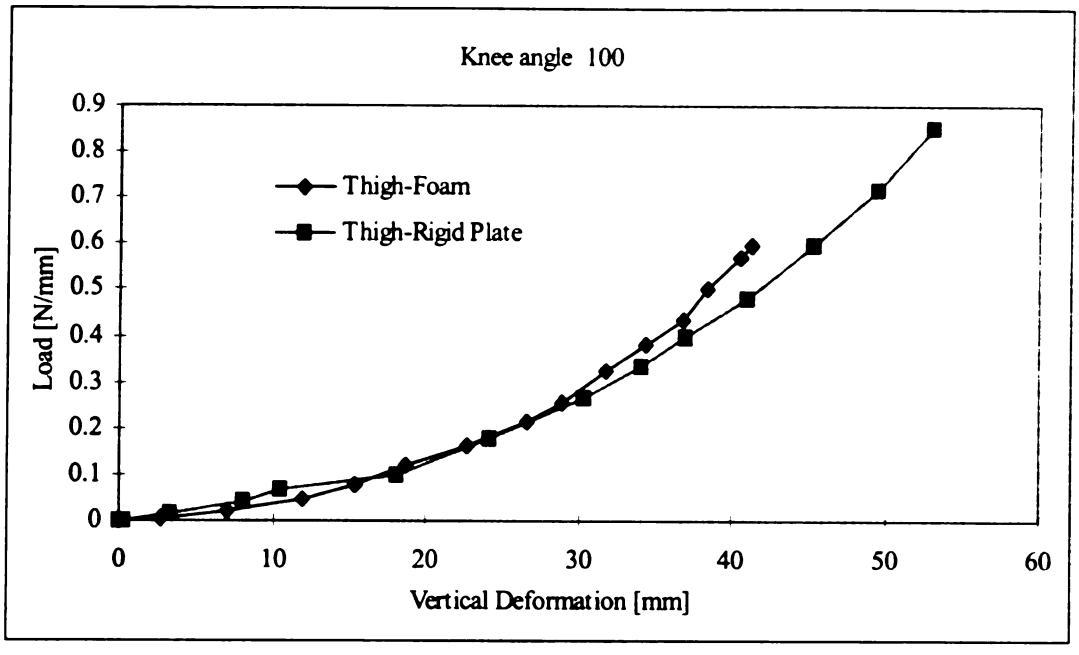

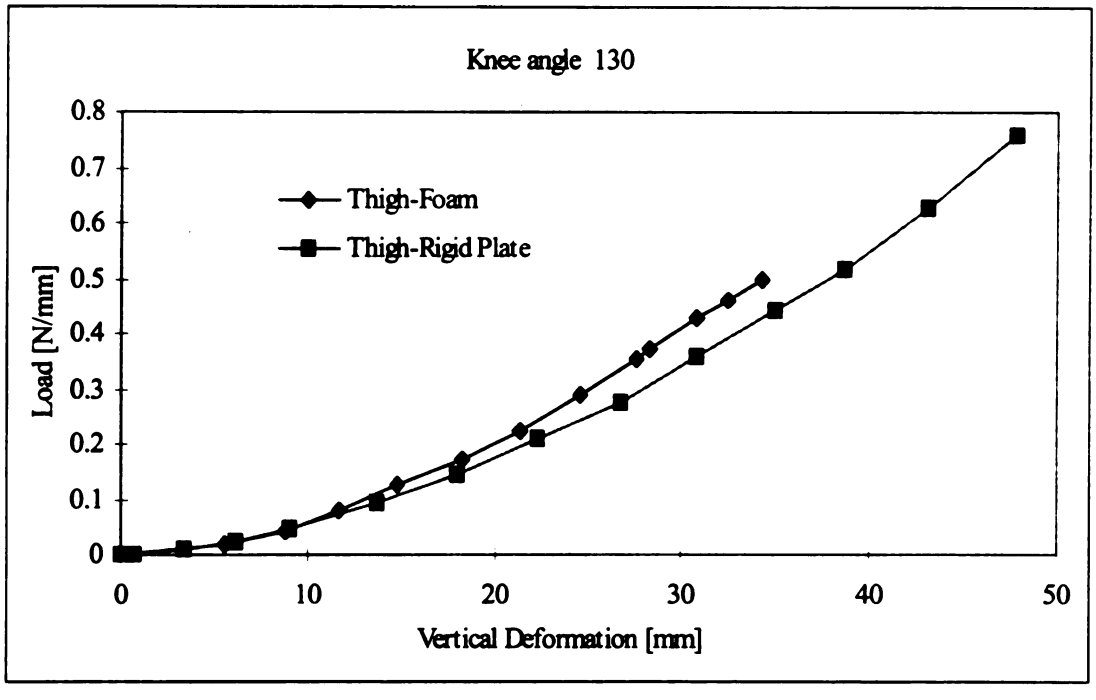

Figure A.77 Load Normalization for Thigh-Foam (43 kg/m^3 Foam Density) Interaction and Thigh-Rigid Plat Tests, Subject No. 3

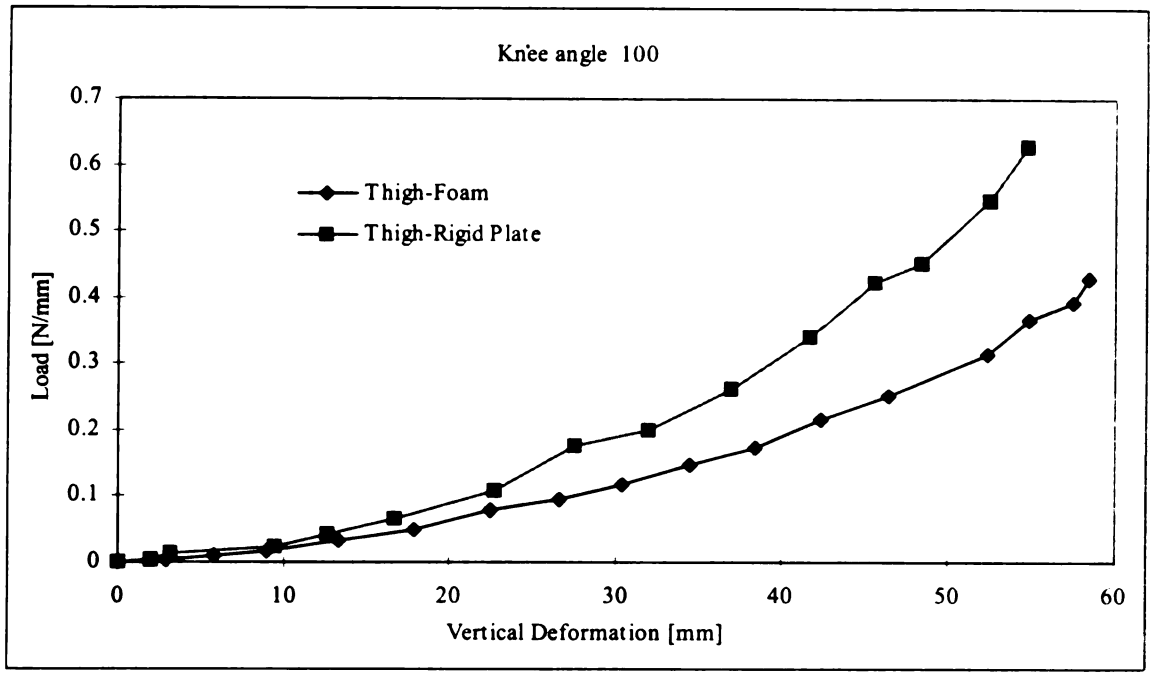

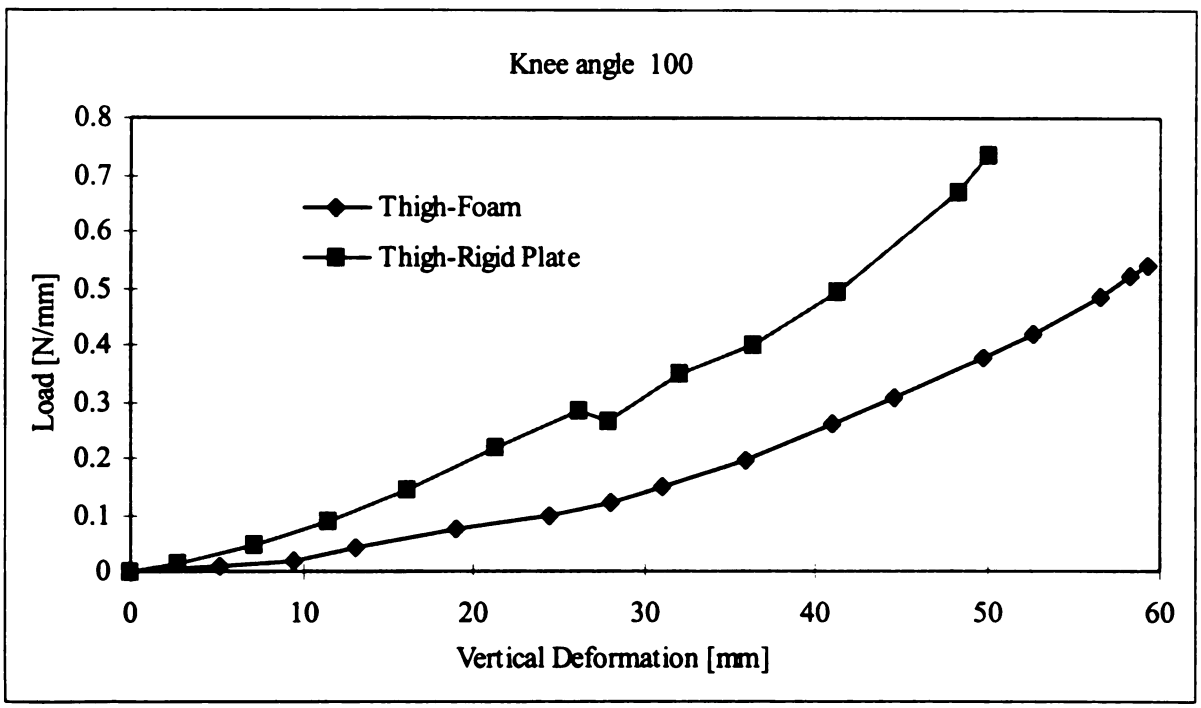

Figure A.78 Load Normalization for Thigh-Foam (43 kg/m^3 Foam Density) Interaction and Thigh-Rigid Plat Tests, Subject No. 4

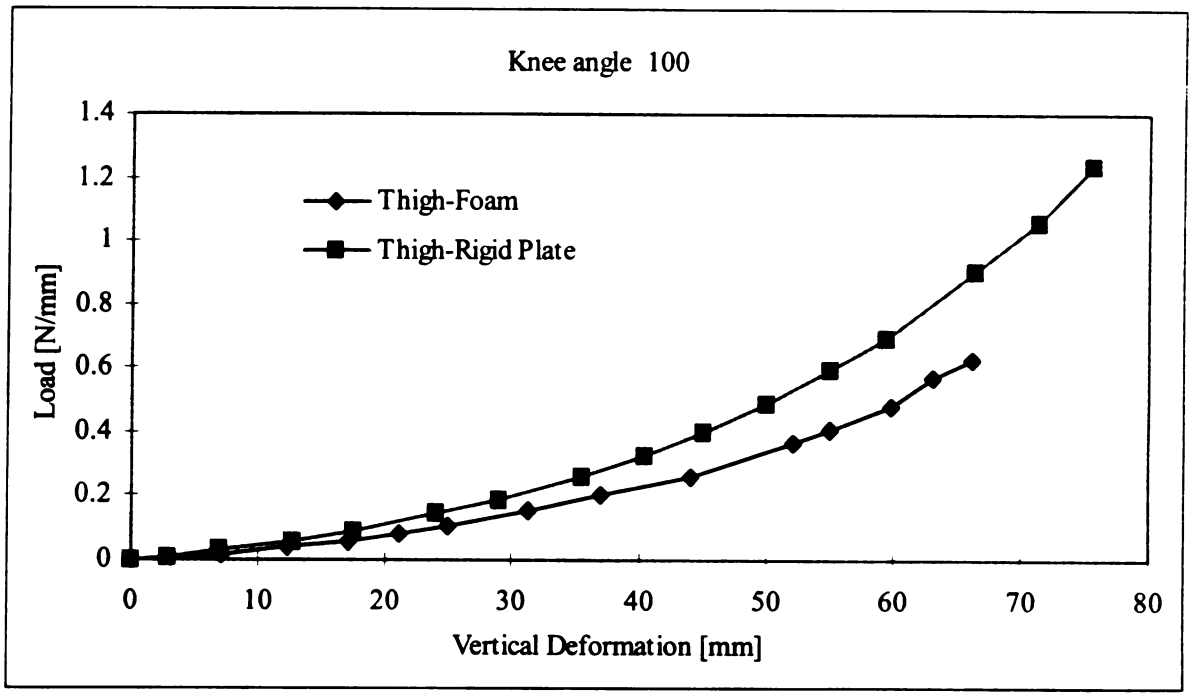

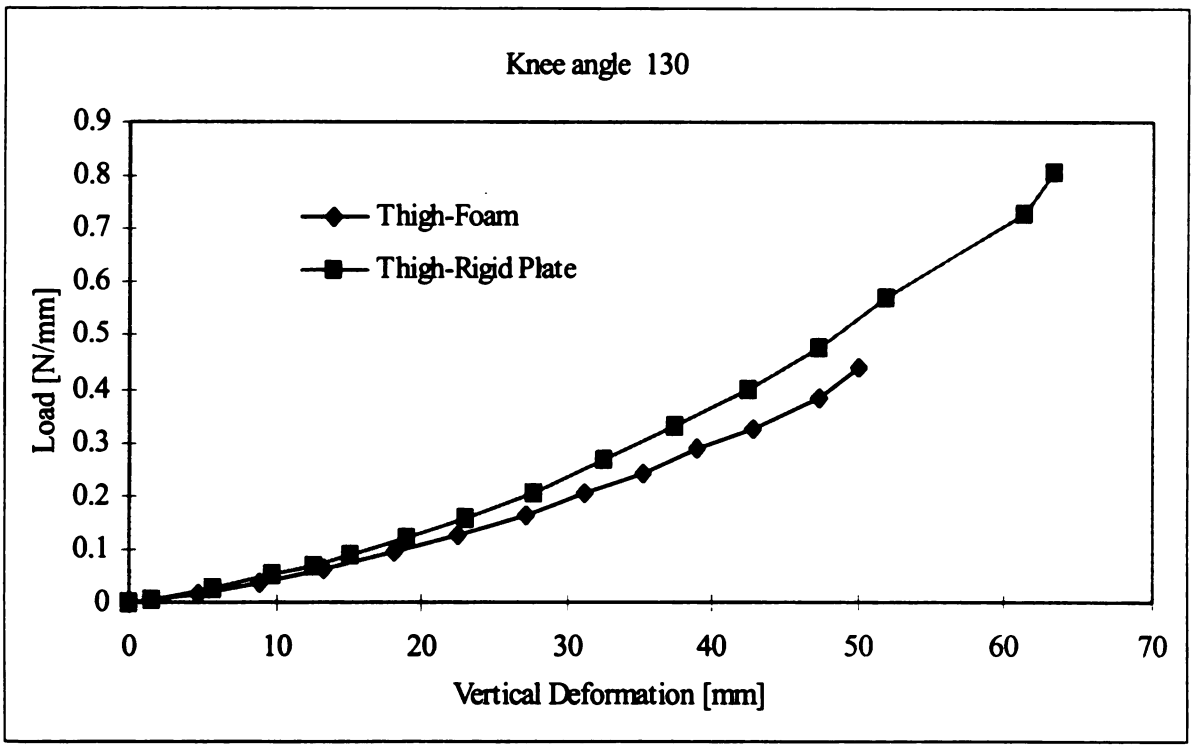

Figure A.79 Load Normalization for Thigh-Foam (43 kg/m^3 Foam Density) Interaction and Thigh-Rigid Plat Tests, Subject No. 5

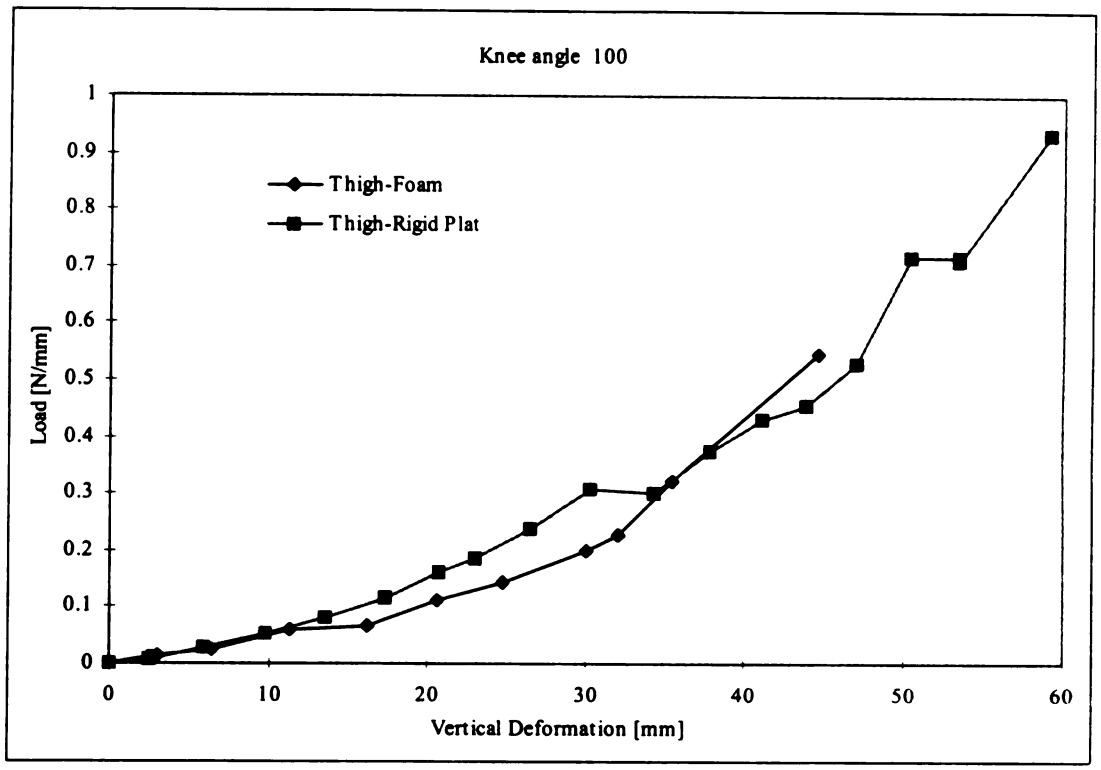

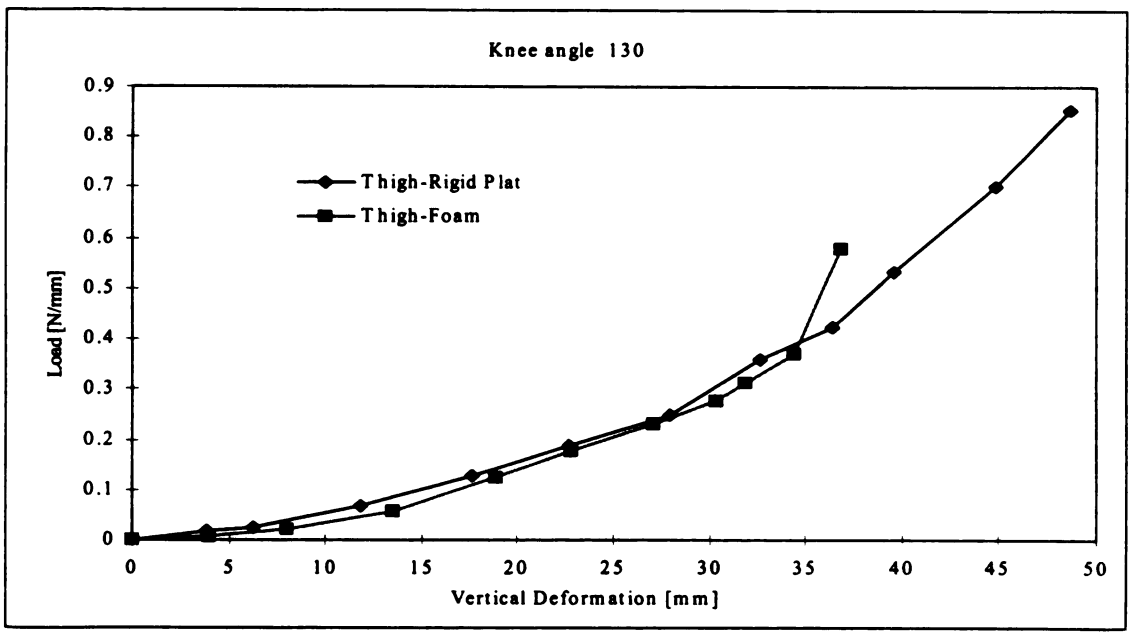

Figure A.80 Load Normalization for Thigh-Foam (A3 kg/m^3 Foam Density) Interaction and Thigh-Rigid Plat Tests, Subject No. 6

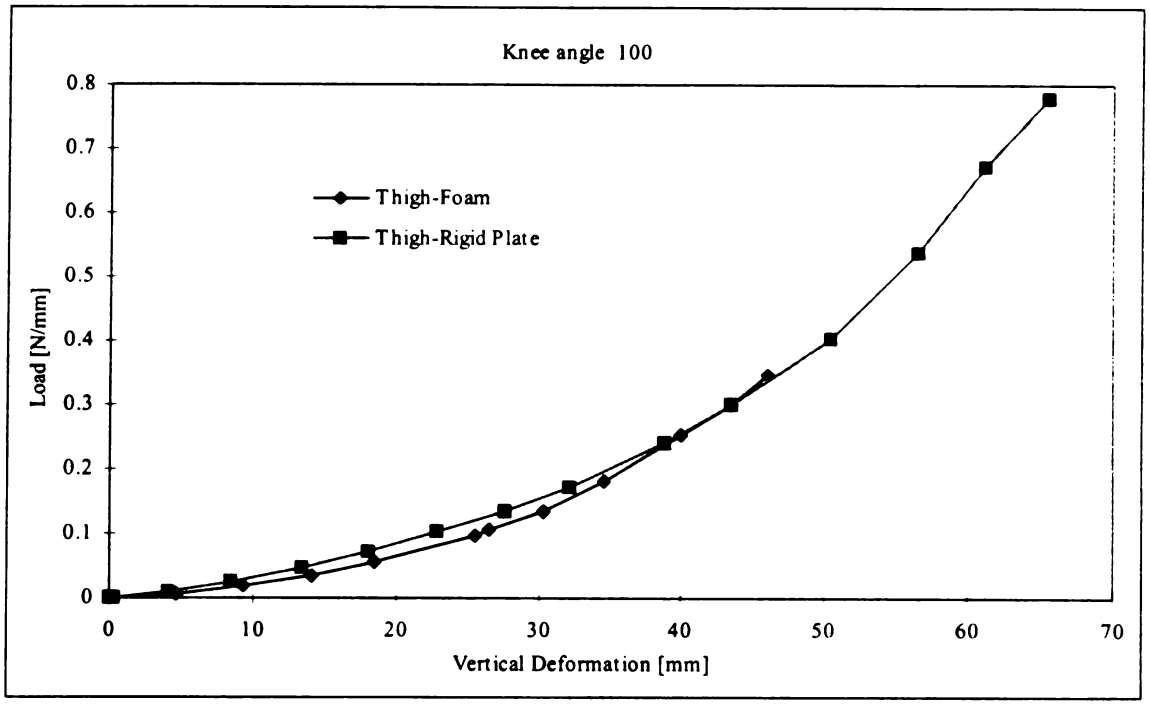

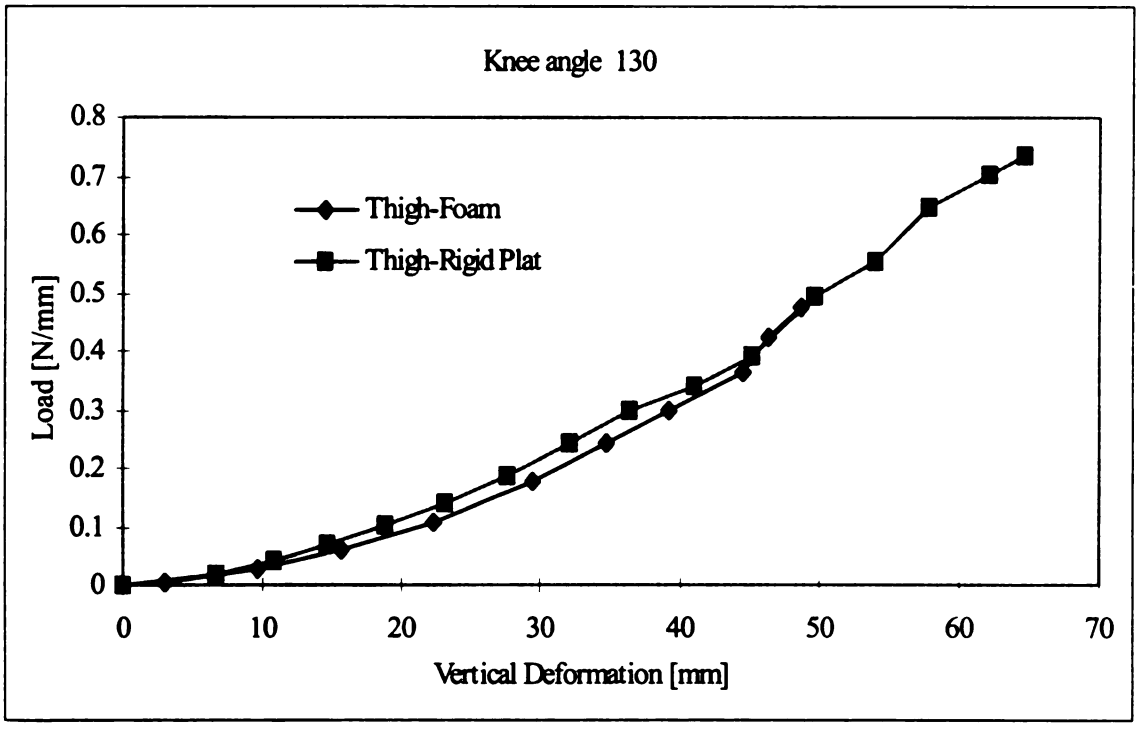

Figure 4.81 Load Normalization for Thigh-Foam (A3 kg/m^3 Foam Density) Interaction and Thigh-Rigid Plat Tests, Subject No. 7

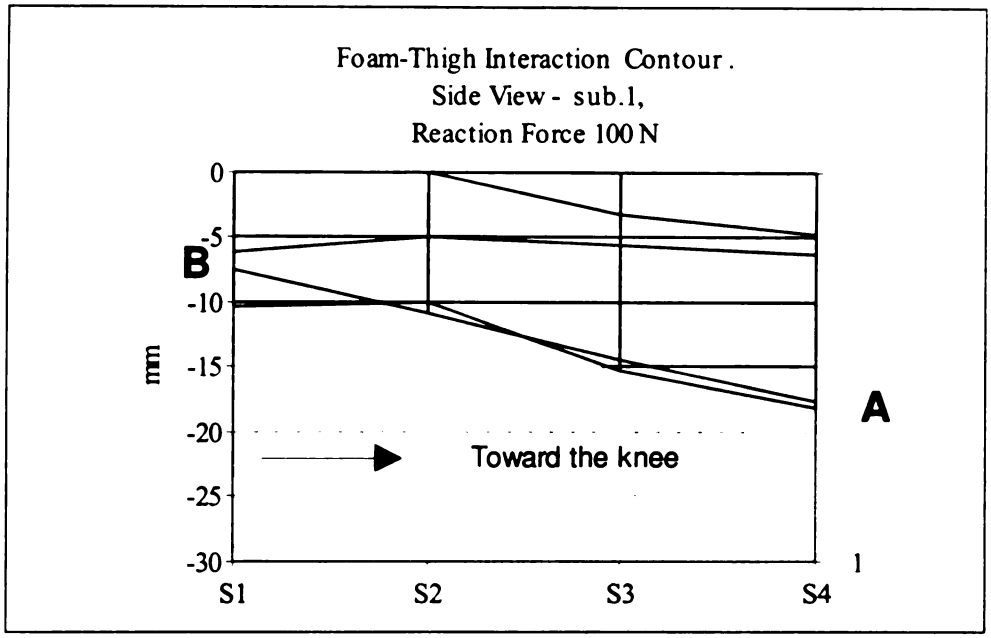

Figure A.82 Side View of Foam-Thigh Interaction Contour, Subject No. 1

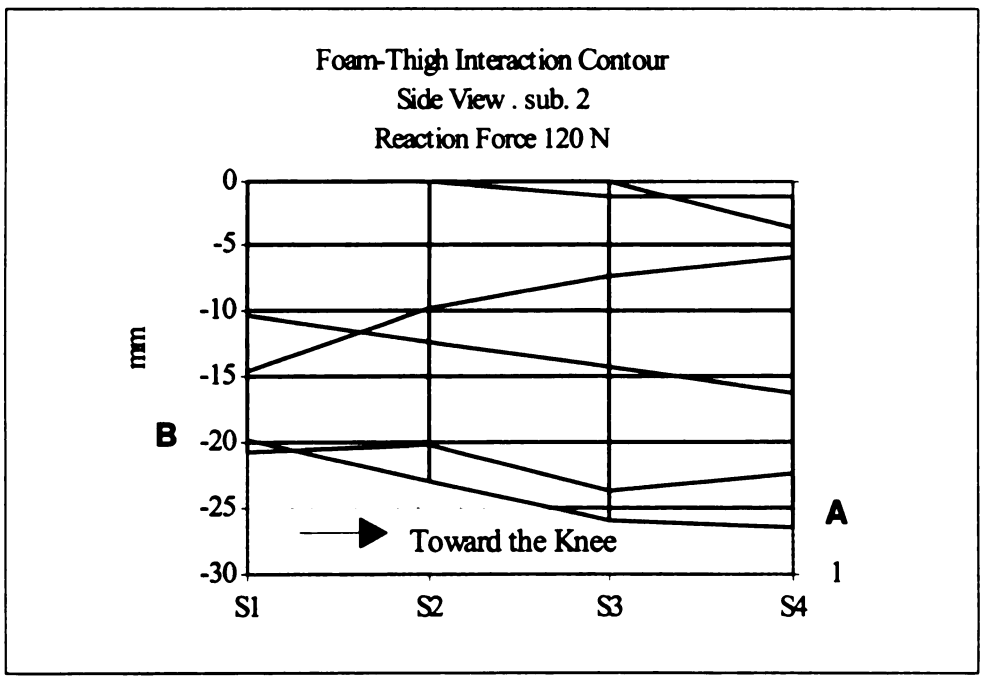

Figure A.83 Side View of Foam-Thigh Interaction Contour, Subject No. 2

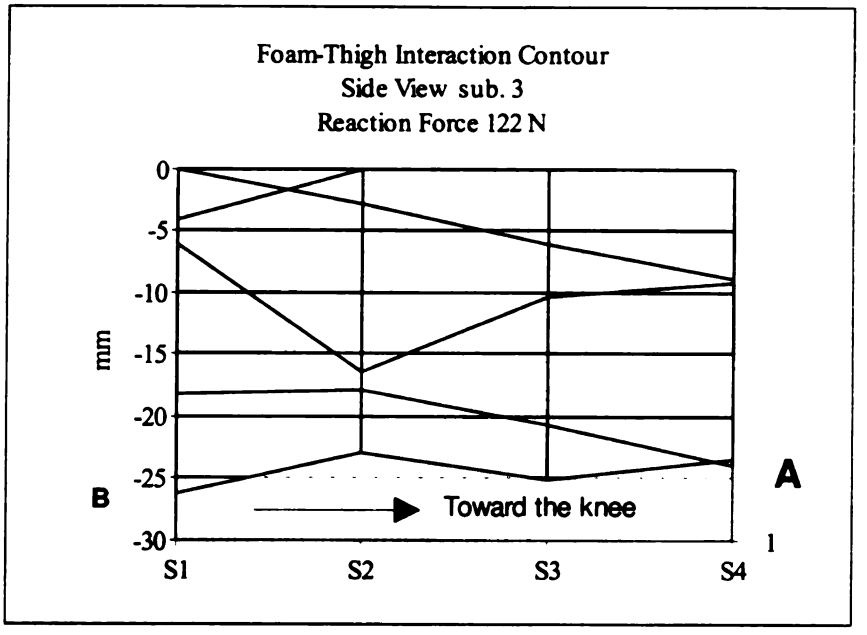

Figure A.84 Side View of Foam-Thigh Interaction Contour, Subject No. 3

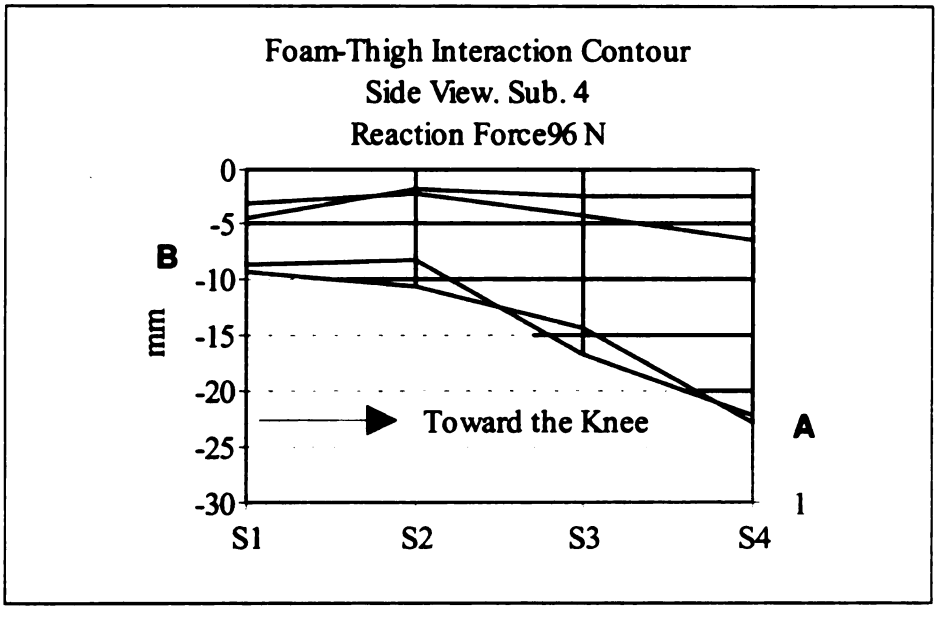

Figure A.85 Side View of Foam-Thigh Interaction Contour, Subject No. 4

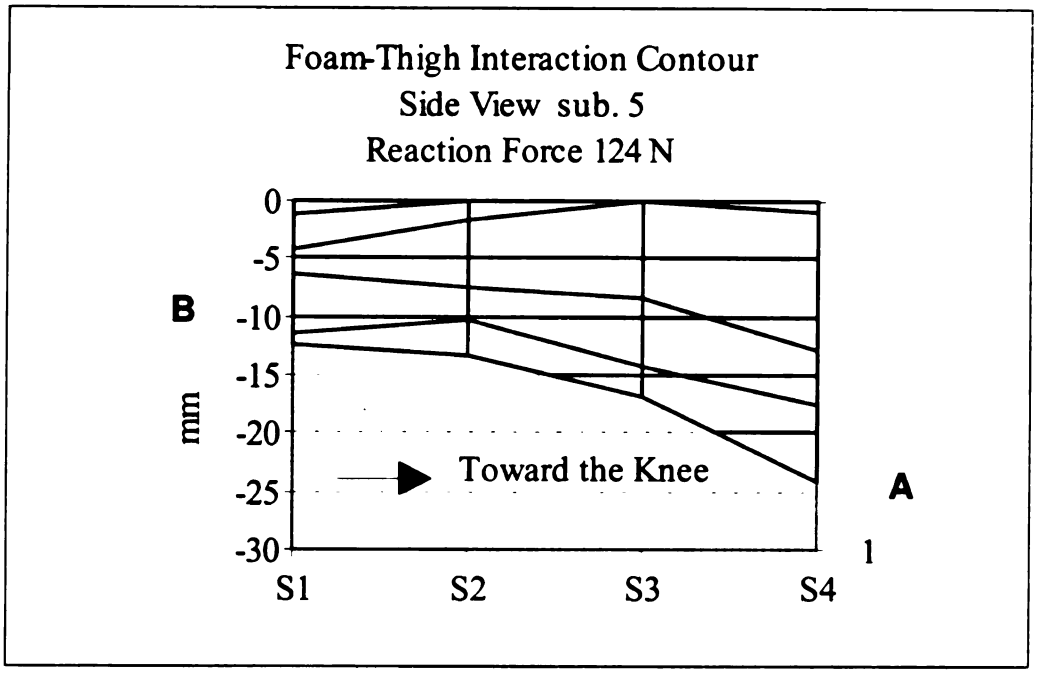

Figure A.86 Side View of Foam-Thigh Interaction Contour, Subject No. 5

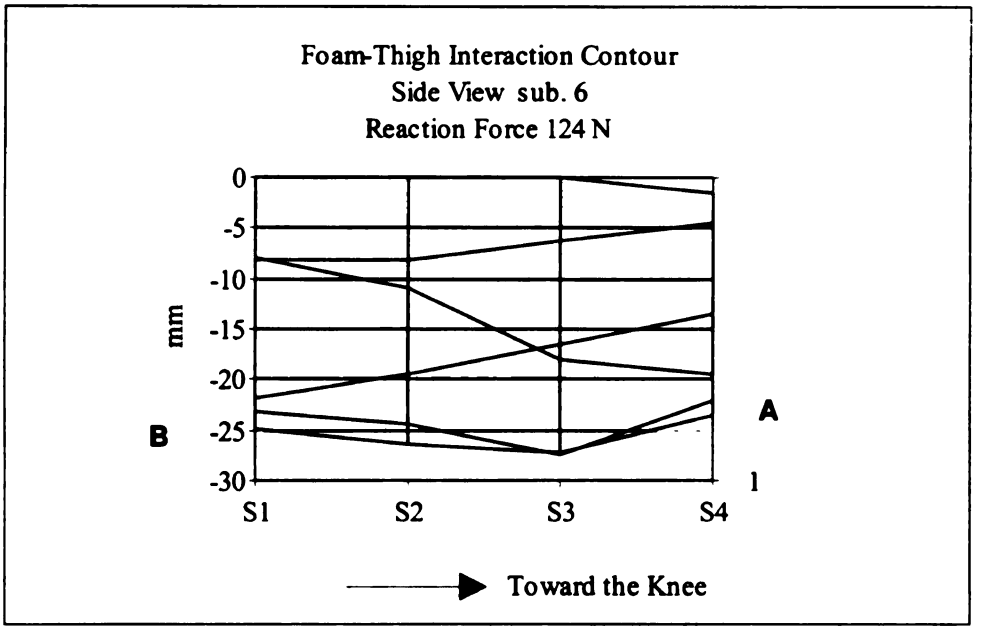

Figure A.87 Side View of Foam-Thigh Interaction Contour, Subject No. 6

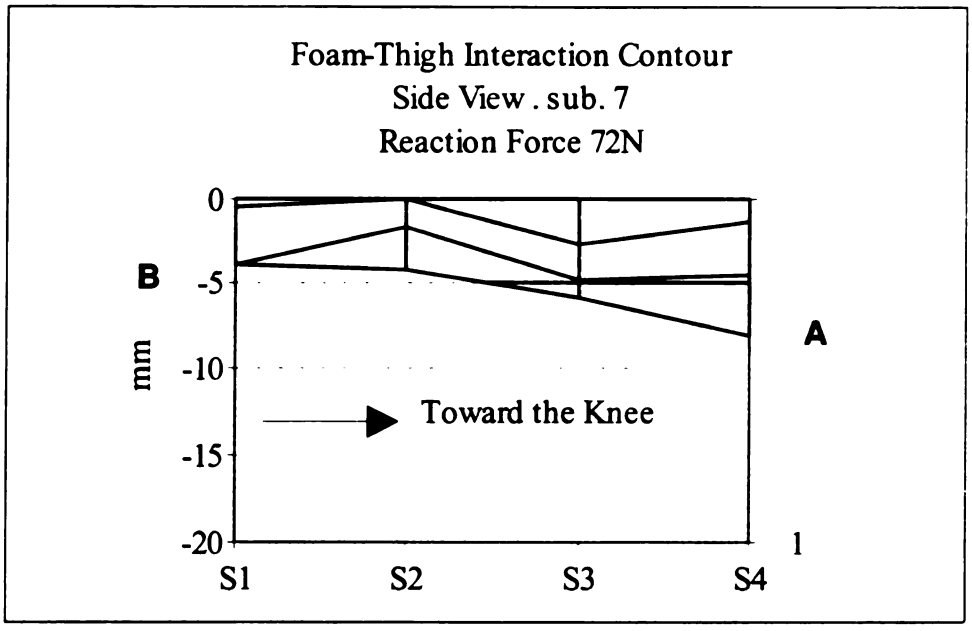

Figure A.88 Side View of Foam-Thigh Interaction Contour, Subject No.7

REFERENCES

REFERENCES

1. Lindan O., et al., "Pressure Distribution on the Surface of the Human Body: 1. Evaluation in lying and Sitting Position Using a Bed of Springs and Nails", Arch. Pays. Med., 39: pp. 623-385, May 1965

2. Mooney et al., "Comparison of Pressure Distribution Qualities in Seat Cushions", Bulletin of Prosthetics Research, pp. 129-143, Spring 1971

3. Canender K. D. and M. R kinkelaa, " Real Time Dynamic Comfort And Performance Factors Of Polyurethane Foam In Automotive Seating", SAE International Congress and Exposition, 1996.

4. PinDot Co product., North brook, IL, 1995

5. Pitman M. I. and Lars Peterson, "Biomechanics of Tissues and Structures of the Musculoskeletal system: Biomechanics of Skeletal Muscle", pp. 89-100,

6. Bruck-Kan R., "Introduction to Human Anatomy", Harper and Row Publishers, 1979.

7. Fung Y.C., "Biomechanics, Mechanical Properties of Living Tissues", Second edition, Springer-Verlag Publishers, 1993.

8. Vannah W. M. and Childress, D. S. "Indentor tests and finite element modeling of bulk muscular tissue in vivo", Journal of Rehabilitation Research and Development Vol. 33, pp. 239-252. 1996

9. Deng B., "Measuring and Modeling Force-Deflection Responses of Human Thighs in Seated Postures", Master of Science thesis, Michigan State University, Department of Materials Science and Mechanics, 1994.

10. Schnider L. W., Pflug M. A.,and Snyder R. G., "Antheropometry Of Motor Vehicle Occupant", volume One , U of M, Transportation Research Institute, 1983.

11. Rohen J. and C Yokochi., in collaboration with E.C.B. Hall-Craggs, "Color Atlas of Anatomy: Photographic Study of the Human Body", Second edition, Igaku-Shoin Medical Publishers, New York, NY, 1988.

12. Jonson R.T., "Elementary Statistics", Fourth Edition, PWS Publishers, 1984.

13. Dobennardo R., and J. Taylor., "Sex Assessment of the Femur: A Test of a New Method", American Journal of Physical Anthropology, Vol. 50: 4, pp. 635-637, 1979.

14. Annual Book of ASTM Standard, D3674-C, Vol. 6, pp.164, 1995.

15. Mow V. and W Hayes, "Basic Orthopedic Biomechanics", Raven Press Publishers, 1991.

16. Yettram A. L., "Material Properties and Stress Analysis in Biomechanics", Manchechester University Press Publishers, 1989.

17. Chou C ,et al., "Development of Foam Model as Applications to Vehicle Interior", Ford Motor Co., MSM seminar, Spring 1995.

18. Pajon M, et al, "Modeling of P.U. Foam Behavior-Applications in the Field of Automotive Seats.", SAE Paper No. 960513, 1996.

19. Ashpy, M. F., "The Metallurgical Properties of Cellular Solids.", Metallurgical Transactions A, 69-1775, 1983.

20. Chow, W. W. and E. I Odell, , "Deformations and Stresses in Soft Body Tissues of a Sitting Person.", Journal of Biomechanical Engineering, Vol. 100, pp. 79-87, May 1978.

21. Beckett, C. l., "Program Developed for Contour Measurement System by Using a Video Camera Interference", MSU, 1996.

22. Husain, T, "An Experimental Study of Some Pressure Effects on Tissues, with Reference to the Bed-sore Problem", Journal of Pathology and Bacteriology, Vol. 66, pp. 347-358, Oct., 1953.

23. Linder, C , Personal communication, Johnson Control Inc., 1996.

24. SENSOTEC catalog, CAT069420, SENSOTEC Inc., 1993.

25. McMaster-Carr catalog, 101, pp. 1750, 1995.